MATERNAL DIETARY OMEGA-3 FATTY ACID INTAKE DURING GESTATION INFLUENCES THE FETAL BRAIN LIPIDOME AND NEURONAL MEMBRANE DYNAMICS

BY

© INNOCENT U. OKAGU

A thesis submitted to the School of Graduate Studies in partial fulfillment of the requirements for the degree of

Masters in Science

Department of Biochemistry, Faculty of Science

Memorial University of Newfoundland

April, 2024

St. John's, Newfoundland and Labrador.

ABSTRACT

Maternal omega (n)-3 polyunsaturated fatty acid (PUFA) intake during gestation has been shown to promote neurodevelopment and reduce the risk of neuropsychiatric disorders. The goals of this thesis were to investigate the effects of maternal diets differing in n-3 PUFA during gestation on fetal brain lipidomic profiles and neuronal membrane dynamics of C57BL/6 mice. A maternal diet high in n-3 PUFA promoted the accretion of ethanolamine, serine, inositol, and glycerol-based glycerophospholipids (GP), while decreasing the levels of choline-based GP in the fetal brain as gestation progressed, compared with low n-3 PUFA diet. A diet high in n-3 PUFA increased the accretion of docosahexaenoic acid (DHA)-containing GP in the fetal brain as gestation progressed, relative to a diet low in n-3 PUFA. Maternal diets high in n-3 PUFA reduced fetal neuronal membrane thickness and increased area per lipid, suggesting increased membrane fluidity. A high n-3 PUFA diet reduced the cholesteryl ester (CE) flip-flop rate, while increasing the formation of ceramide, CE, and phosphatidylethanolamine-enriched lipid domains in the fetal neuronal membrane, which are associated with improved neurotransmission, memory, and cognition. In summary, the data reported in this thesis suggest that adequate amounts of maternal n-3 PUFA during gestation are necessary for proper fetal brain growth, development, and health.

ACKNOWLEDGMENTS

I wish to express my unreserved gratitude to my supervisor, Dr. Sukhinder K. Cheema, for your guidance and criticism throughout my master's program. This thesis work would not have been successful without your scholarly advice and assistance. I deeply appreciate the opportunity of joining your lab and the mentorship; your timely feedback and attention to detail is highly commendable and have shaped my values. My supervisory committee members, Dr. Robert Bertolo and Dr. Robert Brown, were incredibly supportive, and I sincerely appreciate all your efforts.

I thank Dr. Katie Wilson for introducing me to molecular dynamic simulation, an interesting and emerging aspect of computational biochemistry. You are such a great teacher and supportive instructor. I know that you will be recognized widely in the future for your teaching and mentorship skills.

To the past and present members of Dr. Cheema's Lab, especially Anthony, Lea, Bipasha, Nisarg, Nandan, Nancy, Narmada, and Cecilia, thank you for all your assistance during my stay at the Memorial University of Newfoundland. I also thank Tiffany Fillier for guiding me on the analysis of the lipidomics dataset and Thu Huong Pham of Lipidomics Facility, Grenfell campus, for her assistance with the lipidomics (UHPLC/MS^2) analysis of the fetal brain lipid extracts and for guiding me on the analysis of mass spectrometry data. I appreciate the support and assistance of the faculty and technical and administrative staff of the Department of Biochemistry, Memorial University of Newfoundland. You are a great family.

I appreciate the Memorial University of Newfoundland's School of Graduate Studies for the baseline, Dean's Doctoral Award, and Dr. Kevin Keough Graduate Scholarships. I also thank

the Enugu State Government of Nigeria for her bursary to ease my transportation to St. John's through the Enugu State Scholarship and Education Loan Board.

I highly acknowledge the support of the management and staff of the University of Nigeria for granting me study leave with pay since January 2022, when I resumed my studies at Memorial University. To my colleagues at the Department of Biochemistry, Nsukka Campus, thank you for keeping the department running while I am away.

To my best friend and wife, Ijeoma; thank you for all the sacrifices you made to ensure the completion of this program. It was a hard decision to leave you with Ifemy while you were pregnant with Gozirim. You took care of everything without my physical help until Gozirim turned 14 months. You assured me you would fill my absence and kept your word. You also paused your Ph.D. program after committing over three years to it to ensure that we reunite and nurture our kids together in their formative age. I deeply appreciate all you did and continue to do for us. I thank my mom and brothers (Dozie, KC, Obi, Chidi, Chigo, and Okwy), extended family, friends, and well-wishers. Your support is highly appreciated. Thanks for believing in me.

Above all, I sincerely thank the Almighty God, the provider, preserver, healer, and all-knowing! It was as if my life was crashing before me on September 12, 2023, when I was diagnosed with stage 2 hypertension, leading to immediate placement on anti-hypertensives. With hypertension that persisted at stage 2 for some weeks despite a combination of drugs of different classes, I was presented with available options, including continuing and facing any possible complications that might arise, taking a medical break, switching to part-time, or switching from Ph.D. to master's program. As an international student on a study permit, the only reasonable option I am eligible for is to change my program to master's; the most challenging and

“unceremonial” decision I had to make in my 37 years of existence. I struggled to continue, but the warning of the high risk of having a stroke, if I do not reduce stress and modify other lifestyle alongside the medications to control my blood pressure, kept ringing in my head. I could remember the anxiety of working alone in the lab at night and having my wife call every 30 minutes to be sure I was fine. I thank my supervisor, my supervisory committee, Andrew Kim of the School of Graduate Studies, Dr. Sherri Christian (Deputy Head, Graduate Studies), and others who encouraged me to choose health over getting a second PhD. Although I am still on a combination of several antihypertensive drugs and sleep therapy, I am grateful to God Almighty for life. In all situations, give glory to God!

TABLE OF CONTENTS

ABBREVIATIONS

AD	Alzheimer's disease
AGPS	alkylglycerone phosphate synthase
AKT	protein kinase B
ALA	alpha (α)-linolenic acid
AMPA	α-amino-3-hydroxy-5-methyl-4-isoxazolepropionic acid
ANOVA	analysis of variance
APL	area per lipid
ARA	arachidonic acid
BBB	blood-brain barrier
BDNF	brain-derived neurotrophic factor
C30RP	C30 reverse phase liquid chromatography
cAMP	cyclic adenosine monophosphate
CE	cholesteryl esters
Cer	ceramides
$cPLA_2$	cytosolic phospholipase A_2
CREB	cAMP-responsive element binding protein
DG	diacylglycerols
DGAT-2	acyl-CoA:diacylglycerol acyltransferase-2
DHA	docosahexaenoic acid
DOPC	dioleoylphosphatidylcholine
DPA	docosapentaenoic acid
EPA	eicosapentaenoic acid

FDR	false discovery rate
GD	gestation day
GL	glycerolipids
GNPAT	glyceronephosphate O-acyltransferase
GP	glycerophospholipids
GPI	glycosylphosphatidylinositol
HILIC-MS	hydrophilic interaction liquid chromatography-mass spectrometry
HRMS	high-resolution mass spectra
HTG	hypertriglyceridemia
iPLA$_2$	calcium-independent phospholipase A$_2$
LA	linoleic acid
LPC	lysophosphatidylcholine
LPE	lysophosphatidylethanolamine
LTP	long-term potentiation
MD	molecular dynamics
Mfsd2a	major facilitator superfamily domain 2a
MTBE	methyl tert-butyl ether
MUFA	monounsaturated fatty acids
NEFA	non-esterified fatty acids
NMDA	N-methyl-D-aspartate
OA	oleic acid
O-PC	plasmanyl choline
O-PE	plasmanyl ethanolamine

PA	palmitic acid
PA	palmitic acid
PC	diacyl phosphatidylcholine
PCA	principal component analysis
PCA	principal component analysis
PD	Parkinson's disease
PE	diacyl phosphatidylethanolamine
PEMT	PE methyltransferases
PG	diacyl phosphatidylglycerol
PI	diacyl phosphatidylinositol
PI3K	phosphoinositide 3-kinase
PKA	protein kinase A
PKC	protein kinase C
PLs	phospholipases
PLS-DA	partial least squares discriminant analysis
PLS-DA	partial least-squares discriminant analysis
PND	postnatal day
POPC	palmitoyl-oleoylphosphatidylcholine
P-PC	choline plasmalogen
P-PE	ethanolamine plasmalogen
PS	diacyl phosphatidylserine
PSD	PS decarboxylases
PSM	*N*-palmitoyl-sphingomyelin

PSS	phosphatidylserine synthase
PSS	PS synthases
PUFA	polyunsaturated fatty acids
SFA	saturated fatty acids
SM	sphingomyelin
SPP	sphingosine phosphatases
TG	triacylglycerols
UHPLC/MS^2	ultra-high performance liquid chromatography-tandem mass spectrometry
VIP	variability importance in the progression
VMD	visual molecular dynamics

LIST OF TABLES

LIST OF FIGURES

LIST OF APPENDICES

CHAPTER ONE

Introduction

1.1 Brain lipid composition

The brain is a vital organ that coordinates nerve messages within the body. According to the Global Burden of Diseases Study 2019 (GBD, 2019), about 40% of the global population suffers from some form of brain disease, which is estimated to double by 2050. Approximately 60% of total brain dry weight is composed of lipids (Chang *et al*., 2009). Lipids are a source of energy (Nordström *et al*., 2013) and play crucial roles in brain development, metabolism, and function (Cao et al., 2009; Deoni et al., 2018; Hussain et al., 2019). Some brain lipids, such as arachidonic acid (20:4 n-6, ARA) and docosahexaenoic acid (22:6 n-3, DHA) are precursors of bioactive chemicals such as maresins and docosanoids that modulate cognition, memory, and other forms of neurobehavior (Hussain *et al*., 2019; West *et al*., 2020). Inadequate levels of major brain lipids have been shown to result in poor myelination, synaptogenesis (Teigler *et al*., 2009), neurogenesis, and neurotransmission (Mallick *et al*., 2021), all of which affect brain development and function. Hence, adequate accretion of lipids in the brain is crucial for proper brain health.

There are different groups of lipids in the brain. These include glycerophospholipids (GP), sphingolipids, sterols and glycerolipids, and their fatty acyl species (O'Brien *et al*., 1964; O'Brien & Sampson, 1965; Custers *et al*., 2022; Hirabayashi, 2012). GP is a group of lipids with glycerol backbone with one or two fatty acyl groups typically attached at the *sn*-1 and *sn*-2 carbons of glycerol and phosphorylated variable head group at the *sn*-3 carbon of the glycerol. Different classes of GP have been identified in the brain. Based on linkages at the *sn*-1 position of the glycerol backbone, GP are classified into diacyl, plasmanyl (or 1-*O*-alkyl-linked), and plasmalogen (plasmenyl or 1-*O*-alk-1′-enyl-linked) GP (Maeba *et al*., 2018). GP are also classified based on the headgroup attached to the *sn*-3 position of the glycerol backbone. These include choline-based GP such as diacyl phosphatidylcholine (PC), plasmanyl choline (O-PC), choline plasmalogens (P-PC,

plasmenyl choline), and lysophosphatidylcholine (LPC). Another class of GP is ethanolamine-based GP, such as diacyl phosphatidylethanolamine (PE), ethanolamine plasmalogens (P-PE, plasmenyl ethanolamine), plasmanyl ethanolamine (O-PE) and lysophosphatidylethanolamine (LPE). Other GP classes found in the brain include serine-based GP (diacyl phosphatidylserine, PS), inositol-based GP (diacyl phosphatidylinositol, PI), and glycerol-based GP (diacyl phosphatidylglycerol, PG). Among the GP classes in adult rat brains, ethanolamine-based GP was the most abundant (54%), followed by choline-based GP (30%), PS (8%), and PI (5%), with phosphatidylglycerol (PG) making up about 0.02% of the total GP (Choi *et al*., 2018). Plasmalogens are major reservoirs of DHA in the brain and play key roles in brain and neuronal membrane function (Udagawa & Hino, 2022). In the adult human brain, P-PE consists of 18-20% of total GP (Dorninger *et al*., 2015), while it makes up 11% of total adult mouse brain lipids (Fitzner *et al*., 2020). DHA-containing plasmalogens are abundant in neuronal membranes and contribute to membrane flexibility (Huber *et al*., 2002), and promote optimal brain function (Almsherqi, 2021).

Ethanolamine-based GP are critical in neurogenesis, myelination, neuroprotection and stabilization of membrane structure (Tasseva *et al*., 2012) whereas PS and PG were shown to protect neurons from stress-induced damages (Donoso *et al*., 2020). PG-enriched membrane domains inhibit α-synuclein fibrillation that promote amyloid-β peptide formation (Khammari *et al*., 2020). Unfibrilated α-synuclein regulates membrane fusion and neurotransmitter release (Sun *et al*., 2019); hence, inhibiting α-synuclein fibrillation will enhance neurotransmission. PS and DHA-containing PS promote neurogenesis and myelination (Kim *et al*., 2010), and neuronal cell survival (Kawakita *et al*., 2006). PS also increases the formation of neurotrophins, neuroprotectins, and synaptamide that boost neurogenesis, synaptogenesis, synaptic transmission and

neuroprotection (Kim *et al*., 2019; Kim *et al*., 2022b). Choline-based GP promotes neuronal differentiation through protein kinase A (PKA)/cyclic adenosine monophosphate (cAMP)-responsive element binding protein (CREB) signaling (Montaner *et al*., 2018; Magaquian *et al*., 2021). LPC is a metabolite of PC, and the major form in which DHA is transported in the form of DHA-containing LPC [LPC(22:6); 22 representing the number of carbon atoms and 6 representing the number of double bonds] into the brain through the transporter, major facilitator superfamily domain 2a (Mfsd2a) (Nguyen *et al*., 2014; Bergman *et al*., 2023). LPC(22:6) was reported to inhibit neuroinflammation (Hung *et al*., 2011) and enhance memory and cognition (Sugasini *et al*., 2017). Plasmalogens protect brain cells from neuroinflammation, prevent neurodegeneration, and boost cognitive function (Ifuku *et al*., 2012; Katafuchi *et al*., 2012; Hossain *et al*., 2023). Additionally, DHA-containing ether lipids (plasmalogens and plasmanyl GP) are crucial because they inhibit γ-secretase, the enzyme that synthesizes amyloid-β peptides which are implicated in neurodegenerative diseases (Onodera *et al*., 2015). Generally, GP is involved in neurogenesis, synaptogenesis, neurotransmission, neuroprotection, and anti-apoptosis (Hossain *et al*., 2013; Kim *et al*., 2014; Hossain *et al*., 2016, 2020;). However, little is known about changes in brain GP profile during normal gestation window, demanding studies to fill this gap in knowledge.

Dysregulation in brain GP metabolism has been reported in neurological conditions such as rhizomelic chondrodysplasia punctata (Dorninger *et al*., 2015), Parkinson's disease (PD) (Fabelo *et al*., 2011), Alzheimer's disease (AD) (Goodenowe *et al*., 2007; Dorninger *et al*., 2017, 2019; Su *et al*., 2019), and Zellweger spectrum (Da Silva *et al*., 2012). Depleted DHA-containing GP has been reported in different brain parts of mouse model of AD (*App* KI mice) at 18 months; specifically, DHA-containing PC [PC(16:0/22:6) and PC(18:0/22:6)] and PE [PE(18:0/22:6)] were lower in cortex, and PC(18:0/22:6) and DHA-containing PS [PS(18:0/22:6)] in the hippocampus,

compared with normal mice (Emre *et al*., 2021). On the other hand, ARA-containing PC [PC(18:1/20:4)] and PE [PE(18:1/20:4)] were lower in the cortex, and PE(18:1/20:4), PS(18:1/20:4) and PS(18:0/20:4) in the hippocampus of AD mice, compared with normal mice (Emre *et al*., 2021). Similarly, lower levels of DHA-containing PS were found in human AD brain, compared with healthy age-matched subjects (Cunnane *et al*., 2012).

Sphingolipids (SP) are another group of lipids in the brain. They have a sphingoid base backbone with aliphatic amino alcohols. Based on the polar head group, SP are grouped into sphingomyelins (SM), ceramides (Cer), and glycosphingolipids (Lahiri & Futerman, 2007). Generally, SP improves synaptogenesis and synaptic transmission via glutamate-mediated information pathways (Hirabayashi, 2012; Riganti *et al*., 2016). Specifically, SM promotes cognition and the formation and stability of myelin (Deoni *et al*., 2018; Schneider *et al*., 2019). In general, aberrations in the metabolism of SP in the brain and plasma are implicated in several brain disorders, including AD, PD, Huntington's disease, Krabbe's disease, and Gaucher's disease (Xing *et al*., 2016; Olsen & Færgeman, 2017; Czubowicz *et al*., 2019; Alaamery *et al*., 2021). For instance, higher plasma levels of C22:0 and C24:1 ceramides have been recorded in PD patients compared with healthy controls (Xing *et al*., 2016). Therefore, changes in brain Cer and SM species during the physiological gestation window and by maternal dietary intake need to be studied by lipidomics analysis. Understanding gestational brain SP profiles will open a window for studying how gestational brain SP profiles are associated with risks of brain diseases in postnatal life and how to modify the risk through dietary intervention.

Sterols are another group of lipids found in the brain, and they exist primarily in the unesterified form (free cholesterol) with about 0.1-1% as cholesteryl esters (CE) in the normal adult brain and about 1-5% during the early stage of myelination (Petrov *et al*., 2016). Cholesterol

makes up about 10% of the dry weight of the adult human brain (Alling & Svennerholm, 1969), which is about 20% of the total cholesterol in an adult body (Jurevics & Morell, 1995). At high cholesterol levels, some of the free cholesterol is esterified into cholesteryl esters (CE) to prevent the effects of excess cholesterol, such as high membrane rigidity. However, the fetal brain sterol composition at different gestation stages and the impact of maternal diets differing in n-3 PUFA have not been reported. This is important as cholesterol is crucial in myelination and neuronal membrane structure and function (Saher *et al*., 2005).

Brain lipids also contain glycerolipids (GL), including diacylglycerols (DG) and triacylglycerols (TG). They are found in smaller amounts in the brain, compared with GP. DG are signaling molecules in cannabinoid signaling-mediated synaptic growth, plasticity, and function, and are precursors of TGs and phospholipids (Tu-Sekine & Raben, 2011; Keimpema *et al*., 2013). On the other hand, TG are reservoirs of fatty acids that can be mobilized for energy and for the synthesis of bioactive lipid mediators (Cook, 1981). TG are components of membrane lipid rafts and are typically between membrane leaflets (Pakkanen *et al*., 2011; Caillon *et al*., 2020). There is a growing interest in circulating TG status and brain health in middle age. For example, accumulating evidence shows that hypertriglyceridemia (HTG), a condition characterized by high plasma TGs in middle age, is a contributory factor to the development of impaired cognitive and executive functions, attention disorders, and dementia in old age (Kalmijn *et al*., 2000; Reitz *et al*., 2005; Burgess *et al*., 2006; Parthasarathy *et al*., 2017; Power *et al*., 2018; Lv *et al*., 2019).

The injection of the TG triolein into mice brain impaired neurotransmission mediated by the N-methyl-D-aspartate (NMDA) component of hippocampal long-term potentiation (LTP) (Farr *et al*., 2008). This may explain the relationship between diet-induced HTG and memory impairment (Farr *et al*., 2008), as TG can cross the blood-brain barrier (BBB) (Banks *et al*., 2018)

and increase the permeability of BBB, leading to increased brain inflammation and stress (Lee *et al*., 2017). HTG has also been shown to increase the polymerization and build-up of amyloid-β peptides and neurofibrillary tangles in the brain, leading to impairment of synaptic transmission and other events associated with neurodegeneration (Burgess *et al*., 2006; Choi *et al*., 2016; Nägga *et al*., 2018). This makes HTG and excessive accretion of TG in the adult brain a risk factor for neurological disorders; however, the fetal brain TG profile and impact of maternal dietary n-3 PUFA intake during gestation are not well-known and should be investigated through fetal brain lipidomics analysis.

In addition to major brain lipid groups and classes, brain fatty acids also play a key role in brain health. This is discussed in the next subsection.

1.1.1 Fatty acyl composition of brain lipids

The composition of fatty acids in the brain is critical in brain growth and function. Long-chain PUFA, typically ARA and DHA, make up 25-30% of total fatty acids in the brain depending on the species, different brain sections, diet, age, and health status (Carrié *et al*., 2000; Carver *et al*., 2001; Xiao *et al*., 2005). In the human brain, DHA consists of 15% of total fatty acids and over 90% of n-3 PUFA (Makrides *et al*., 1994), suggesting that DHA has a critical role in brain development and function. In C57BL/6 mice brains, ARA and DHA consist of 5-10% and 10-15%, respectively; the highest ARA level in the brain is in the hypothalamus (~10%), while the highest DHA level is in the prefrontal cortex (~15%) (Joffre *et al*., 2016).

There is a rapid accretion of DHA in the brain during late gestation and early postnatal life when substantial development of brain tissues, including myelination (Kinney *et al*., 1988; Yarnykh *et al*., 2018) and synaptogenesis occur (Sarnat & Flores-Sarnat, 2015; Sarnat, 2023).

Moreover, DHA has been demonstrated to promote synaptogenesis by upregulating the expression of several synaptic proteins, leading to an increase in synaptic function, including synaptic plasticity and LTP, which are associated with learning and memory (Sakamoto *et al*., 2007; Cao *et al*., 2009; Kim *et al*., 2011; Lee *et al*., 2016; Kim *et al*., 2022). Furthermore, the accretion of DHA and DHA-containing lipids in the developing brain is critical because poor myelination due to low brain DHA during brain development has been linked to a higher risk of cognitive impairment (Deoni *et al*., 2018). Low brain DHA also alters synaptic function, influences memory and cognition, and negatively impacts behavior (Cohen *et al*., 2005; Salem *et al*., 2001). Higher prevalence of neurodevelopmental defects such as schizophrenia (SCZ), attention-deficit/hyperactivity disorder, and autism spectrum disorder (Rommel *et al*., 2017; Anderson *et al*., 2021) and psychiatric disorders such as psychosis and mood disorders (Vanes *et al*., 2022) has been recorded in preterm-born individuals. Moreover, people with these conditions are reported to have low brain DHA compared with their healthy counterparts (McNamara, 2010), suggesting that low brain DHA status during early brain development may predispose to neurodevelopmental and psychiatric disorders across the lifespan. Additionally, preterm-born individuals with high DHA status exhibited higher brain development and better cognitive behavior (Tam *et al*., 2016), indicating that accretion of adequate DHA during early brain development will promote neurodevelopment and brain health.

DHA is a precursor for the synthesis of neuromodulatory chemicals, including neurotransmitters, synaptamides, docosanoids, neuroprotectins, resolvins, and maresins (Dinicolantonio & O'Keefe, 2020; Kim et al., 2022). These chemicals are known to prevent the development and progression of several neurodegenerative events in both *in vitro* (Rey *et al*., 2016) and *in vivo* models (De Smedt-Peyrusse *et al*., 2008; Orr *et al*., 2013). They enhance neuronal

expansion and maturation and stimulate neuritogenesis and growth of cell membranes through several pathways, including upregulating proteins implicated in membrane transport and neurite outgrowth, such as syntaxin 3 (Darios & Davletov, 2006). They also stimulate neurogenesis and protect brain cells against oxidation and inflammation (Palacios-Pelaez *et al*., 2010; Bazan *et al*., 2011; Bazan, 2013, 2018). Dietary DHA supplementation (at 14% of total fat) for eight weeks was shown to promote brain DHA-containing GP of adult senescence-accelerated mouse-prone 8 mice, which alleviated memory and cognitive impairment associated with these mouse models between 8-12 months of life (Petursdottir *et al*., 2008b). However, it is highly unlikely that this high amount of dietary DHA intake will be sustained in a population with low DHA intake in early life. Hence, the accretion of adequate DHA in the brain during early brain development is critical for brain health, as summarized in Figure **1.1**.

1.2 Changes in brain lipid composition with age

Brain development starts with the formation of the neural tube at the third week of gestation in humans (Newville *et al*., 2018), which corresponds to gestation day (GD) 8.5-9.5 in mice (Chen *et al*., 2017), and continues until parturition and early adulthood. As the brain develops, its lipid content (including the lipid groups, classes and their associated fatty acyl species) changes in amount and composition (Hazel, 1990; Mota-Martorell *et al*., 2022). For example, total choline-based GP in a healthy human brain decreases by half at eight years, compared with the amount at birth, while human total brain SM increased by 8-fold between this age window (Dawson, 2015).

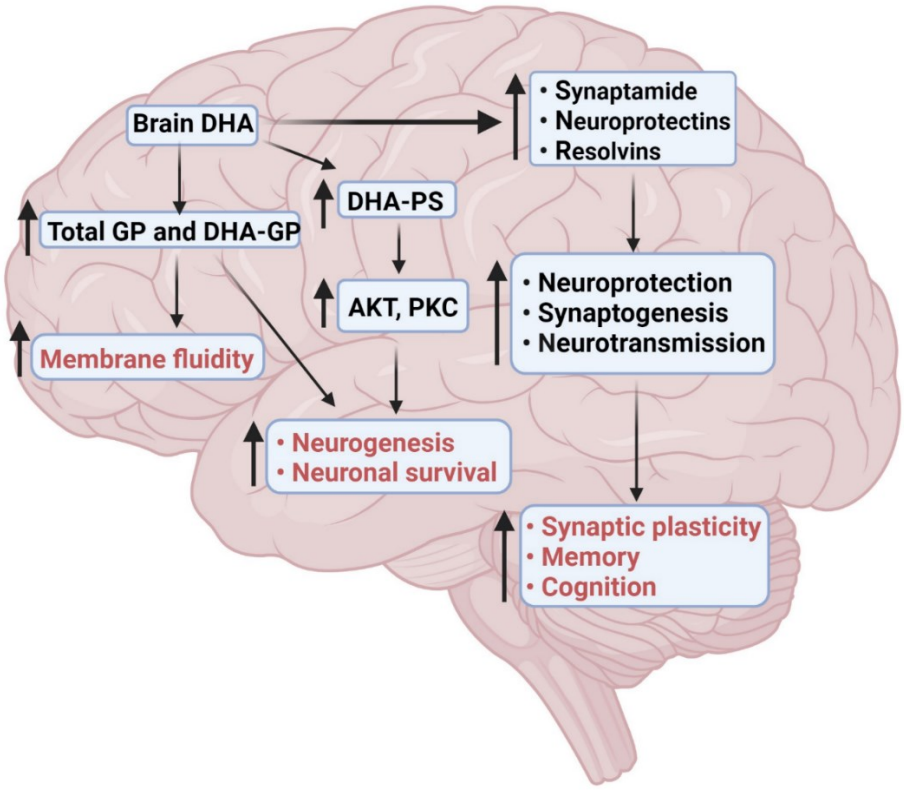

Figure 1.1: Summary of benefits of docosahexaenoic acid (DHA) in the brain and neuronal membrane. *Dietary n-3 PUFA increases brain DHA leading to an increase in total glycerophospholipids (GP) and DHA-containing GP (DHA-GP) which are crucial in increasing neuronal membrane fluidity. Increase in DHA-containing GP also increases neurogenesis and neuronal survival. DHA also increases levels of total and DHA-containing diacyl phosphatidylserine (PS) that activates protein kinase B (AKT) and protein kinase C (PKC) signaling that also promote neurogenesis and neuronal survival. DHA are precursors of synaptamide, neuroprotectins and resolvins which protect neurons from assaults and promote synaptogenesis and neurotransmission. Promotion of synaptic transmission increases synaptic plasticity, memory, and cognition. Block arrows pointing up show increase while line arrows show direction of events. The image was created using Biorender.com.*

Regarding brain fatty acids and fatty acyl species of major lipid groups/classes in the brain, palmitic acid (PA, C16:0) was the most abundant fatty acyl content in rat brain PC and it increased dramatically from full-term pregnancy (GD21) to postnatal day (PND) 9, while DHA was the most abundant fatty acyl species in PE and it increased sharply from GD21 to PND3 and from PND6 to PND9 (Cunnane & Chen, 1992).

In the normal aging human brain, n-6 PUFA-containing GP [PC(18:0/20:4), PE(18:0/22:4), PE(16:0/22:4), PS(18:0/22:4) and PS(18:0/20:4)] progressively decrease between 20 and 100 years, whereas DHA-containing GP [PE(18:/22:6), PS(18:0/22:6) and LPE(22:6)] increased with age (Hancock *et al*., 2015). Contrarily, lower levels of PA, eicosapentaenoic acid (EPA, 20:5n-3), and DHA-containing PS (Cunnane *et al*., 2012) and choline plasmalogens [PC(P-18:0/22:6) and PC(P-18:0/20:4)] (Otoki *et al*., 2021) were reported in AD human brain compared with healthy counterparts. Similarly, a marked reduction in DHA-containing PS [PS(18:0/22:6) and ARA-containing PI [PI(16:0/20:4)] in the gray matter of the prefrontal cortex has been reported in aged human schizophrenia patients relative to age-matched healthy control (Matsumoto *et al*., 2017). These observations suggest that DHA-containing GP may be essential in preventing the development of AD and SCZ. The findings reviewed above showed that changes in brain GP during postnatal life are well-known; however, little is known about changes in fetal brain GP profile during the gestation window, warranting studies to fill this knowledge gap through lipidomic analysis of fetal brain at different stages of gestation.

For the brain sterols, there is a substantial increase in CE between gestation weeks 28 and 38 in humans (Alling & Svennerholm, 1969), which correlates with the onset of myelination. Brain CE substantially decreases around the full term and during early postnatal, with almost all the cholesterol being in the unesterified form at 60 years (Adams & Davison, 1959; Alling &

Svennerholm, 1969). In general, there is a progressive switching of brain total cholesterol from the esterified form during prenatal life and early infancy to all being in the non-esterified form during adulthood (Quan *et al*., 2003; Dietschy & Turley, 2004). This suggests that both free and esterified cholesterol are important in the determination of the sterol profile of the fetal brain.

Brain SP metabolism also changes with age and has been associated with the risk of neurodegenerative disorders (Wang & Bieberich, 2018). In the human hippocampus, the total Cer and SM levels were shown to increase with age (Couttas *et al*., 2018). This could be attributed to the previously reported increase in activities of Cer and SM synthases with age in rat brain (Sacket *et al*., 2009). Looking at the specific Cer and SM species, erucic acid (C22:1) and nervonic acid (C24:1)-containing Cer and erucic acid (C22:1)-containing SM were reported to increase, whereas sphingosine 1-phosphate (S1P), a neuroprotective signaling SP decreased with age in hippocampus (Couttas *et al*., 2018). In C57BL/6 mice, an age-dependent increase in nervonic acid (C24:1)-containing ceramide [Cer(d18:1/24:1)] and hexosylceramide [HexCer(d18:1/24:1)] in hippocampus was reported at 12 and 21 months relative to three months, whereas stearic acid (C18:0)-containing ceramide [Cer(d18:1/18:0)] decreased with age (Vozella *et al*., 2017). These changes were explained by the upregulated gene expression of ceramide synthase 2 (CerS2), which is responsible for the synthase of very long-chain ceramides like C24:0 and C24:1, whereas CerS1, which catalyzes the synthesis of long-chain ceramides like C18:0-containing ceramides decreased during between 12 and 21 months (Vozella *et al*., 2017). Interestingly, the expression of genes for the enzymes that catalyze the rate-limiting step in the synthesis of C24:1, stearoyl-CoA desaturases, were markedly increased at 21 months relative to three and 12 months in mice. Sphingomyelin [SM(d42:2)], which was speculated to contain C24:1 fatty acid molecular species, was shown to increase in mice hippocampi between three and 21 months (Vozella *et al*., 2017). A

similar result was previously reported in rat brain: SM(d24:1) significantly increased between two and half and 21.5 months, whereas SM(d18:0) decreased (Giusto *et al*., 1992).

Changes in brain lipid composition during the postnatal period (infancy to late adulthood) have been reported in both healthy and diseased brains (Nussbaum *et al*., 1971; Clandinin *et al*., 1980; Cunnane & Chen, 1992; J. Choi *et al*., 2018). However, little is known about changes to the fetal brain lipidome (all lipids in the brain), especially the fatty acid components of major brain lipids at different stages of gestation. Altered brain lipids during gestation have been shown to influence brain development and function that extend to adulthood (Suzuki *et al*., 1998). Hence, understanding the entire fetal brain lipidome at different stages of normal gestation is crucial.

Our laboratory previously showed that the fetal brain fatty acid profile changes during gestation; as gestation progress, the total monounsaturated fatty acids (MUFA) and palmitoleic acid (C16:1) and oleic acid (C18:1, OA), and n-6 PUFA and linoleic acid (C18:2-n6, LA) decrease, whereas total n-3 PUFA and DHA in the fetal brain increase during gestation (Akerele & Cheema, 2020). Our laboratory also showed that MUFA, OA and eicosenoic acid (C20:1) composition of offspring brain increases from weaning to 16 weeks postweaning (Balogun & Cheema, 2014), suggesting a switch from decrease during progress of gestation to increase during early postnatal until adulthood. However, the lipid classes and specific fatty acyl species in the fetal and offspring brains in the above reports were not studied.

As mentioned previously, PUFA such as DHA and ARA make up major components of brain total fatty acid and they accrue in developing brain – typically during the third trimester and early postnatal life (Wainwright, 2002). DHA and DHA-containing GP boost neurogenesis, myelination, and synaptogenesis, and protect brain cells from damages. As shown in several

models of membranes such as rat bile canalicular plasma membrane (Hashimoto et al., 2001), membrane extracted from Y-79 retinoblastoma cells (Treen et al., 1992), artificial membrane formed with cholesterol-to-phospholipid (1.5:1 ratio) (Mason et al., 2016), and membrane prepared using small unilamellar vesicles (Jacobs et al., 2021), DHA also increases fluidity and permeability of membrane. ARA also contributes to membrane fluidity and permeability to enhance membrane transport function (Beck *et al*., 1998). At high concentrations, ARA induces inflammation that can cause damage to brain cells, leading to alteration in pathways involved in cognition and memory, including glutamate receptor 5, Aβ oligomers affect the activity and recycling of the NMDA and α-amino-3-hydroxy-5-methyl-4-isoxazolepropionic acid (AMPA) signaling (Bagga *et al*., 2003; Thomas *et al*., 2017).

Metabolites of ARA, endocannabinoids modulate synaptic communication, learning and memory (Atwood & Lovinger, 2017). Hence, adequate amount of these lipids in the brain may be beneficial against neurodevelopmental and neurodegenerative disorders. These studies highlight the importance of analysis of normal brain lipidome at all stages of life, from prenatal through the lifespan. The results may provide crucial information with diagnostic implications on the etiology of some brain diseases.

1.3 Importance of dietary essential fatty acids in brain development and function

Diet is another important modifiable factor that affects brain lipid composition. Maternal gestational diets have been shown to influence the fetal brain lipid composition. Maternal n-3 PUFA intake during gestation is crucial because dietary n-3 PUFA have several health benefits, including improving cardiometabolic health (Balogun *et al*., 2013, 2014; Balogun & Cheema, 2016), neurotrophin signaling (Balogun & Cheema, 2014; Feltham *et al*., 2019; Akerele &

Cheema, 2020) and reducing cognitive impairment associated with neurodegenerative diseases (Ruxton *et al*., 2005; Katakura *et al*., 2009; Gil *et al*., 2012; Gil & Gil, 2015). It has been shown previously in our laboratory that maternal diets enriched in fish oil-based n-3 PUFA during gestation improved maternal lipogenesis to meet the high demand of fatty acids by developing mouse fetal brain (Akerele & Cheema, 2017), altered fetal brain lipid composition, and regulated neurotrophin signaling (Akerele & Cheema, 2020). Maternal cord DHA level, an indicator of maternal n-3 PUFA status, has been reported to be directly associated with fetal DHA status (Montgomery *et al*., 2003).

Human offspring from mothers with high cord DHA levels were shown to have higher DHA levels and better neurological functionality at five and half years (Escolano-Margarit *et al*., 2011). Breastmilk lipid composition is another indicator of n-3 PUFA status; our laboratory has previously shown that breastmilk of mice on a high n-3 PUFA diet (10% of total fatty acid composition) had higher n-3 PUFA content, including DHA, EPA, and docosapentaenoic acid (C22:5 n-3, DPA), compared with mice on low n-3 PUFA diet (2% of total fatty acid composition) (Balogun *et al*., 2014). Interestingly, offspring from dams with high breastmilk n-3 PUFA had higher brain *BDNF* and *CREB* gene expression (Balogun *et al*., 2014). Human offspring of mothers with high breastmilk n-3 PUFA were shown to have better cognitive performance, compared with formula-fed counterparts (with low dietary n-3 PUFA) (Makrides *et al*., 1994; Gibson *et al*., 1996; Smith & Rouse, 2017).

Inadequate supply of n-3 PUFA (0.3% α-linolenic acid, C18:3-n3, ALA) during prenatal life of a mouse was shown to result in progressive decline of its brain DHA during early postnatal life, typically within the first 30 days of life. This depletion of brain DHA resulted in downregulated expression of *BDNF* (Madore *et al*., 2014). Similarly, insufficient supply of n-3

PUFA (0.3% ALA) was reported to deplete DHA-containing PE and PS in brain and retina of rhesus monkeys which were not completely restored by supplying of n-3 PUFA-enriched diet (7.7% ALA) (Anderson *et al*., 2005). Human offspring whose mothers received fish oil or n-3 PUFA supplementation during pregnancy had higher cognitive performance, visual acuity, and brain growth (Campoy *et al*., 2012; Larqué *et al*., 2006, 2012). Remarkably, the impact of n-3 PUFA on fetal brain health is higher when n-3 PUFA is initiated by pregnancy week 20 (Tahaei *et al*., 2022).

DHA accretion during early life is crucial as studies have shown that poor DHA accretion during neurodevelopmental stages increases the risk of neurological disorders, including AD (Lauritzen et al., 2016). Once these conditions have set in, the impact of DHA supplementation and accretion is limited. In individuals with poor brain DHA accretion during early life requires a high dose of DHA (1000 mg/day or more) supplementation to prevent/alleviate the impact of defective neurodevelopment (Stonehouse et al., 2013).

Our laboratory has shown previously that maternal diets high in fish oil-based n-3 PUFA improve the accretion of total n-3 PUFA, especially DHA with concomitant reduction in total n-6 PUFA and LA in mouse fetal brain during gestation (Akerele & Cheema, 2020). However, the entire fetal brain lipid profile was not studied to understand the lipid classes which the DHA are associated with and the specific fatty acyl species that are impacted by diets during gestation. Our laboratory also showed that the accretion of DHA in fetal brain of fetuses prenatally fed high n-3 PUFA diet correlated with increased expression of *BDNF* and its receptors (Akerele & Cheema, 2020). BDNF is crucial in neurogenesis, neuronal plasticity, memory and cognition (Miranda *et al*., 2019), and in protecting brain cells against assaults and degeneration (Nagahara *et al*., 2009). This implies that the n-3 PUFA improves neurogenesis, synaptogenesis and synaptic function

through upregulation of BDNF signaling (Cao et al., 2009). Other mechanisms through which n-3 PUFA (typically DHA) promote brain growth, in addition to increasing BDNF signaling, includes upregulation of transcription factors involved in neuronal differentiation and maturation such as retinoid X receptors, neurogenin, neuronal differentiation 1, and Achaete-scute homolog 1 (Calderon & Kim, 2004; Beltz *et al*., 2007; Katakura *et al*., 2009; Cao *et al*., 2009a; Crupi *et al*., 2013; Dyall, 2011, 2014). Hence, accretion of DHA in the developing brain (especially during prenatal life) is crucial because some neurodevelopmental defects associated with inadequate supply of DHA in the brain during early development may not be fully-remedied by postnatal dietary n-3 PUFA intake (McNamara & Carlson, 2006). Therefore, consumption of diets enriched in n-3 PUFA during pregnancy may promote brain growth and prevent neurodegenerative diseases.

The essential n-3 PUFA, ALA and essential n-6 PUFA, LA cannot be synthesized in humans and hence must be derived from diet. The major sources of ALA are flaxseed, soybean, rapeseed and some green vegetables (Burdge & Calder, 2006), while LA is mainly found in safflower oil, sunflower oil, meats, and eggs (Whelan & Fritsche, 2013). When consumed, ALA and LA can be converted to their long-chain PUFA (LC-PUFA) counterparts such as EPA, DPA and DHA from ALA, and ARA and adrenic acid (22:4 n-6, ADA) from LA in the body (Figure **1.2**).

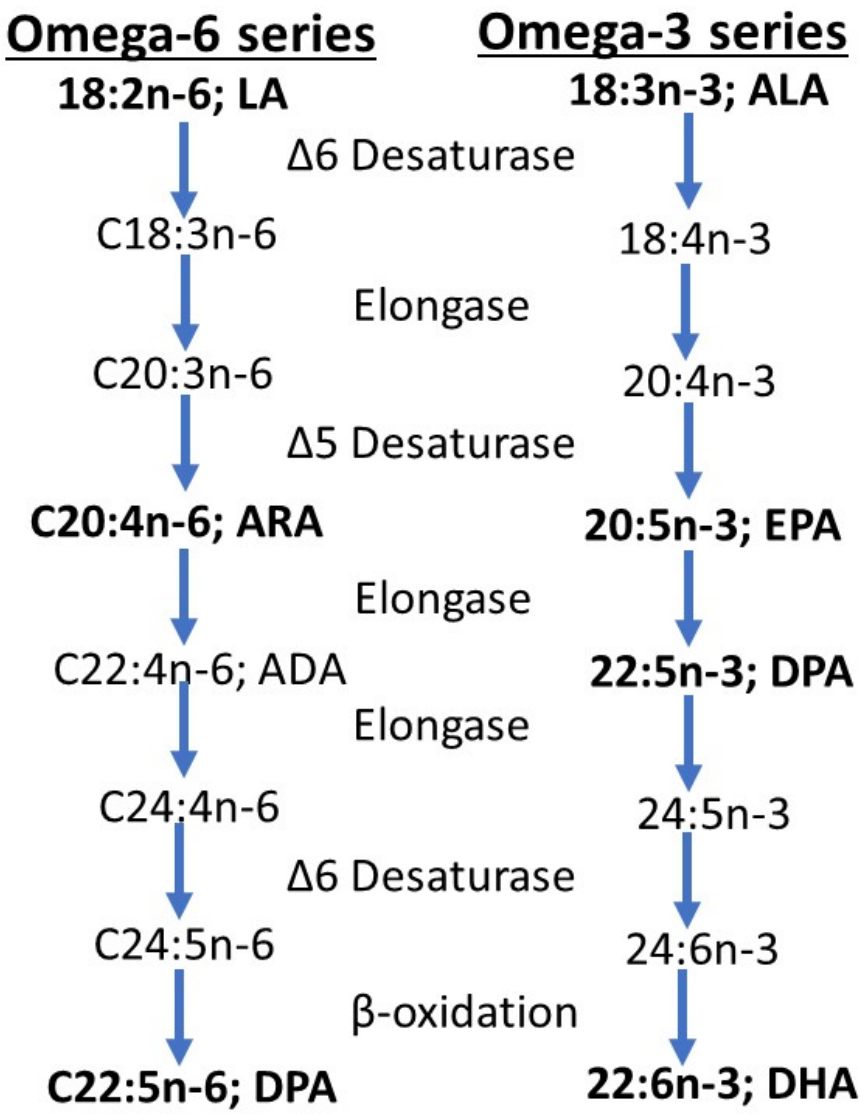

Figure 1.2: Bioconversion of essential fatty acids to their long-chain and very long-chain polyunsaturated fatty acid derivatives. *Modified from (Akerele & Cheema, 2016). Journal of Nutrition & Intermediary Metabolism, 5; 23–33. C18:2n-6 = linoleic acid (LA), C18:3n-6 = γ-linolenic acid (GLA), C20:3n-6 = dihomo-γ-linolenic acid (DGLA), C20:4n-6 = arachidonic acid (ARA), C22:4n-6 = adrenic acid (ADA), C22:5n-6 = docosapentaenoic acid (DPA), C18:3 n-3 = α-linolenic acid (ALA), C18:4n-3 = stearidonic acid (SA), C20:4n-3 = eicosatetraenoic acid (ETA), C20:5n-3 = eicosapentaenoic acid (EPA), C22:5n-3 = docosapentaenoic acid (DPA), C22:6n-3 = docosahexaenoic acid (DHA).*

Although the endogenous conversion of essential fatty acids is possible, as shown in Figure **1.2**, the efficiency is low (Swanson *et al*., 2012). The conversion also depends on age and sex and is influenced by other constituents of diets. For example, using stable isotope-labeled ALA, a study showed that the conversion rate of ALA to EPA, DPA, and DHA after 48 hours in adult men is 2.8%, 1.2%, and 0.04%, respectively (Burdge *et al*., 2003), whereas the conversion rate of ALA to EPA, DPA, and DHA in adult women of reproductive age were 21%, 6%, and 9%, respectively (Burdge & Wootton, 2002). During pregnancy, the conversion of ALA to DHA has been speculated to double due to metabolic adaptation associated with increased estrogen (Williams & Burdge, 2006), hence, confirming the importance of DHA during gestation. Our laboratory reported non-detectable levels of ALA in erythrocytes of dams on a low n-3 PUFA diet (2.72% ALA) using gas chromatography technique (Akerele & Cheema, 2017), suggesting a total conversion of all the ALA to longer-chain n-3 PUFA. However, the conversion rate of ALA to DHA in human does not meet the DHA requirement during fetal brain development, highlighting the importance of consuming preformed EPA and DHA in the form of fatty fish, fish oil, or n-3 PUFA supplement (Jia *et al*., 2015; Best *et al*., 2022).

Brain PUFA composition can be improved through diet; our laboratory previously showed that the consumption of n-3 PUFA-enriched diet containing preformed DHA at both prenatal and postnatal stages promoted accretion of brain DHA and total n-3 PUFA levels, which upregulated BDNF signaling to promote brain health (Balogun & Cheema, 2014; Feltham *et al*., 2019; Akerele & Cheema, 2020). In these studies, the specific lipid classes with which the DHA in the fetal brain were associated were not studied. Hence, it is crucial to understand the specific lipids and the associated fatty acyl species influenced by diet which could provide more information with diagnostic implications on brain health.

Maternal diets containing a n-6/n-3 PUFA ratio of 4:1 (including preformed DHA) during gestation and lactation were shown to improve the accretion of total n-3 PUFA and DHA in all parts of the mouse offspring's brain, including the cortex, brainstem, cerebellum and subcortical regions, at PND30 and PND60, compared to diet containing a n-6/n-3 PUFA ratio of 303:1 which showed very poor accretion of total n-3 PUFA and DHA in the mouse offspring's brain (Janssen et al., 2015). The accretion of DHA in fetal brain of the offspring is associated with improved behavior, such as motor and cognitive functions and memory (Janssen et al., 2015). Adequate accretion of DHA in the brain due to n-3 PUFA-enriched diet during gestation and lactation is sustained through adulthood to improve brain development and function. Our laboratory previously showed that maternal diets containing a n-6/n-3 PUFA ratio of 5:1 (including preformed DHA) for two weeks before and during gestation promoted accretion of total n-3 PUFA and DHA (Akerele & Cheema, 2020). The high n-3 PUFA diet further upregulated neurotrophin signaling with depletion in total n-6 PUFA in the fetal brain, compared to maternal diets containing ratio of 40:1 which showed lower effect on DHA accretion and neurotrophin signaling and higher fetal brain total n-6 PUFA level (Akerele & Cheema, 2020). Maternal diets containing a n-6/n-3 PUFA ratio of 6:1 (including preformed DHA) during gestation until PND7 improved neurogenesis and brain growth whereas diet containing n-6/n-3 PUFA ratio of 16:1 elicited neuronal apoptosis (Fan *et al*., 2015). Reducing the n-6/n-3 ratio in maternal diets during gestation and lactation was reported to improve human offspring brain development and neurobehavior in infancy (Bernard *et al*., 2013; Kim *et al*., 2017). Furthermore, recent meta-analyses of randomized controlled trials concluded that n-3 PUFA supplementation (1000 mg DHA + EPA combined) twice weekly during gestation is beneficial by reducing the risks of preeclampsia, preterm birth and prenatal fetal death, and increasing fetal birth weight (Abdelrahman *et al*., 2023). These findings agree with the

hypothesis from our laboratory that a balance between n-3 PUFA and n-6 PUFA intake during pregnancy and lactation is critical for fetal/offspring health (Akerele & Cheema, 2016).

1.4 Brain lipids and neuronal membranes

Lipids are major components of cellular membranes, including neuronal membranes. Lipids play a barrier function in the membrane by forming a bilayer in aqueous environment to separate the internal and external environment of cells. Membrane GP are crucial in cellular trafficking, signaling, proliferation, differentiation, migration and death, and regulation of membrane protein (Morita & Ikeda, 2022). For example, PS and PG play roles in activating protein kinase C (PKC) (Murray *et al*., 1998; Bittova *et al*., 2001). PKC is a membrane protein involved in several cellular processes such as induction of LTP through the AMPA receptor (Son *et al*., 1996; Sweatt *et al*., 1998).

Membrane SP, typically Cer is involved in formation of microdomains that are involved in some cellular functions. For example, Cer-enriched membrane domains promote the clustering of receptors involved in cellular signaling and amplify signal transduction (Zhang *et al*., 2009), including activation of phosphoinositide 3-kinase (PI3K)/protein kinase B (AKT) signaling (Ladjohounlou *et al*., 2020). PI3K/AKT signaling pathways promote neurogenesis and neuronal survival (Chen *et al*., 2017), and LTP, synaptic plasticity and cognition (Horwood *et al*., 2006; Sui *et al*., 2008; Bruel-Jungerman *et al*., 2009).

Cholesterol is a major component of plasma membrane and regulates the movement of lipid tails to increase orderliness and rigidification of membranes whereas membrane fluidity is reduced (Kutchai *et al*., 1983; Arora *et al*., 2004). Therefore, membranes with higher cholesterol content are more rigid and ordered than membranes with low cholesterol content. Cholesterol also

modulates the activities of membrane proteins, including ion channels and receptors associated with signaling transduction and induces domain formation (Wang *et al*., 2005; Sheng *et al*., 2012). At low concentration, cholesterol participates in transbilayer dimerization through van der Waals interactions between the bulky ring to form microdomains (Mukherjee & Chattopadhyay, 1996; Rukmini *et al*., 2001). The hydroxyl functional group of cholesterol interacts with GP through the carbonyl functional group and the bulky ring with hydrocarbon chain of the fatty acyl molecular species of GP (Xu & London, 2000). Cholesterol also interacts with SP through the *N*-linked acyl chain to form lipid domains (Pandit *et al*., 2004; Ramstedt & Slotte, 2006; Bakht *et al*., 2007). The interaction between cholesterol and SP-like SM is more pronounced than GP (Leftin *et al*., 2014). As cholesterol interacts more with saturated fatty acid-containing GP compared with PUFA-rich GP (Engberg *et al*., 2016), membranes with higher PUFA-containing GP are less rigid and have higher fluidity (characterized by higher area per lipid, APL). APL is a crucial membrane dynamic parameter determined by calculating local Voronoi cells and estimating APL from the area of each cell (Buchoux, 2017) . APL is an index of membrane fluidity; hence, the higher the APL, the higher the membrane fluidity. Membranes with high PUFA content, especially DHA are reported to have higher APL (Ollila *et al*., 2007).

Lipid flip-flop between membrane leaflets is an important membrane dynamic parameter that represents the movement of lipids from one membrane leaflet to another (Ueda *et al*., 2014). Membrane lipids such as cholesterol, DG and Cer have been shown to flip between neuronal membrane bilayers with cholesterol having a higher flip-flop rate, followed by DG and Cer having very small flip-flop rates (Ingólfsson *et al*., 2017). Oxidation of cholesterol has been shown to decrease the cholesterol flip-flop rate between membrane bilayer by over 20-fold (Wilson, *et al*., 2021); however, CE flip-flop rates in neuronal membrane have not been studied previously. As

CE is found in the brain and membrane, it would be interesting to evaluate if CE flip between membrane bilayer like free cholesterol and to compare the flip-flop rate with free cholesterol.

Membrane thickness, the distance between the lipid head groups of membrane bilayers is another membrane parameter. Membrane thickness modulates the organization and interaction of membrane proteins and transmembrane permeability to small molecules (Paula *et al*., 1996; Mathai *et al*., 2008; Shinoda, 2016); thicker membranes have lower permeability to molecules compared with thinner membranes. As already described, membrane physiochemical properties are influenced by its lipid composition; hence, change in membrane lipid composition alters its physicochemical properties and behavior. For example, membranes containing a higher degree of unsaturated lipids, especially PUFA-enriched GP have been reported to have higher APL, compared with membranes with lower unsaturated lipid contents (Wilson *et al*., 2020). Oxidation of phospholipids and the presence of cholesterol was shown to increase membrane bilayer thickness and lipid orderliness but decrease APL (Schumann-gillett & Mara, 2019). In addition, oxidation of cholesterol (to 27-OH-cholesterol) in membranes was shown computationally to disturb the integrity of the membrane leading to increased permeability of water and hydrophilic small molecules, whereas oxidation of cholesterol to 7β-OH-cholesterol did not affect the permeability (Kulig *et al*., 2020).

DHA is a major component of neuronal membrane phospholipids, especially ethanolamine-based GP. It promotes membrane fluidity and membrane function (Mason et al., 2016). In neurodevelopmental disorders such as schizophrenia, lower membrane fluidity and higher membrane thickness have been reported (Horrobin *et al*., 1994; Horrobin, 1998; Mason *et al*., 2016). This altered membrane dynamic corresponds to low brain DHA levels reported in schizophrenia (McNamara *et al*., 2007; McEvoy *et al*., 2013; Li *et al*., 2022). Our laboratory

showed that high n-3 PUFA diet increased the accretion of DHA in fetal brain during gestation (Akerele & Cheema, 2020); however, the lipid classes and fatty acyl species that are crucial in brain growth and function, and neuronal membrane structure and function, were not studied. Proper understanding of the fetal brain lipidomic profile during gestation and impact of maternal dietary n-3 PUFA intake will clarify if accretion of specific lipids during gestation will impact fetal neuronal membrane dynamics.

The effects of changes in lipid composition and other factors on membrane structure and functions are assessed computationally by determining the dynamic parameters. Hence, lipidomics data can be used to construct membranes which are computationally studied to predict the behavior of the membrane. Adult brain lipidomic data have been applied for studying idealized complex neuronal membrane computationally; hence, fetal brain lipidomics data can be utilized to study how maternal dietary status influences fetal brain lipidomic profile, and how the impact on fetal brain lipidomic profiles affect neuronal membrane structure and behavior during gestation.

1.4.1 Molecular dynamic simulation for studying membrane properties

The behavior of membrane composed of different lipid species, and how changes to the variety and concentration of lipid species influence the physicochemical properties of membranes, has been computationally studied. For example, computational studies have used membrane lipids [such as palmitoyl-oleoylphosphatidylcholine (POPC), dioleoylphosphatidylcholine (DOPC), or mix of these and *N*-palmitoyl-sphingomyelin (PSM), and cholesterol] to generate artificial membranes for studying the impact of ratio of POPC, DOPC, SM and cholesterol and head group size on membrane properties such as permeability and thickness (Björkbom *et al*., 2010; Orsi & Essex, 2012; Reddy *et al*., 2012; Frallicciardi *et al*., 2022). Although these strategies have

successfully provided insights on the impact of internal (such as composition and oxidative status of the lipids) and external factors (such as temperature) on membrane behavior, the influence of interaction of diverse lipids classes as seen in a typical plasma membrane may not be entirely accounted for using simple membrane models.

Recent computational studies are adapting lipidomic profiles of whole cells and tissues to idealize the complexity of lipids in plasma membranes. This involves using lipidomics data to computationally study membrane dynamics at molecular level by molecular dynamics (MD) simulation (Ingólfsson *et al*., 2017; Wilson *et al*., 2020; Wilson *et al*., 2021). Ingólfsson *et al*. (2017) showed that cholesterol concentration and degree of tail saturation also have huge impact on model neuronal membrane structure and behavior, including APL and membrane thickness. As membrane lipid compositions are derived from whole cells or tissues, it is not certain if the types and molar ratios of the lipids used in constructing membrane for dynamic simulation are exactly the same as those found in the plasma membranes. However, utilizing whole tissue lipidomics data for MD simulation of membrane lipids helps to predict how changes in class, oxidative state and concentration of membrane lipids influence membrane properties and behaviors. As mentioned above, Ingólfsson *et al*. (2017) utilized adult brain lipidomics data to computationally construct a model of human neuronal plasma membrane for MD simulation; this study provided features of idealized complex human neuronal plasma membrane and compared them with the averaged plasma membrane. Another computational study, utilized a similar complex neuronal membrane model to show that site of cholesterol oxidation influences domain formation of adult neuronal plasma membrane (Wilson *et al*., 2021). However, fetal neuronal membrane has not been computationally studied. Understanding the fetal neuronal membrane dynamics will predict if fetal

neuronal membranes differ from adult neuronal membranes, and will open the window for further understanding of the link between fetal neuronal membrane and brain diseases.

Overall, brain lipidomic profiles during postnatal life have been well studied but little is known about changes in brain lipidomic profiles during the gestation. Research from our laboratory previously demonstrated that maternal diets high in n-3 PUFA promoted the accretion of DHA and total n-3 PUFA in fetal brain during gestation (Akerele & Cheema, 2020), but the effect of maternal dietary n-3 PUFA intake on the entire fetal brain lipidome during gestation has not been studied. As inadequate levels of brain lipids influence brain development and function, understanding changes in fetal brain lipidomic profiles and the effect of maternal dietary n-3 PUFA intake during gestation may promote further research to elucidate the role of each lipid species in the fetal brain on brain structure and function during postnatal life. The lipid composition of membranes influences membrane properties and function. Lipidomic data are being utilized to construct membranes for molecular dynamic simulations to study how the composition of membranes, oxidative state and site of oxidation of lipid components of the membrane influence membrane behaviour (Ingólfsson *et al*., 2017; Wilson *et al*., 2021). While such work was computationally studied with adult neuronal membranes (Ingólfsson *et al*., 2017), no one has computationally studied the fetal neuronal membrane. It would be interesting to computationally study fetal neuronal membranes by predicting how the impact of maternal dietary n-3 PUFA intake during gestation on the fetal brain lipidome will influence fetal neuronal membrane dynamics.

1.5 Mouse as an animal model

Despite differences in size and complexity between human and mouse brains (Wong *et al*., 2023), there are substantial genetic and physio-anatomical similarities (Nakajima *et al*., 2021;

Beauchamp *et al*., 2022) and susceptibilities to metabolic and brain disorders (Paigen *et al*., 1990; Yang *et al*., 1997; Harper, 2010). C57BL/6 mice were used in the current research because it is a strain widely adopted for investigating the influence of diets on neurodevelopment and brain function across lifespan (Janssen *et al*., 2015; Fernandes *et al*., 2021; Wang *et al*., 2021; Bordeleau *et al*., 2022; Westmark *et al*., 2022; Wu *et al*., 2023). It is also an ideal model for studying changes in brain development and function with age (Shoji *et al*., 2016), and it is the strain from which many models of metabolic and brain disorders were generated (Paigen *et al*., 1990; The Dutch-Belgian Fragile X Consorthium *et al*., 1994; Fontaine & Davis, 2016). Hence, the adoption of C57BL/6 mice for this study opens the window for extending our investigation on transgenic mice models of neurodevelopmental defects.

1.6 Rationale for the study

The impact of dietary n-3 PUFA intake during postnatal life on brain lipid metabolism has been well investigated (Petursdottir *et al*., 2008; Balogun & Cheema, 2014); however, little is known about the impact of n-3 PUFA intake during gestation on fetal brain lipidomic profiles. Our laboratory has previously analyzed the effect of maternal diets differing in n-3 PUFA content on the fetal brain fatty acid profiles to show that maternal diets high in n-3 PUFA increased the accretion of total n-3 PUFA and DHA in the fetal brain while LA and total n-6 PUFA decreased in high n-3 PUFA group compared with low n-3 PUFA intake (Akerele & Cheema, 2020). In this previous study, the effect of maternal dietary n-3 PUFA intake on the entire fetal lipidomic profile was not studied. As lipid makes up over half of the brain and several neurodevelopmental defects manifest in the postnatal stage when irreparable alterations have occurred in the brain, understanding the brain lipidomic profile during gestation, a time of rapid brain development, is crucial. The physicochemical properties of a membrane are dependent on its lipid composition as

lipids are major components of the membrane. Hence, it is worthwhile to predict how changes in the fetal lipidomic profile resulting from different maternal dietary n-3 PUFA intake during gestation impact fetal neuronal membrane dynamics.

1.6.1 Overall hypothesis

The overall hypothesis of this thesis is that maternal diets high in n-3 PUFA during gestation will promote the accretion of specific lipids and fatty acids in the fetal brain and influence fetal neuronal membrane dynamics.

1.6.2 Specific aims

Aim 1: To investigate the effects of a maternal diet high (9%, n-6/n-3 PUFA ratio 5:1) or low (1%, n-6/n-3 PUFA ratio 40:1) in n-3 PUFA during gestation on the accretion of specific lipids and fatty acyl species in the fetal brain at gestation days 12.5 and 18.5.

Hypothesis: It was hypothesized that maternal diets high in n-3 PUFA during gestation would promote the accretion of specific lipids and fatty acid species crucial for brain development and function.

Aim 2: To predict whether maternal diets high (9%, n-6/n-3 PUFA ratio 5:1) or low (1%, n-6/n-3 PUFA ratio 40:1) in n-3 PUFA during gestation impact fetal neuronal membrane dynamics.

Hypothesis: It is hypothesized that maternal diets containing high n-3 PUFA during gestation will increase area per lipid and reduce membrane thickness in fetal neuronal membrane dynamics.

CHAPTER TWO

Materials and Methods

Diet preparation, animal feeding, and fetal brain tissue collection were done by Dr. Cheema and her former PhD student, Anthony Akerele.

2.1 Experimental diet

The experimental diets used in this study were high-fat diets prepared by adding known amounts of Menhaden fish oil (Sigma-Aldrich, St. Louis, MO, USA; Cat. No. 8002-50-4 and product number - F8020); safflower oil, extra-virgin olive oil, and lard that were procured from domestic grocery stores with same lot numbers. These oils providing n-3 PUFA, n-6 PUFA, MUFA, and SFA, were added to a custom ordered fat-free semi-synthetic diet (MP Biomedicals, Santa Ana, CA, USA; Cat No. 999999 and lot number - X2448) to control for fat content of final diets at 20% w/w. The composition of the semi-synthetic base diet as per the provider is presented in Appendix **1**. To make one kilogram of the experimental diets, each of the oils were mixed in specific ratios to make a 200 g oil mixture (20% total fat), as shown in Appendix **2**. The resulting total diets contained either 9% n-3 PUFA with n-6/n-3 PUFA ratio of 5:1 (high n-3 PUFA diet) or 1% n-3 PUFA with n-6/n-3 PUFA ratio of 40:1 (low n-3 PUFA diet). In the two diets, the total amounts of saturated, monosaturated, and polyunsaturated fatty acids were kept constant while the amount of total n-6 and n-3 PUFA varied. The 5:1 n-6/n-3 PUFA ratio diet has been shown in previous studies in our laboratory to promote physiological health during pregnancy and fetal development (Akerele *et al*., 2021; Akerele & Cheema, 2018, 2020) and is the recommended diet with adequate n-3 PUFA, while the 40:1 n-6/n-3 PUFA ratio diet is very low in n-3 PUFA and is characteristic of vegetarian diets in some urban communities in India (Mani & Kurpad, 2016; Simopoulos, 2016). The 20% fat diet represents approximately 40% of total calories from fat, which is higher than the quantity (20-35% of total calories) recommended by the Food and

Agriculture Organization (2010). The diets were stored in black bags to protect from light at -20°C and under nitrogen to prevent oxidation of their fatty acids.

2.2 Experimental design

Prior to animal procurement and handling, the experimental protocols received the approval of the Memorial University's Animal Care Committee (approval number - 22-02-SC). All animal experiments were executed following the Canadian Council on Animal Care guidelines for the use of animals for research (CCAC, 2022). Female C57BL/6 mice (seven weeks old) were purchased from Charles Rivers Laboratories (MA, USA) and were separately caged to habituate with the laboratory environment (temperature of 21 ± 1°C, humidity of 35 ± 5%, and 12 h light/12 h dark period cycle) for seven days. The mice had unrestricted access to standard rodent chow purchased from Prolab RMH 3000 (MI nutrition, USA) and drinking water. After the seven-day period, the females were divided into two groups and were fed either low or high n-3 PUFA diets from two weeks prior to mating and throughout gestation (Figure 2.1). Gestation was established when a vaginal plug was observed in the morning of the day after an overnight mating, which represents gestation day (GD) 0.5. On either GD12.5 or GD18.5, mice from each diet group were euthanized and fetal brains were collected for fetal brain total lipid extraction. Fetal brains from the same dam were pooled together to represent n = 1.

2.3 Extraction of fetal brain total lipids and lipidomic analysis

The fetal brain total lipids were extracted and lipidomic analysis was performed at the Lipidomics Facilities by Dr. Raymond Thomas, Grenfell Campus, Memorial University of Newfoundland.

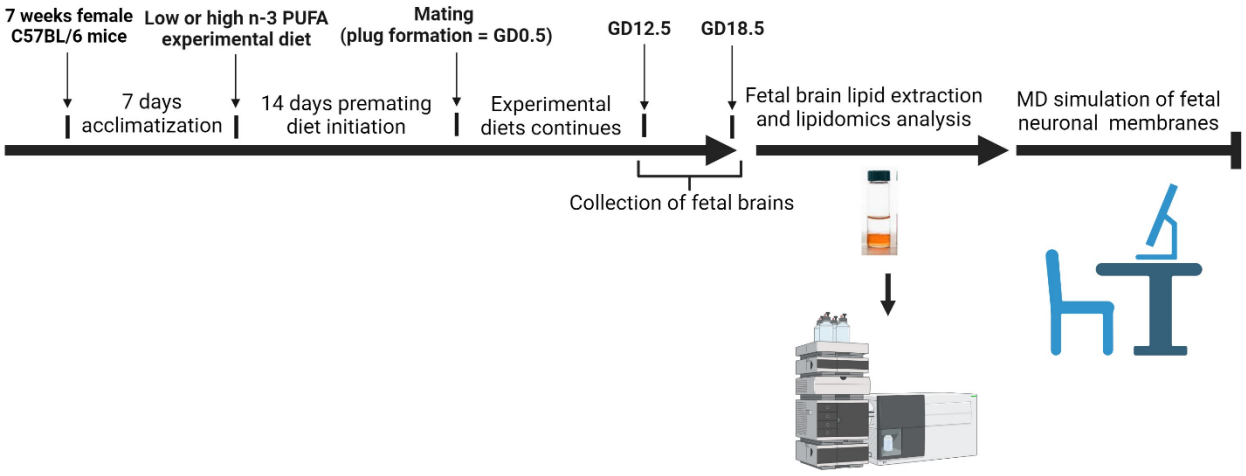

Figure 2.1: Experimental design of the study. *Female C57BL/6 mice used in this study were fed either of the two experimental diets differing only in the amount of n-3 PUFA described as "High" or "Low" n-3 PUFA diets for two weeks prior to breeding. The High and Low n-3 PUFA describes n-6/n-3 PUFA of 5:1 and n-6/n-3 PUFA of 40:1, respectively. After successful mating (determined by plug formation after male and female pairing and confirmed by a progressive increase in body weight), the females were maintained on the assigned diet throughout the experimental period. n-3 PUFA = omega-3 polyunsaturated fatty acid.*

2.3.1 Lipid extraction

The fetal brain tissues (~80 mg) were cryo-homogenized (Potter-Elvehjem homogenizer, USA) with 2 mL of 0.1% ammonium acetate in water. Ten microliters of SPLASH® internal lipid standard mix (Avanti Polar Lipids, Birmingham; Catalogue number - 330710X-1EA) were added to 500 µL of each of the tissue homogenate in a glass tube. Two microliters of methyl *tert*-butyl ether (MTBE)/methanol/water (10:3:2.5, v/v/v, i.e 2 mL MTBE, 0.6 mL methanol, and 0.5 mL deionized water) were added to the glass tube, caped and vortexed. The tube was centrifuged for 15 min at 1200 xg (Cryomill, Retsch, Germany) to separate the contents into two layers. The organic layer containing the extracted lipids (upper layer) was transferred into a new glass Teflon-lined cap tube and stored at -20°C for lipidomic analysis (Matyash *et al*., 2008).

2.3.2 Lipidomic analysis

Lipidomics platforms described previously (Pham *et al*., 2019) using ultra-high-performance liquid chromatography (UHPLC) coupled with high-resolution mass spectrometry (HRMS) were adopted for this study. Both hydrophilic interaction (HILIC) and C30 reverse phase (C30RP) columns were used: HILIC chromatography was the best for resolving the polar lipid classes in the negative ion mode with ammonium acetate buffer (Anesi & Guella, 2015).

For the HILIC chromatography, UHPLC was managed by Chromeleon software (Dionex UltiMate 3000 UHPLC, ThermoScientifc, MO, USA). An Acquity BEH HILIC 1.7 µm particle Size, 2.1 mm x 150 mm (Waters, MA, USA) column was used. The mobile phase consisted of solvents A (pure acetonitrile) and solvent B (10 mM ammonium acetate in HPLC-grade water). The mobile phase gradient was set as follows: initially set as 97% solvent A and 3% solvent B for 2 min, then increased to 10% solvent B over 23 min, 10-20% solvent B for 10 min, and maintained

as 85% solvent A and 20% solvent B for 5 min. The column was re-equilibrated with only solvent A for 10 min before the injection of every new sample.

For the C30RP chromatography, the mobile phase system consisted of solvent A (acetonitrile:water 60:40 v/v) and solvent B (iso-propanol:acetonitrile:water 90:10:1 v/v/v) both containing 10 mM ammonium formate and 0.1% formic acid. Solvent gradient and run conditions were: 30% of solvent B for 3 min and increasing to 43% within a 5-min interval. This was followed by increasing solvent B increased to 50% for 1 min, followed by 90% for 9 min, and 99% for 4 min. Solvent A set at 70% for 5 min was used to reset the column prior to every fresh sample injection.

The high-resolution tandem mass spectrometry was achieved using a Q-Exactive™ Plus Hybrid Quadrupole-Orbitrap™ mass spectrometer managed by X-Calibur version 4.0 software (ThermoScientifc, MO, USA). The system conditions for the mass spectrometer were set to a mass range (200–2000 *m/z*), resolution (70,000 *m/z*), sheath gas (45 arbitrary units), auxiliary gas (15 arbitrary units), ion spray voltage (3.2 kV), capillary temperature (300°C), S-lens RF (30V), collision energy (35 eV), isolation window (1 *m/z*), and automatic gain control target ($1x10^5$ arbitrary units). The platforms were first calibrated using positive and negative ion calibration solutions (ThermoScientifc, MO, USA), and the working conditions optimized using non-natural standard lipids (Avanti Polar Lipids, Alabama, USA) in both negative and positive ion modes. Fetal brain lipid extracts (10 µL) were injected into the UHPLC-HRMS with column temperature and a flow rate set at 30°C and 0.2 mL/min, respectively. Details of how the lipidomic data were analyzed are provided in the "lipidomics data and statistical analysis" section.

2.3.3 Pathway analysis

The fetal brain lipid species were visualized in a heatmap to observe the enrichment and depletion of species by maternal diets during gestation. The number of lipid metabolic pathways and hits influenced by maternal diets during gestation were predicted using MetaboAnalyst software 5.0 (https://new.metaboanalyst.ca/MetaboAnalyst/) (Dhariwal et al., 2017). Compound (lipid species) matching were done using human metabolic databases (HMDB), hypergeometric test was used as the enrichment method, and *Mus musculus* small molecule pathway database pathway library were used. The cut off for statistical significance was set at $p \leq 0.05$.

2.4 Formulation of fetal neuronal membrane model, molecular dynamics simulation and analysis of membrane dynamics

Previously published MD simulation protocols (Ingólfsson *et al*., 2017; Wilson *et al*., 2020; Wilson *et al*., 2021) were followed to computationally construct molecular models of neuronal membranes using the lipidomics data (Appendix **4**). The chemical composition of lipid species head groups and linkers used to compose the fetal neuronal membrane are shown in Appendix **5**. A custom-version of the Insane Package from Wassenaar (Wassenaar *et al*., 2015) was used to construct the fetal neuronal membrane corresponding to each of the four experimental groups. All lipid species found in the fetal brain with a molar ratio ≥ 0.001 were included (and those not detected such as free cholesterol were excluded). Lipid species with related tails, as shown in Appendix **4,** were combined, and each system was composed of ~4007 lipids and was solvated using 82581-83305 polarizable MARTINI water molecules (Yesylevskyy *et al*., 2010) and 150 mM sodium chloride (~972 sodium and ~855 chloride ions) (Appendix **6**). The initial positions of the lipids in the bilayer were randomly placed, and each replicate had a different random

placement of lipids. All bilayers were oriented in the x−y plane of a solvated rectangular box with dimensions of 35 nm × 35 nm × 12 nm. Periodic boundary conditions were applied in all directions. Each membrane system was solvated using the polarizable MARTINI water model (Yesylevskyy *et al*., 2010), and was energy-minimized using the steepest descent algorithm and equilibrated over three 5 ns simulations with increasing time step (10 fs, 20 fs and 25 fs) at constant temperature and pressure.

All simulations were conducted using the GROMACS 2022.4 molecular dynamics engine (Abraham *et al*., 2015; Berendsen *et al*., 1995; De Jong *et al*., 2016; Hess *et al*., 2008; Kutzner *et al*., 2022; Lindahl *et al*., 2001; Páll *et al*., 2015; Pronk *et al*., 2013; Van Der Spoel *et al*., 2005) under periodic boundary conditions, adopting the MARTINI 2.2P coarse-grained force field parameters (De Jong *et al*., 2013). Each membrane underwent 10 μs production simulation at temperature of 310 K, [maintained using the Bussi thermostat (Bussi *et al*., 2007) with a coupling constant of 1.0 ps] and pressure of 1.0 bar [maintained using a semi-isotropic Parrinello–Rahman barostat (Parrinello & Rahman, 1980, 1981) with a compressibility of 3×10^{-4} bar^{-1} and a coupling constant of 12 ps], using a time step of 25 fs in triplicates.

2.4.1 Analysis of effects of gestation and maternal dietary n-3 PUFA status on fetal neuronal membrane parameters

Parameters indicative of membrane physicochemical properties were determined. The density of the four membranes representing four experimental groups was determined using GROMACS to confirm that the fetal neuronal membrane model constructed (Appendix **7**) agrees with typical neuronal membrane (Ingólfsson *et al*., 2017). The lateral self-diffusibility of each lipid class was calculated using GROMACS and was averaged to obtain the average diffusion rate.

Membrane thickness was determined using FATSLiM software (Buchoux, 2017), while APL and CE flip-flop rate were determined using the LiPyphilic python package (Smith & Lorenz, 2021). The formation of lipid domains in membrane – assembling of lipid species and lipid classes with each other was determined by calculating contact fraction as previously reported (Koldsø *et al*., 2014; Wilson *et al*., 2020) using the LiPyphilic python package (Smith & Lorenz, 2021). The relative collocation (enrichment/depletion) of lipid species *B* around lipid species *A* was calculated by comparing the local molar ratio within the 1.2 nm cut-off to the global molar ratio of species *B*.

$$C_{AB} = \frac{N_{AB}}{[N_B]} \qquad \text{Equation 1}$$

Where; C is the contact fraction, N_{AB} = number of lipid species *B* around species *A*, $[N_B]$ = mean number of species *B* around any species. Notably, contact fractions were evaluated over the entire membrane rather than by each leaflet and the values were averaged over all lipid species within the lipid class. This was done for the GP and SP headgroup beads. Lipid domains with contact fractions < 0.8 are depleted, lipid domains with contact fraction ≥ 1.2 are enriched, while lipid domains with contact fraction ≥ 0.8 and < 1.2 are neither enriched nor depleted.

Visualization of simulations were done using visual molecular dynamics (VMD) software (Humphrey *et al*., 1996). Membrane parameters were assessed over the entire membrane and not by membrane leaflets.

2.5 Lipidomics data and statistical analysis

2.5.1 Lipidomics data analysis: The raw UHPLC/MS2 data of the fetal brain lipid profile was first subjected to multivariate analyses in XLSTAT 2022 (Addinsoft Software, New York). Partial least-squares discriminant analysis (PLS-DA) was used to rank the effects of gestation and maternal n-

3 PUFA status on the 127 lipid species identified in fetal brain based on lipid group/class of interest. In each lipid group or class considered, lipid species whose variable importance in the projection (VIP) scores were ≥ 1.0 were considered substantially varied by diet and/or gestation, while lipid species with moderate to low variability (VIP scores < 1.0) were not included in further analysis. Lipid species with VIP ≥ 1.0 were subjected to principal component analysis (PCA), another multivariate analysis tool to visualize the distribution of species with related variability.

2.5.2 Statistical analysis: The main effects and the interaction of gestation stage and maternal dietary n-3 PUFA status on lipid species clustered in the same quadrant of PCA biplot were determined using two-way ANOVA and Bonferroni multiple comparisons in GraphPad Prism, version 9.3.1 (GraphPad Software, San Diego). The lipidomics data were presented as mean ± standard deviation (SD), with sample size per group (n) as 8 dams (fetal brains from the same dam were pooled as n =1). Data for each lipid species [fatty acyl molecular species of each lipid] were expressed as nmol% of each lipid group or class; $p < 0.05$ was considered significant.

The raw data of molecular dynamics simulations of the fetal neuronal membrane were subjected to 2-way ANOVA to understand the main effects and the interaction of gestation stage and maternal dietary n-3 PUFA status on molecular dynamics parameters using GraphPad Prism, version 9.3.1 (GraphPad Software, San Diego). The results were presented as mean ± standard error of the mean (SEM) in triplicate runs for each membrane.

CHAPTER THREE

Results

3.1 Fetal brain lipidomic profile

The HILIC-MS base peak chromatogram of a fetal brain lipid extract from a representative of high n-3 PUFA at GD18.5 group showing the separation of lipids based on their polarity and the headgroups is shown in Figure **3.1 (A)**. The major brain lipid classes detected in negative ion mode include Cer, non-esterified fatty acids (NEFA, C16:0 or FA 16:0), PG, PI, PE, PS, PC, and SM. An example of HILIC-MS^2 spectra with the structures of precursor ions is presented in Figure **3.1 (B-E)** showing the typical fragmentation of their headgroup class. Cer and NEFA belong to neutral lipids category which are not retained in HILIC column and as a result, elute first in the HILIC-MS chromatogram. Figure **3.1 (B)** shows the fragmentation of major Cer molecular species seen in Figure **3.1 (A)** at *m/z* 624.56 $[M+CH_3COO]^-$. The two main fragments at *m/z* 308.30 and 237.22 resulted from the most energy favourable pathway of cleaving C-C bond in conjunction with the double bond in the sphingosine backbone, giving the identification of Cer(d18:1_18:0) molecular species. The fragmentations of PE, PC, and PS in negative ion mode were well-known with the formation of headgroup characteristic ions: *m/z* 140.01 for phosphoethanolamine (from ethanolamine-containing lipids), *m/z* 168.04 for phosphocholine (from choline-containing lipids), and *m/z* 152.99 from glycerophosphate in PS headgroup. Their molecular species were identified by the fatty acyl product ions at *m/z* 255.23 (C16:0), *m/z* 283.26 (C18:0), *m/z* 303.23 (C20:4), and *m/z* 327.23 (C22:6), confirming the identity of PE(18:0_20:4), PC(16:0_20:4) and PS(18:0_22:6) (Figure **3.1C-E**), respectively. PE(18:0_20:4) represents PE with 2 fatty acid molecular species - C18:0 and C20:4; these fatty acid molecular species can be either in *sn*-1 or *sn*-2 position of the glycerol backbone.

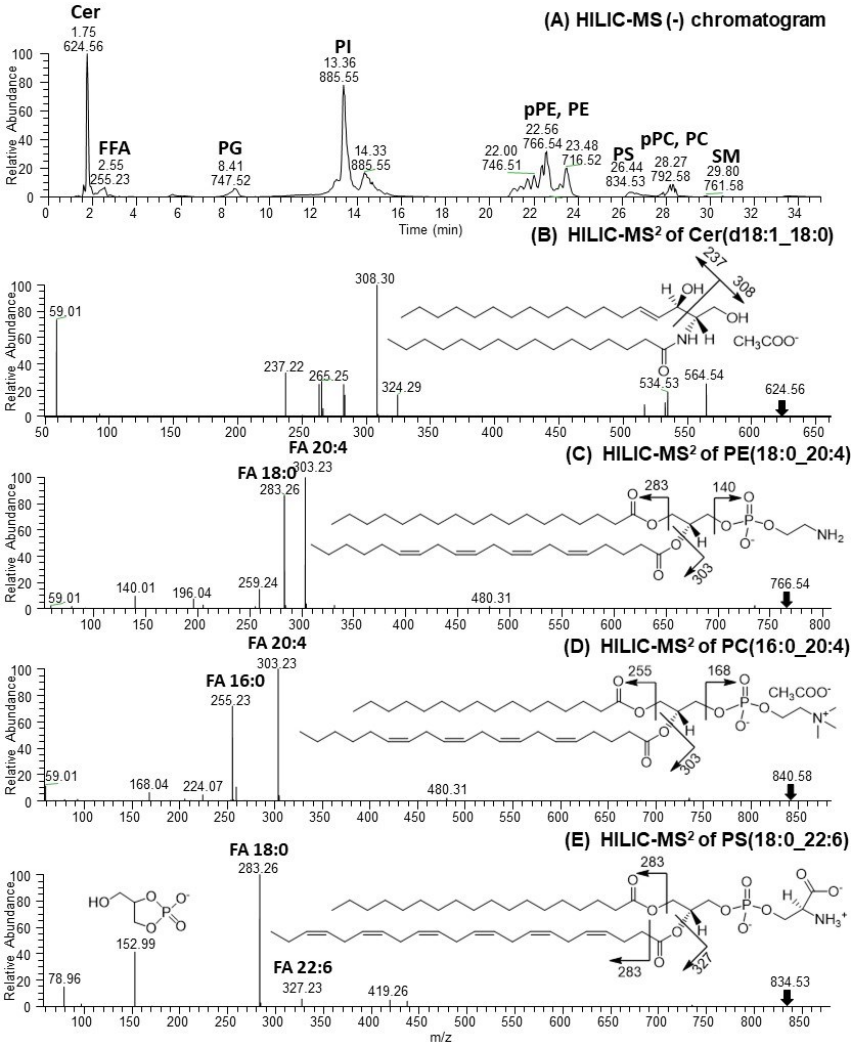

Figure 3.1: Ultra-high-performance liquid chromatography (UHPLC) coupled with high-resolution mass spectrometry (HRMS) conducted in negative ion mode of a representative fetal brain lipid extract from high n-3 PUFA at GD18.5 group. A) Hydrophilic interaction (HILIC-MS) base peak chromatogram of fetal brain lipid extract**.** *HILIC-MS^2 spectra showing the typical fragmentation of their headgroup class from the precursor ions:* ***B)*** *Cer(d18:1_18:0) [M+CH$_3$COO]$^-$ at m/z 624.56,* ***C)*** *PE(18:0_20:4) [M-H]$^-$ at m/z 766.54,* ***D)*** *PC(16:0_20:4) [M+CH$_3$COO]$^-$ at m/z 840.58 and* ***E)*** *PS(18:0_22:6) [M-H]$^-$ at m/z 834.53. Ceramides (Cer), phosphatidylglycerol (PG, phosphatidylinositol (PI), phosphatidylethanolamine (PE), phosphatidylserine (PS, phosphatidylcholine (PC), and sphingomyelin (SM).*

Subclasses of PC and PE, including plasmanyl choline (O-PC), plasmanyl ethanolamine (O-PE), choline plasmalogen (P-PC), and ethanolamine plasmalogen (P-PE) were also detected in the fetal brain lipid extract. Examples of major P-PE and O-PC molecular species are shown in Appendices **8** and **9**, respectively. Full MS spectra of PE and PC classes were achieved [Appendix **8 (A)** and Appendix **9 (A)**] due to the inter-class separation capacity of the HILIC column. The resolution of plasmanyl and plasmalogen PC and PE were achieved using both HILIC and C30RP column HRMS. Fragmentation of P-PE [PE(P-18:1_22:6) and PE(P-18:0_22:5)] are shown in Appendix **8 (B** and **C)**. Two additional product ions, *m/z* 462.30 and 444.29, in Appendix **8 (B)** were signatures from P-18:1, while *m/z* 464.31 and 446.30 in Appendix **8 (C)** resulted from P-18:0 plasmalogen linkage. It is noted that *m/z* 283.24 and *m/z* 285.26 fragment ions in Appendix **8 (B** and **C)** resulted from the loss of CO_2 (44 Da), which is typical of the PUFAs, C22:6 and C22:5, respectively. HILIC-MS^2 spectra of PE(18:0_22:6) and PE(18:0_22:5) in Appendix **8 (D** and **E)** show the two major fatty acyl ions from each molecular species in addition to *m/z* 140 PE headgroup characteristic ions. Similarly, HILIC-MS^2 spectra of some major PC species, including PC(16:0_18:1), PC(16:0_16:0), PC(16:0_14:0) and ether PC(O-16:0_16:0) are displayed in Appendix **8**.

Figure **3.2 (A)** shows the C30RP-MS chromatogram of fetal brain lipid extract, separating two lipid categories, GP and TG, at different regions on the chromatograms based on the *m/z* and their fatty acyl chain length and unsaturation degree. In contrast to HILIC, where TG was eluted upfront together with all other nonpolar lipids, TG was separated and resolved very well at the end of C30RP chromatography, even at low concentrations.

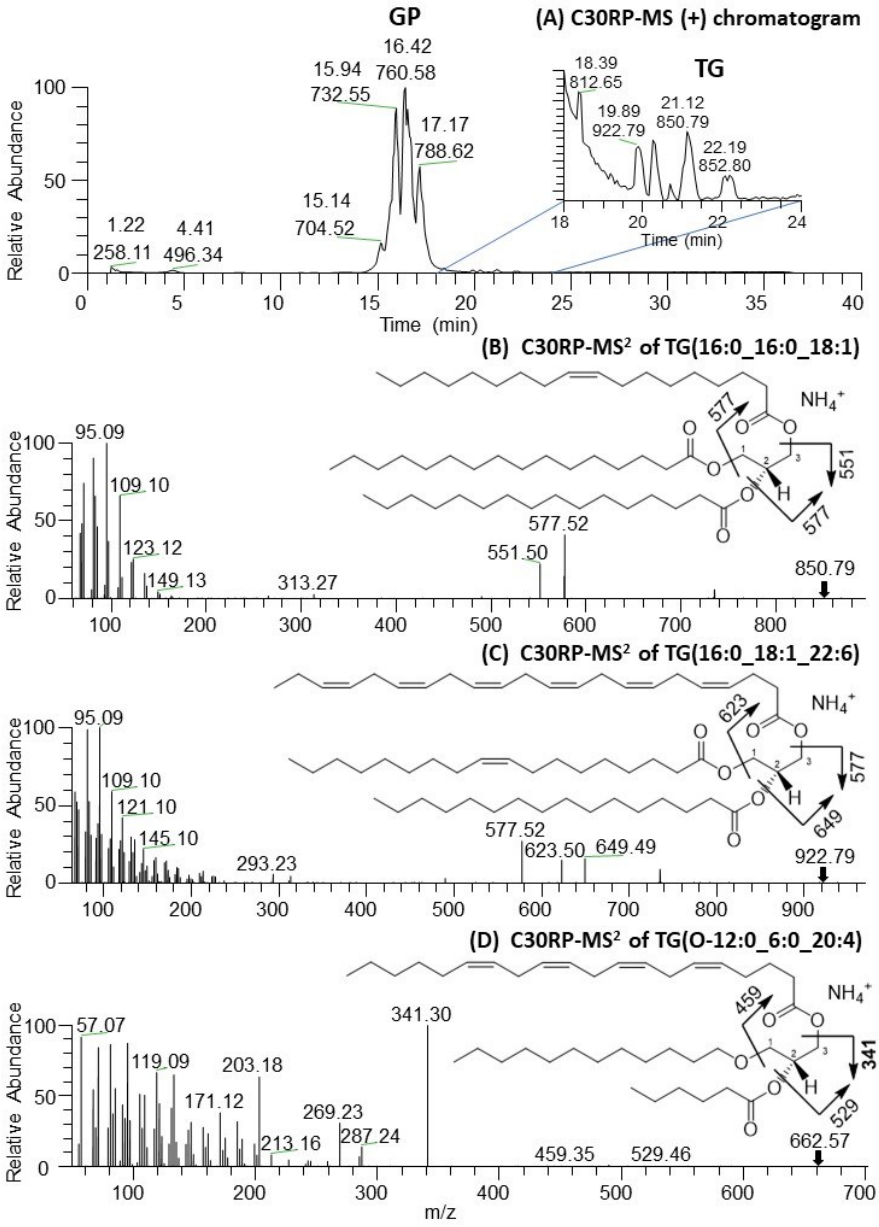

Figure 3.2: C30 reverse phase ultra-high-performance liquid chromatography coupled with high-resolution mass spectrometry (C30RP-HRMS) chromatogram conducted in positive ion mode for a representative fetal brain lipid extract from high n-3 PUFA at GD18.5 group. A) *C30RP-MS^2 spectra of some major TG molecular species:* ***B)*** *TG(16:0_16:0_18:1) $[M+NH_4]^+$ at m/z 850.79,* ***C)*** *TG(16:0_18:1_22:6) $[M+NH_4]^+$ at m/z 922.79, and* ***D)*** *ether TG(O-12:0_6:0_20:4) $[M+NH_4]^+$ at m/z 662.57. Glycerophospholipids (GP), and triacylglycerols (TG).*

Some major TG molecular species in the fetal brain samples were selected for showing C30RP-MS^2 spectra as in Figure **3.2 (B-D)**. All TG molecular species were observed as ammonium adducts $[M+NH_4]^+$ in the positive ion mode. The fragmentation of the most abundant TG seen at *m/z* 850.79 was shown in the inserted structure in Figure **3.2 (B)**, whose accurate *m/z* already assigned the total carbon number and number of double bonds as TG(50:1) $[M+NH_4]^+$ precursor ion. Two product ions observed at *m/z* 577.52 and 551.50 were corresponding to the neutral losses of 273 Da ($-C_{15}H_{31}COONH_4$) and 299 Da ($-C_{17}H_{33}COONH_4$), respectively. From these characteristic neutral losses of C16:0 and C18:1 (in form of ammonium salts), the identification of TG(16:0_16:0_18:1) was confirmed. Where TG molecules consisted of three different fatty acyls, such as TG(16:0_18:1_22:6), there were 3 characteristic neutral losses of ammonium salts C16:0, C18:1 and C22:6 forming *m/z* 649.49, 623.50 and 577.52 product ions seen in Figure **3.2 (C)**. The relative position (*sn*-1,2, 3) of FA on the glycerol backbone of TG molecular species could be assigned due to much higher neutral loss of *sn*-1/3 FA as compared with *sn*-2 FA loss (Herrera *et al*., 2010; Pham *et al*., 2019). Ether O-TG subclass was also observed and C30RP-MS^2 spectrum of TG(O-12:0_6:0_20:4) $[M+NH_4]^+$ at *m/z* 662.57 shown in Figure **3.2 (D)**.

Using the above-described algorithm, 127 lipid molecular species were identified in the fetal brain lipid extract at each gestation stage (Appendix **10**).

Further data analysis was conducted based on lipid major head groups and lipid species per lipid classes to evaluate the impact of gestation and maternal dietary n-3 PUFA intake on fetal brain lipidome.

3.2 Effects of gestation and maternal n-3 PUFA intake on major lipid groups and classes in total lipids

The effects of gestation and maternal diet on the proportion of major lipid groups, viz, ethanolamine-based [diacyl phosphatidylethanolamine (PE), plasmanyl ethanolamine (O-PE) and ethanolamine plasmalogen (P-PE) and lyso-PE (LPE)], choline-based [diacyl phosphatidylcholine (PC), plasmanyl choline (O-PC) and choline plasmalogen (P-PC) and lyso-PC (LPC)];glycerolipids [triacylglycerols (TG) and diacylglycerols (DG)], and minor brain lipids [phosphatidylserine (PS), phosphatidylinositol (PI), phosphatidylglycerol (PG), CE, ceramides (Cer) and sphingomyelins (SM)], classes and subclasses in the fetal brain total lipids, were first analyzed (Figure **3.3**).

Gestation and maternal diets had significant effects on ethanolamine-based, choline-based, minor brain lipids, and glycerolipids in the fetal brain total lipids (Figure **3.3**). As gestation progressed, ethanolamine-based and minor brain lipids significantly ($p < 0.0001$) increased, whereas choline-based lipids ($p < 0.0001$) and glycerolipids ($p = 0.0002$) decreased in both low and high n-3 PUFA group. A maternal diet high in n-3 PUFA significantly increased the accretion of ethanolamine-based lipids ($p < 0.0001$) and minor brain lipids ($p = 0.0003$) in the fetal brain as gestation progressed, whereas maternal diet high in n-3 PUFA showed significantly lower ($p < 0.0001$) choline-based lipids, compared with low n-3 PUFA diet (Figure **3.3**). Diet had no significant effect on the glycerolipids in fetal brain during gestation. Unlike other major brain lipid groups, there was significant interaction between diet and gestation ($p < 0.0001$) in choline-based lipids (Figure **3.3**).

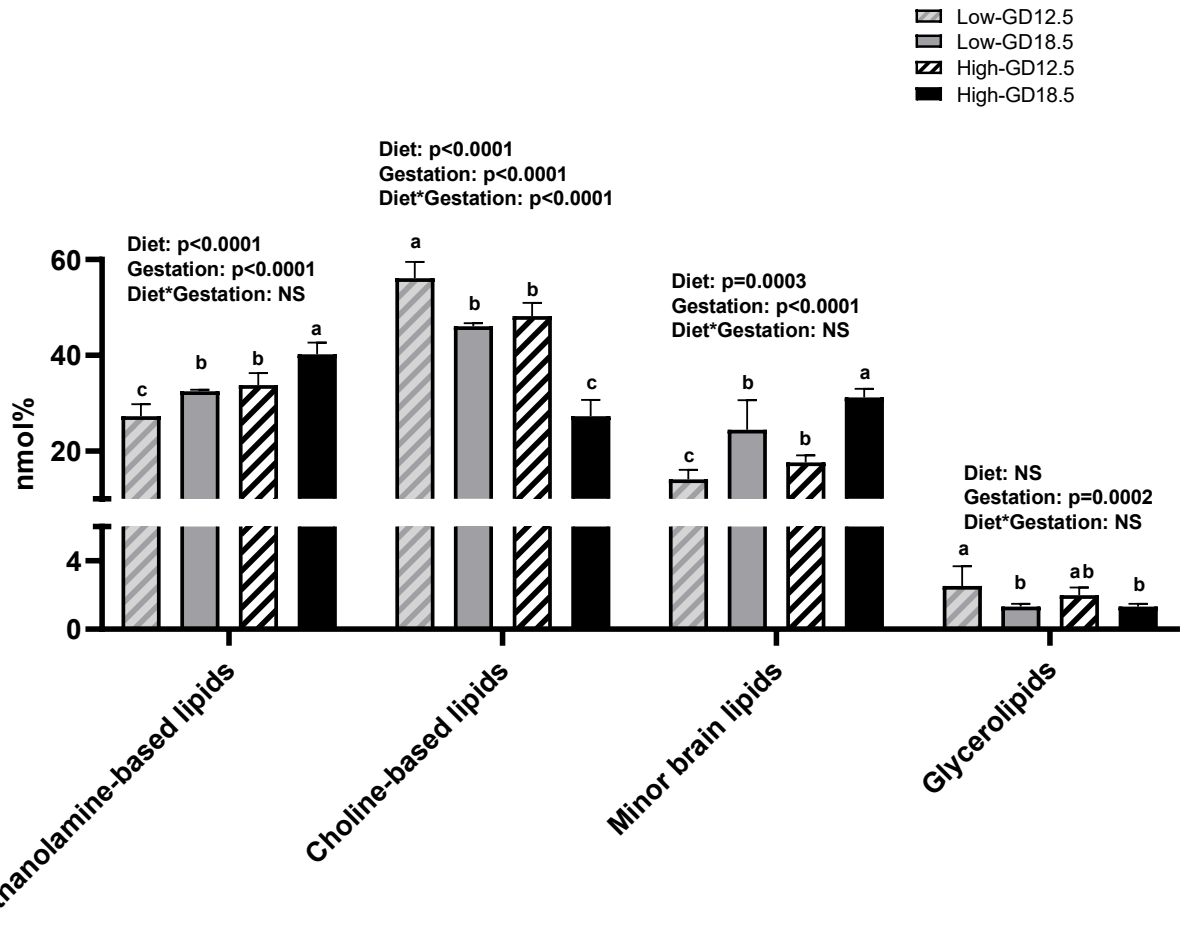

Figure 3.3: Effects of gestation and maternal n-3 PUFA intake on major lipid groups in total lipids. *Data were analyzed using two-way ANOVA to determine the main effects and the interactions between maternal diet and gestation stage; pairwise comparison using Bonferroni's correction was used to determine differences. Data represent the mean ± SD of nmol% of sum of each of the lipid group in total lipids. Mean values with different superscript letters (a, b, c & d) are significantly different; p<0.05 (n = 8 dams per group). ethanolamine-based = diacyl phosphatidylethanolamine (PE), ethanolamine plasmalogens (P-PE), plasmanyl ethanolamine (O-PE), and lyso-PE (LPE); choline-based = diacyl phosphatidylcholine (PC), plasmanyl choline (O-PC) and choline plasmalogen (P-PC) and lyso-PC (LPC); glycerolipids = triacylglycerols (TGs) and diglycerides (DGs); minor brain lipids = diacyl phosphatidylserine (PS), diacyl phosphatidylinositol (PI), diacyl phosphatidylglycerol (PG), cholesteryl esters (CE), ceramides (Cer), and sphingomyelins (SM).*

Thereafter, we analyzed the effect of gestation and diet on each of the lipid class or subclass of the major lipid groups in the fetal brain total lipids (Table **3.1**). Gestation had a significant effect on the proportion of diacyl phosphatidylethanolamine (PE) and plasmanyl ethanolamine (O-PE) in fetal brain total lipids; PE and O-PC increased significantly ($p < 0.0001$) as gestation progressed from GD12.5 to GD18.5 in both low and high n-3 PUFA groups (Table **3.1**). Diet had a significant effect on the proportion of PE and O-PE in the fetal brain total lipids; a maternal diet high in n-3 PUFA significantly increased PE ($p = 0.001$) and O-PC ($p < 0.0001$) levels in the fetal brain total lipids at both gestation stages, compared with a low n-3 PUFA diet (Table **3.1**).

There was a significant interaction between diet and gestation ($p = 0.01$) for the ethanolamine plasmalogen (P-PE) in the fetal brain total lipids revealing a significant diet-dependent effect with no significant gestation-dependent effect (Table **3.1**). A maternal diet high in n-3 PUFA showed a significantly lower ($p = 0.01$) level of P-PE in the fetal brain total lipids at GD18.5 only, compared with a low n-3 PUFA diet (Table **3.1**). Both gestation and diet had no significant effect on the lysophosphatidylethanolamine (LPE) levels in the fetal brain total lipids (Table **3.1**). Gestation and maternal diets had significant effects on ethanolamine-based fatty acyl species in the fetal brain total lipids (Table **3.1**). As gestation progressed, ethanolamine-based fatty acyl species in the fetal brain total lipids significantly increased ($p < 0.0001$) in both low and high n-3 PUFA groups (Table **3.1**). A maternal diet high in n-3 PUFA significantly ($p = 0.001$) increased the sum of ethanolamine-based fatty acyl species in the fetal brain total lipids, compared with low n-3 PUFA diet (Table **3.1**).

Table 3.1. nmol% of lipid group/class/subclass found in fetal brain total lipids

Lipid species	Low-GD12.5	Low-GD18.5	High-GD12.5	High-GD18.5	Diet	Gestation	Diet* Gestation	Diet effect	Gestation effect
∑Ethanolamine-based lipids	27.26 ± 2.35^{c}	35.47 ± 3.95^{b}	32.89 ± 3.30^{b}	40.18 ± 2.33^{a}	$p < 0.0001$	$p < 0.0001$	NS	↑	↑
PE	12.45 ± 2.43^{c}	17.46 ± 4.32^{b}	15.91 ± 2.33^{ab}	22.27 ± 2.02^{a}	$p = 0.001$	$p < 0.0001$	NS	↑	↑
O-PE	3.51 ± 0.97^{c}	5.62 ± 1.42^{b}	5.82 ± 0.86^{b}	8.29 ± 0.69^{a}	$p < 0.0001$	$p < 0.0001$	NS	↑	↑
P-PE	10.84 ± 1.70^{a}	11.61 ± 1.94^{a}	10.77 ± 1.46^{a}	8.66 ± 0.43^{b}	$p = 0.01$	NS	$p = 0.01$	-	↓
LPE	0.46 ± 0.19^{a}	0.78 ± 0.47^{a}	0.39 ± 0.16^{a}	0.96 ± 0.57^{a}	NS	NS	NS	-	-
∑Choline-based lipids	56.10 ± 3.14^{a}	38.77 ± 9.71^{b}	46.06 ± 6.23^{b}	27.29 ± 3.18^{c}	$p < 0.0001$	$p < 0.0001$	$p < 0.0001$	↓	↓
PC	54.42 ± 3.49^{a}	36.89 ± 10.10^{b}	43.88 ± 6.21^{b}	25.22 ± 3.32^{c}	$p = 0.0001$	$p < 0.0001$	NS	↓	↓
O-PC	0.11 ± 0.03^{a}	0.14 ± 0.02^{a}	0.12 ± 0.03^{a}	0.12 ± 0.01^{a}	NS	NS	NS	-	-
P-PC	0.94 ± 0.22^{a}	0.58 ± 0.12^{ab}	1.06 ± 0.28^{a}	0.34 ± 0.11^{b}	NS	$p < 0.0001$	NS	-	↓
LPC	0.63 ± 0.28^{b}	1.17 ± 0.43^{a}	1.00 ± 0.24^{b}	1.61 ± 0.39^{a}	$p = 0.004$	$p = 0.0002$	NS	↑	↑
PS	5.94 ± 1.02^{c}	12.66 ± 3.50^{b}	7.26 ± 2.86^{c}	16.80 ± 0.84^{a}	$p = 0.006$	$p < 0.0001$	NS	↑	↑
PG	0.80 ± 0.11^{c}	1.99 ± 0.48^{b}	1.97 ± 0.42^{b}	3.61 ± 0.23^{a}	$p < 0.0001$	$p < 0.0001$	NS	↑	↑
PI	5.50 ± 0.95^{b}	7.63 ± 2.19^{a}	7.60 ± 1.44^{a}	8.97 ± 1.01^{a}	$p = 0.006$	$p = 0.005$	NS	↑	↑
∑SP	1.17 ± 0.24^{b}	2.00 ± 0.43^{a}	1.10 ± 0.14^{b}	1.48 ± 0.17^{b}	$p = 0.006$	$p < 0.0001$	$p = 0.02$	↓	↑
Cer	1.06 ± 0.22^{bc}	1.91 ± 0.42^{a}	0.98 ± 0.09^{c}	1.37 ± 0.14^{b}	$p = 0.003$	$p < 0.0001$	$P = 0.02$	↑	↑
SM	0.10 ± 0.02^{a}	0.09 ± 0.01^{a}	0.12 ± 0.04^{a}	0.11 ± 0.03^{a}	NS	NS	NS	-	-
CE	0.70 ± 0.51^{ab}	0.15 ± 0.11^{c}	1.12 ± 0.40^{a}	0.35 ± 0.10^{b}	$p = 0.01$	$p < 0.0001$	NS	↓	↓
∑Glycerolipids	2.53 ± 1.07^{a}	1.33 ± 0.14^{b}	1.99 ± 0.42^{ab}	1.32 ± 0.15^{b}	NS	$p = 0.0002$	NS	↓	↓
DG	0.97 ± 0.34^{a}	0.49 ± 0.10^{b}	1.04 ± 0.29^{a}	0.61 ± 0.07^{b}	NS	$p < 0.0001$	NS	-	↓
TG	1.56 ± 0.12^{a}	0.84 ± 0.15^{b}	0.96 ± 0.22^{ab}	0.71 ± 0.09^{b}	NS	$p = 0.001$	NS	-	↓

Female mice were fed diets containing 1% n-3 PUFA (low n-3 PUFA diet) and 9% n-3 PUFA (high n-3 PUFA) during gestation, and fetal brain lipidomic profile at gestation days (GD)12.5 and GD18.5 was determined. Data were analyzed using two-way ANOVA to determine the main effects and the interactions between maternal diet and gestation stage; pairwise comparison using Bonferroni's correction was used to determine differences. Data represent mean ± SD *nmol percentage of major lipid group/class/sub-class found in fetal brain total lipid extract. Mean values with different superscript letters (a, b, c & d) are significantly different; $p<0.05$ (n = 8 dams per group). ethanolamine-based = diacyl phosphatidylethanolamine (PE), ethanolamine plasmalogens (P-PE), plasmanyl ethanolamine (O-PE), and lyso-PE (LPE); choline-based = diacyl phosphatidylcholine (PC), plasmanyl choline (O-PC) and choline plasmalogen (P-PC) and lyso-PC (LPC); glycerolipids = triacylglycerols (TGs) and diglycerides (DGs); minor brain lipids = diacyl phosphatidylserine (PS), diacyl phosphatidylinositol (PI), diacyl phosphatidylglycerol (PG), cholesteryl esters (CE), ceramides (Cer), sphingomyelins (SM), ∑GP = sum of glycerophospholipids, ∑SP = sum of sphingolipids, and ∑GL = sum of glycerolipids. For gestation effect column, ↑ = increase as gestation progressed from GD12.5 to GD18.5, while ↓ = decrease as gestation progressed. For the diet effect column, ↑ = higher levels in high n-3 PUFA diet group, compared with low n-3 PUFA diet group, while ↓ = lower levels in high n-3 PUFA diet group, compared with low n-3 PUFA diet group. - = no effect of diet and/or gestation.*

Among the lipid (sub)classes in choline-based fatty acyl species in the fetal brain total lipids, gestation had a significant effect on diacyl phosphatidylcholine (PC), choline plasmalogen (P-PC) and lysophosphatidylcholine (LPC), but not on plasmanyl choline (O-PC) levels in the fetal brain total lipids (Table **3.1**). As gestation progressed, PC in the fetal brain total lipids significantly decreased ($p < 0.0001$) in both low and high n-3 PUFA diet groups, whereas P-PC significantly decreased ($p < 0.0001$) in the high n-3 PUFA diet group. Diet had a significant effect on PC; a maternal diet high in n-3 PUFA showed a significantly lower ($p = 0.0001$) level of PC in the fetal brain total lipids in both gestation stages, compared to a low n-3 PUFA diet (Table **3.1**). As gestation progressed, the proportion of LPC in the fetal brain total lipids significantly increased ($p = 0.0002$) in both low and high n-3 PUFA groups. Diet had a significant effect on the proportion of LPC in the fetal brain total lipids; a maternal diet high in n-3 PUFA significantly increased ($p = 0.004$) LPC levels in the fetal brain total lipids at both gestation stages, compared with a low n-3 PUFA diet (Table **3.1**). Total choline-based fatty acyl species in the fetal brain total lipids showed significant interaction between diet and gestation revealing a significant decrease ($p < 0.0001$) in both low and high n-3 PUFA diet groups as gestation progressed from GD12.5 to GD18.5 (Table **3.1**). Diet had a significant effect on the total choline-based fatty acyl species in the fetal brain total lipids; a maternal diet high in n-3 PUFA showed significantly lower ($p < 0.0001$) total choline-based fatty acyl species in the fetal brain total lipids, compared with low n-3 PUFA diet (Table **3.1**).

Gestation had a significant effect on PS and PG in fetal brain total lipids; the PS and PG levels in fetal brain total lipids significantly increased ($p < 0.0001$) in low and high n-3 PUFA diet groups (Table **3.1**). Diet had a significant effect on PS and PG in the fetal brain total lipids; a maternal diet high in n-3 PUFA diet significantly increased PS ($p = 0.006$) and PG ($p < 0.0001$)

levels in the fetal brain total lipids (Table **3.1**). Gestation had a significant effect on phosphatidylinositol (PI) in the fetal brain total lipids; as gestation progressed, PI level in the fetal brain total lipids significantly increased ($p = 0.005$) in low n-3 PUFA group with no significant change in high n-3 PUFA group (Table **3.1**).

Gestation had a significant effect on Cer level in the fetal brain total lipids; Cer level in the fetal brain total lipids significantly increased ($p < 0.0001$) in both low and high n-3 PUFA groups as gestation progressed (Table **3.1**). Diet had a significant effect on Cer level in the fetal brain total lipids; a maternal diet high in n-3 PUFA showed significantly lower ($p = 0.003$) level of Cer in the fetal brain total lipids at GD18.5 only, compared to low n-3 PUFA group (Table **3.1**). Neither gestation nor diet had a significant effect on sphingomyelin (SM) in the fetal brain total lipids (Table **3.1**). Our findings show a significant interaction between diet and gestation ($p = 0.02$) for total SP in the fetal brain total lipids revealing significantly increased ($p < 0.0001$) in the low n-3 PUFA group with no significant change in the high n-3 PUFA group as gestation progressed from GD12.5 to GD18.5 (Table **3.1**). Diet had a significant effect on total SP in the fetal brain total lipids; a maternal diet high in n-3 PUFA showed lower ($p = 0.006$) total SP in the fetal brain total lipids at GD18.5, compared with a low n-3 PUFA diet (Table **3.1**).

CE in fetal brain total lipids showed gestation and diet-dependent effects revealing a significant decrease ($p < 0.0001$) in CE level in the total lipids as gestation progressed from GD12.5 to GD18.5 in both low and high n-3 PUFA groups. A maternal diet high in n-3 PUFA showed a significantly higher ($p = 0.01$) level of CE in the fetal brain total lipids at both gestation stages, compared with low n-3 PUFA diet (Table **3.1**).

Gestation had a significant effect on the DG and TG levels in the fetal brain total lipids; as gestation progressed, DG level in the fetal brain total lipids significantly decreased ($p < 0.0001$) in both low and high n-3 PUFA diet groups, whereas TG level significantly decreased ($p = 0.001$) in low n-3 PUFA diet group (Table **3.1**). Diet had no significant effect on DG and TG levels in the fetal brain total lipids. Gestation had a significant effect on ∑glycerolipids in the fetal brain total lipids; as gestation progressed, ∑glycerolipids in the fetal brain total lipids significantly decreased ($p = 0.0002$) in low n-3 PUFA group with no significant change in the high n-3 PUFA group (Table **3.1**). Diet had no significant effect on ∑glycerolipids in the fetal brain total lipids (Table **3.1**).

3.3 Effects of gestation and maternal n-3 PUFA intake on fetal brain glycerophospholipids

Gestation had significant effects on all fetal brain GP; as gestation progressed, ethanolamine-based [diacyl phosphatidylethanolamine (PE), ethanolamine plasmalogens (P-PE), plasmanyl ethanolamine (O-PE), and lyso-PE (LPE)] ($p < 0.0001$), serine-based [diacyl phosphatidylserine (PS)] ($p < 0.0001$), glycerol-based [diacyl phosphatidylglycerol (PG)] ($p < 0.0001$) and inositol-based [diacyl phosphatidylinositol (PI)] ($p = 0.006$) GP in fetal brain total GP increased in both low and high n-3 PUFA groups, whereas choline-based [choline-based = diacyl phosphatidylcholine (PC), plasmanyl choline (O-PC) and choline plasmalogen (P-PC) and lyso-PC (LPC)] GP in fetal brain total GP decreased in both low and high n-3 PUFA groups (Figure **3.4**). Maternal diets high in n-3 PUFA significantly increased the accretion of ethanolamine-based, inositol-based, serine-based, and glycerol-based GP in the fetal brain ($p = 0.0002$, $p = 0.005$, $p = 0.006$ and $p = 0.0001$, respectively) as gestation progressed, compared with low n-3 PUFA diets. On the other hand, a diet high in n-3 PUFA showed significantly lower ($p = 0.0001$) levels of choline-based GP in fetal brain total GP, compared with the low n-3 PUFA diet.

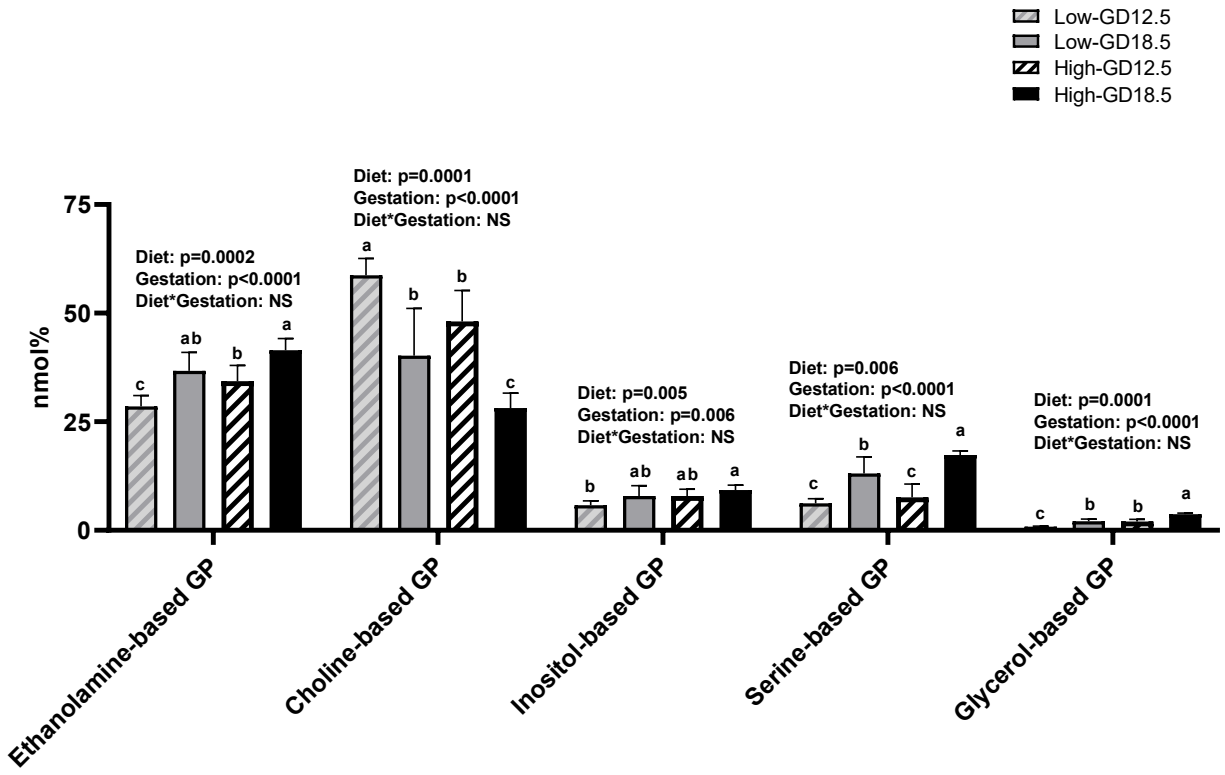

Figure 3.4: Effects of gestation and maternal n-3 PUFA intake on fetal brain glycerophospholipids. *Female mice were fed diets containing 1% n-3 PUFA (low n-3 PUFA diet) and 9% n-3 PUFA (high n-3 PUFA) during gestation, and fetal brain lipidomic profile at gestation days (GD)12.5 and GD18.5 was determined. Data represent the mean ± SD of nmol% of sum of each of the GP classes. Mean values with different superscript letters (a, b, c & d) are significantly different; p<0.05 (n = 8 dams per group). Ethanolamine-based GP= diacyl phosphatidylethanolamine (PE), ethanolamine plasmalogen (P-PE), plasmanyl ethanolamine (O-PE), and lyso-PE (LPE); choline-based GP = diacyl phosphatidylcholine (PC), plasmanyl choline (O-PC) and choline plasmalogen (P-PC) and lyso-PC (LPC); Inositol-based GP = diacyl phosphatidylinositol (PI), serine-based GP = diacyl phosphatidylserine (PS) and glycerol-based GP = diacyl phosphatidylglycerol (PG).*

3.4 Effects of maternal diets high or low in n-3 PUFA on ethanolamine-based glycerophospholipids in the fetal brain during gestation

Next, we investigated the effect of diet and gestation on each ethanolamine-based GP fatty acyl species among total GP in fetal brain. Of the 34 ethanolamine-containing GP species subjected to PLS-DA analysis, 22 had VIP score ≥ 1.0, suggesting substantial alteration by either or both diet and gestation (Figure **3.5 A**). The 22 ethanolamine-based fatty acyl species with VIP scores ≥ 1.0 were subjected to PCA analysis; these species were clustered into four quadrants (Q) 1-4 in the PCA biplot with accumulated variability components, F1 and F2, explaining the 78.39% variation in the fatty acyl species (Figure **3.5 B**). Oleic acid (18:1, OA)-containing ethanolamine-based GP [PE(16:0_18:1), PE(16:1_18:1) and PE(18:1_18:1)], palmitoleic acid (16:1)-containing ethanolamine-based fatty acyl species [PE(16:0_16:1)] and ARA-containing ethanolamine-based fatty acyl species [PE(O-16:0_20:4)] were clustered in Q1 of the PCA biplot, corresponding to high n-3 PUFA diet at GD12.5 centroid (Figure **3.5 B**). ARA-containing [PE(P-16:0_20:4)], OA-containing [PE(P-16:0_18:1)], EPA-containing [PE(P-16:0_22:5) and PE(P-18:0_22:5)], adrenic acid (22:4, ADA)-containing [PE(P-16:0_22:4) and P-18:0_22:4)] and palmitic acid-containing [PE(P-16:0_16:0] ethanolamine-based fatty acyl species were clustered in Q2 of the PCA biplot, corresponding to low n-3 PUFA diet group at GD12.5 centroid (Figure **3.5 B**). DHA-containing [PE(16:0_22:6)], ARA-containing [PE(18:0_20:4)], ADA-containing [PE(18:0_22:4)] and EPA-containing [PE(18:0_22:5)] ethanolamine-based fatty acyl species were clustered in Q3 of PCA biplot, corresponding to low n-3 PUFA diet at GD18.5 centroid (Figure **3.5 B**). OA-containing [PE(18:0_18:1)] and DHA-containing [PE(18:0_22:6), PE(O-16:1_22:6), and PE(O-18:1_22:6)] ethanolamine-based fatty acyl species were clustered in Q4 of the PCA biplot corresponding to high n-3 PUFA diet at GD18.5 centroid (Figure **3.5 B**).

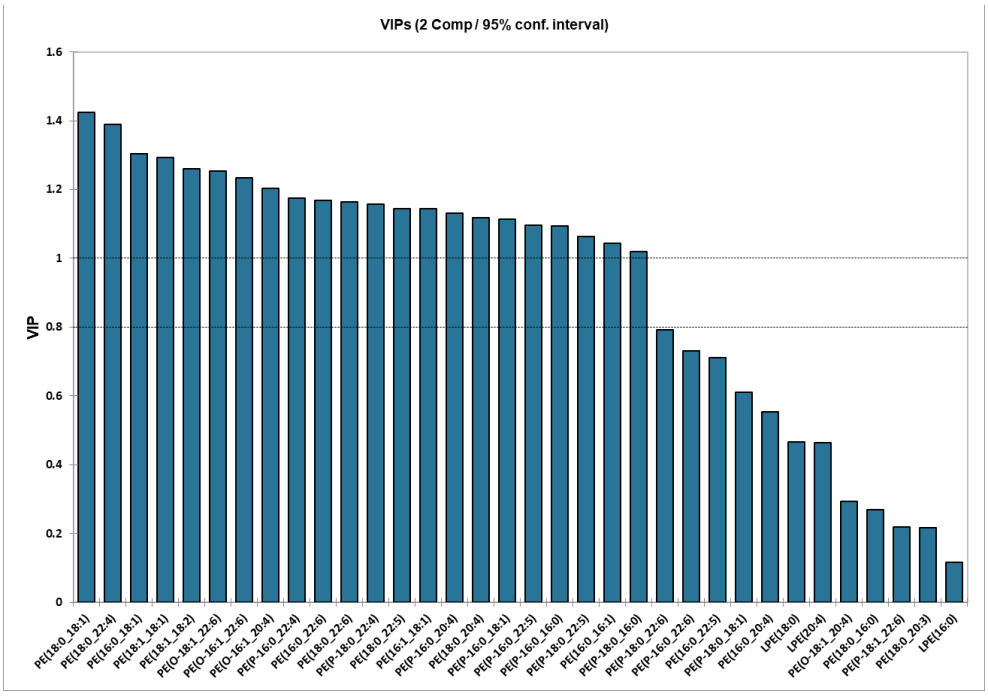
VIPs (2 Comp / 95% conf. interval)
VIP
1.6
1.4
1.2
1
0.8
0.6
0.4
0.2
0
PE(18:0_18:1)
PE(18:0_22:4)
PE(16:0_18:1)
PE(18:1_18:1)
PE(18:1_18:2)
PE(O-18:1_22:6)
PE(O-16:1_22:6)
PE(O-16:1_20:4)
PE(P-16:0_22:4)
PE(16:0_22:6)
PE(18:0_22:6)
PE(P-18:0_22:4)
PE(18:0_22:5)
PE(16:1_18:1)
PE(P-16:0_20:4)
PE(18:0_20:4)
PE(P-16:0_18:1)
PE(P-16:0_22:5)
PE(P-16:0_16:0)
PE(P-18:0_22:5)
PE(16:0_16:1)
PE(P-18:0_16:0)
PE(P-18:0_22:6)
PE(P-16:0_22:6)
PE(16:0_22:5)
PE(P-18:0_18:1)
PE(16:0_20:4)
LPE(18:0)
LPE(20:4)
PE(O-18:1_20:4)
PE(18:0_16:0)
PE(P-18:1_22:6)
PE(18:0_20:3)
LPE(16:0)

A

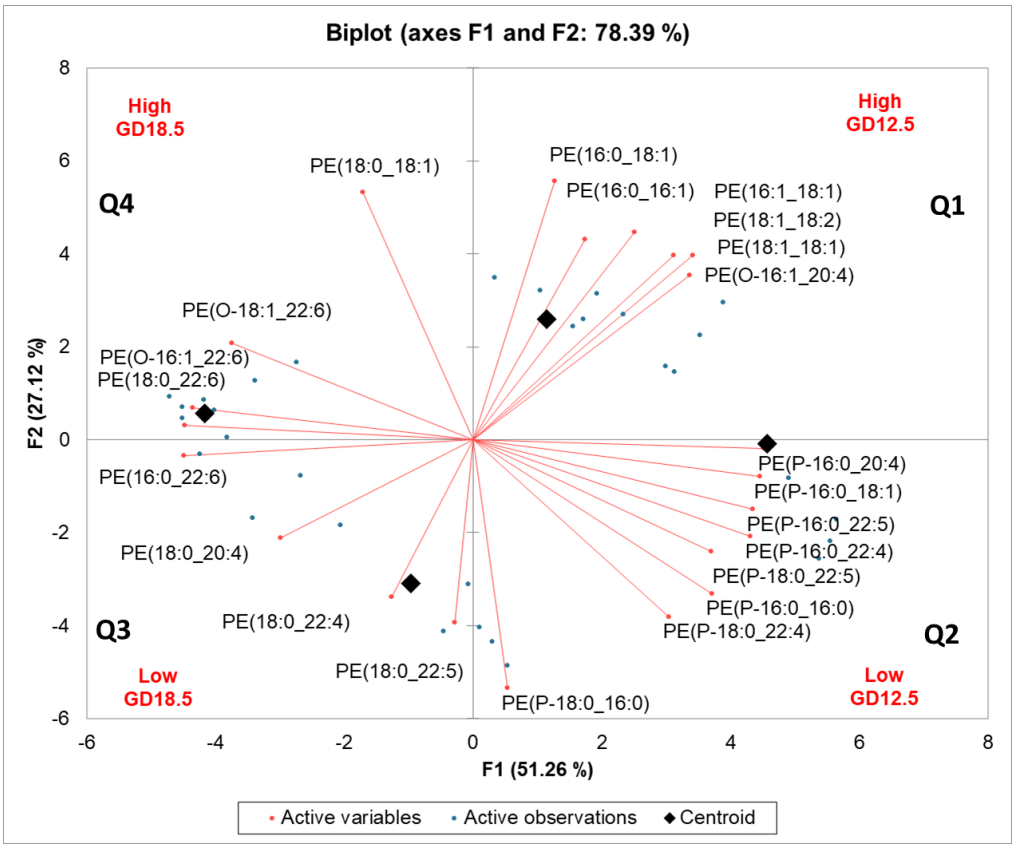
Biplot (axes F1 and F2: 78.39 %)
High GD18.5
High GD12.5
Q4
Q1
Q3
Q2
Low GD18.5
Low GD12.5
PE(18:0_18:1)
PE(16:0_18:1)
PE(16:0_16:1)
PE(16:1_18:1)
PE(18:1_18:2)
PE(18:1_18:1)
PE(O-16:1_20:4)
PE(O-18:1_22:6)
PE(O-16:1_22:6)
PE(18:0_22:6)
PE(16:0_22:6)
PE(P-16:0_20:4)
PE(P-16:0_18:1)
PE(P-16:0_22:5)
PE(P-16:0_22:4)
PE(P-18:0_22:5)
PE(P-16:0_16:0)
PE(P-18:0_22:4)
PE(18:0_20:4)
PE(18:0_22:4)
PE(18:0_22:5)
PE(P-18:0_16:0)
F2 (27.12 %)
F1 (51.26 %)
8
6
4
2
0
-2
-4
-6
Active variables
Active observations
Centroid

B

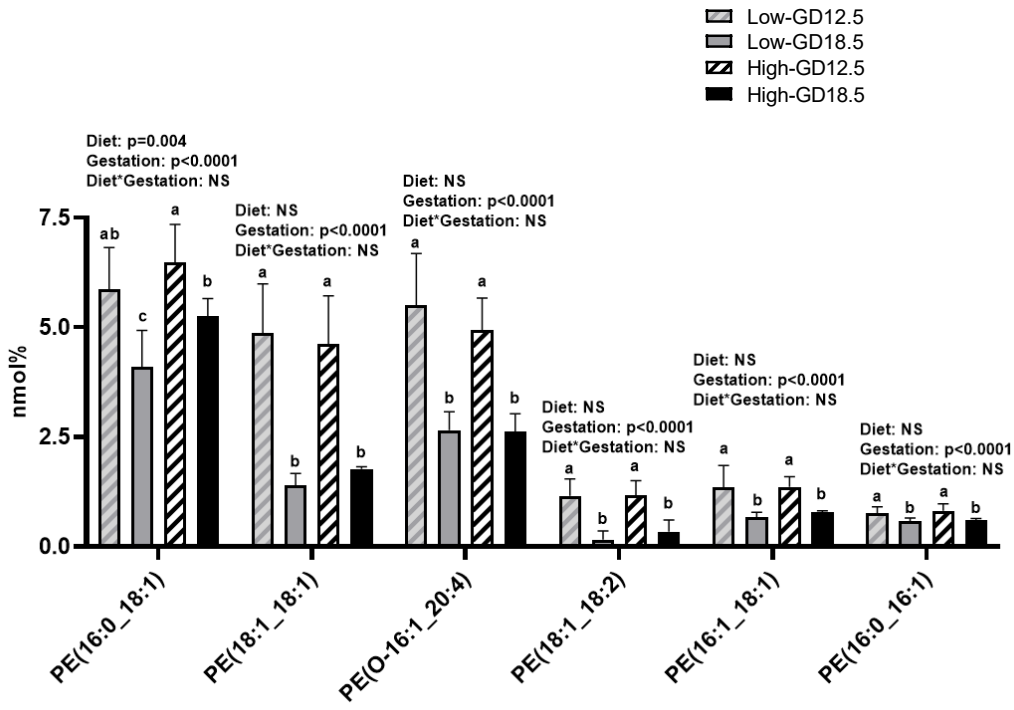
Low-GD12.5
Low-GD18.5
High-GD12.5
High-GD18.5
nmol%
7.5
5.0
2.5
0.0
Diet: p=0.004
Gestation: p<0.0001
Diet*Gestation: NS
Diet: NS
Gestation: p<0.0001
Diet*Gestation: NS
Diet: NS
Gestation: p<0.0001
Diet*Gestation: NS
Diet: NS
Gestation: p<0.0001
Diet*Gestation: NS
Diet: NS
Gestation: p<0.0001
Diet*Gestation: NS
Diet: NS
Gestation: p<0.0001
Diet*Gestation: NS
PE(16:0_18:1)
PE(18:1_18:1)
PE(O-16:1_20:4)
PE(18:1_18:2)
PE(16:1_18:1)
PE(16:0_16:1)

C

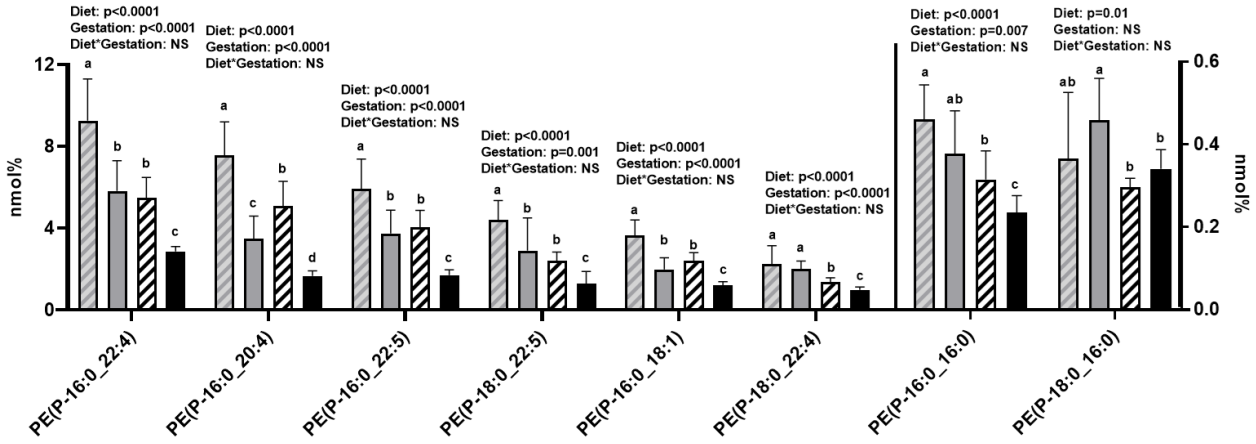
nmol%
12
8
4
0
0.6
0.4
0.2
0.0
Diet: p<0.0001
Gestation: p<0.0001
Diet*Gestation: NS
Diet: p<0.0001
Gestation: p<0.0001
Diet*Gestation: NS
Diet: p<0.0001
Gestation: p<0.0001
Diet*Gestation: NS
Diet: p<0.0001
Gestation: p=0.001
Diet*Gestation: NS
Diet: p<0.0001
Gestation: p<0.0001
Diet*Gestation: NS
Diet: p<0.0001
Gestation: p<0.0001
Diet*Gestation: NS
Diet: p<0.0001
Gestation: p=0.007
Diet*Gestation: NS
Diet: p=0.01
Gestation: NS
Diet*Gestation: NS
PE(P-16:0_22:4)
PE(P-16:0_20:4)
PE(P-16:0_22:5)
PE(P-18:0_22:5)
PE(P-16:0_18:1)
PE(P-18:0_22:4)
PE(P-16:0_16:0)
PE(P-18:0_16:0)

D

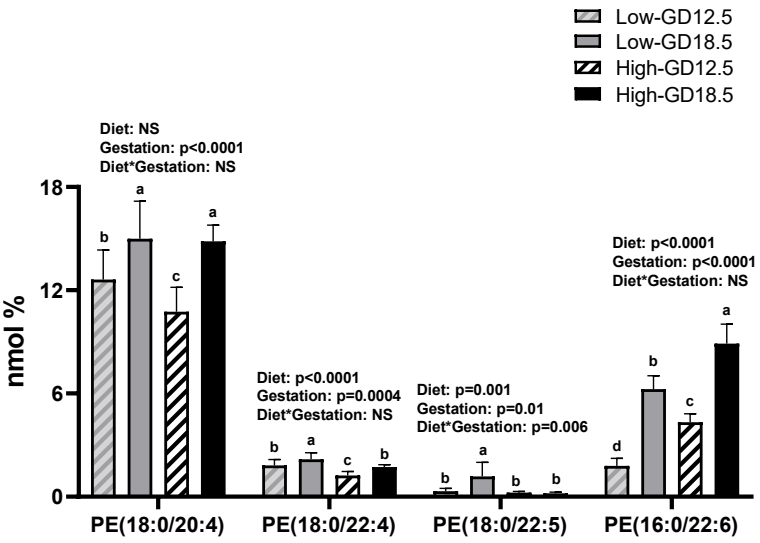

E

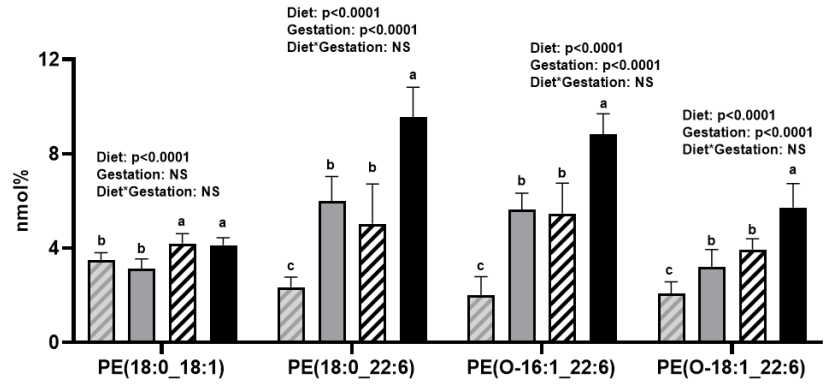

F

Figure 3.5: Effects of maternal diets high or low in n-3 PUFA on ethanolamine-based fatty acyl species in fetal brain during gestation. ***A)*** *Partial least-squares discriminant analysis (PLS-DA) score plot showing their variability importance in the progression (VIP);* ***B)*** *Principal component analysis (PCA) score plot of the ethanolamine-based lipid species in total lipids; ethanolamine-based fatty acyl species clustered in -* ***C)*** *quadrant 1;* ***D)*** *quadrant 2,* ***E)*** *quadrant 3, and* ***F)*** *quadrant 4. Female mice were fed diets containing 1% n-3 PUFA (low n-3 PUFA diet) and 9% n-3 PUFA (high n-3 PUFA) during gestation, and fetal brain ethanolamine-based fatty acyl species at gestation days (GD)12.5 and GD18.5 were determined. Data were analysed using two-way*

ANOVA to determine the main effects and the interactions between maternal diet and gestation stage; pairwise comparison using Bonferroni's correction was used to determine differences when there was an observed interaction. Data represent the mean ± SD of nmol% of each of ethanolamine-based fatty acyl species in total ethanolamine-based species. Mean values with different superscript letters (a, b, c & d) are significantly different; $p<0.05$ ($n = 8$ dams per group). Diacyl phosphatidylethanolamine (PE), plasmanyl ethanolamine (O-PE), and ethanolamine plasmalogen (P-PE).

Thereafter, we conducted a two-way ANOVA on the ethanolamine-based lipids based on the quadrants (Q1-Q4) the lipid species were clustered in the PCA biplot. Gestation had a significant ($p < 0.0001$) effect on all ethanolamine-based fatty acyl species clustered in the first quadrant (Q1) of PCA output (Figure **3.5 C**). Oleic acid (18:1)-containing- [PE(16:0_18:1), PE(18:1_18:1) and PE(16:1_18:1)], ARA-containing [PE(O-16:1_20:4)], LA-containing [PE(18:1_18:2)], and palmitoleic acid-containing [PE(16:0_16:1)] ethanolamine-based fatty acyl species, generally decreased as gestation progressed from GD12.5 to GD18.5 (Figure **3.5 C**). Diet had a significant effect on PE(16:0_18:1) only; a diet high in n-3 PUFA significantly increased level of PE(16:0_18:1), $p = 0.004$ in fetal brain, compared with low n-3 PUFA diet (Figure **3.5 C**). Gestation had significant effects on ethanolamine-based lipids clustered in Q2 of the PCA biplot, except PE(P-18:0/16:0) where gestation had no significant effect ($p > 0.05$) (Figure **3.5 D**). As gestation progressed from GD12.5 to GD18.5, ethanolamine-based fatty acyl species [PE(P-16:0_22:4), PE(P-16:0_20:4), PE(P-16:0_22:5), PE(P-18:0_22:5), PE(P-16:0_18:1), $p < 0.0001$, $p < 0.0001$, $p < 0.0001$, $p = 0.001$ and $p < 0.0001$, respectively], significantly decreased in both low and high n-3 PUFA groups, whereas PE(P-18:0_22:4) and PE(P-16:0_16:0), $p < 0.0001$ and $p = 0.007$, respectively, significantly decreased in high n-3 PUFA group only (Figure **3.5 D**). Diet had a significant effect on all the ethanolamine-based lipids clustered in Q2 of the PCA biplot. Compared with low n-3 PUFA diet, a maternal diet high in n-3 PUFA showed lower levels of ethanolamine-based fatty acyl species [PE(P-16:0_22:4), PE(P-16:0_20:4), PE(P-16:0_22:5), PE(P-18:0_22:5), PE(P-16:0_18:1), PE(P-18:0_22:4) and PE(P-16:0_16:0), $p < 0.000$] as gestation progressed from GD12.5 to GD18.5, whereas PE(P-18:0_16:0) was significantly lower ($p = 0.01$) at GD18.5 only (Figure **3.5 D**).

Gestation had a significant effects on all the ethanolamine-based fatty acyl species clustered in Q3 of PCA biplot; as gestation progressed from GD12.5 to GD18.5, PE(18:0_20:4) and PE(18:0_22:4)] significantly increased ($p < 0.0001$ and $p = 0.0004$, respectively) in both low and high n-3 PUFA groups, whereas PE(18:0_22:5) increased ($p = 0.01$) in low n-3 PUFA group only (Figure **3.5 E**). Diet had no significant effect ($p > 0.05$) on PE(18:0_20:4) level in the fetal brain; however, a diet high in n-3 PUFA showed lower levels of PE(18:0_22:4) at both gestation stages and PE(18:0_22:5) at GD18.5 only, compared with the low n-3 PUFA diet (Figure **3.5 E**). DHA-containing ethanolamine-based fatty acyl species [PE(16:0_22:6)] significantly increased ($p < 0.0001$) in the fetal brain as gestation progressed from GD12.5 to GD18.5. A maternal diet high in n-3 PUFA significantly promoted the accretion of PE(16:0_22:6) in the fetal brain by 2-fold, $p < 0.0001$ as gestation progressed from GD12.5 to GD18.5, compared with a low n-3 PUFA diet (Figure **3.5 E**).

As shown in Figure **3.5 F**, gestation had a significant effect on the ethanolamine-based fatty acyl species clustered in the 4th quadrant (Q4), except OA-containing ethanolamine-based fatty acyl species [PE(18:0_18:1)]. DHA-containing ethanolamine-based fatty acyl species [PE(18:0_22:6), PE(O-16:1_22:6), and PE(O-18:1_22:6)] significantly increased ($p < 0.0001$) in both low and high n-3 PUFA groups as gestation progressed from GD12.5 to GD18.5 (Figure **3.5 F**).

Diet also had a significant effect on all the ethanolamine-based fatty acyl species clustered in the 4th quadrant (Q4). As gestation progressed from GD12.5 to GD18.5, maternal diets high in n-3 PUFA significantly increased ($p < 0.0001$) the levels of OA-containing ethanolamine-based GP [PE(18:0_18:1)], compared with low n-3 PUFA diets. Maternal diets high in n-3 PUFA promoted the accretion of DHA-containing ethanolamine-based fatty acyl species [PE(18:0_22:6),

PE(O-16:1_22:6), and PE(O-18:1_22:6), $p < 0.0001$] species by approximately 2-fold, compared with low n-3 PUFA diets (Figure **3.5 F**). Interestingly, the accretion of DHA-enriched PE species in the high n-3 PUFA group at GD12.5 was equivalent to that of low n-3 PUFA group at GD18.5. (Figure **3.5 F**).

3.5 Effects of maternal diets high or low in n-3 PUFA on choline-based fatty acyl species in the fetal brain during gestation

We conducted PLAS-DA analysis on the 40 choline-based fatty acyl species and 16 of the species with VIP scores ≥ 1.0 (Figure **3.6 A**) were subjected to PCA analysis. As shown in the PCA biplot (Figure **3.6 B**), these 16 choline-based fatty acyl species were clearly separated into four quadrants with accumulated variability components, F1 and F2, explaining the 74.90% variation in clustering. Palmitoleic acid-containing [PC(O-16:0_16:1)], DHA-containing [PC(16:1_22:6), PC(16:0_22:6) and LPC(22:6)], 20:3-containing [PC(18:0_20:3)] and arachidic acid-containing [PC(18:1_20:0)] choline-based fatty acyl species were clustered in quadrant (Q)1, corresponding with high n-3 PUFA at GD18.5 (Figure **3.6 B**). Stearic acid-containing [PC(18:1_18:0) and PC(16:0_18:0)] and palmitoleic acid-containing [PC(14:0_16:1) and PC(16:1_16:1)] choline-based fatty acyl species were clustered in Q2, corresponding with low n-3 PUFA at GD18.5 (Figure 3.6 B). ARA-containing [PC(18:1_20:4) and PC(16:0_20:4)] choline-based fatty acyl species were clustered in Q3, corresponding with low n-3 PUFA at GD12.5 (Figure **3.6 B**). Dihomo-γ-linolenic acid (20:3n-6; DGLA)-containing [PC(16:0_20:3)] and DHA-containing [PC(18:0_22:6)] choline-based fatty acyl species were clustered in Q4, corresponding with high n-3 PUFA at GD12.5 (Figure **3.6 B**).

As gestation progressed, DHA-containing choline-based fatty acyl species [PC(16:0_22:6) and LPC(22:6), $p = 0.01$ and $p < 0.0001$, respectively] increased in both low and high n-3 PUFA groups, whereas arachidic acid-containing PC [PC(18:1_20:0), $p < 0.0001$] significantly increased ($p < 0.0001$) at GD18.5 only (Figure **3.6 C**). Gestation had no significant effect on PC(18:0_20:3), PC(16:1_22:6) and PC(O-16:0_16:1) species clustered in quadrant (Q) 1 of PCA biplot (Figure **3.6 C**). A diet high in n-3 PUFA significantly increased the accretion of DHA-containing choline-based [PC(16:0_22:6) and LPC(22:6), $p < 0.0001$ and $p < 0.0001$, respectively] at both gestation stages, whereas DGLA-containing [PC(18:0_20:3) ($p = 0.001$)], DHA-containing [PC(16:1_22:6), $p < 0.0001$)], arachidic acid-containing [PC(18:1_20:0), $p < 0.0001$], and palmitoleic acid-containing [PC(O-16:0_16:1), $p = 0.0005$] choline-based fatty acyl species increased at GD18.5 only (Figure **3.6 C**). There was significantly interaction between diet and gestation for PC(18:1_20:0) and LPC(22:6), $p = 0.01$ and $p = 0.0009$, respectively (Figure **3.6 C**).

Figure **3.6 D** shows that as gestation progressed, choline-based fatty acyl species clustered in Q2 of PCA biplot [PC(16:1_16:1), PC(18:1_18:0), PC(16:0_18:0), and PC(14:0_16:1)] significantly increased ($p < 0.0001$) in both low and high n-3 PUFA groups. Diet had a significant effects on choline-based fatty acyl species clustered in Q2, except PC(16:1_16:1). As gestation progressed, maternal diets high in n-3 PUFA increased the level of stearic acid-containing choline-based fatty acyl species [PC(18:1_18:0), $p < 0.0001$] in fetal brain at both gestation stages, whereas PC(18:1_18:0) and PC(14:0_16:1) significantly increased ($p = 0.007$ and $p = 0.006$, respectively) at GD18.5 only (Figure **3.6 D**). There was a significant interaction between diet and gestation ($p = 0.004$) for PC(16:1_16:1) (Figure **3.6 D**).

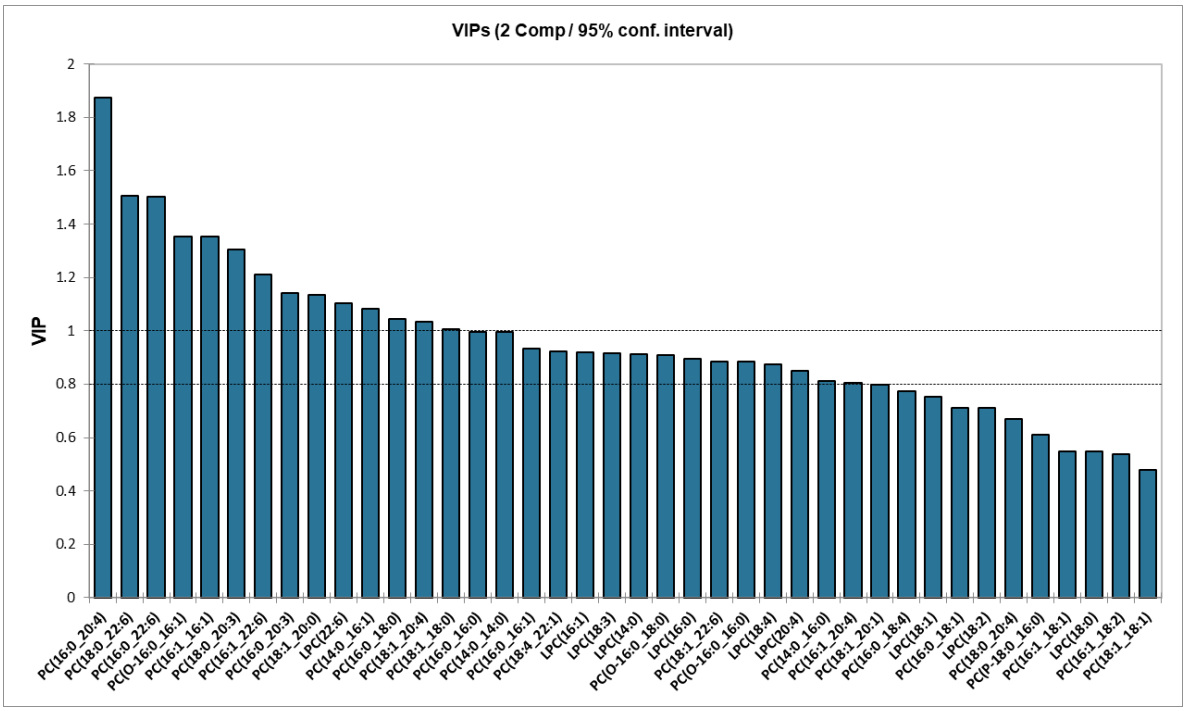
VIPs (2 Comp / 95% conf. interval)
VIP
2
1.8
1.6
1.4
1.2
1
0.8
0.6
0.4
0.2
0
PC(16:0_20:4)
PC(18:0_22:6)
PC(16:0_22:6)
PC(O-16:0_16:1)
PC(16:1_16:1)
PC(18:0_20:3)
PC(16:1_22:6)
PC(16:0_20:3)
PC(18:1_20:0)
LPC(22:6)
PC(14:0_16:1)
PC(16:0_18:0)
PC(18:1_20:4)
PC(18:1_18:0)
PC(16:0_16:0)
PC(14:0_14:0)
PC(16:0_16:1)
PC(18:4_22:1)
LPC(16:1)
LPC(18:3)
LPC(14:0)
PC(O-16:0_18:0)
LPC(16:0)
PC(18:1_22:6)
PC(O-16:0_16:0)
LPC(18:4)
LPC(20:4)
PC(14:0_16:0)
PC(16:1_20:4)
PC(18:1_20:1)
PC(16:0_18:4)
LPC(18:1)
PC(16:0_18:1)
LPC(18:2)
PC(18:0_20:4)
PC(P-18:0_16:0)
PC(16:1_18:1)
LPC(18:0)
PC(16:1_18:2)
PC(18:1_18:1)

A

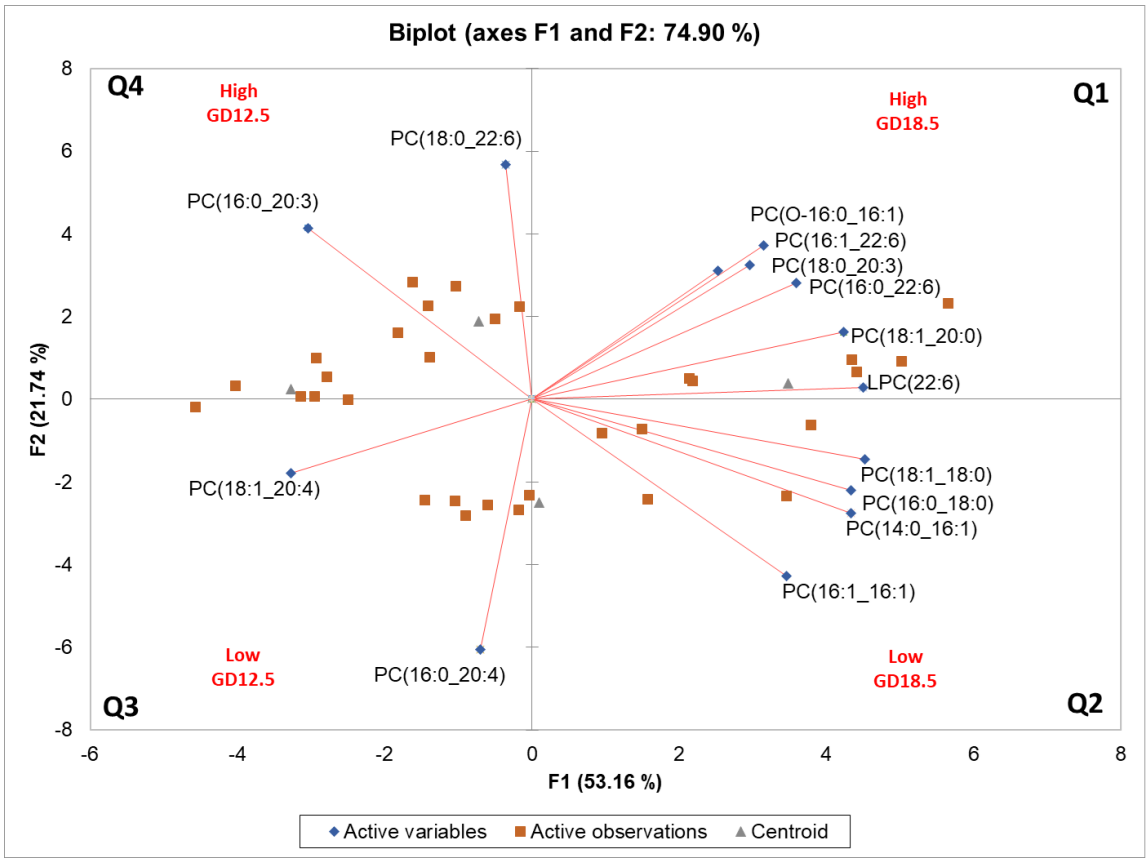
Biplot (axes F1 and F2: 74.90 %)
Q4
High
GD12.5
Q1
High
GD18.5
Q3
Low
GD12.5
Q2
Low
GD18.5
PC(18:0_22:6)
PC(16:0_20:3)
PC(O-16:0_16:1)
PC(16:1_22:6)
PC(18:0_20:3)
PC(16:0_22:6)
PC(18:1_20:0)
LPC(22:6)
PC(18:1_20:4)
PC(18:1_18:0)
PC(18:1_18:0)
PC(16:0_18:0)
PC(14:0_16:1)
PC(16:1_16:1)
PC(18:1_20:4)
PC(16:0_20:4)
F2 (21.74 %)
F1 (53.16 %)
8
6
4
2
0
-2
-4
-6
-8
-6
-4
-2
0
2
4
6
8
Active variables
Active observations
Centroid

B

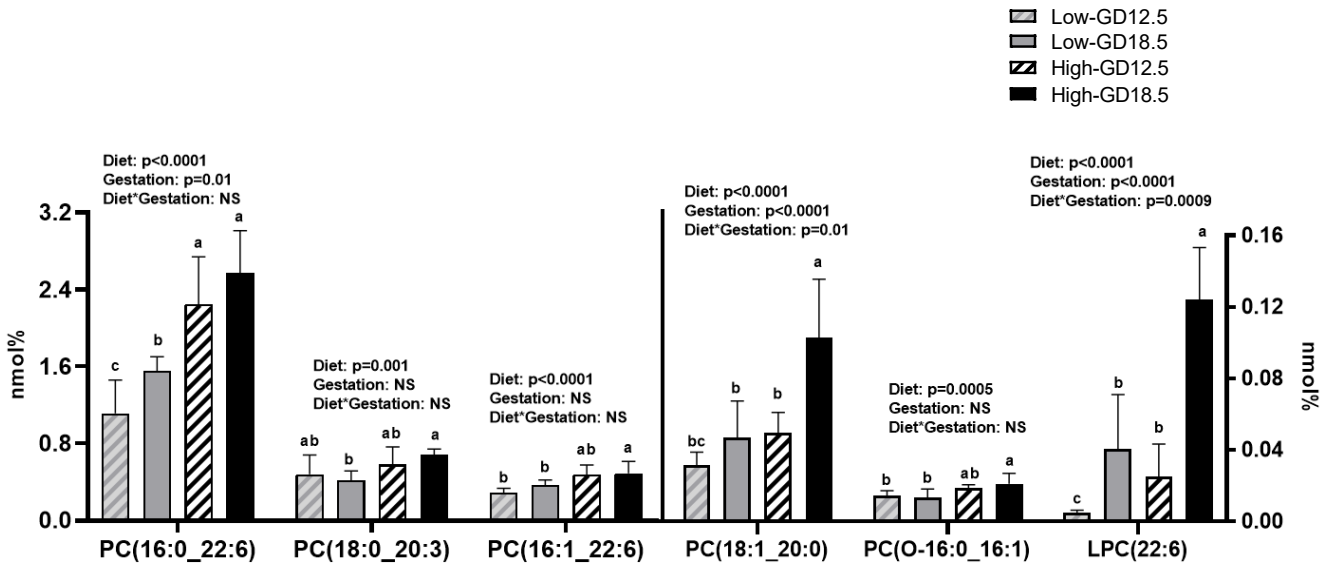
Low-GD12.5
Low-GD18.5
High-GD12.5
High-GD18.5
nmol%
Diet: p<0.0001
Gestation: p=0.01
Diet*Gestation: NS
Diet: p=0.001
Gestation: NS
Diet*Gestation: NS
Diet: p<0.0001
Gestation: NS
Diet*Gestation: NS
Diet: p<0.0001
Gestation: p<0.0001
Diet*Gestation: p=0.01
Diet: p=0.0005
Gestation: NS
Diet*Gestation: NS
Diet: p<0.0001
Gestation: p<0.0001
Diet*Gestation: p=0.0009
PC(16:0_22:6)
PC(18:0_20:3)
PC(16:1_22:6)
PC(18:1_20:0)
PC(O-16:0_16:1)
LPC(22:6)

C

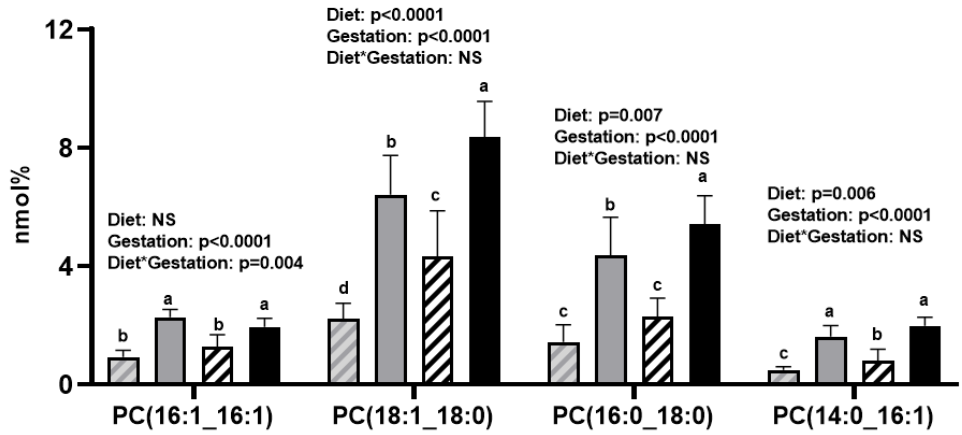
nmol%
Diet: NS
Gestation: p<0.0001
Diet*Gestation: p=0.004
Diet: p<0.0001
Gestation: p<0.0001
Diet*Gestation: NS
Diet: p=0.007
Gestation: p<0.0001
Diet*Gestation: NS
Diet: p=0.006
Gestation: p<0.0001
Diet*Gestation: NS
PC(16:1_16:1)
PC(18:1_18:0)
PC(16:0_18:0)
PC(14:0_16:1)

D

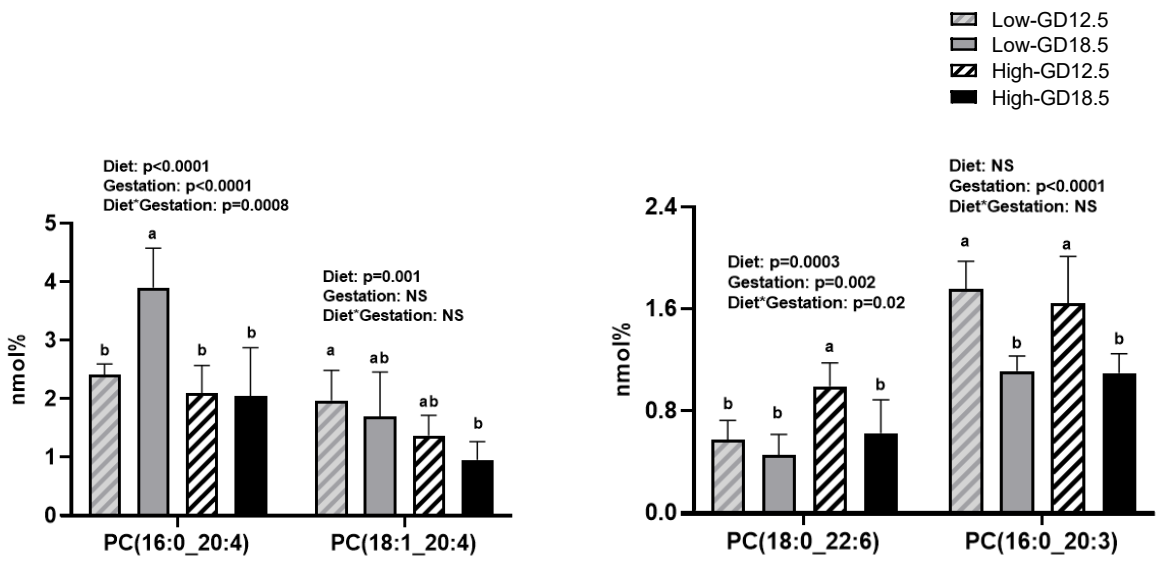

E F

Figure 3.6: Effects of maternal diets high or low in n-3 PUFA on choline-based fatty acyl species in fetal brain during gestation. ***A)*** *Partial least-squares discriminant analysis (PLS-DA) score plot showing their variability importance in the progression (VIP);* ***B)*** *Principal component analysis (PCA) score plot of the choline-based fatty acyl species; choline-based fatty acyl species clustered in -* ***C)*** *quadrant 1;* ***D)*** *quadrant 2,* ***E)*** *quadrant 3, and* ***F)*** *quadrant 4. Female mice were fed diets containing 1% n-3 PUFA (low n-3 PUFA diet) and 9% n-3 PUFA (high n-3 PUFA) during gestation and fetal brain choline-based fatty acyl species at gestation days (GD)12.5 and GD18.5 were determined. Data were analyzed using two-way ANOVA to determine the main effects and the interactions between maternal diet and gestation stage; pairwise comparison using Bonferroni's correction was used to determine differences. Data represent the mean ± SD of nmol% of each of choline-based fatty acyl species in total choline-based fatty acyl species. Mean values with different superscript letters (a, b, c & d) are significantly different; $p<0.05$ ($n = 8$ dams per group). Diacyl phosphatidylcholine (PC) and polyunsaturated fatty acids (PUFA), gestation day (GD).*

Gestation had a significant effect on PC(16:0_20:4), but not on PC(18:1_20:4) which were clustered in Q3; as gestation progressed, PC(16:0_20:4) significantly increased ($p < 0.0001$) in low n-3 PUFA diet group only without significant change in high n-3 PUFA group (Figure **3.6 E**). Diet had a significant effect on PC(16:0_20:4) and PC(18:1_20:4); a maternal diet high in n-3 PUFA showed significantly lower level of PC(16:0_20:4), $p < 0.0001$ at GD18.5 only, whereas a high n-3 PUFA diet showed significantly lower level of PC(18:1_20:4), $p = 0.001$ at GD18.5 compared with low n-3 PUFA diet at GD12.5. There was significant interaction between diet and gestation for PC(16:0_20:4), $p = 0.0008$ (Figure **3.6 E**).

Gestation had a significant effect on lipid species clustered in Q4 of PCA biplot; as gestation progressed, DHA-containing PC [PC(18:0_22:6)] significantly decreased ($p = 0.002$) only in high n-3 PUFA diet group with no significant change ($p > 0.05$) in low n-3 PUFA group, whereas PC(16:0_20:3) significantly decreased ($p < 0.0001$) in both low and high n-3 PUFA groups (Figure **3.6 F**). Diet had significant effects on choline-based GP species clustered in Q4 of PCA biplot [PC(16:0_22:6)] but not PC(16:0_20:3) (Figure **3.6 F**). A maternal diet high in n-3 PUFA significantly promoted accretion of PC(16:0_22:6), $p = 0.0003$ at GD18.5 only, compared with low n-3 PUFA diet. There was a significant interaction between diet and gestation ($p = 0.02$) on PC(16:0_22:6) (Figure **3.6 F**).

3.6 Effects of maternal diets high or low in n-3 PUFA on minor brain lipids in the fetal brain during gestation

As shown in the PLS-DA score plot (Figure **3.7 A**), 13 of 26 minor brain lipids (PG, PS, CE, Cer, and PI) had VIP score ≥ 1.0, showing that they are affected by either or both diet and gestation. There was a clear separation of these 13 minor lipid species into different quadrants in

the PCA biplot with accumulated variability components, F1 and F2 explaining 80.59% variance in clustering of the lipid species (Figure **3.7 B**).

DHA-containing CE [CE(22:6)], OA-containing PG [PG(18:1_18:1) and PG(18:0_18:1)] and PA-containing PG [PG(16:0_16:0)] were clustered in Q1, corresponding with high n-3 PUFA diet at GD12.5 (Figure **3.7 B**, High-GD12.5, Q1). OA-containing PG [PG(16:0_18:1)], DHA-containing PS [PS(18:0_22:6)], palmitoleic acid-containing PG [PG(16:0_16:1)] and stearic acid-containing Cer [Cer(d18:2_18:0) and Cer(d18:1_18:0)] were clustered in Q2 of PCA biplot, corresponding with high n-3 PUFA diet at GD18.5 (Figure **3.7 B**, High-GD18.5, Q2). EPA-containing PS [PS(18:0_22:5)] was the only minor brain lipid species clustered in Q3 of PCA biplot, corresponding with low n-3 PUFA diet at GD18.5 (Figure **3.7 B**, Low-GD18.5, Q3). ARA-containing PI [PI(18:0_20:4)], PA-containing Cer [Cer(d18:1_16:0)] and ADA-containing PS [PS(18:0_22:4)] were clustered in Q4 of PCA biplot, corresponding with low n-3 PUFA diet at GD12.5 (Figure **3.7 B**, Low-GD12.5, Q4).

Gestation had a significant effect on all the minor brain lipids clustered in Q1 of PCA biplot; as gestation progressed, oleic acid (18:1)-containing PG [PG(18:1_18:1)] significantly decreased ($p = 0.0008$) in high n-3 PUFA diet group, with no significant change in low n-3 PUFA group, whereas PG(18:0_18:1) and PG(16:0_18:1) significantly increased ($p < 0.0001$) in both low and high n-3 PUFA groups (Figure **3.7 C**). DHA-containing CE [CE(22:6)] significantly decreased ($p < 0.0001$) as gestation progressed from GD12.5 to GD18.5 in the high n-3 PUFA diet group only with no significant change in low n-3 PUFA groups (Figure **3.7 C**).

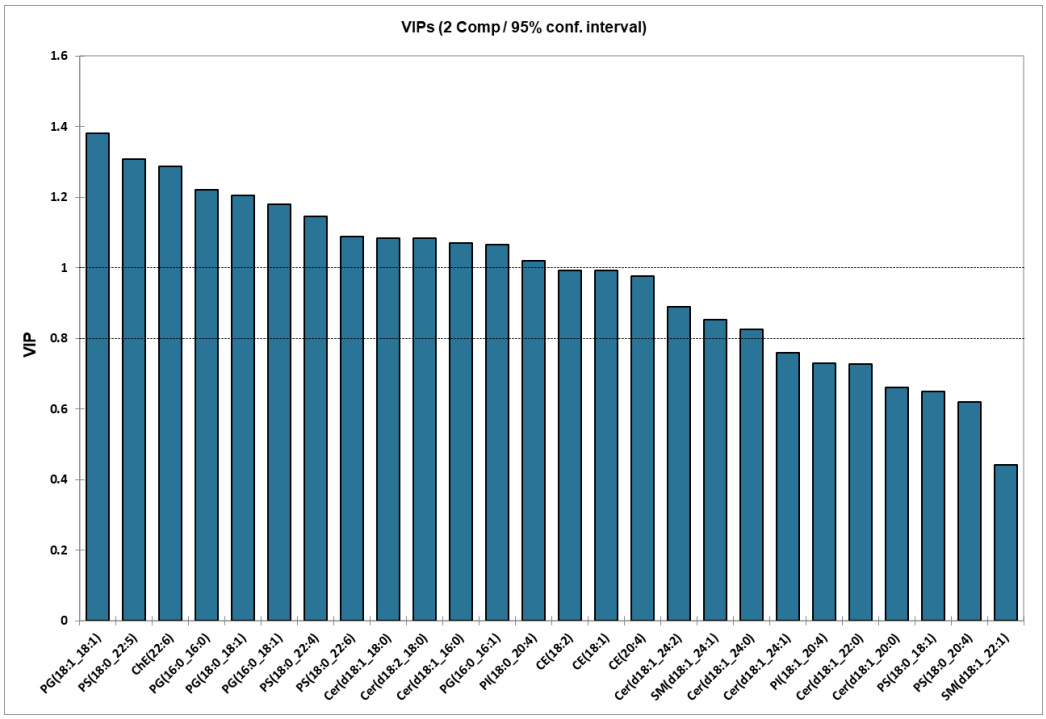
VIPs (2 Comp / 95% conf. interval)
VIP
1.6
1.4
1.2
1
0.8
0.6
0.4
0.2
0
PG(18:1_18:1)
PS(18:0_22:5)
CholE(22:6)
PG(16:0_16:0)
PG(18:0_18:1)
PG(16:0_18:1)
PS(18:0_22:4)
PS(18:0_22:6)
Cer(d18:1_18:0)
Cer(d18:2_18:0)
Cer(d18:1_16:0)
PG(16:0_16:1)
PI(18:0_20:4)
CE(18:2)
CE(18:1)
CE(20:4)
Cer(d18:1_24:2)
SM(d18:1_24:1)
Cer(d18:1_24:0)
Cer(d18:1_24:1)
PI(18:1_20:4)
Cer(d18:1_22:0)
Cer(d18:1_20:0)
PS(18:0_18:1)
PS(18:0_20:4)
SM(d18:1_22:1)

A

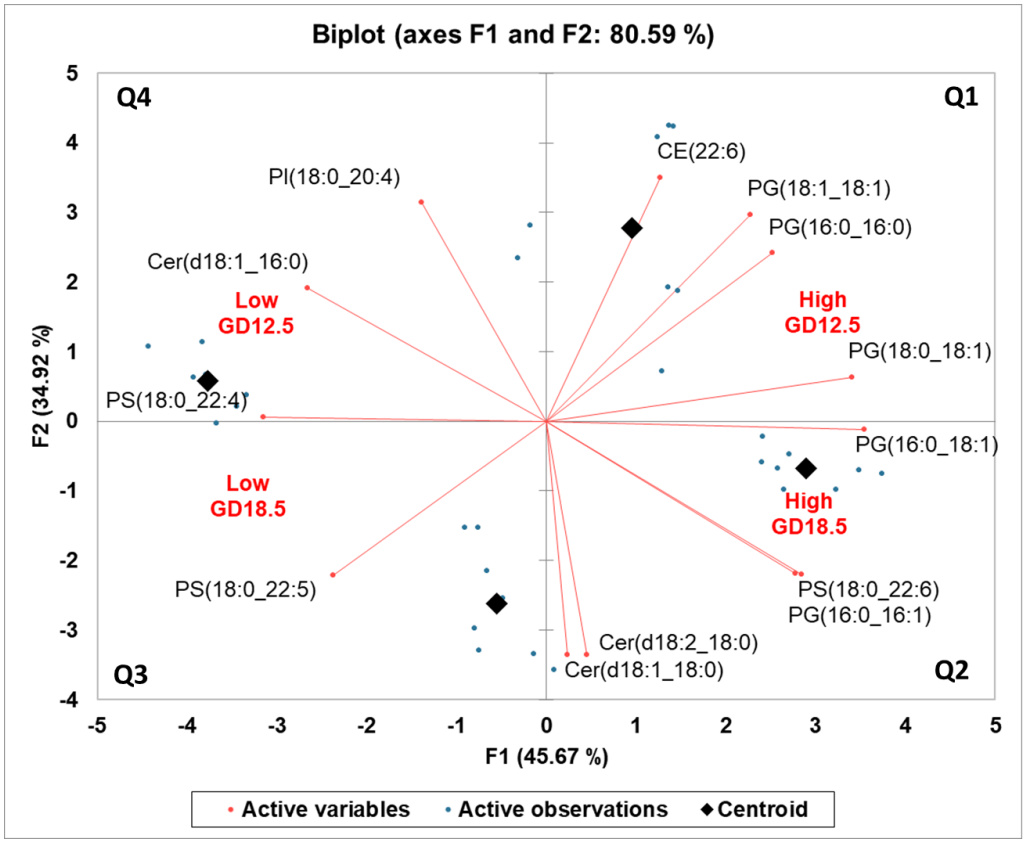
Biplot (axes F1 and F2: 80.59 %)
Q4
Q1
Q3
Q2
CE(22:6)
PI(18:0_20:4)
PG(18:1_18:1)
PG(16:0_16:0)
Cer(d18:1_16:0)
Low
GD12.5
High
GD12.5
PG(18:0_18:1)
PS(18:0_22:4)
PG(16:0_18:1)
Low
GD18.5
High
GD18.5
PS(18:0_22:5)
PS(18:0_22:6)
PG(16:0_16:1)
Cer(d18:2_18:0)
Cer(d18:1_18:0)
F2 (34.92 %)
F1 (45.67 %)
5
4
3
2
1
0
-1
-2
-3
-4
-5
Active variables
Active observations
Centroid

B

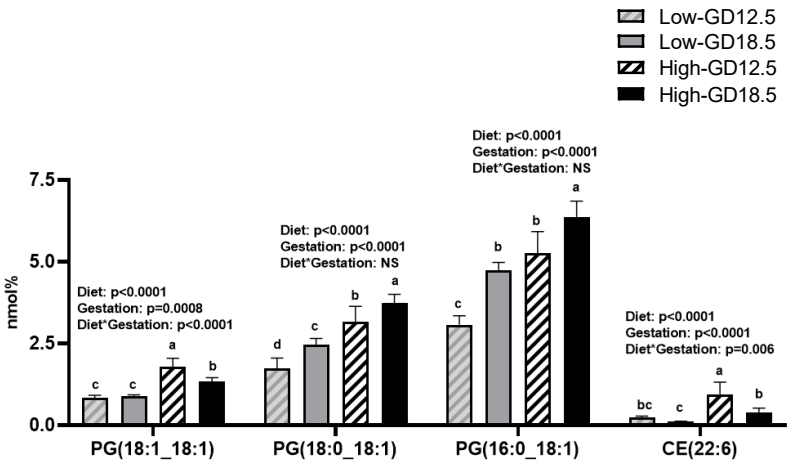
Low-GD12.5
Low-GD18.5
High-GD12.5
High-GD18.5
nmol%
7.5
5.0
2.5
0.0
Diet: p<0.0001
Gestation: p=0.0008
Diet*Gestation: p<0.0001
Diet: p<0.0001
Gestation: p<0.0001
Diet*Gestation: NS
Diet: p<0.0001
Gestation: p<0.0001
Diet*Gestation: NS
Diet: p<0.0001
Gestation: p<0.0001
Diet*Gestation: p=0.006
PG(18:1_18:1)
PG(18:0_18:1)
PG(16:0_18:1)
CE(22:6)

C

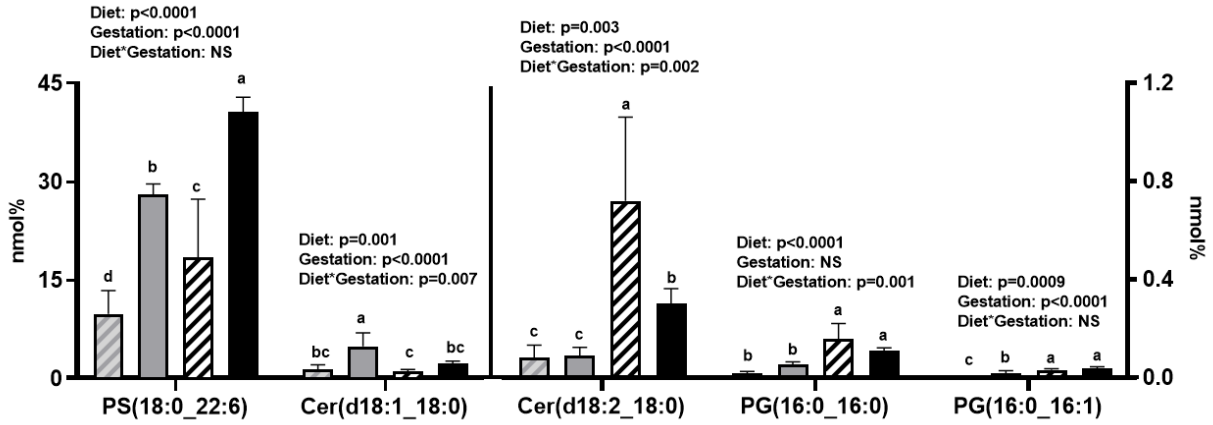
Diet: p<0.0001
Gestation: p<0.0001
Diet*Gestation: NS
Diet: p=0.003
Gestation: p<0.0001
Diet*Gestation: p=0.002
nmol%
45
30
15
0
1.2
0.8
0.4
0.0
Diet: p=0.001
Gestation: p<0.0001
Diet*Gestation: p=0.007
Diet: p<0.0001
Gestation: NS
Diet*Gestation: p=0.001
Diet: p=0.0009
Gestation: p<0.0001
Diet*Gestation: NS
PS(18:0_22:6)
Cer(d18:1_18:0)
Cer(d18:2_18:0)
PG(16:0_16:0)
PG(16:0_16:1)

D

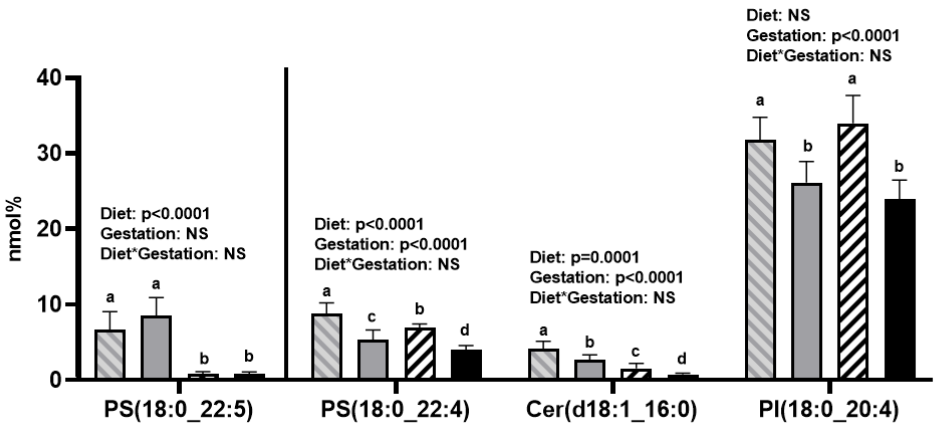
Diet: NS
Gestation: p<0.0001
Diet*Gestation: NS
nmol%
40
30
20
10
0
Diet: p<0.0001
Gestation: NS
Diet*Gestation: NS
Diet: p<0.0001
Gestation: p<0.0001
Diet*Gestation: NS
Diet: p=0.0001
Gestation: p<0.0001
Diet*Gestation: NS
PS(18:0_22:5)
PS(18:0_22:4)
Cer(d18:1_16:0)
PI(18:0_20:4)

E

Figure 3.7: Effects of maternal diets high or low in n-3 PUFA on minor brain lipid fatty acyl species in fetal brain during gestation. ***A)*** *Partial least-squares discriminant analysis (PLS-DA) score plot showing their variability importance in the progression (VIP);* ***B)*** *Principal component analysis (PCA) score plot of the minor brain lipid fatty acyl species; minor brain lipid fatty acyl species clustered in -* ***C)*** *quadrant 1;* ***D)*** *quadrant 2,* ***E)*** *quadrants 3 and 4. Female mice were fed diets containing 1% n-3 PUFA (low n-3 PUFA diet) and 9% n-3 PUFA (high n-3 PUFA) during gestation and fetal brain minor brain lipids fatty acyl species at gestation days (GD)12.5 and GD18.5 were determined. Data were analysed using two-way ANOVA to determine the main effects and the interactions between maternal diet and gestation stage; pairwise comparison using Bonferroni's correction was used to determine differences when there was an observed interaction. Data represent the mean ± SD of nmol% of each of minor brain lipid fatty acyl species in total of each of the minor brain lipid class. Mean values with different superscript letters (a, b, c & d) are significantly different; $p<0.05$ ($n = 8$ dams per group). Phosphatidylglycerol (PG), cholesteryl esters (CE), phosphatidylserine (PS), phosphatidylinositol (PI), ceramide (Cer), polyunsaturated fatty acids (PUFA), and gestation day (GD).*

A maternal diet high in n-3 PUFA significantly increased oleic acid (18:1)-containing PG [PG(18:1_18:1), PG(18:0_18:1) and PG(16:0_18:1), $p = 0.0008$, $p < 0.0001$ and $p < 0.0001$, respectively] and DHA-containing CE [CE(22:6), $p < 0.0001$] minor brain lipids, compared with low n-3 PUFA diet (Figure **3.7 C**). There were significant interaction between diet and gestation in PG(18:0_18:1) and CE(22:6), $p < 0.0001$ and $p = 0.006$, respectively (Figure **3.7 C**). As gestation progressed from GD12.5 to GD18.5, DHA-containing PS [PS(18:0_22:6), $p < 0.0001$] significantly increased in both low and high n-3 PUFA groups, whereas stearic acid (18:0)-containing Cer [Cer(d18:1_18:0), $p < 0.0001$] and palmitoleic acid (16:1)-containing PG [PG(16:0_16:1), $p < 0.0001$] significantly increased in the low n-3 PUFA group (Figure **3.7 D**). Stearic acid-containing Cer [Cer(d18:2_18:0)] significantly decreased ($p < 0.0001$) as gestation progressed in the high n-3 PUFA group only, whereas gestation had no significant effect on PG(16:0_16:0) (Figure **3.7 D**).

Diet had a significant effect on all the minor brain lipids clustered in Q2 of PCA biplot; a maternal diet high in n-3 PUFA significantly increased DHA-containing PS [PS(18:0_22:6), $p < 0.0001$] in the fetal brain at both gestation stages. A maternal diet high in n-3 PUFA showed significantly lower level ($p = 0.001$) of Cer(d18:1_18:0) at GD18.5, whereas a high n-3 PUFA diet showed significantly higher level of Cer(d18:2_18:0), PG(16:0_16:0) and PG(16:0_16:1), $p = 0.003$, $p < 0.0001$ and $p = 0.0009$, respectively at both gestation stages (Figure **3.7 D**). There was a significant interaction between diet and gestation for Cer(d18:1_18:0), Cer(d18:2_18:0) and PG(16:0_16:0), $p = 0.007$, $p = 0.002$ and $p = 0.001$, respectively (Figure **3.7 D**).

3.7 Effects of maternal diets high or low in n-3 PUFA on glycerolipids in the fetal brain during gestation

Fifteen GL species, including tri (TG) and di (DG)-acylglycerols had VIP score ≥ 1.0 showing that either or both diet and gestation influenced these species (Figure **3.8 A**). The PCA biplot showed a significant separation of these 15 species into four quadrants with combined variability components F1 and F2 explaining 71.49% variance in clustering of the lipid species (Figure **3.8 B**). OA-containing [DG(16:0_18:1)] DHA-containing GL species [TG(16:0_16:0_22:6) and TG(16:0_18:1_22:6)] and DGLA-containing [TG(16:0_20:3_20:3)] GL species were clustered in Q1 of PCA biplot, corresponding with high n-3 PUFA diet at GD18.5 (Figure **3.8 B**, High-GD18.5, Q1). ARA-containing [TG(O-12:0_6:0_20:4), TG(18:0_18:1_20:4) and TG(16:0_16:0_20:4)], PA-containing [TG(18:0_16:0_16:0) and TG(16:0_16:0_16:0)] and ALA-containing [TG(18:1_18:1_18:3)] GL species were clustered in Q2 of PCA biplot, corresponding with low n-3 PUFA diet at GD18.5 (Figure **3.8 B**, Low-GD18.5, Q2). LA-containing [TG(18:1_18:2_18:2) and TG(18:1_18:1_18:2)] and [TG(16:0_18:2_18:2)] GL species were clustered in Q3 of PCA biplot, corresponding with low n-3 PUFA diet at GD12.5 (Figure **3.8 B**, Low-GD12.5, Q3). Octanoic acid-containing [TG(8:0_8:0_8:0)] and stearic acid-containing [DG(18:0_18:0)] GL species were clustered in Q4 of PCA biplot, corresponding with high n-3 PUFA diet at GD12.5 (Figure **3.8 B**, High-GD12.5, Q4).

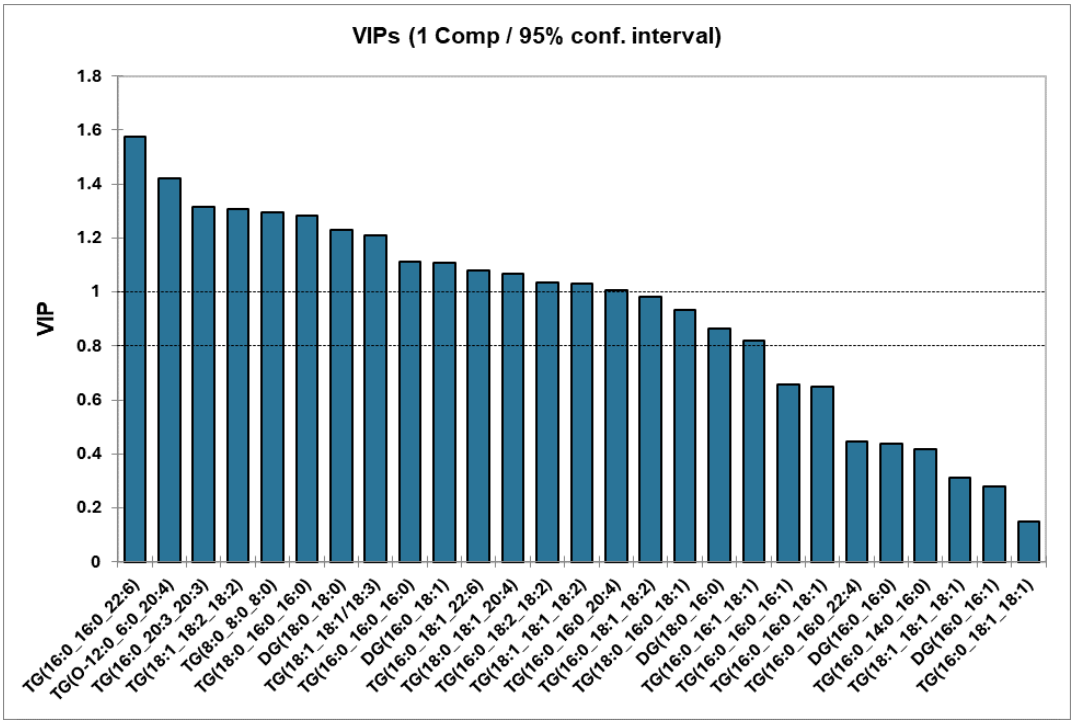
VIPs (1 Comp / 95% conf. interval)
VIP
1.8
1.6
1.4
1.2
1
0.8
0.6
0.4
0.2
0
TG(16:0_16:0_22:6)
TG(O-12:0_6:0_20:4)
TG(16:0_20:3_20:3)
TG(18:1_18:2_18:2)
TG(8:0_8:0_8:0)
TG(18:0_16:0_16:0)
DG(18:0_18:0)
TG(18:1_18:1/18:3)
TG(16:0_16:0_16:0)
DG(16:0_18:1)
TG(16:0_18:1_22:6)
TG(18:0_18:1_20:4)
TG(16:0_18:2_18:2)
TG(18:1_18:1_18:2)
TG(16:0_16:0_20:4)
TG(16:0_18:1_18:2)
TG(18:0_16:0_18:1)
DG(18:0_16:0)
TG(16:0_16:1_18:1)
TG(16:0_16:0_16:1)
TG(16:0_16:0_18:1)
TG(16:0_16:0_22:4)
DG(16:0_16:0)
TG(16:0_14:0_16:0)
TG(18:1_18:1_18:1)
DG(16:0_16:1)
TG(16:0_18:1_18:1)

A

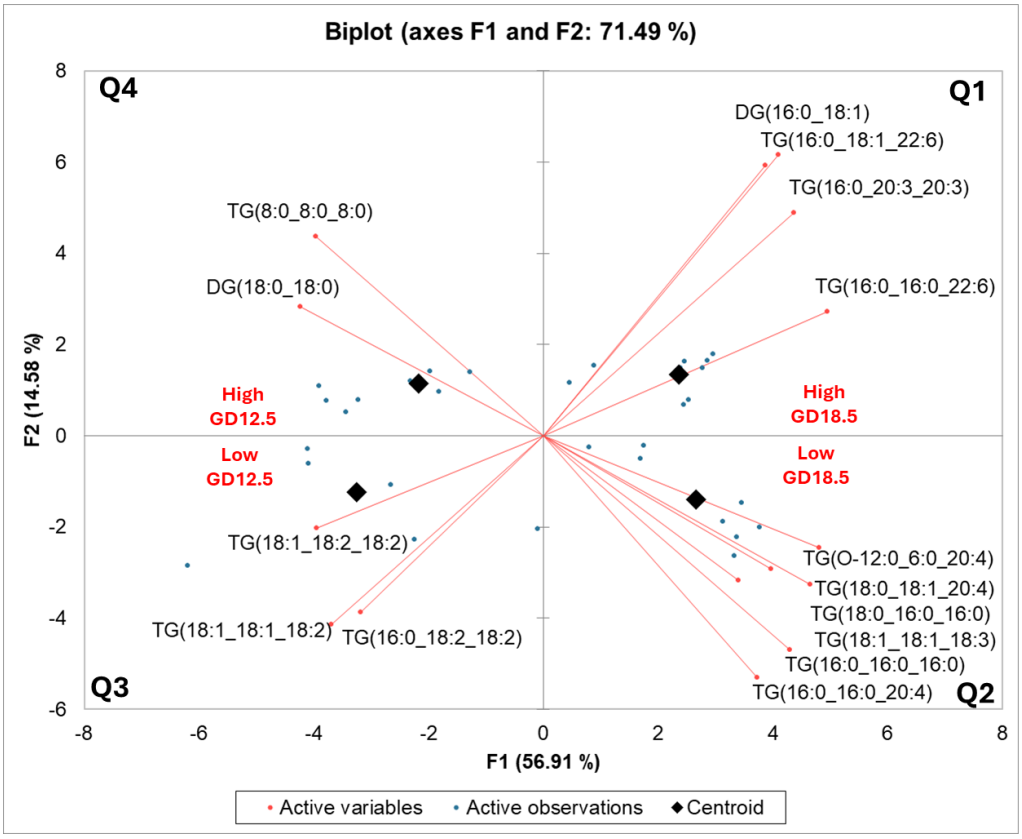
Biplot (axes F1 and F2: 71.49 %)
Q4
Q1
Q3
Q2
DG(16:0_18:1)
TG(16:0_18:1_22:6)
TG(16:0_20:3_20:3)
TG(8:0_8:0_8:0)
DG(18:0_18:0)
TG(16:0_16:0_22:6)
High GD12.5
Low GD12.5
High GD18.5
Low GD18.5
TG(18:1_18:2_18:2)
TG(O-12:0_6:0_20:4)
TG(18:0_18:1_20:4)
TG(18:0_16:0_16:0)
TG(18:1_18:1_18:3)
TG(16:0_16:0_16:0)
TG(18:1_18:1_18:2)
TG(16:0_18:2_18:2)
TG(16:0_16:0_20:4)
F2 (14.58 %)
F1 (56.91 %)
8
6
4
2
0
-2
-4
-6
-8
Active variables
Active observations
Centroid

B

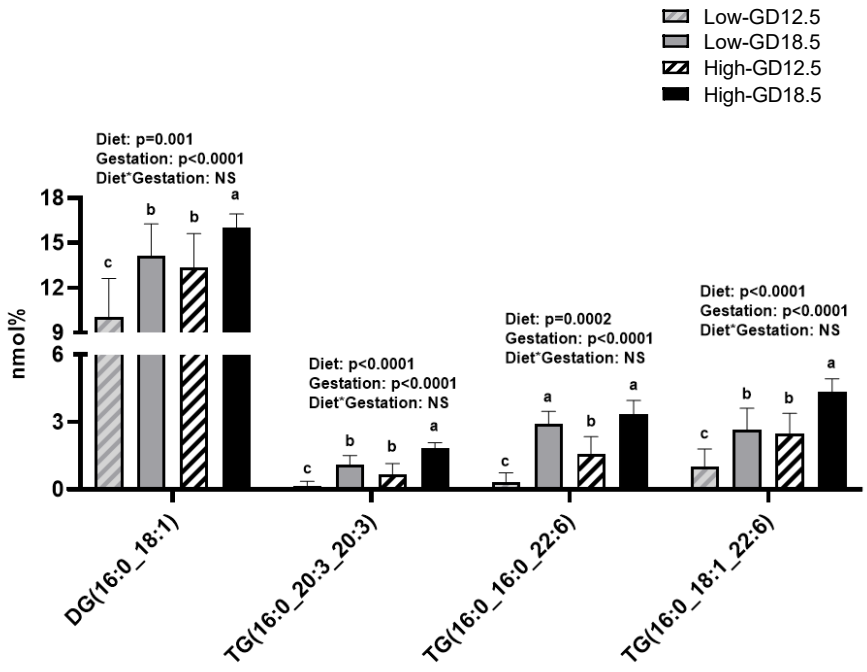
Low-GD12.5
Low-GD18.5
High-GD12.5
High-GD18.5
nmol%
Diet: p=0.001
Gestation: p<0.0001
Diet*Gestation: NS
Diet: p<0.0001
Gestation: p<0.0001
Diet*Gestation: NS
Diet: p=0.0002
Gestation: p<0.0001
Diet*Gestation: NS
Diet: p<0.0001
Gestation: p<0.0001
Diet*Gestation: NS
DG(16:0_18:1)
TG(16:0_20:3_20:3)
TG(16:0_16:0_22:6)
TG(16:0_18:1_22:6)

C

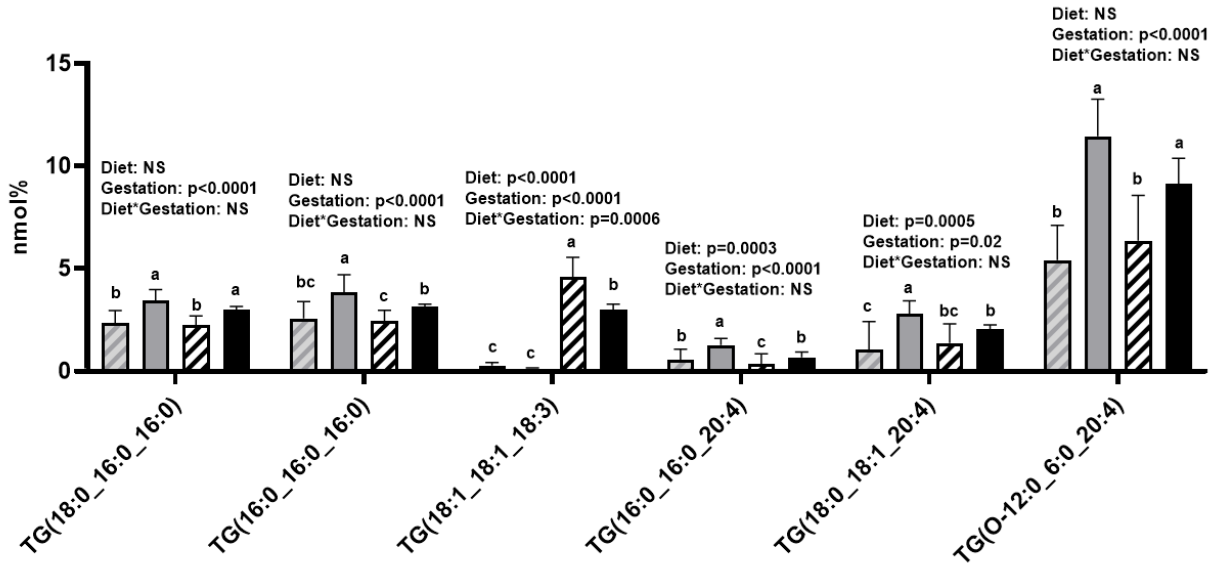
nmol%
Diet: NS
Gestation: p<0.0001
Diet*Gestation: NS
Diet: NS
Gestation: p<0.0001
Diet*Gestation: NS
Diet: p<0.0001
Gestation: p<0.0001
Diet*Gestation: p=0.0006
Diet: p=0.0003
Gestation: p<0.0001
Diet*Gestation: NS
Diet: p=0.0005
Gestation: p=0.02
Diet*Gestation: NS
Diet: NS
Gestation: p<0.0001
Diet*Gestation: NS
TG(18:0_16:0_16:0)
TG(16:0_16:0_16:0)
TG(18:1_18:1_18:3)
TG(16:0_16:0_20:4)
TG(18:0_18:1_20:4)
TG(O-12:0_6:0_20:4)

D

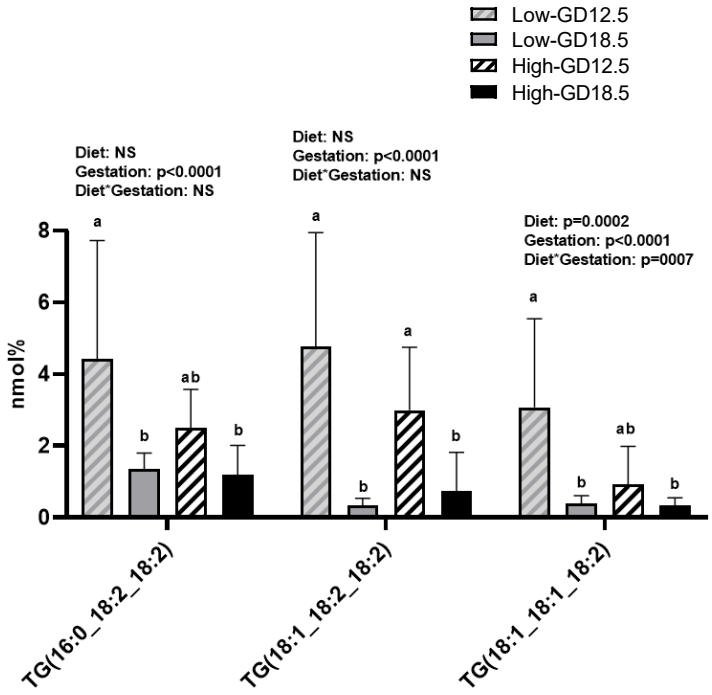

E

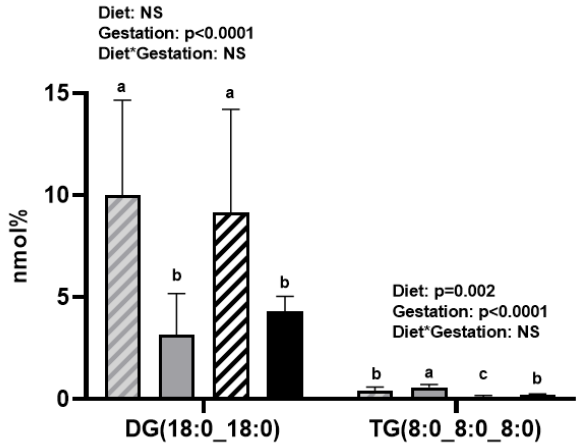

F

Figure 3.8: Effects of maternal diets high or low in n-3 PUFA on glycerolipids in the fetal brain during gestation. ***A)*** *Partial least-squares discriminant analysis (PLS-DA) score plot showing their variability importance in the progression (VIP);* ***B)*** *Principal component analysis (PCA) score plot of the glycerolipids fatty acyl species; glycerolipids fatty acyl species clustered in -* ***C)*** *quadrant 1;* ***D)*** *quadrant 2,* ***E)*** *quadrant 3, and* ***F)*** *quadrant 4. Female mice were fed diets*

containing either 1% n-3 PUFA (low n-3 PUFA diet) and 9% n-3 PUFA (high n-3 PUFA) during gestation and fetal brain glycerolipids (DG and TG) fatty acyl species at gestation days (GD)12.5 and GD18.5 were determined. Data were analyzed using two-way ANOVA to determine the main effects and the interactions between maternal diet and gestation stage; pairwise comparison using Bonferroni's correction was used to determine differences. Data represent the mean ± SD of nmol% of each fatty acyl species in the fetal brain total diacylglycerols and total triacyglycerols. Mean values with different superscript letters (a, b, c & d) are significantly different; $p < 0.05$ ($n = 8$ dams per group). Diacylglycerols (DG), triacylglycerols (TG), polyunsaturated fatty acids (PUFA), and gestation day (GD).

Gestation had a significant effect on the accretion of fetal brain GL species clustered in Q1 of PCA biplot; as gestation progressed, OA-containing DG [DG(16:0_18:1), $p < 0.0001$], DGLA-containing TG [TG(16:0_20:3_20:3), $p < 0.0001$], DHA-enriched [TG(16:0_16:0_22:6) and TG(16:0_18:1_22:6), $p < 0.0001$] GL species increased significantly in both low and high n-3 PUFA groups (Figure **3.8 C**). Diet had a significant effect on fetal brain GL species clustered in Q1 of PCA biplot; a maternal diet high in n-3 PUFA significantly increased the levels of DG(16:0_18:1), $p = 0.001$; TG(16:0_20:3_20:3), $p < 0.0001$; TG(16:0_16:0_22:6), $p = 0.0002$ and TG(16:0_18:1_22:6), $p < 0.0001$ as gestation progressed (Figure **3.8 C**).

Gestation had a significant effect on the accretion of fetal brain glycerolipids clustered in Q2 of PCA biplot; as gestation progressed, PA-containing [TG(18:0_16:0_16:0) and TG(16:0_16:0_16:0), $p < 0.0001$], ALA-containing [TG(18:1_18:1_18:3), $p < 0.0001$], ARA-containing [TG(18:0_18:1_20:4), and TG(O-12:0_6:0_20:4), $p < 0.0001$ and $p < 0.0001$, respectively] GL species significantly increased in both low and high n-3 PUFA groups, whereas TG(16:0_16:0_20:4) significantly increased at GD12.5 only (Figure **3.8 D**). Diet had a significant effect on ALA-containing [TG(18:1_18:1_18:3)] and ARA-containing [TG(18:0_18:1_20:4) and TG(16:0_16:0_20:4)]; a maternal diet high in n-3 PUFA showed significantly higher ($p < 0.0001$) level of TG(18:1_18:1_18:3) at both gestation stages, compared with low n-3 PUFA diet (Figure 3.16 B). High n-3 PUFA diet showed significantly lower ($p = 0.0003$) level of TG(16:0_16:0_20:4) at both gestation stages, whereas a maternal diet high in n-3 PUFA showed significantly lower ($p = 0.0005$) level of TG(18:0_18:1_20:4) at GD18.5 only, compared to low n-3 PUFA diet (Figure **3.8 D**). There was a significant interaction between diet and gestation in ALA-containing [TG(18:1_18:1_18:3), $p = 0.0006$ (Figure **3.8 D**).

Gestation had a significant effect on fetal brain glycerolipids clustered in Q3 of PCA biplot; LA-containing TG [TG(16:0_18:2_18:2 and TG(18:1_18:1_18:2), $p < 0.0001$] decreased as gestation progressed in low n-3 PUFA group only, whereas TG(18:1_18:2_18:2), $p < 0.0001$ decreased in both low and high n-3 PUFA groups as gestation progressed (Figure **3.8 E**). Maternal diet high in n-3 PUFA showed lower level of TG(18:1_18:1_18:2), $p = 0.0002$ in fetal brain at GD12.5 only, compared with low n-3 PUFA diet. There was a significant interaction between diet and gestation for TG(18:1_18:1_18:2), $p = 0.0007$ (Figure **3.8 E**).

Gestation had a significant effect on glycerolipids clustered in Q4 of PCA biplot; stearic acid-containing DG [DG(18:0_18:0)] and octanoic acid-containing TG [TG(8:0_8:0_8:0)] significantly decreased ($p < 0.0001$) as gestation progressed in both low and high n-3 PUFA group (Figure **3.8 F**). Diet had no significant effect on GL clustered in Q4 of PCA biplot (Figure **3.8 F**).

3.8 Heatmap visualization of actively variable fetal brain lipid species

The clustering of the actively varied fetal brain lipid species was visualized in a heatmap using MetaboAnalyst software 5.0 (https://new.metaboanalyst.ca/MetaboAnalyst/). Figure **3.9** shows that all the DHA-containing lipid species in fetal brain clustered with the high n-3 PUFA diet at GD18.5 region, irrespective of the lipid class. Results also showed that n-6 PUFA-containing lipid species decreased as gestation progressed, with lower levels found in high n-3 PUFA diet group, compared with low n-3 PUFA diet group. The results of the heatmap summarizes the results presented in previous subsections that as gestation progressed, the accretion of DHA-enriched lipid species increased and that maternal diets high in n-3 PUFA boost the accretion of DHA-enriched GP (Figure **3.9**).

3.9 Lipid metabolic pathways analysis and predicted effects of maternal n-3 PUFA diet on lipid metabolic pathways during gestation

Lipid metabolic analysis was performed using MetaboAnalyst software 5.0. Eight lipid pathways, including glycerophospholipids, steroid, glycosylphosphatidylinositol-anchor biosynthesis, glycerolipids, sphingolipid, arachidonic acid, linoleic acid, and α-linolenic acid metabolism pathways were impacted by n-3 PUFA diet (Figure **3.10 A).** Interestingly, the glycerophospholipid pathway had the highest number of hits (4 hits), whereas other pathways had only one hit each. Although sphingolipid pathways had only one hit, the pathway impact score (0.27) was higher than glycerophospholipids with 4 hits and an average pathway impact score of 0.26 (Table **3.2)**. Glycerolipid metabolic pathway with 1 hit has a pathway impact score of 0.014, while the GPI-anchor biosynthesis pathway has one hit and a pathway impact score of 0.004. Other pathways had very low pathway impact score less than 0.001 (Table **3.2)**. Statistically, glycerophospholipids and steroid metabolic pathways were significantly impacted by maternal n-3 PUFA diet with $p \leq 0.05$, whereas other lipid metabolic pathways were not statistically significantly ($p > 0.05$) impacted by maternal diet (Table **3.2**).

The impact of n-3 PUFA on major lipid species and predicted pathways implicated are shown in Figure **3.10 B**. Interestingly, the fold change of DHA-containing lipids showed that they were enriched (green arrows) while oleic acid, LA and some ARA-containing lipid species were depleted (black arrows) by high n-3 PUFA diets. It was speculated that the effect of maternal diets on fetal brain lipidome was through the predicted pathways by influencing the activities of key enzymes associated with speculated pathways (shown in yellowish-brown texts in Figure **3.10 B**).

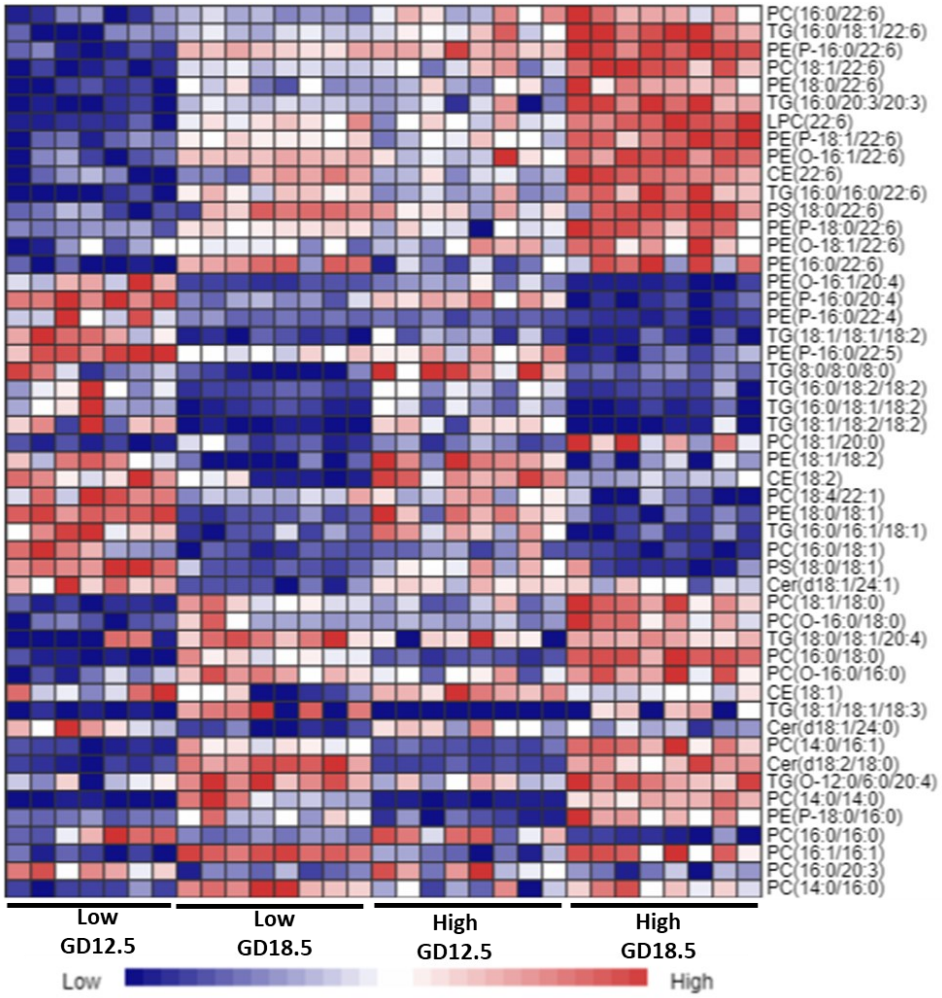

Figure 3.9: Heatmap visualization of major lipid species. *Lipid species in fetal brain were entered in MetaboAnalyst software 5.0 to visualize the enrichment (red cells) and depletion (blue cells) of different fetal lipid species in the experimental groups. Within low or high n-3 PUFA groups, lipid species with red cells at gestation day (GD)12.5 and blue cells at the GD18.5 shows depletion as gestation progressed from GD12.5 to GD18.5, whereas within GD12.5 and GD18.5, lipid species with blue cells in low n-3 PUFA and red cells at in high n-3 PUFA shows that maternal diet high in n-3 PUFA promoted the enrichment in the fetal brain. Note: the variation in nomenclature of lipids species in Figure 3.9 compared to other data is because MetaboAnalyst can only accepts the nomenclature shown in this Figure, and not the nomenclature on the other Figures/Tables.*

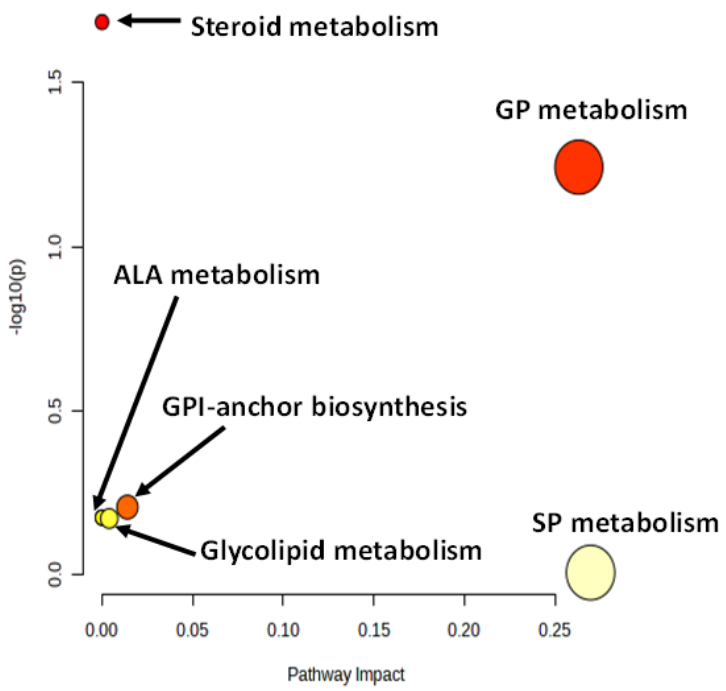

A

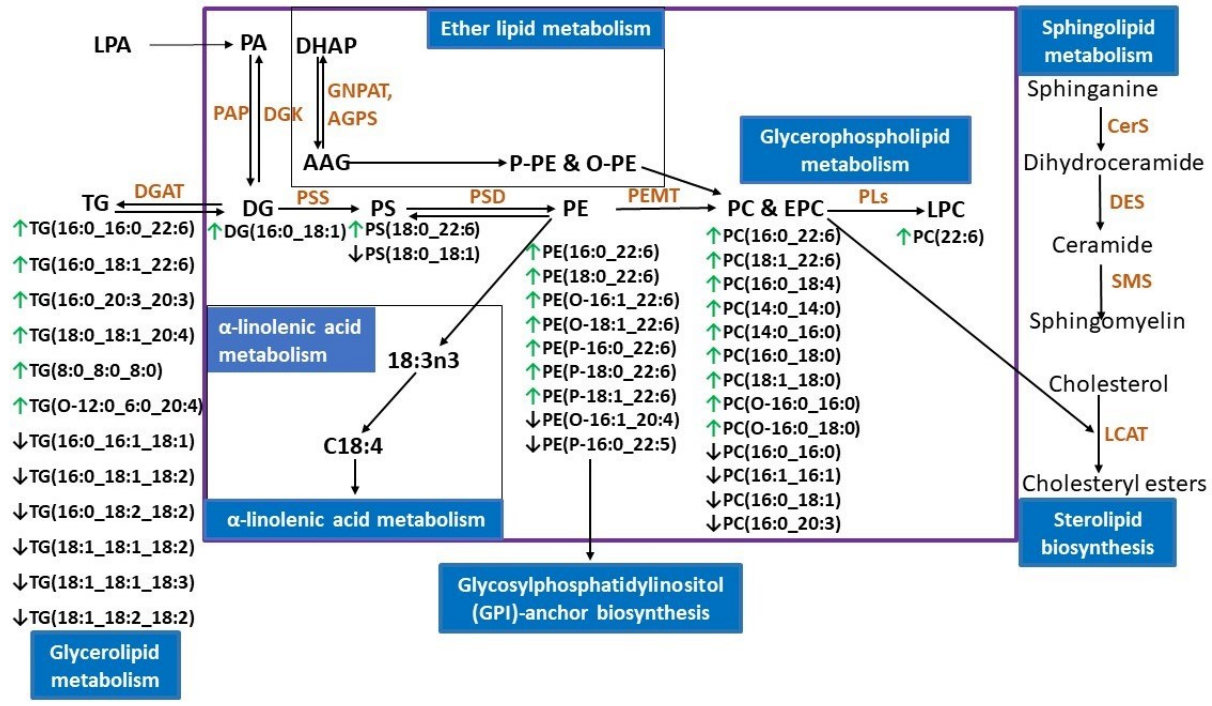

B

Figure 3.10: Lipid metabolic pathways analysis and predicted effects of maternal n-3 PUFA diet on lipid metabolic pathways during gestation. A) *Lipid species in fetal brain were entered in*

MetaboAnalyst software 5.0 to analyze the impact of diet on lipid metabolic pathways by matching fetal brain lipid species with compounds in human metabolic database of lipid metabolic pathways. The number of matching lipid species with compounds in a metabolic pathway database is identified as hits while the influence of diet on the pathways is ranked as pathway impact scores. Pathway score > 0.10 is considered substantially impacted by treatment under consideration (ex. n-3 PUFA) (Liu et al., 2019). ***B)*** *The difference between the mean of nmol% of high n-3 PUFA and low n-3 PUFA for each lipid species in fetal brain was calculated and species positive values represent enriched species (↑) while species with negative values were considered depleted species (↓). Based on the metabolic pathway the lipid species belong to, we predicted that the changes in levels of lipid species by n-3 PUFA could be linked with alteration in expression of key enzymes of the pathway (shown in yellowish brown texts). It was predicted that n-3 PUFA could affect the referenced pathways by altering the key enzymes of the pathways; the increased or decrease of glycerolipids species (DG and TG) could be attributed to alteration in specific phosphatidic acid phosphatase (PAP) and acyl-CoA:diacylglycerol acyltransferase (DGAT), respectively. We also predicted that n-3 PUFA could influence plasmalogens and plasmanyl species metabolism by altering the expression of glyceronephosphate O-acyltransferase (GNPAT) = alkylglycerone phosphate synthase (AGPS), by altering the key enzymes of ether lipids. For GP metabolic pathways, it was predicted that n-3 PUFA influenced DHA-containing PS, PE, PC and LPC species by altering PS synthases (PSS), PS decarboxylase (PSD), PE methyltransferase (PEMT) and phospholipases (PLs), respectively. For the SP and sterolipids metabolic pathways, the enzymes predicted to be affected were sphingosine phosphatases (SPP) and lecithin cholesterol acyl transferase (LCAT), respectively. Glycerophospholipids (GP); glycosylphosphatidylinositol (GPI); α-linolenic acid (ALA); sphingolipids (SP); phosphatidylserine (PS), phosphatidylcholine (PC); ethanolamine plasmalogens (P-PE); plasmanyl ethanolamine (O-PE), and plasmanyl choline (O-PC).*

We predicted that the increase in DHA-containing LPC by n-3 PUFA diet is predicted to be increased activity of specific phospholipases (PLs), while the increase in DHA-containing PE and PS species could be attributed to availability of DHA for synthesis of PE and an increase in the activity of PS synthase (PSS) and PS decarboxylase (PSD) in fetal brain. We also predicted that the influence of n-3 PUFA on glycerolipid metabolism (DG and TG species) could be attributed to altered expression of phosphatidic acid phosphatase and acyl-CoA:diacylglycerol acyltransferase-2 (DGAT-2), respectively (Figure **3.10 B)**.

As shown in Figure **3.10 B**, it is predicted that n-3 PUFA could influence metabolism of ether lipids, including ethanolamine plasmalogen, plasmanyl ethanolamine and plasmanyl choline, by altering the expression of glyceronephosphate O-acyltransferase (GNPAT) and alkylglycerone phosphate synthase (AGPS), the key enzymes of ether lipid metabolic pathways. Furthermore, alterations in GP metabolic pathways such as PS, PE, PC and LPC metabolism by n-3 PUFA could be attributed to influence on PS synthases (PSS), PS decarboxylases (PSD), PE methyltransferases (PEMT) and phospholipases (PLs), respectively, whereas that of sphingolipid metabolism could be attributed to alteration of sphingosine phosphatases (SPP) (Figure **3.10 B**).

3.10 Effects of maternal n-3 PUFA diets during gestation on the concentration of lipid headgroups in computationally constructed fetal neuronal membranes

Lipidomics data were used to computational construct neuronal membranes models representing the four experimental groups (see methods and Appendices **2-6** for details, Figure **3.11**). Choline-based lipids were more concentrated in the outer leaflet, ethanolamine-based lipids were more concentrated in the inner leaflet, while PS and PI were exclusively found in the inner leaflet (Figure **3.11)**.

Table 3.2: Summary of the metabolic pathway analysis of fetal brain lipid species

Pathway name	Total compounds	Hits	Impacts	Raw p-value	-log10(p)
Steroid biosynthesis	42	1	0.0000	0.0206	1.6861
GP metabolism	36	4	0.2630	0.0572	1.2426
Glycerolipid metabolism	16	1	0.0140	0.6200	0.2076
Arachidonic acid metabolism	36	1	0.0000	0.6700	0.1739
Linoleic acid metabolism	5	1	0.0000	0.6700	0.1739
ALA metabolism	13	1	0.0000	0.6700	0.1739
GPI-anchor biosynthesis	14	1	0.0040	0.6700	0.1739
Sphingolipid metabolism	21	1	0.2700	0.9900	0.0044

Data presented in the table represent the pertubation of different lipid metabolic pathways by n-3 PUFA; the total number of lipid species (total compounds) in database of each metabolic pathway and number of lipid species in the fetal brain (Hits). Lipid pathways with higher number of hits and pathway impacts are altered more by the treatment (n-3 PUFA diet in our study). Total compounds = the total number of metabolites in the pathway; Hits = the actual number of lipid species matched from our data; Impact = the pathway impact value calculated from pathway topology analysis; GPI = glycosylphosphatidylinositol; GP = Glycerophospholipid; ALA = α-Linolenic acid.

Maternal diets high in n-3 PUFA revealed higher concentration of ethanolamine-based lipids in the fetal neuronal membrane as gestation progressed, compared with low n-3 PUFA diet, whereas high n-3 PUFA diets showed higher concentration of choline-based lipids in the fetal neuronal membrane as gestation progressed (Figure **3.11**). The concentrations of lipid species in the fetal neuronal membrane models described above were dependent on the membrane model set-up from lipidomics data as reported previous (Ingólfsson et al., 2017). CE and TG were observed to flip-flop between the leaflets (characteristic of membrane lipids with poor polarity) while GP and SP remained in their original locations in the inner and outer membrane leaflets (Figure **3.11**).

3.11 Effects of maternal diets high in n-3 PUFA on the thickness, area per lipid, and CE flip-flop rate of fetal neuronal membrane

Gestation had a significant ($p < 0.0001$) effect on the fetal neuronal membrane thickness; as gestation progressed, there was a decrease in fetal membrane thickness in both low and high n-3 PUFA diet groups (Figure **3.12 A**). Diet had a significant ($p < 0.0001$) effect on the fetal membrane thickness; a maternal diet high in n-3 PUFA showed lower membrane thickness at GD12.5 (39.16 ± 0.00 Å), compared with low n-3 PUFA diet (38.80 ± 0.00 Å) (Figure **3.12 A**). However, at GD18.5, a higher membrane thickness was observed in high n-3 PUFA diet group (38.40 ± 0.00 Å), compared with low n-3 PUFA diet group (38.20 ± 0.00 Å). There was a significant interaction between diet and gestation for the fetal neuronal membrane thickness ($p < 0.0001$) (Figure **3.12 A**).

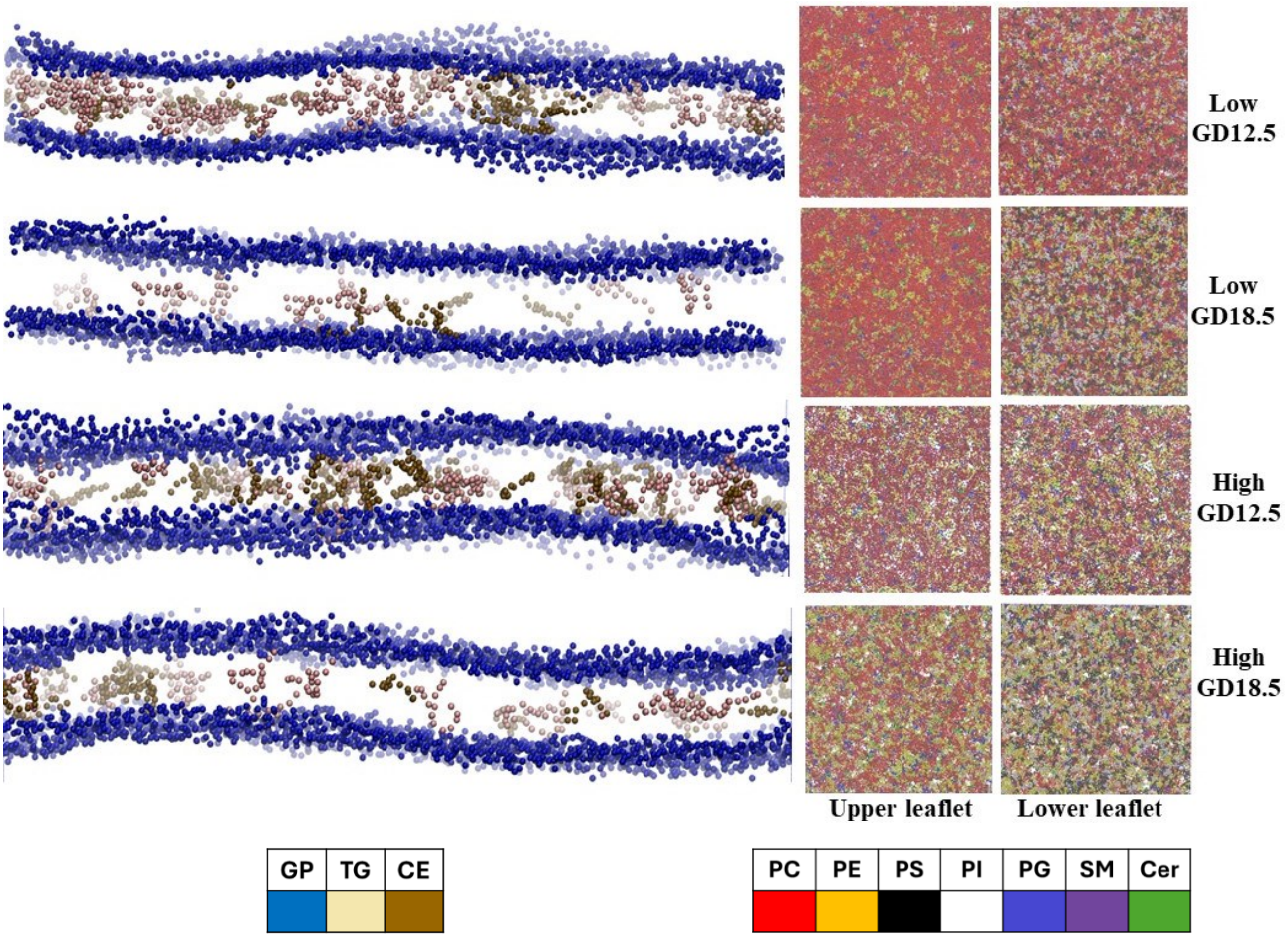

Figure 3.11: Representative snapshots from 10 µs molecular dynamics simulations of fetal neuronal membrane to show the location of the glycerophospholipids (GP) headgroups, cholesteryl esters (CE), and triacyglycerols (TG), and the clustering of lipid species in the upper, and lower leaflets of fetal neuronal plasma membrane models. *Image were created using visual molecular dynamics (VMD) (Humphrey et al., 1996); For the membranes shown in the left-hand side, dark-blue beads represent GP headgroups, ochre beads represent CE and light pink beads represent TG. For the leaflets shown in the right-hand side, red beads represent PC, yellow beads represent PE, black beads represent PS, white beads represent PI, blue beads represent PG, purple beads represent SM, and green beads represent Cer. GD = gestation day.*

Gestation had a significant ($p < 0.0001$) effect on the APL of fetal neuronal membrane; the APL of fetal neuronal membrane increased in both low and high n-3 PUFA diet groups as gestation progressed (Figure **3.12 B**). Diet had a significant ($p < 0.0001$) effect on the APL of fetal neuronal membrane; a maternal diet high in n-3 PUFA diet showed higher APL at both gestation stages (70.00 ± 0.00 Å^2 and 71.13 ± 0.01 Å^2 for GD12.5 and GD18.5, respectively), compared with low n-3 PUFA diet (68.95 ± 0.01 Å^2 and 69.92 ± 0.01 Å^2 for GD12.5 and GD18.5, respectively). There was a significant interaction between diet and gestation for APL in fetal neuronal membrane ($p < 0.0001$) (Figure **3.12 B**).

Gestation had a significant ($p < 0.0001$) effect on CE flip-flop rate in fetal neuronal membrane; as gestation progressed in both low and high n-3 PUFA diet groups, CE flip-flop rate decreased ($p < 0.0001$) (Figure **3.12 C**). Diet had significant ($p < 0.0001$) effect on CE flip-flop rate; as gestation progressed, high n-3 PUFA diet showed lower CE flip-flip rate ($9.81 \pm 0.09 \times 10^6$ s^{-1} and $6.47 \pm 0.23 \times 10^6$ s^{-1} at GD12.5 and GD18.5, respectively) between fetal neuronal membrane leaflets, compared with low n-3 PUFA diet ($12.28 \pm 0.05 \times 10^6$ s^{-1} and $7.64 \pm 0.10 \times 10^6$ s^{-1} at GD12.5 and GD18.5, respectively). There was a significant interaction between diet and gestation for CE flip-flop rate ($p < 0.0001$) (Figure **3.12 C**).

Maternal n-3 PUFA diets had no significant effect on the average lipid diffusion rate (6.25 ± 0.20 vs 6.42 ± 0.25 10^{-7} cm^2/s at GD12.5; 6.73 ± 0.17 vs 6.86 ± 0.15 10^{-7} cm^2/s at GD18.5, for both low and high n-3 PUFA groups, respectively) (Appendix **11**).

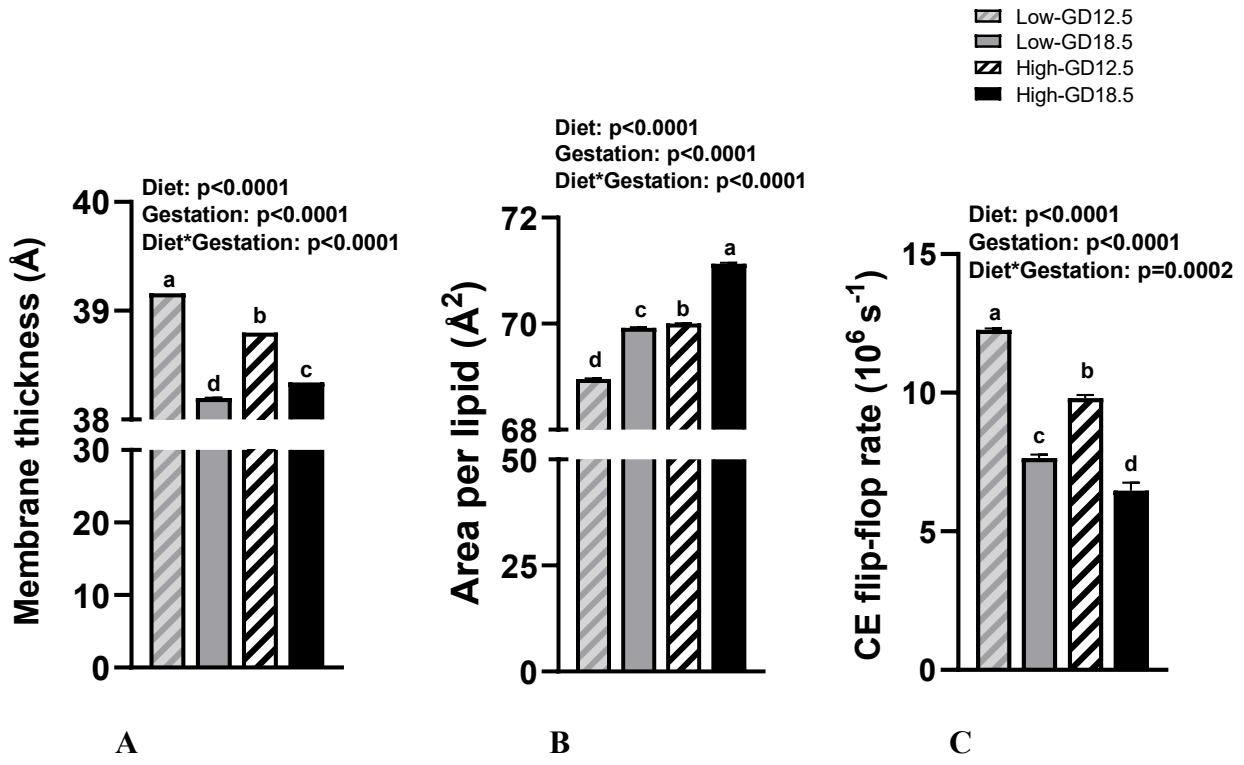

Figure 3.12: Effects of maternal diets high in n-3 PUFA on the membrane dynamic parameters in fetal neuronal membrane. A) membrane thickness; B) area per lipid; C) CE flip-flop rate. *Molecular dynamic simulation of the computed membrane data was done in triplicate for 10* μs. *The membrane thickness was analyzed using FATSLiM software (Buchoux, 2017), area per lipid (APL), and cholesteryl esters (CE) flip-flop rate were analyzed using LiPyphilic software (P. Smith & Lorenz, 2021). The simulation data were analysed using two-way ANOVA to determine the main effects and the interactions between maternal diet and gestation stage; pairwise comparison using Bonferroni's correction was used to determine differences when there was an observed interaction. Significant level was set at $p < 0.05$ (n = 3 per group).*

3.12 Maternal n-3 PUFA dietary intake during gestation influenced the formation of lipid domains in fetal neuronal membrane

Lipid domains PG/SM, PI/Cer, PI/PE, and SM/Cer were enriched in high n-3 PUFA fetal neuronal membrane at both gestation stages; however, they were neither enriched nor depleted in the low n-3 PUFA fetal neuronal membrane at both gestation stages (Table **3.3**). The contact fraction values of the above domains increased as gestation progressed in the high n-3 PUFA diet membranes (Table **3.3**). Lipid domains CE/CE, CE/PE, Cer/PC, PC/CE, and PE/PE were enriched in all the domains except in the low n-3 PUFA diet at GD12.5 membrane, which was neither enriched nor depleted. Additionally, the contact fraction values of these enriched domains increased as gestation progressed in the high n-3 PUFA diet membranes (Table **3.3**).

Lipid domains PC/PS, PS/PE, and PS/SM were enriched in all the membranes except in the high n-3 PUFA diet at GD18.5 membrane, which was neither enriched nor depleted. As gestation progressed, the contact fraction values of these domains decreased, and they were lower in the high n-3 PUFA diet membrane compared with the low n-3 PUFA diet membrane (Table **3.3**).

Lipid domain PC/SM was enriched only in the high n-3 PUFA diet at GD18.5 membrane and was neither enriched nor depleted in other membranes (Table **3.3**). On the other hand, PE/PI was enriched in the low n-3 PUFA diet at GD12.5 membrane and was neither enriched nor depleted in other membranes (Table **3.3**).

Lipid domain CE/PG was enriched in the low n-3 PUFA diet at GD18.5 and high n-3 PUFA diet at GD18.5 membranes but was neither enriched nor depleted in other membranes (Table **3.3**). Meanwhile, Cer/PG was enriched in the low n-3 PUFA diet at GD18.5 membrane but was neither enriched nor depleted in other membranes (Table **3.3**).

Table 3.3: Maternal n-3 PUFA dietary intake during gestation influenced the formation of lipid domains in fetal neuronal membranes

Domains	Groups			
	Low-GD12.5	**Low-GD18.5**	**High-GD12.5**	**High-GD18.5**
PG/SM	1.09 ± 0.07	0.85 ± 0.08	1.20 ± 0.18	1.46 ± 0.22
PI/Cer	1.06 ± 0.06	1.12 ± 0.12	1.20 ± 0.01	1.49 ± 0.05
PI/PE	1.10 ± 0.04	1.15 ± 0.02	1.21 ± 0.03	1.37 ± 0.02
SM/Cer	1.08 ± 0.06	1.15 ± 0.10	1.34 ± 0.01	1.49 ± 0.18
CE/CE	1.09 ± 0.02	1.41 ± 0.08	1.30 ± 0.04	1.51 ± 0.05
CE/PE	1.14 ± 0.03	1.45 ± 0.03	1.26 ± 0.02	1.48 ± 0.02
Cer/PC	1.10 ± 0.06	1.30 ± 0.10	1.30 ± 0.10	1.40 ± 0.22
PE/CE	1.09 ± 0.03	1.39 ± 0.02	1.20 ± 0.02	1.39 ± 0.02
PE/PE	1.10 ± 0.03	1.35 ± 0.05	1.19 ± 0.05	1.32 ± 0.04
PC/PS	1.37 ± 0.00	1.32 ± 0.00	1.24 ± 0.00	1.06 ± 0.00
PS/PE	1.37 ± 0.19	1.32 ± 0.16	1.24 ± 0.12	1.05 ± 0.03
PS/SM	1.35 ± 0.00	1.29 ± 0.01	1.21 ± 0.01	1.03 ± 0.00
PC/SM	1.06 ± 0.03	1.12 ± 0.06	1.13 ± 0.06	1.29 ± 0.14
PE/PI	1.21 ± 0.11	0.90 ± 0.10	1.13 ± 0.06	1.04 ± 0.02
CE/PG	1.03 ± 0.02	1.20 ± 0.09	1.14 ± 0.02	1.24 ± 0.03
Cer/PG	0.99 ± 0.05	1.22 ± 0.00	1.00 ± 0.00	1.10 ± 0.00
CE/SM	0.80 ± 0.03	0.41 ± 0.06	0.60 ± 0.03	0.45 ± 0.03
CE/PC	0.84 ± 0.04	0.42 ± 0.06	0.64 ± 0.04	0.45 ± 0.02
PS/Cer	0.59 ± 0.02	0.61 ± 0.02	0.67 ± 0.02	0.82 ± 0.05
SM/PE	0.68 ± 0.14	0.65 ± 0.20	0.72 ± 0.09	0.86 ± 0.09
PE/PS	0.88 ± 0.00	0.78 ± 0.01	0.25 ± 0.00	0.96 ± 0.01
PG/PI	0.80 ± 0.13	0.82 ± 0.08	0.73 ± 0.16	0.64 ± 0.17
SM/PI	0.87 ± 0.02	0.85 ± 0.00	0.77 ± 0.01	0.65 ± 0.00
PG/PG	0.70 ± 0.02	0.80 ± 0.08	0.90 ± 0.05	1.00 ± 0.02
PS/PG	0.91 ± 0.02	0.88 ± 0.05	0.83 ± 0.08	0.67 ± 0.17

Molecular dynamic simulation of the fetal neuronal membrane was done in triplicate for 10 µs.

The formation of lipid domains in the fetal neuronal membranes were determined by calculating contact fractions. Contact fraction of lipid species B around species A within 1.2 nm was calculated by dividing the number of molecules of species B around species A (N_{AB}) by the mean

number of species B around any species [N_B] using LiPyphilic software (P. Smith & Lorenz, 2021). The mean ± standard error of the mean (SEM) (n = 3 per group) was determined and presented in the Table 3.3. Lipid domains with contact fraction values < 0.8 (in red color cells) represent depleted domains, domains with contact fraction values > 0.8 and less than 1.2 (in yellow color cells) represent domains that were neither depleted nor enriched and domains with contact fraction values ≥ 1.2 (in blue color cells) represent enriched domains. Only domains that were enriched and/or depleted by diet or gestation in 1-3 membranes were shown in Table 3.3, while domains that were enriched, depleted, or neither enriched nor depleted in all the four membranes were shown in Appendix 12.

The lipid domains CE/SM and CE/PC were depleted in all the membranes except in the low n-3 PUFA diet at GD12.5 membranes, which were neither enriched nor depleted, whereas PS/Cer and SM/PE were depleted in all the membranes except in the high n-3 PUFA diet at GD18.5 membranes, which was neither enriched nor depleted (Table **3.3**).

Lipid domain PE/PS was depleted in low n-3 PUFA diet at GD18.5 and high n-3 PUFA diet at GD12.5 membranes but was neither enriched nor depleted in the low n-3 PUFA diet at GD12.5 and high n-3 PUFA diet at GD18.5 membranes (Table 3.3). Lipid domains PG/PI and SM/PI were depleted in the high n-3 PUFA diet membranes at both gestation stages but were neither enriched nor depleted in the low n-3 PUFA diet at both gestation stages (Table **3.3**). Lipid domain PG/PG was neither enriched nor depleted in all the membranes except in the low n-3 PUFA diet at GD12.5 membranes, which was depleted. On the other hand, PS/PG was neither enriched nor depleted in all the membranes except in the high n-3 PUFA diet at GD18.5 membranes, which was depleted (Table **3.3**).

Lipid domains CE/PI, CE/Cer, Cer/Cer, Cer/PE, Cer/SM, PC/PC, PE/PG, PE/Cer, PI/PS, SM/SM, and SM/PC were enriched in all the membranes (Appendix **12**). The contact fraction of these domains increased as gestation progressed, and higher levels in the high n-3 PUFA diet, compared with the low n-3 PUFA diet, except Cer/Cer and PI/PS, which decreased as gestation progressed and lower l in the high n-3 PUFA compared with low n-3 PUFA diet membranes (Appendix **12**). Meanwhile, CE/PS, PC/PG, PC/Cer, PG/Cer, PI/PG, and PI/PI were neither enriched nor depleted in all the membranes. On the other hand, Cer/CE, Cer/PS, Cer/PI, PC/PI, PC/PE, PC/CE, PE/SM, PE/PC, PG/CE, PG/PC, PG/PS, PG/PE, PI/CE, PI/PC, PI/SM, PS/PC, PS/CE, SM/PG, and SM/PS were depleted in all the membranes (Appendix **12**).

CHAPTER FOUR

Discussion

4.1. Gestation stages and diet affect brain lipidome

Our laboratory have previously showed that total brain DHA increases in fetal brain from mid (GD12.5) to late (GD18.5) gestation stages, and that maternal diets enriched in n-3 PUFA further increases the accretion of total DHA in the fetal brain during gestation (Akerele & Cheema, 2020). However, the fatty acid profile was studied in total extracted brain lipids; the specific lipid species with which DHA was associated was not investigated. Furthermore, changes in all lipid classes and their associated fatty acyl species during gestation were not studied.

Results of the present study show for the first time that fetal brain lipidome changes within pregnancy window, and diets low and high in n-3 PUFA further influenced brain lipidomics profile as summarized in our heatmap (Figure **3.9**). The overall summary of our findings show that maternal diets high in n-3 PUFA promoted the accretion of DHA-enriched ethanolamine-based lipids and increased indices of membrane fluidity and formation of lipid domains that are associated with neurogenesis, memory and cognition (as summarized in Appendices, 13, 14 and 15).

We found that maternal diet high in n-3 PUFA promoted the enrichment of total ethanolamine-based GP and total PE, compared to low n-3 PUFA diet in fetal brain as gestation progressed. The ability of high n-3 PUFA diet to promote accretion of ethanolamine-based GP, specifically PE, as early as GD12.5 is interesting because ethanolamine-based GP are critical in neurogenesis, myelinogenesis, neuroprotection and stabilization of membrane structure (Tasseva *et al*., 2012). Interestingly, there was an interaction between diet and gestation for P-PE, revealing lower levels in the high n-3 PUFA diet at late gestation, compared to low n-3 PUFA diet. On the other hand, O-PE increased as gestation progressed, and was higher in the high n-3 PUFA group

compared to the low n-3 PUFA group. The higher amounts of O-PE with concomitant lower P-PE in the high n-3 PUFA group suggest a reduction in the activity of phosphatidate phosphohydrolase (PPH), as predicted in our pathway analysis (Figure **3.10 B**). PPH is the enzyme that converts 1-alkyl-glycerol-3-phosphate to alkylacylglycerophosphate for synthesizing plasmalogens (Farooqui *et al*., 2008; Messias *et al*., 2018). As the precursor of P-PE, the accretion of O-PE in the fetal brain may benefit the developing brain by boosting cognitive function and protecting brain cells from damages (Ifuku *et al*., 2012; Katafuchi *et al*., 2012; Hossain *et al*., 2023).

Our results further show that MUFA-containing PE [PE(16:0_18:1), PE(18:1_18:1), PE(16:1_18:1), and PE(16:0_16:1)], and P-PE [PE(P-16:0_18:1)] decreased as gestation progressed, and the levels of PE(16:0_18:1) and PE(P-16:0_18:1) were lower in high n-3 PUFA group. It has been previously shown that total MUFA, palmitoleic acid, and OA in the fetal brain decreased as gestation progressed, and with a diet high in n-3 PUFA (Kuipers *et al*., 2012; Akerele & Cheema, 2020). In the current study, the reduction in fetal brain MUFA profile during gestation is likely partly associated with a decrease in palmitoleic acid and OA-containing PE/O-PE/P-PE species. A reduction in MUFA-containing PE/O-PE (especially C16:1 and C18:1) could be due to the conversion of these species to longer-chain MUFA that are essential for myelination and axonal function (Velasco *et al*., 2003).

As gestation progressed, n-6 PUFA-containing PE/P-PE [PE(18:1_18:2), PE(P-16:1_20:4), PE(P-16:0_20:4), PE(P-16:0_22:4), and PE(P-18:0_22:4)] significantly decreased ($p < 0.0001$) in all groups. This aligns with our previous findings that showed a decrease in total n-6 PUFA and LA in fetal brain total lipid extract as gestation progressed (Akerele & Cheema, 2020). The decrease in the n-6 PUFA-containing PE/O-PE species could be attributed to the gestation-related increase in mobilization and oxidation of n-6 PUFA by cytosolic phospholipase A_2 ($cPLA_2$)

activity during gestation (Skannal *et al*., 1997). Mobilized ARA could also serve as a precursor for the synthesis of endocannabinoids that are crucial in brain development and function (Wei *et al*., 2016, 2017). The lower ARA-containing PE/O-PE could also be a compensatory response to the accretion of DHA-containing PE/O-PE (Wainwright *et al*., 1991) and to minimize the impact of increased ARA on impairing *BDNF* signaling needed for neurogenesis, cognition, and memory (Fan *et al*., 2016). The high n-3 PUFA group generally showed lower levels of n-6 PUFA [PE(P-16:0_20:4), PE(P-16:0_22:4), and PE(P-18:0_22:4)]-containing PE/O-PE species, compared with the low n-3 PUFA groups. Our previous findings showed lower levels of n-6 PUFA in fetal and offspring's brains of dams fed high fed high n-3 PUFA diet (Balogun & Cheema, 2014; Feltham *et al*., 2019; Akerele & Cheema, 2020); our current results suggest that reduction in the fetal brain n-6 PUFA profile is likely partly associated with P-PE/PE.

DPA-containing P-PE [PE(P-16:0_22:5), PE(P-18:0_22:5)] and PE [PE(18:0_22:5) decreased as gestation progressed, and showed lower levels in high n-3 PUFA group, compared with low n-3 PUFA group. These findings agree with our previous findings where fetal brain showed a reduction in DPA level fed similar diets as gestation progressed (Akerele & Cheema, 2020). The lower amount of DPA-containing ethanolamine-based GP is likely due to increased conversion of DPA to DHA for incorporation into ethanolamine-based GP as predicted by pathway analysis (Figure **3.10 B**).

According to the literature review, the effect of maternal dietary n-3 PUFA on fetal brain DHA-containing PE profile has not been previously reported. A diet high in n-3 PUFA boosted the accretion of DHA-containing PE and O-PE by over 2-fold as early as GD12.5, compared with a low n-3 PUFA diet. Akerele & Cheema (2020) previously showed similar findings; however, the current findings suggest that the accretion of DHA in the fetal brain by a high n-3 PUFA diet is

associated with PE/O-PE. Suzuki *et al*. (1998) reported that intake of a high n-3 PUFA diet for 12 months increased adult mice brain DHA-containing PE levels. It is interesting to note that in our study, maternal diets high in n-3 PUFA also caused fetal brain enrichment of DHA in PE and O-PE during gestation. One mechanism through which n-3 PUFA could achieve this is via inhibition of calcium-independent $iPLA_2$ to suppress the mobilization of DHA incorporated in brain GP (Bousserouel *et al*., 2003; Rao *et al*., 2007). N-3 PUFA may increase fetal brain DHA-containing O-PE by upregulating expression and/or activities of GNPAT and AGPS, the rate-determining enzymes in ether lipid biosynthesis as predicted by our pathway analysis (Fig. **3.10 B**). The increase in DHA-containing ether lipids is crucial because they increase *BDNF* expression (Hossain *et al*., 2022) and inhibit γ-secretase, the enzyme that synthesizes amyloid-β peptides implicated in neurodegeneration (Onodera *et al*., 2015). We previously showed that maternal diets high in n-3 PUFA improved the accretion of DHA in fetal brain that correlated with upregulation of *BDNF* expression (Akerele & Cheema, 2020). As *BDNF* promotes neurogenesis and neuroprotection (Numakawa *et al*., 2018), the results of the present study suggest that prenatal exposure to the high n-3 PUFA diet will improve brain development and overall brain health, and reduce the risk of neurodegenerative diseases in postnatal life due to correlation of DHA accretion, *BDNF* and lower risk of neurodegenerative diseases. Although the functional difference between diacyl and ether-containing GPs is unclear, the presence of vinyl ether bonds in ether-linked phospholipids may influence their physicochemical properties and health benefits such as modulating membrane fluidity, anti-inflammatory and antioxidant properties (Hossain *et al*., 2013).

Our results showed a significant interaction between diet and gestation, revealing a decline in total choline-based GP, and PC as gestation progressed, with lower levels of P-PC in the high

n-3 PUFA group, compared with the low n-3 PUFA group. This agrees with the previous report that fetal brain total PC declines during late gestation (Burdge & Postle, 1995). As far as we know, there are no publications to date showing the influence of diets high or low in n-3 PUFA on fetal brain choline-based GP during gestation window. A diet high in n-3 PUFA promoted the accretion of DHA-containing PC as gestation progressed, compared with a low n-3 PUFA diet. Our research group has previously shown accretion of DHA in the fetal brain from dams fed a high n-3 PUFA diet. However, this was measured in the total fetal brain. Our current findings suggest that the accretion of DHA in the fetal brain by a maternal high n-3 PUFA diet is associated with PC. The accretion of DHA-containing PC during fetal brain development is crucial because it has been reported to alleviate oxidative stress, inflammation, apoptosis, and spatial deficits in Aβ1–40 rats and improve learning performance (Wen *et al*., 2016). Aβ1–40 rats are AD models known to be associated with oxidative stress, one of the pathogenetic mechanisms of AD (Ul Amin et al., 2017).

ARA-containing PC [PC(16:0_20:4)] showed a significant interaction of diet and gestation, revealing an increase as gestation progressed, and lower levels of PC(16:0_20:4) and PC(18:1_20:4) in high n-3 PUFA group, compared with high n-3 PUFA diet. A similar finding was shown previously by our research group on mice fed a similar diet (Akerele & Cheema, 2020), and show that the depletion of ARA in the fetal brain is likely associated with PC. The mechanism behind the lower ARA-containing PC via a gestation-dependent increase in higher $iPLA_2$ activity might be a protective strategy as ARA regulates *BDNF* signaling, leading to impairment of neurogenesis and upregulation of apoptosis of neuronal cells (Fan *et al*., 2016); hence, the lower level of ARA-containing PC in the fetal brain may promote *BDNF* signaling and the associated benefits on memory and cognitive performance. Additionally, elevated PC(16:0_20:4) was associated with reactive microglia and astrocytes (indicators of neuroinflammation) in peripheral

nervous injury (Xu *et al*., 2016), suggesting that reduction in this species during gestation and by high n-3 PUFA will protect the developing brain from neuroinflammatory assaults.

Stearic acid-containing PC [PC(18:1_18:0) and PC(16:0_18:0)] a significantly increased as gestation progressed with higher levels in the high n-3 PUFA group, compared with the low n-3 PUFA group. The increase in stearic acid-containing PC in the fetal brain and in the high n-3 PUFA group could be linked to increased fatty acid biosynthesis during gestation and by high n-3 PUFA diet in response to a high lipid demand during gestation (Akerele & Cheema, 2017). Accretion of stearic acid in the fetal brain is beneficial due to its protective nature against brain cells' assaults (Wang et al., 2006); it is also a precursor of erucic acid and nervonic acid, which are crucial for myelination (Namiecinska et al., 2024).

A maternal diet high in n-3 PUFA increased the accretion of LPC in the fetal brain, with further accretion as gestation progressed. The increase in LPC with the concomitant decrease in PC could be attributed to the increased breakdown of PC to LPC by PLA_2 during gestation (Besenboeck *et al*., 2016). The increase in LPC during gestation and by high n-3 PUFA diet is interesting because LPC is a major pathway for transporting DHA and other n-3 PUFA into the brain through *Mfsd2a* (Nguyen *et al*., 2014; Bergman *et al*., 2023). DHA-containing LPC [LPC(22:6)] showed a significant interaction between diet and gestation, revealing a significant increase as gestation progressed, and over 2-fold higher level in the high n-3 PUFA diet, compared with the low n-3 PUFA diet. Our research group previously showed that maternal diets high in n-3 PUFA upregulated *Mfsd2a* expression in the fetal brain during gestation (Akerele & Cheema, 2020). The accretion of LPC(22:6) in the fetal brain during gestation may reduce the risk of neurological diseases associated with neuroinflammation (Gilhus & Deuschl, 2019), and improve

memory and cognitive function as LPC(22:6) was reported to inhibit neuroinflammation (Hung *et al*., 2011) and enhance memory and cognition (Sugasini *et al*., 2017).

Minor brain lipids (sum of PS, PG, PI, Cer, SM, and CE) in fetal brain total lipids increased as gestation progressed with a higher level in the high n-3 PUFA group, compared with the low n-3 PUFA group. We further analyzed the effect of gestation and diet on individual lipid classes that make up the minor brain lipids. Our findings showed that PS increased as gestation progressed, with a higher level in the high n-3 PUFA diet, compared with the low n-3 PUFA diet. N-3 PUFA has been reported to increase PS synthesis in cultured neuronal cells (Guo *et al*., 2007), supporting the higher PS level in the high n-3 PUFA group, compared with the low n-3 PUFA group in our study. We speculate that n-3 PUFA may increase fetal brain PS level by increasing phosphatidylserine synthase I (PSS-1)-mediated conversion of PC to PS (Bergo *et al*., 2002) as can be deduced from the enrichment of PS with a concomitant depletion PC in the high n-3 PUFA group, compared with low n-3 PUFA group. N-3 PUFA may have also increased the synthesis of PS from DG by PSS-2, as predicted from our pathway analysis (Figure **3.10 B**). The accretion of PS in the fetal brain during brain development is critical because PS promotes neurotransmission and prevents neuroinflammation (Zhao *et al*., 2018), and increases the formation of neurotrophins, neuroprotectins, and synaptamide that boost synaptogenesis and synaptic transmission through Akt and cAMP/PKA/CREB signaling pathways (Kim *et al*., 2019; Kim *et al*., 2022). Moreover, mice fed n-3-deficient diets from *in-utero* until two months old had lower brain total PS levels (Hamilton *et al*., 2000). This report further demonstrates that consumption of adequate n-3 PUFA during gestation to boost fetal brain PS will promote fetal brain development and function, by promoting synaptogenesis and synaptic neurotransmission and protecting brain cells against assaults (Park *et al*., 2021). For the first time, we report that a high n-3 PUFA diet promoted the accretion of

DHA-containing PS [PS(18:0_22:6)] in the fetal brain as early as GD12.5 and by approximately 2 fold, with further increases as gestation progressed from GD12.5 to GD18.5. DHA-containing PS is critical for neurogenesis and myelination (Kim *et al*., 2010), and neuronal cell survival (Kawakita *et al*., 2006); hence, the accretion of DHA-containing PS in the fetal brain as gestation progressed by n-3 PUFA diet will promote brain development and protect developing brain from assaults. Our results further support the need for the consumption of adequate amounts of n-3 PUFA during gestation as n-3 PUFA-deficient diets during gestation until eight weeks showed depleted brain DHA-containing PS, which resulted in cognitive impairment (Hamilton *et al*., 2000); hence, the accretion of DHA-containing PS in fetal brain may promote cognitive function across the lifespan.

Our findings showed a drastically lower DPA-containing PS [PS(18:0_22:5)] level in the high n-3 PUFA group, compared with the low n-3 PUFA group. Akerele & Cheema (2020) previously showed a similar reduction in DPA of the fetal brain fed high n-3 PUFA, suggesting that lower fetal brain DPA in the high n-3 PUFA diet is associated with PS. Our findings suggest that n-3 PUFA diet increases the conversion of DPA to DHA (Hamilton *et al*., 2000). Our results also show that n-6 PUFA-containing PS [PS(18:0_22:4)] decreased as gestation progressed, and lower levels in the high n-3 PUFA group, compared to the low n-3 PUFA group. This is in accordance with the results of our research group showing a lower n-6 PUFA in the fetal brain (Akerele & Cheema, 2020), and indicate that a reduction in n-6 PUFA is associated with PS(18:0_22:4). The lower amount of PS(18:0_22:4) in the fetal brain could be attributed to the lower conversion rate of LA to ADA due to the inhibitory effects of n-3 PUFA (Lands *et al*., 1990).

Little attention has been given to the brain PG profile, probably due to the smaller proportion of PG compared with other GP classes (Choi *et al*., 2018). Our results show a

significantly higher accretion of total PG in the high n-3 PUFA group, compared with the low n-3 PUFA group with further increases as gestation progressed. There was an interaction between diet and gestation for OA-containing PG [PG(18:1_18:1)] revealing higher levels in the high n-3 PUFA group, compared with the low n-3 PUFA group, with further increase in PG(18:0_18:1) and PG(16:0_18:1) as gestation progressed. The accretion of total PG and OA-containing PG in the fetal brain is interesting because PG and OA-containing PG are reported to inhibit inflammation through toll-like receptor/nuclear factor kappa B/tumor necrotic factor alpha (Choudhary *et al*., 2019; Klein *et al*., 2020) and PLA_2-mediated release of inflammatory mediators (Wu *et al*., 2003); hence, will protect the developing brain from neuroinflammation. We also found a significant interaction between diet and gestation for PA-containing PG [PG(16:0_16:0)], revealing higher levels in high n-3 PUFA groups compared with low n-3 PUFA diet at both gestation stages. N-3 PUFA increases lipogenesis (Akerele & Cheema, 2017), which may explain the increased PA-containing PG in the fetal brain of the high n-3 PUFA group, compared with the low n-3 PUFA group. Th accretion of palmitic acid-enriched species in the brain will serve as a reservoir of palmitic acid for elongation to longer-chain fatty acids, and for palmitoylation of synaptic proteins during synaptic plasticity, which is needed for cognition (Fukata & Fukata, 2010).

A maternal diet high in n-3 PUFA showed higher PI levels, compared with the low n-3 PUFA group, and further increased as gestation progressed. The increase in PI is speculated to result from DG conversion to PI by PI synthase (Vance, 2015) as can be deduced from the increase in PI with concomitant decrease in DG. PI plays a role in neurogenesis and neurotransmission through the PI3K/Akt signaling pathway (Peng *et al*., 2004; Papadopoulos *et al*., 2017) and promote myelination (Logan *et al*., 2017). ARA-containing PI species [PI(18:0_20:4)] decreased as gestation progressed, which aligns with our previous findings (Akerele & Cheema, 2020), and

confirms that reductions in fetal brain n-6 PUFA profile found in our previous studies were partly associated with PI.

Cer is a major class of SP in the brain and neuronal membrane which increases with age in postnatal life (Sacket *et al*., 2009; Vozella *et al*., 2017; Couttas *et al*., 2018); however, little is known about changes in brain Cer levels during gestation. Our findings showed an interaction of diet and gestation for total SP and Cer, revealing an increase as gestation progressed and lower levels in the high n-3 PUFA groups, compared with the low n-3 PUFA group. The higher total SP and Cer levels during gestation will benefit myelination and formation of Cer-enriched domains in neuronal membrane critical for brain development and function (Zhang *et al*., 2009; Ladjohounlou *et al*., 2020). We found significant interaction between diets and gestation for Cer(d18:1_18:0) and Cer(d18:2_18:0) levels in the fetal brain, revealing an increase as gestation progressed in low n-3 PUFA group for Cer(d18:1_18:0) and decrease as gestation progressed in high n-3 PUFA group for Cer(d18:2_18:0). A maternal diet high in n-3 PUFA showed lower Cer(d18:1_18:0) and Cer(d18:1_16:0) levels and higher Cer(d18:2_18:0) level in the fetal brain, compared with low n-3 PUFA diet. Literature review suggests that the difference in functions of these ceramide species in the brain is unknown. The result of the present study suggests that CerS catalyze the attachment of fatty acids to sphingosine or sphinganine to produce specific ceramides, thereby determining the brain ceramide profile (Stiban *et al*., 2010), are differentially expressed in the fetal brain during gestation and are differentially impacted by n-3 PUFA diet (Camacho-Muñoz *et al*., 2022), as predicted by our pathway analysis (Figure **3.10 B**).

Free cholesterol consists of about 80% of total sterol in the fetal brain (Yusuf *et al*., 1981); however, free cholesterol was not detected using the lipidomic method adopted in this study because free cholesterol has poor ionization efficiency due to its low proton affinity and acidity

(Wu *et al*., 2009). However, CE was detected in the fetal brain and decreased as gestation progressed, with lower levels in the high n-3 PUFA group compared with the low n-3 PUFA group. There was a significant interaction of diet and gestation for DHA-containing CE [CE(22:6)], revealing a decrease as gestation progressed with higher levels in the high n-3 PUFA group, compared with the low n-3 PUFA group. Our pathway analysis predicted that n-3 PUFA may have increased fetal brain CE(22:6) level by upregulating LCAT, the enzyme that catalyzes the esterification of free cholesterol with PC (such as DHA-containing PC) (Figure **3.10 B**). N-3 PUFA may also increase fetal brain CE(22:6) level by increasing the activity of acyl coenzyme-A cholesterol acyltransferase (ACAT) (Davis, 1992). ACAT is the enzyme that esterifies cholesterol with activated fatty acids like docosahexaenoyl coenzyme-A to form CE(22:6) (Zhang & Liu, 2015). CE is the storage and transport form of cholesterol in lipid droplets, typically during cholesterol surplus (Wechsler *et al*., 2003); thus, the higher accretion of CE(22:6) in the developing brain will serve as a reservoir of cholesterol and DHA for neuronal membrane formation in developing fetal brain.

Our results show that total GL, DG, and TG in the fetal brain total lipids decreased as gestation progressed with no significant effects of diet. High n-3 PUFA diet increased the accretion of OA-containing DG, and DGLA and DHA-containing TG, compared with low n-3 PUFA diet as gestation progressed. N-3 PUFA is speculated to increase the accretion of the aforementioned TG species by upregulating DGAT-2, an enzyme that catalyzes TG synthesis (Akerele & Cheema, 2017). This will make DHA available for remodeling into other brain lipids and for conversion to bioactive DHA metabolites such as docosanoids that prevent neuroinflammation and promote brain growth and development (Basak *et al*., 2020). The increase in OA-containing DG in the fetal brain is interesting because DG is a second messenger and a signal transduction molecule crucial

in modulating axonal growth, synaptic plasticity (Keimpema *et al*., 2013), memory, and cognition (Schurman *et al*., 2019).

Overall, OA and ARA, ADA and DPA-containing lipid species decreased as gestation progressed, with lower levels in high n-3 PUFA diet group, compared with low n-3 PUFA diet groups as summarized in our heatmap (Figure **3.9**). On the other hand, DHA-containing lipids increased as gestation progressed in both diet groups, and a maternal diet high in n-3 PUFA further promoted the accretion of DHA-containing lipids in the high n-3 PUFA group, compared with low n-3 PUFA group (Figure **3.9**).

4.2. Gestation stages and diet affect computationally-constructed neuronal membrane dynamics

The composition of membrane lipids influences its structure and physicochemical properties. We are the first to report that fetal neuronal membranes are thinner, compared to the adult neuronal membranes. There was a significant interaction of diet and gestation for membrane thickness revealing a decrease as gestation progressed, and lower thickness in high n-3 PUFA diet at GD12.5. Our results are remarkable to show that fetal neuronal membranes are thinner (39.16 ± 0.00 Å and 38.80 ± 0.00 Å in the high and low n-3 PUFA groups at GD12.5, respectively and 38.40 ± 0.00 Å and 38.20 ± 0.00 Å in the high and low n-3 PUFA groups at GD18.5, respectively) than adult neuronal membrane (42.63 ± 0.17 Å) (Wilson *et al*., 2021) and average mammalian PM mixture (41.09 ± 0.00 Å) (Ingólfsson *et al*., 2017). Free cholesterol is known to increase membrane thickness (Chakraborty *et al*., 2020; Boonnoy *et al*., 2021; Oh *et al*., 2021; Chen *et al*., 2023); however, we did not detect free cholesterol in the fetal brain lipids due to adopted analytical method and hence, we cannot directly compare our result and that of previous studies (Ingólfsson *et al*., 2017). Thinner membranes have higher ability to transport molecules across the membrane,

and interaction between membrane components such as neuromodulatory molecules and their receptors associated with brain development and neurotransmission (Cohen, 2018).

Both diet and gestation affected APL, revealing an increase by 0.95 $Å^2$ and 1.13 $Å^2$ in low n-3 and high n-3 PUFA groups, respectively at GD18.5 compared with GD12.5. APL was higher in the high n-3 PUFA group by 1.05 $Å^2$ and 1.21 $Å^2$ at GD12.5 and GD18.5, respectively, compared with low n-3 PUFA diet. APL is associated with higher membrane fluidity and interaction of membrane components needed for neuronal differentiation and brain growth (Noutsi *et al*., 2016). The higher APL in fetal neuronal membrane in our study (70.00 ± 0.00 $Å^2$ and 71.13 ± 0.01 $Å^2$ at GD12.5 and GD18.5, respectively for high n-3 PUFA diet and 68.95 ± 0.01 $Å^2$ and 69.92 ± 0.01 $Å^2$ at GD12.5 and GD18.5, respectively for low n-3 PUFA diet), compared with adult neuronal membrane (49.67 ± 15.35 $Å^2$ and 54.74 ± 16.00 $Å^2$, respectively for the extracellular and intracellular leaflets) (Ingólfsson *et al*., 2017) suggest that the fetal neuronal membrane is more fluid than the adult neuronal membrane. Free cholesterol has been shown to reduce APL (Philips, 1972); however, we did not detect free cholesterol using the analytical methods in this study. Hence, we were unable to determine the impact of free cholesterol on the APL of the fetal neuronal membrane and hence cannot accurately compared our results and that of previous studies. Accretion of DHA-enriched PE in adult mice brain fed high n-3 PUFA diet has been shown to correlate with increased synaptic membrane fluidity and improved cognitive function (Suzuki *et al*., 1998). Our results suggest that the accretion of DHA-containing PE in the fetal brain of high n-3 PUFA group is involved in higher APL in the high n-3 PUFA diet membranes, relative to low n-3 PUFA diet membranes.

Lipid flip-flop between membrane bilayer, the number transbilayer movement of lipids from one bilayer to another per minutes, regulates membrane tension and structures (Devaux *et*

al., 2008). Free cholesterol flip-flop between membrane leaflets have been reported in computational studies on adult neuronal membrane (Ingólfsson *et al*., 2017); however, CE flip-flop between membrane bilayers has not been reported. Our results show an interaction between diet and gestation for CE flip-flop rate, revealing a decrease as gestation progressed, and a lower rate in high n-3 PUFA group, compared with a low n-3 PUFA group. Our findings showed higher CE flip-flop rate in the fetal neuronal membrane (12.28 ± 0.05 s^{-1} and 7.64 ± 0.10 s^{-1} for low n-3 PUFA at GD12.5 and GD18.5, respectively and 9.81 ± 0.09 s^{-1} and 6.47 ± 0.23 s^{-1} for high n-3 PUFA at GD12.5 and GD18.5, respectively), compared with free cholesterol flip-flop rate reported in computationally constructed adult neuronal membrane (2.64 ± 0.01 s^{-1}) (Ingólfsson *et al*., 2017). CE flip-flop rate has not been studied previously; hence, there was a scarcity of findings to compare with our result. Several factors have been shown to influence the cholesterol flip-flop rate, including the degree of unsaturation of membrane lipids, the site of cholesterol oxidation, and cholesterol concentration (Ingólfsson *et al*., 2017; Wilson *et al*., 2021). Membranes with a higher degree of unsaturation have been shown to have a lower rate of lipid flip-flop between the membrane bilayers (Alwarawrah *et al*., 2016); however, we did not find an association between the degree of unsaturation and CE flip-flop rate. As mentioned earlier, we did not detect free cholesterol using the analytical method adopted in this study; hence, we do not know if the presence and concentration of free cholesterol influence the CE flip-flop rate.

We found that a high n-3 PUFA diet promoted the formation of some Cer-enriched (Cer/PC, PI/Cer, and SM/Cer), SM-enriched (SM/Cer, and PG/SM), and PC-enriched (PC/CE, and Cer/PC) domains in the fetal neuronal membrane, with further increase as gestation progressed. Interestingly, high n-3 PUFA promoted the formation of the lipid domain, PC/SM at GD18.5 only. Cer-enriched domains have been shown to contribute to the clustering of receptors, some of which

are involved in signal transduction and stress modulation (Ladjohounlou *et al*., 2020), that are critical in neurotransmission, memory, and cognition. Cer-enriched domains also form channels for small molecules like cytochrome *c* involved in cellular respiration (Siskind & Colombini, 2000). Therefore, the increase in Cer-enriched domains in the fetal neuronal membrane by a high n-3 PUFA diet suggests that consuming adequate n-3 PUFA diets during gestation will improve fetal brain growth and function that may extend throughout the lifetime. Similarly, SM-enriched domains promote cellular cytokinesis, a process involved in cellular differentiation (Abe *et al*., 2012), whereas PC-enriched domains are important in neuronal regeneration (Marcucci *et al*., 2010); hence, n-3 PUFA diet will boost neurogenesis and neuronal survival.

High n-3 PUFA diet promoted the formation of PE-enriched (PE/PE, CE/PE, and PI/PE), and CE-enriched (CE/CE, CE/PE, and PE/CE) domains in the fetal neuronal membrane, which increased as gestation progressed. The specific role of CE and PE-enriched domains in the neuronal membrane is unclear; however, due to the charged ethanolamine head group, PE-enriched domains may promote neurotransmission and favour the synthesis and folding of some neuronal membrane proteins, including GPI-anchored proteins to their most active form (Patel & Witt, 2017). PE-enriched domains possess intrinsic negative curvature and promote membrane fusion (Lee *et al*., 2020; Joardar *et al*., 2021). As a major reservoir of DHA, PE-enriched domains may enhance the production of synaptamide, a DHA metabolite that promotes synaptic development and neurogenesis through the activation of orphan adhesion G-protein-coupled receptor 110 signaling (Kim et al., 2022), and prevention of neuroinflammation through cAMP/PKA/CREB signaling (Park *et al*., 2016).

Interestingly, a high n-3 PUFA diet promoted the formation of PG-enriched (PG/SM) domain in the fetal neuronal membrane as gestation progressed. PG-enriched domains inhibit the

assembly of α-Synuclein into α-synuclein fibrils that promote amyloid-β peptide formation (Khammari *et al*., 2020). Unfibrilated α-synuclein is essential in regulating membrane fusion, synaptic vesicle release, and transport and neurotransmitter release (Sun *et al*., 2019); hence, inhibiting α-synuclein fibrillation will enhance neurotransmission. Therefore, consumption of adequate n-3 PUFA diets (9% n-3 PUFA diet) during gestation will boost fetal brain PG and enrich the formation of PG-enriched domains in the fetal neuronal membrane, which are crucial in brain development and neurotransmission that may extend across the lifespan.

Cholesterol has been shown to influence lipid domain formation in membranes (Javanainen *et al*., 2017; Xu & London, 2000); however, we did not detect free cholesterol in the fetal neuronal membrane using the analytical method adopted in this study and could not determine the effect of cholesterol on domain formation in the fetal neuronal membrane.

4.3 Limitations of the study and future directions

The findings from the current thesis demonstrate that maternal diets high in n-3 PUFA promote the accretion of DHA-containing PE in the fetal brain, increased indicators of membrane fluidity, and formation of lipid domains associated with neurotransmission; however, the molecular mechanisms involved were not studied, and should be explored in future. In addition, free cholesterol was not detected in our study by the electrospray ionization MS used in this study because free cholesterol has poor ionization efficiency due to its low proton affinity and acidity (Wu *et al*., 2009). Since cholesterol plays an important role in brain function, future studies should derivatize the fetal brain lipid extract by treating the extract with betaine aldehyde or acetyl chloride to convert free cholesterol to hemiacetal salt or cholesteryl acetate to enable its quantification by

HPLC-MS (Higashi & Shimada, 2004; Liebisch *et al*., 2006; Wu *et al*., 2009; Li *et al*., 2019) to investigate whether gestation stage or diets high/low in n-3 PUFA alter cholesterol levels.

We computationally predicted the impact of maternal diets differing in n-3 PUFA during gestation on fetal neuronal membrane using the whole fetal brain lipidomic profile to show that high n-3 PUFA diet reduced membrane thickness and CE flip-flop, and increased APL and formation of lipid domains were associated with neuronal transmission, memory, and cognition. Computational studies on membrane dynamics using lipidomics data is accumulating in literature (Ingólfsson *et al*., 2017; Wilson *et al*., 2020; Wilson *et al*., 2021); however, isolating fetal neuronal membranes, extracting lipids and analyzing the lipidomic profile before using the data for computational examination will provide a direct relationship between neuronal membrane lipidome and membrane dynamics.

4.4 Overall conclusion and take-home message

Overall, the findings of this study demonstrated that maternal diets containing an adequate amount of n-3 PUFA promoted accretion of DHA-containing PE in the fetal brain. The accretion of DHA-containing PE in the fetal brain resulted in a reduction in neuronal membrane thickness and increase in APL, indicating increased membrane fluidity. High n-3 PUFA also increased the formation of domains which are associated with neurogenesis, synaptogenesis, synaptic transmission, memory, and cognition. The take home message from this research is that intake of adequate n-3 PUFA (9% n-3 PUFA, n-6/n-3 PUFA ratio of 5:1) before and during gestation promoted the accretion of DHA-containing PE in fetal brain as gestation progressed from GD12.5 to GD18.5. Adequate n-3 PUFA improved area per lipid and formation of Cer, PG, SM, and PE-enriched domains, and reduced membrane thickness at GD12.5 in fetal neuronal membrane

(Figure **4.1**, Appendix **14**). Therefore, it is strongly recommended that women of childbearing age should consume adequate n-3 PUFA, including preformed DHA during gestation for better offspring brain health across the lifespan.

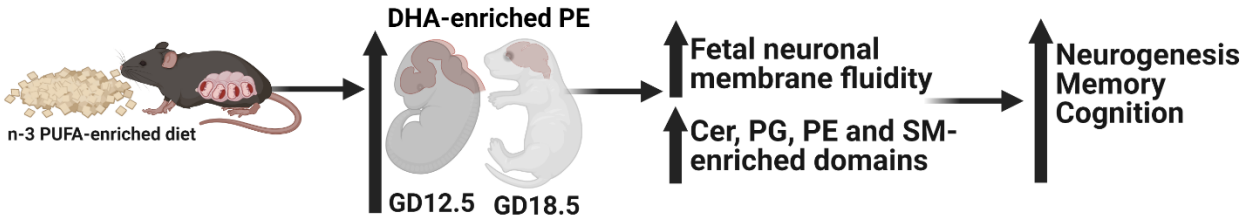

Figure 4.1: Schematic summary of thesis findings. *Maternal diets high in n-3 polyunsaturated fatty acids (PUFA) during gestation increases the accretion of DHA-enriched phosphoatidylethanolamine (PE) in fetal brain with concomitant increase in fetal neuronal membrane fluidity and formation of Cer, PG, PE, and SM-enriched membranes domains are associated with improved neurogenesis, memory, and cognition. Therefore, consuming diets containing high n-3 PUFA during gestation will not only promote accretion of DHA-containing PE in the fetal brain but also promote brain growth and function.*

BIBLIOGRAPHY

Abdelrahman, M. A., Osama, H., Saeed, H., Madney, Y. M., Harb, H. S., & Abdelrahim, M. E. A. (2023). Impact of n-3 polyunsaturated fatty acid intake in pregnancy on maternal health and birth outcomes: Systematic review and meta-analysis from randomized controlled trails. *Archives of Gynecology and Obstetrics*, *307*(1), 249–262. https://doi.org/10.1007/S00404-022-06533-0/METRICS

Abe, M., Makino, A., Hullin-Matsuda, F., Kamijo, K., Ohno-Iwashita, Y., Hanada, K., Mizuno, H., Miyawaki, A., & Kobayashi, T. (2012). A role for sphingomyelin-rich lipid domains in the accumulation of phosphatidylinositol-4,5-bisphosphate to the cleavage furrow during cytokinesis. *Molecular and Cellular Biology*, *32*(8), 1396–1407. https://doi.org/10.1128/mcb.06113-11

Abraham, M. J., Murtola, T., Schulz, R., Páll, S., Smith, J. C., Hess, B., & Lindah, E. (2015). GROMACS: High performance molecular simulations through multi-level parallelism from laptops to supercomputers. *SoftwareX*, *1–2*, 19–25. https://doi.org/10.1016/J.SOFTX.2015.06.001

Adams, C. W. M., & Davison, A. N. (1959). The occurrence of esterified cholesterol in the developing nervous system. *Journal of Neurochemistry*, *4*(4), 282–289. https://doi.org/10.1111/j.1471-4159.1959.tb13207.x

Akerele, O. A., & Cheema, S. K. (2016). A balance of omega-3 and omega-6 polyunsaturated fatty acids is important in pregnancy. *Journal of Nutrition & Intermediary Metabolism*, *5*, 23–33. https://doi.org/10.1016/J.JNIM.2016.04.008

Akerele, O. A., & Cheema, S. K. (2017). A low-fat diet enriched in fish oil increased lipogenesis and fetal outcome of C57BL/6 mice. *Reproduction*, *154*(2), 153–165. https://doi.org/10.1530/REP-17-0068

Akerele, O. A., & Cheema, S. K. (2018). A diet enriched in longer chain omega-3 fatty acids reduced placental inflammatory cytokines and improved fetal sustainability of C57BL/6 mice. *Prostaglandins, Leukotrienes and Essential Fatty Acids*, *137*, 43–51. https://doi.org/10.1016/J.PLEFA.2018.08.002

Akerele, O. A., & Cheema, S. K. (2020). Maternal diet high in Omega-3 fatty acids upregulate genes involved in neurotrophin signalling in fetal brain during pregnancy in C57BL/6 mice. *Neurochemistry International*, *138*, 104778. https://doi.org/10.1016/J.NEUINT.2020.104778

Akerele, O. A., Manning, S. J., Dixon, S. E., Lacey, A. E., & Cheema, S. K. (2021). Maternal omega-3 fatty acids maintained positive maternal lipids and cytokines profile, and improved pregnancy outcomes of C57BL/6 mice. *The Journal of Nutritional Biochemistry*, *98*, 108813. https://doi.org/10.1016/J.JNUTBIO.2021.108813

Alaamery, M., Albesher, N., Aljawini, N., Alsuwailm, M., Massadeh, S., Wheeler, M. A., Chao, C. C., & Quintana, F. J. (2021). Role of sphingolipid metabolism in neurodegeneration. *Journal of Neurochemistry*, *158*(1), 25–35. https://doi.org/10.1111/jnc.15044

Alling, C., & Svennerholm, L. (1969). Concentration and fatty acid composition of cholesteryl esters of normal human brain. *Journal of Neurochemistry*, *16*(5), 751–759. https://doi.org/10.1111/J.1471-4159.1969.TB06453.X

Almsherqi, Z. A. (2021). Potential role of plasmalogens in the modulation of biomembrane morphology. *Frontiers in Cell and Developmental Biology*, *9*, 1648. https://doi.org/10.3389/FCELL.2021.673917/BIBTEX

Alwarawrah, M., Hussain, F., & Huang, J. (2016). Alteration of lipid membrane structure and dynamics by diacylglycerols with unsaturated chains. *Biochimica et Biophysica Acta - Biomembranes*, *1858*(2), 253–263. https://doi.org/10.1016/j.bbamem.2015.11.014

Anderson, G. J., Neuringer, M., Lin, D. S., & Connor, W. E. (2005). Can prenatal N-3 fatty acid deficiency be completely reversed after birth? Effects on retinal and brain biochemistry and visual function in rhesus monkeys. *Pediatric Research*, *58*(5), 865–872. https://doi.org/10.1203/01.pdr.0000182188.31596.5a

Anderson, P. J., de Miranda, D. M., Albuquerque, M. R., Indredavik, M. S., Evensen, K. A. I., Van Lieshout, R., Saigal, S., Taylor, H. G., Raikkonen, K., Kajantie, E., Marlow, N., Johnson, S., Woodward, L. J., Austin, N., Nosarti, C., Jaekel, J., Wolke, D., Cheong, J. L., Burnett, A., … Doyle, L. W. (2021). Psychiatric disorders in individuals born very preterm/very low-birth weight: An individual participant data (IPD) meta-analysis. *EClinicalMedicine*, *42*, 101216. https://doi.org/10.1016/J.ECLINM.2021.101216

Anesi, A., & Guella, G. (2015). A fast liquid chromatography-mass Spectrometry methodology for membrane lipid profiling through hydrophilic interaction liquid chromatography. *Journal of Chromatography A*, *1384*, 44–52. https://doi.org/10.1016/J.CHROMA.2015.01.035

Arora, A., Raghuraman, H., & Chattopadhyay, A. (2004). Influence of cholesterol and ergosterol

on membrane dynamics: A fluorescence approach. *Biochemical and Biophysical Research Communications*, *318*(4), 920–926. https://doi.org/10.1016/J.BBRC.2004.04.118

Atwood, B. K., & Lovinger, D. M. (2017). Endocannabinoid-dependent synaptic plasticity in the striatum. In M. Melis (Ed.), *Endocannabinoids and Lipid Mediators in Brain Functions* (pp. 109–153). Springer, Cham. https://doi.org/10.1007/978-3-319-57371-7

Bagga, D., Wang, L., Farias-Eisner, R., Glaspy, J. A., & Reddy, S. T. (2003). Differential effects of prostaglandin derived from ω-6 and ω-3 polyunsaturated fatty acids on COX-2 expression and IL-6 secretion. *Proceedings of the National Academy of Sciences of the United States of America*, *100*(4), 1751–1756. https://doi.org/10.1073/pnas.033421110

Bakht, O., Pathak, P., & London, E. (2007). Effect of the structure of lipids favoring disordered domain formation on the stability of cholesterol-containing ordered domains (lipid rafts): Identification of multiple raft-stabilization mechanisms. *Biophysical Journal*, *93*(12), 4307–4318. https://doi.org/10.1529/biophysj.107.114967

Balogun, K. A., Albert, C. J., Ford, D. A., Brown, R. J., & Cheema, S. K. (2013). Dietary omega-3 polyunsaturated fatty acids alter the fatty acid composition of hepatic and plasma bioactive lipids in C57BL/6 mice: A lipidomic approach. *PLoS ONE*, *8*(11), 1–16. https://doi.org/10.1371/journal.pone.0082399

Balogun, K. A., & Cheema, S. K. (2014). The expression of neurotrophins is differentially regulated by omega-3 polyunsaturated fatty acids at weaning and postweaning in C57BL/6 mice cerebral cortex. *Neurochemistry International*, *66*(1), 33–42. https://doi.org/10.1016/J.NEUINT.2014.01.007

Balogun, K. A., & Cheema, S. K. (2016). Dietary omega-3 fatty acids prevented adipocyte hypertrophy by downregulating DGAT-2 and FABP-4 in a sex-dependent fashion. *Lipids*, *51*(1), 25–38. https://doi.org/10.1007/S11745-015-4105-X

Balogun, K. A., Randunu, R. S., & Cheema, S. K. (2014). The effect of dietary omega-3 polyunsaturated fatty acids on plasma lipids and lipoproteins of C57BL/6 mice is age and sex specific. *Prostaglandins Leukotrienes and Essential Fatty Acids*, *91*(1–2), 39–47. https://doi.org/10.1016/j.plefa.2014.05.002

Banks, W. A., Farr, S. A., Salameh, T. S., Niehoff, M. L., Rhea, E. M., Morley, J. E., Hanson, A. J., Hansen, K. M., & Craft, S. (2018). Triglycerides cross the blood-brain barrier and induce central leptin and insulin receptor resistance. *International Journal of Obesity*, *42*, 391–397. https://doi.org/10.1038/IJO.2017.231

Basak, S., Vilasagaram, S., & Duttaroy, A. K. (2020). Maternal dietary deficiency of n-3 fatty acids affects metabolic and epigenetic phenotypes of the developing fetus. *Prostaglandins Leukotrienes and Essential Fatty Acids*, *158*(April), 102109. https://doi.org/10.1016/j.plefa.2020.102109

Bazan, N. G. (2013). The docosanoid neuroprotectin D1 induces homeostatic regulation of neuroinflammation and cell survival. *Prostaglandins, Leukotrienes and Essential Fatty Acids*, *88*(1), 127–129. https://doi.org/10.1016/J.PLEFA.2012.08.008

Bazan, N. G. (2018). Docosanoids and elovanoids from omega-3 fatty acids are pro-homeostatic modulators of inflammatory responses, cell damage and neuroprotection. *Molecular Aspects of Medicine*, *64*, 18. https://doi.org/10.1016/J.MAM.2018.09.003

Bazan, N. G., Musto, A. E., & Knott, E. J. (2011). Endogenous signaling by omega-3 docosahexaenoic acid-derived mediators sustains homeostatic synaptic and circuitry integrity. *Molecular Neurobiology*, *44*(2), 216–222. https://doi.org/10.1007/S12035-011-8200-6/FIGURES/1

Beauchamp, A., Yee, Y., Darwin, B. C., Raznahan, A., Mars, R. B., & Lerch, J. P. (2022). Whole-brain comparison of rodent and human brains using spatial transcriptomics. *ELife*, *11*, e79418. https://doi.org/10.7554/ELIFE.79418

Beck, R., Bertolino, S., Abbot, S. E., Aaronson, P. I., & Smirnov, S. V. (1998). Modulation of arachidonic acid release and membrane fluidity by albumin in vascular smooth muscle and endothelial cells. *Circulation Research*, *83*(9), 923–931. https://doi.org/10.1161/01.RES.83.9.923

Beltz, B. S., Tlusty, M. F., Benton, J. L., & Sandeman, D. C. (2007). Omega-3 fatty acids upregulate adult neurogenesis. *Neuroscience Letters*, *415*(2), 154–158. https://doi.org/10.1016/j.neulet.2007.01.010

Berendsen, H. J. C., van der Spoel, D., & van Drunen, R. (1995). GROMACS: A message-passing parallel molecular dynamics implementation. *Computer Physics Communications*, *91*(1–3), 43–56. https://doi.org/10.1016/0010-4655(95)00042-E

Bergman, S., Cater, R. J., Plante, A., Mancia, F., & Khelashvili, G. (2023). Substrate binding-induced conformational transitions in the omega-3 fatty acid transporter MFSD2A. *Nature Communications*, *14*(1). https://doi.org/10.1038/s41467-023-39088-y

Bergo, M. O., Gavino, B. J., Steenbergen, R., Sturbois, B., Parlow, A. F., Sanan, D. A., Skarnes,

W. C., Vance, J. E., & Young, S. G. (2002). Defining the importance of phosphatidylserine synthase 2 in mice. *Journal of Biological Chemistry*, *277*(49), 47701–47708. https://doi.org/10.1074/jbc.M207734200

Bernard, J. Y., De Agostini, M., Forhan, A., de Lauzon-Guillain, B., Charles, M. A., Heude, B., Annesi-Maesano, I., Botton, J., Charles, M. A., Dargent-Molina, P., De Agostini, M., de Lauzon-Guillain, B., Ducimetière, P., Foliguet, B., Forhan, A., Fritel, X., Germa, A., Goua, V., Hankard, R., … Thiebaugeorges, O. (2013). The dietary n6:n3 fatty acid ratio during pregnancy is inversely associated with child neurodevelopment in the EDEN mother-child cohort. *The Journal of Nutrition*, *143*(9), 1481–1488. https://doi.org/10.3945/JN.113.178640

Besenboeck, C., Cvitic, S., Lang, U., Desoye, G., & Wadsack, C. (2016). Going into labor and beyond: Phospholipase A2 in pregnancy. *Reproduction*, *151*(6), R91–R102. https://doi.org/10.1530/REP-15-0519

Best, K. P., Gibson, R. A., & Makrides, M. (2022). ISSFAL statement number 7 – Omega-3 fatty acids during pregnancy to reduce preterm birth. *Prostaglandins, Leukotrienes and Essential Fatty Acids*, *186*, 102495. https://doi.org/10.1016/J.PLEFA.2022.102495

Bittova, L., Stahelin, R. V, & Cho, W. (2001). Roles of ionic residues of the C1 domain in protein kinase C-α activation and the origin of phosphatidylserine specificity. *The Journal of Biological Chemistry*, *276*(6), 4218–4226. https://doi.org/10.1074/jbc.M008491200

Björkbom, A., Róg, T., Kaszuba, K., Kurita, M., Yamaguchi, S., Lönnfors, M., Nyholm, T. K. M., Vattulainen, I., Katsumura, S., & Slotte, J. P. (2010). Effect of sphingomyelin

headgroup size on molecular properties and interactions with cholesterol. *Biophysical Journal*, *99*(10), 3300–3308. https://doi.org/10.1016/j.bpj.2010.09.049

Boonnoy, P., Jarerattanachat, V., Karttunen, M., & Wong-ekkabut, J. (2021). Role of cholesterol flip-flop in oxidized lipid bilayers. *Biophysical Journal*, *120*(20), 4525–4535. https://doi.org/10.1016/J.BPJ.2021.08.036

Bordeleau, M., Comin, C. H., Fernández de Cossío, L., Lacabanne, C., Freitas-Andrade, M., González Ibáñez, F., Raman-Nair, J., Wakem, M., Chakravarty, M., Costa, L. da F., Lacoste, B., & Tremblay, M. È. (2022). Maternal high-fat diet in mice induces cerebrovascular, microglial and long-term behavioural alterations in offspring. *Communications Biology*, *5*, 26. https://doi.org/10.1038/s42003-021-02947-9

Bousserouel, S., Brouillet, A., Béréziat, G., Raymondjean, M., & Andréani, M. (2003). Different effects of n-6 and n-3 polyunsaturated fatty acids on the activation of rat smooth muscle cells by interleukin-1β. *Journal of Lipid Research*, *44*(3), 601–611. https://doi.org/10.1194/jlr.M200092-JLR200

Bruel-Jungerman, E., Veyrac, A., Dufour, F., Horwood, J., Laroche, S., & Davis, S. (2009). Inhibition of PI3K-Akt signaling blocks exercise-mediated enhancement of adult neurogenesis and synaptic plasticity in the dentate gyrus. *PloS One*, *4*(11), e7901. https://doi.org/10.1371/JOURNAL.PONE.0007901

Buchoux, S. (2017). FATSLiM: A fast and robust software to analyze MD simulations of membranes. *Bioinformatics*, *33*(1), 133–134. https://doi.org/10.1093/bioinformatics/btw563

Burdge, G. C., & Calder, P. C. (2006). Dietary α-linolenic acid and health-related outcomes: A

metabolic perspective. *Nutrition Research Reviews*, *19*(1), 26–52. https://doi.org/10.1079/nrr2005113

Burdge, G. C., Finnegan, Y. E., Minihane, A. M., Williams, C. M., & Wootton, S. A. (2003). Effect of altered dietary n-3 fatty acid intake upon plasma lipid fatty acid composition, conversion of [13C]α-linolenic acid to longer-chain fatty acids and partitioning towards β-oxidation in older men. *British Journal of Nutrition*, *90*(2), 311–321. https://doi.org/10.1079/BJN2003901

Burdge, G. C., & Postle, A. D. (1995). Phospholipid molecular species composition of developing fetal guinea pig brain. *Lipids*, *30*(8), 719–724. https://doi.org/10.1007/BF02537798

Burdge, G. C., & Wootton, S. A. (2002). Conversion of α-linolenic acid to eicosapentaenoic, docosapentaenoic and docosahexaenoic acids in young women. *British Journal of Nutrition*, *88*(4), 411–420. https://doi.org/10.1079/BJN2002689

Burgess, B. L., McIsaac, S. A., Naus, K. E., Chan, J. Y., Tansley, G. H. K., Yang, J., Miao, F., Ross, C. J. D., van Eck, M., Hayden, M. R., van Nostrand, W., St. George-Hyslop, P., Westaway, D., & Wellington, C. L. (2006). Elevated plasma triglyceride levels precede amyloid deposition in Alzheimer's disease mouse models with abundant A beta in plasma. *Neurobiology of Disease*, *24*(1), 114–127. https://doi.org/10.1016/J.NBD.2006.06.007

Bussi, G., Donadio, D., & Parrinello, M. (2007). Canonical sampling through velocity rescaling. *Journal of Chemical Physics*, *126*, 014101. https://doi.org/10.1063/1.2408420/186581

Caillon, L., Nieto, V., Gehan, P., Omrane, M., Rodriguez, N., Monticelli, L., & Thiam, A. R.

(2020). Triacylglycerols sequester monotopic membrane proteins to lipid droplets. *Nature Communications*, *11*(1), 1–12. https://doi.org/10.1038/s41467-020-17585-8

Calderon, F., & Kim, H. Y. (2004). Docosahexaenoic acid promotes neurite growth in hippocampal neurons. *Journal of Neurochemistry*, *90*(4), 979–988. https://doi.org/10.1111/J.1471-4159.2004.02520.X

Camacho-Muñoz, D., Niven, J., Kucuk, S., Cucchi, D., Certo, M., Jones, S. W., Fischer, D. P., Mauro, C., & Nicolaou, A. (2022). Omega-3 polyunsaturated fatty acids reverse the impact of western diets on regulatory T cell responses through averting ceramide-mediated pathways. *Biochemical Pharmacology*, *204*(August), 115211. https://doi.org/10.1016/j.bcp.2022.115211

Campoy, C., Escolano-Margarit, V., Anjos, T., Szajewska, H., & Uauy, R. (2012). Omega 3 fatty acids on child growth, visual acuity and neurodevelopment. *British Journal of Nutrition*, *107*(S2), S85–S106. https://doi.org/10.1017/S0007114512001493

Cao, D., Kevala, K., Kim, J., Moon, H. S., Jun, S. B., Lovinger, D., & Kim, H. Y. (2009). Docosahexaenoic acid promotes hippocampal neuronal development and synaptic function. *Journal of Neurochemistry*, *111*(2), 510–521. https://doi.org/10.1111/J.1471-4159.2009.06335.X

Carrié, I., Clément, M., Javel, D. De, Francès, H., Inserm, U., Neuro-pharmaco-nutrition, U. De, & Ponroy, L. (2000). Specific phospholipid fatty acid composition of brain regions in mice: Effects of n – 3 polyunsaturated fatty acid deficiency and phospholipid supplementation. *Journal of Lipid Research*, *41*, 465–472. https://doi.org/10.1016/S0022-2275(20)34485-0

Carver, J. D., Benford, V. J., Han, B., & Cantor, A. B. (2001). The relationship between age and the fatty acid composition of cerebral cortex and erythrocytes in human subjects. *Brain Research Bulletin*, *56*(2), 79–85. https://doi.org/10.1016/S0361-9230(01)00551-2

CCAC. (2022). *Canadian Council on Animal Care Guidelines*. https://ccac.ca/en/standards/guidelines/

Chakraborty, S., Doktorova, M., Molugu, T. R., Heberle, F. A., Scott, H. L., Dzikovski, B., Nagao, M., Stingaciu, L. R., Standaert, R. F., Barrera, F. N., Katsaras, J., Khelashvili, G., Brown, M. F., & Ashkar, R. (2020). How cholesterol stiffens unsaturated lipid membranes. *Proceedings of the National Academy of Sciences of the United States of America*, *117*(36), 21896–21905. https://doi.org/10.1073/pnas.2004807117

Chang, C.-Y., Ke, D.-S., & Chen, J.-Y. (2009). Essential fatty acids and human brain. *Acta Neurol Taiwan*, *18*(4), 231–241. https://doi.org/10.3389/fcell.2022.823857

Chen, S., Liu, Y., Rong, X., Li, Y., Zhou, J., & Lu, L. (2017). Neuroprotective role of the PI3 Kinase/Akt signaling pathway in Zebrafish. *Frontiers in Endocrinology*, *8*(FEB), 238048. https://doi.org/10.3389/FENDO.2017.00021/BIBTEX

Chen, T., Ghosh, A., & Enderlein, J. (2023). Cholesterol-Induced Nanoscale Variations in the Thickness of Phospholipid Membranes. *Nano Letters*, *23*(6), 2421–2426. https://doi.org/10.1021/acs.nanolett.2c04635

Chen, V. S., Morrison, J. P., Southwell, M. F., Foley, J. F., Bolon, B., & Elmore, S. A. (2017). Histology atlas of the developing prenatal and postnatal mouse central nervous system, with emphasis on prenatal days E7.5 to E18.5. *Toxicologic Pathology*, *45*(6), 705.

https://doi.org/10.1177/0192623317728134

Choi, H. J., Byun, M. S., Yi, D., Choe, Y. M., Sohn, B. K., Baek, H. W., Lee, J. H., Kim, H. J., Han, J. Y., Yoon, E. J., Kim, Y. K., Woo, J. I., & Lee, D. Y. (2016). Association between serum triglycerides and cerebral amyloidosis in cognitively normal elderly. *The American Journal of Geriatric Psychiatry*, *24*(8), 604–612. https://doi.org/10.1016/J.JAGP.2016.03.001

Choi, J., Yin, T., Shinozaki, K., Lampe, J. W., Stevens, J. F., Becker, L. B., & Kim, J. (2018). Comprehensive analysis of phospholipids in the brain, heart, kidney, and liver: Brain phospholipids are least enriched with polyunsaturated fatty acids. *Molecular and Cellular Biochemistry*, *442*(1–2), 187–201. https://doi.org/10.1007/S11010-017-3203-X/FIGURES/11

Choudhary, V., Uaratanawong, R., Patel, R. R., Patel, H., Bao, W., Hartney, B., Cohen, E., Chen, X., Zhong, Q., Isales, C. M., & Bollag, W. B. (2019). Phosphatidylglycerol inhibits toll-like receptor–mediated inflammation by danger-associated molecular patterns. *Journal of Investigative Dermatology*, *139*(4), 868–877. https://doi.org/10.1016/j.jid.2018.10.021

Clandinin, M. T., Chappell, J. E., Leong, S., Heim, T., Swyer, P. R., & Chance, G. W. (1980). Intrauterine fatty acid accretion rates in human brain: Implications for fatty acid requirements. *Early Human Development*, *4*(2), 121–129. https://doi.org/10.1016/0378-3782(80)90015-8

Cohen, B. E. (2018). Membrane thickness as a key factor contributing to the activation of osmosensors and essential ras signaling pathways. *Frontiers in Cell and Developmental*

Biology, *6*(JUL), 76. https://doi.org/10.3389/FCELL.2018.00076/BIBTEX

Cohen, J. T., Bellinger, D. C., Connor, W. E., & Shaywitz, B. A. (2005). A quantitative analysis of prenatal intake of n-3 polyunsaturated fatty acids and cognitive development. *American Journal of Preventive Medicine*, *29*(4), 366–374. https://doi.org/10.1016/j.amepre.2005.06.008

Cook, H. W. (1981). Metabolism of triacylglycerol in developing rat brain. *Neurochemical Research*, *6*(11), 1217–1229. https://doi.org/10.1007/BF00966679

Couttas, T. A., Kain, N., Tran, C., Chatterton, Z., Kwok, J. B., & Don, A. S. (2018). Age-dependent changes to sphingolipid balance in the human hippocampus are gender-specific and may sensitize to neurodegeneration. *Journal of Alzheimer's Disease*, *63*(2), 503–514. https://doi.org/10.3233/JAD-171054

Crupi, R., Marino, A., & Cuzzocrea, S. (2013). N-3 fatty acids: Role in neurogenesis and neuroplasticity. *Current Medicinal Chemistry*, *20*(24), 2953–2963. https://doi.org/10.2174/09298673113209990140

Cunnane, S. C., & Chen, Z. Y. (1992). Quantitative changes in long-chain fatty acids during fetal and early postnatal development in rats. *The American Journal of Physiology*, *262*(1 Pt 2). https://doi.org/10.1152/AJPREGU.1992.262.1.R14

Cunnane, S. C., Schneider, J. A., Tangney, C., Tremblay-Mercier, J., Fortier, M., Bennett, D. A., & Morris, M. C. (2012). Plasma and brain fatty acid profiles in mild cognitive impairment and Alzheimer's disease. *Journal of Alzheimer's Disease : JAD*, *29*(3), 691–697. https://doi.org/10.3233/JAD-2012-110629

Custers, Emma, E. M., Kiliaan, & Amanda, J. (2022). Dietary lipids from body to brain. *Progress in Lipid Research*, *85*, 101144. https://doi.org/10.1016/J.PLIPRES.2021.101144

Czubowicz, K., Jęśko, H., Wencel, P., Lukiw, W. J., & Strosznajder, R. P. (2019). The role of ceramide and sphingosine-1-phosphate in Alzheimer's disease and other neurodegenerative disorders. *Molecular Neurobiology*, *56*(8), 5436–5455. https://doi.org/10.1007/S12035-018-1448-3

Da Silva, T. F., Sousa, V. F., Malheiro, A. R., & Brites, P. (2012). The importance of ether-phospholipids: A view from the perspective of mouse models. *Biochimica et Biophysica Acta*, *1822*(9), 1501–1508. https://doi.org/10.1016/J.BBADIS.2012.05.014

Darios, F., & Davletov, B. (2006). Omega-3 and omega-6 fatty acids stimulate cell membrane expansion by acting on syntaxin 3. *Nature*, *440*(7085), 813–817. https://doi.org/10.1038/nature04598

Davis, P. J. (1992). n-3 and n-6 polyunsaturated fatty acids have different effects on acyl-CoA:cholesterol acyltransferase in J774 macrophages. *Biochemistry and Cell Biology = Biochimie et Biologie Cellulaire*, *70*(12), 1313–1318. https://doi.org/10.1139/o92-178

Dawson, G. (2015). Measuring brain lipids. *Biochimica et Biophysica Acta*, *1851*, 1026–1039. https://doi.org/10.1016/J.BBALIP.2015.02.007

De Jong, D. H., Baoukina, S., Ingólfsson, H. I., & Marrink, S. J. (2016). Martini straight: Boosting performance using a shorter cutoff and GPUs. *Computer Physics Communications*, *199*, 1–7. https://doi.org/10.1016/J.CPC.2015.09.014

De Jong, D. H., Singh, G., Bennett, W. F. D., Arnarez, C., Wassenaar, T. A., Schäfer, L. V., Periole, X., Tieleman, D. P., & Marrink, S. J. (2013). Improved parameters for the martini coarse-grained protein force field. *Journal of Chemical Theory and Computation*, *9*(1), 687–697. https://doi.org/10.1021/ct300646g

De Smedt-Peyrusse, V., Sargueil, F., Moranis, A., Harizi, H., Mongrand, S., & Layé, S. (2008). Docosahexaenoic acid prevents lipopolysaccharide-induced cytokine production in microglial cells by inhibiting lipopolysaccharide receptor presentation but not its membrane subdomain localization. *Journal of Neurochemistry*, *105*(2), 296–307. https://doi.org/10.1111/J.1471-4159.2007.05129.X

Deoni, S., Dean, D., Joelson, S., O'Regan, J., & Schneider, N. (2018). Early nutrition influences developmental myelination and cognition in infants and young children. *NeuroImage*, *178*, 649. https://doi.org/10.1016/J.NEUROIMAGE.2017.12.056

Devaux, P. F., Herrmann, A., Ohlwein, N., & Kozlov, M. M. (2008). How lipid flippases can modulate membrane structure. *Biochimica et Biophysica Acta (BBA) - Biomembranes*, *1778*(7–8), 1591–1600. https://doi.org/10.1016/J.BBAMEM.2008.03.007

Dhariwal, A., Chong, J., Habib, S., King, I. L., Agellon, L. B., & Xia, J. (2017). MicrobiomeAnalyst: a web-based tool for comprehensive statistical, visual and meta-analysis of microbiome data. *Nucleic Acids Research*, *45*(W1), W180–W188. https://doi.org/10.1093/NAR/GKX295

Dietschy, J. M., & Turley, S. D. (2004). Thematic review series: Brain lipids. Cholesterol metabolism in the central nervous system during early development and in the mature

animal. *Journal of Lipid Research*, *45*(8), 1375–1397. https://doi.org/10.1194/JLR.R400004-JLR200

Dinicolantonio, J. J., & O'Keefe, J. H. (2020). The importance of marine omega-3s for brain development and the prevention and treatment of behavior, mood, and other brain disorders. *Nutrients*, *12*, 2333. https://doi.org/10.3390/NU12082333

Donoso, F., Schverer, M., Rea, K., Pusceddu, M. M., Roy, B. L., Dinan, T. G., Cryan, J. F., & Schellekens, H. (2020). Neurobiological effects of phospholipids in vitro: Relevance to stress-related disorders. *Neurobiology of Stress*, *13*(September). https://doi.org/10.1016/j.ynstr.2020.100252

Dorninger, F., Brodde, A., Braverman, N. E., Moser, A. B., Just, W. W., Forss-Petter, S., Brügger, B., & Berger, J. (2015). Homeostasis of phospholipids — The level of phosphatidylethanolamine tightly adapts to changes in ethanolamine plasmalogens. *Biochimica et Biophysica Acta (BBA) - Molecular and Cell Biology of Lipids*, *1851*(2), 117–128. https://doi.org/10.1016/J.BBALIP.2014.11.005

Dorninger, F., Forss-Petter, S., & Berger, J. (2017). From peroxisomal disorders to common neurodegenerative diseases - the role of ether phospholipids in the nervous system. *FEBS Letters*, *591*(18), 2761–2788. https://doi.org/10.1002/1873-3468.12788

Dorninger, F., König, T., Scholze, P., Berger, M. L., Zeitler, G., Wiesinger, C., Gundacker, A., Pollak, D. D., Huck, S., Just, W. W., Forss-Petter, S., Pifl, C., & Berger, J. (2019). Disturbed neurotransmitter homeostasis in ether lipid deficiency. *Human Molecular Genetics*, *28*(12), 2046–2061. https://doi.org/10.1093/HMG/DDZ040

Dyall, S. C. (2011). The role of omega-3 fatty acids in adult hippocampal neurogenesis. *Oléagineux, Corps Gras, Lipides*, *18*(5), 242–245. https://doi.org/10.1051/OCL.2011.0392

Dyall, S. C. (2014). The Role of Omega-3 Fatty Acids in Hippocampal Neurogenesis. *Omega-3 Fatty Acids in Brain and Neurological Health*, *18*(5), 251–263. https://doi.org/10.1016/B978-0-12-410527-0.00021-1

Emre, C., Do, K. V., Jun, B., Hjorth, E., Alcalde, S. G., Kautzmann, M. A. I., Gordon, W. C., Nilsson, P., Bazan, N. G., & Schultzberg, M. (2021). Age-related changes in brain phospholipids and bioactive lipids in the APP knock-in mouse model of Alzheimer's disease. *Acta Neuropathologica Communications 2021 9:1*, *9*(1), 1–26. https://doi.org/10.1186/S40478-021-01216-4

Engberg, O., Hautala, V., Yasuda, T., Dehio, H., Murata, M., Slotte, J. P., & Nyholm, T. K. M. (2016). The affinity of cholesterol for different phospholipids affects lateral segregation in bilayers. *Biophysical Journal*, *111*(3), 546–556. https://doi.org/10.1016/j.bpj.2016.06.036

Escolano-Margarit, M. V., Ramos, R., Beyer, J., Csábi, G., Parrilla-Roure, M., Cruz, F., Perez-Garcia, M., Hadders-Algra, M., Gil, A., Koletzko, T. D., & Campoy, C. (2011). Prenatal DHA status and neurological outcome in children at age 5.5 years are positively associated. *Journal of Nutrition*, *141*(6), 1216–1223. https://doi.org/10.3945/jn.110.129635

Fabelo, N., Martín, V., Santpere, G., Marín, R., Torrent, L., Ferrer, I., & Díaz, M. (2011). Severe alterations in lipid composition of frontal cortex lipid rafts from Parkinson's disease and incidental Parkinson's disease. *Molecular Medicine (Cambridge, Mass.)*, *17*(9–10), 1107–1118. https://doi.org/10.2119/MOLMED.2011.00119

Fan, C., Fu, H., Dong, H., Lu, Y., Lu, Y., & Qi, K. (2016). Maternal n-3 polyunsaturated fatty acid deprivation during pregnancy and lactation affects neurogenesis and apoptosis in adult offspring : associated with DNA methylation of brain-derived neurotrophic factor transcripts. *Nutrition Research*, *36*(9), 1013–1021. https://doi.org/10.1016/j.nutres.2016.06.005

Fan, C., Sun, W., Fu, H., Dong, H., Xia, L., Lu, Y., Deckelbaum, R. J., & Qi, K. (2015). Dietary ratios of n-6/n-3 polyunsaturated fatty acids during maternal pregnancy affect hippocampal neurogenesis and apoptosis in mouse offspring. *Nutricion Hospitalaria*, *32*(3), 1170–1179. https://doi.org/10.3305/nh.2015.32.3.9259

Farooqui, A. A., Farooqui, T., & Horrocks, L. A. (2008). Biosynthesis of Plasmalogens in Brain. In *Metabolism and Functions of Bioactive Ether Lipids in the Brain* (1st ed., p. PP. 17-37). Springer. https://doi.org/10.1007/978-0-387-77401-5/COVER

Farr, S. A., Yamada, K. A., Butterfield, D. A., Abdul, H. M., Xu, L., Miller, N. E., Banks, W. A., & Morley, J. E. (2008). Obesity and hypertriglyceridemia produce cognitive impairment. *Endocrinology*, *149*(5), 2628–2636. https://doi.org/10.1210/EN.2007-1722

Feltham, B. A., Balogun, K. A., & Cheema, S. K. (2019). Perinatal and postweaning diets high in omega-3 fatty acids have age- and sex-specific effects on the fatty acid composition of the cerebellum and brainstem of C57BL/6 mice. *Prostaglandins Leukotrienes and Essential Fatty Acids*, *148*, 16–24. https://doi.org/10.1016/j.plefa.2019.07.006

Fernandes, D. J., Spring, S., Roy, A. R., Qiu, L. R., Yee, Y., Nieman, B. J., Lerch, J. P., & Palmert, M. R. (2021). Exposure to maternal high-fat diet induces extensive changes in the

brain of adult offspring. *Translational Psychiatry*, *11*, 149. https://doi.org/10.1038/s41398-021-01274-1

Fitzner, D., Bader, J. M., Penkert, H., Bergner, C. G., Su, M., Weil, M. T., Surma, M. A., Mann, M., Klose, C., & Simons, M. (2020). Cell-type- and brain-region-resolved mouse brain lipidome. *Cell Reports*, *32*, 108132. https://doi.org/10.1016/j.celrep.2020.108132

Fontaine, D. A., & Davis, D. B. (2016). Attention to background strain is essential for metabolic research: C57BL/6 and the International knockout mouse consortium. *Diabetes*, *65*(1), 25–33. https://doi.org/10.2337/DB15-0982

Food and Agriculture Organization of the United Nations. (2010). Fats and fatty acids in human nutrition. Report of an expert consultation. In *Fats and fatty acids in human nutrition: Report of an expert consultation*. Food and Agriculture Organization of the United Nations. https://www.fao.org/3/i1953e/i1953e00.pdf

Frallicciardi, J., Melcr, J., Siginou, P., Marrink, S. J., & Poolman, B. (2022). Membrane thickness, lipid phase and sterol type are determining factors in the permeability of membranes to small solutes. *Nature Communications*, *13*(1), 1–12. https://doi.org/10.1038/s41467-022-29272-x

Fukata, Y., & Fukata, M. (2010). Protein palmitoylation in neuronal development and synaptic plasticity. *Nature Reviews Neuroscience*, *11*(3), 161–175. https://doi.org/10.1038/nrn2788

GBD. (2019). *The Global Burden of Disease. Institute of Health Metrics and Evaluation*. https://vizhub.healthdata.org/gbd-results/

Gibson, R. A., Neumann, M. A., & Makrides, M. (1996). Effect of dietary docosahexaenoic acid on brain composition and neural function in term infants. *Lipids*, *31*(3 SUPPL.), 177–181. https://doi.org/10.1007/bf02637072

Gil, A., & Gil, F. (2015). Fish, a Mediterranean source of n-3 PUFA: Benefits do not justify limiting consumption. *British Journal of Nutrition*, *113*(S2), S58–S67. https://doi.org/10.1017/S0007114514003742

Gil, A., Serra-Majem, L., Calder, P. C., & Uauy, R. (2012). Systematic reviews of the role of omega-3 fatty acids in the prevention and treatment of disease. *British Journal of Nutrition*, *107*(S2), S1–S2. https://doi.org/10.1017/S0007114512001420

Gilhus, N. E., & Deuschl, G. (2019). Neuroinflammation — a common thread in neurological disorders. *Nature Reviews Neurology*, *15*(8), 429–430. https://doi.org/10.1038/s41582-019-0227-8

Giusto, N. M., Roque, M. E., & Ilincheta de Boschero, M. G. (1992). Effects of aging on the content, composition and synthesis of sphingomyelin in the central nervous system. *Lipids*, *27*(11), 835–839. https://doi.org/10.1007/BF02535859

Goodenowe, D. B., Cook, L. L., Liu, J., Lu, Y., Jayasinghe, D. A., Ahiahonu, P. W. K., Heath, D., Yamazaki, Y., Flax, J., Krenitsky, K. F., Sparks, D. L., Lerner, A., Friedland, R. P., Kudo, T., Kamino, K., Morihara, T., Takeda, M., Wood, P. L., Goodenowe, D.-B., … Takeda, M. (2007). Peripheral ethanolamine plasmalogen deficiency: A logical causative factor in Alzheimer's disease and dementia. *Journal of Lipid Research*, *48*(11), 2485–2498. https://doi.org/10.1194/JLR.P700023-JLR200

Guo, M., Stockert, L., Akbar, M., & Kim, H. Y. (2007). Neuronal specific increase of phosphatidylserine by docosahexaenoic acid. *Journal of Molecular Neuroscience : MN*, *33*(1), 67–73. https://doi.org/10.1007/S12031-007-0046-Z

Hamilton, J., Greiner, R., Salem N., J., & Kim, H. Y. (2000). N-3 fatty acid deficiency decreases phosphatidylserine accumulation selectively in neuronal tissues. *Lipids*, *35*(8), 863–869. https://doi.org/10.1007/S11745-000-0595-X

Hancock, S. E., Friedrich, M. G., Mitchell, T. W., Truscott, R. J. W., & Else, P. L. (2015). Decreases in phospholipids containing adrenic and arachidonic acids occur in the human hippocampus over the adult lifespan. *Lipids*, *50*(9), 861–872. https://doi.org/10.1007/s11745-015-4030-z

Harper, A. (2010). Mouse models of neurological disorders—A comparison of heritable and acquired traits. *Biochimica et Biophysica Acta (BBA) - Molecular Basis of Disease*, *1802*(10), 785–795. https://doi.org/10.1016/J.BBADIS.2010.05.009

Hashimoto, M., Hossain, M. S., Shimada, T., Yamasaki, H., Fujii, Y., & Shido, O. (2001). Effects of docosahexaenoic acid on annular lipid fluidity of the rat bile canalicular plasma membrane. *Journal of Lipid Research*, *42*(7), 1160–1168. https://doi.org/10.1016/s0022-2275(20)31607-2

Hazel, J. (1990). The role of alterations in membrane lipid composition in enabling physiological adaptation of organisms to their physical environment. *Progress in Lipid Research*, *29*(3), 167–227. https://doi.org/10.1016/0163-7827(90)90002-3

Herrera, L. C., Potvin, M. A., & Melanson, J. E. (2010). Quantitative analysis of positional

isomers of triacylglycerols via electrospray ionization tandem mass spectrometry of sodiated adducts. *Rapid Communications in Mass Spectrometry : RCM*, *24*(18), 2745–2752. https://doi.org/10.1002/RCM.4700

Hess, B., Kutzner, C., Van Der Spoel, D., & Lindahl, E. (2008). GRGMACS 4: Algorithms for highly efficient, load-balanced, and scalable molecular simulation. *Journal of Chemical Theory and Computation*, *4*(3), 435–447. https://doi.org/10.1021/CT700301Q/ASSET/IMAGES/LARGE/CT700301QF00006.JPEG

Higashi, T., & Shimada, K. (2004). Derivatization of neutral steroids to enhance their detection characteristics in liquid chromatography-mass spectrometry. *Analytical and Bioanalytical Chemistry*, *378*(4), 875–882. https://doi.org/10.1007/s00216-003-2252-z

Hirabayashi, Y. (2012). A world of sphingolipids and glycolipids in the brain —Novel functions of simple lipids modified with glucose—. *Proceedings of the Japan Academy. Series B, Physical and Biological Sciences*, *88*(4), 129. https://doi.org/10.2183/PJAB.88.129

Horrobin, D. F. (1998). The membrane phospholipid hypothesis as a biochemical basis for the neurodevelopmental concept of schizophrenia. *Schizophrenia Research*, *30*(3), 193–208. https://doi.org/10.1016/S0920-9964(97)00151-5

Horrobin, D. F., Glen, A. I. M., & Vaddadi, K. (1994). The membrane hypothesis of schizophrenia. *Schizophrenia Research*, *13*(3), 195–207. https://doi.org/10.1016/0920-9964(94)90043-4

Horwood, J. M., Dufour, F., Laroche, S., & Davis, S. (2006). Signalling mechanisms mediated by the phosphoinositide 3-kinase/Akt cascade in synaptic plasticity and memory in the rat.

The European Journal of Neuroscience, *23*(12), 3375–3384. https://doi.org/10.1111/J.1460-9568.2006.04859.X

Hossain, M. S., Ifuku, M., Take, S., Kawamura, J., Miake, K., & Katafuchi, T. (2013). Plasmalogens rescue neuronal cell death through an activation of AKT and ERK survival signaling. *PloS One*, *8*(12), e83508. https://doi.org/10.1371/JOURNAL.PONE.0083508

Hossain, M. S., Mawatari, S., & Fujino, T. (2020). Biological functions of plasmalogens. In *Peroxisome biology: Experimental models, peroxisomal disorders and neurological diseases* (pp. 171–193). Springer. https://doi.org/10.1007/978-3-030-60204-8_13/COVER/

Hossain, M. S., Mawatari, S., & Fujino, T. (2022). Plasmalogens, the vinyl ether-linked glycerophospholipids, enhance learning and memory by regulating brain-derived neurotrophic factor. *Frontiers in Cell and Developmental Biology*, *10*, 153. https://doi.org/10.3389/FCELL.2022.828282/BIBTEX

Hossain, M. S., Mawatari, S., & Fujino, T. (2023). Plasmalogens inhibit neuroinflammation and promote cognitive function. *Brain Research Bulletin*, *192*(November 2022), 56–61. https://doi.org/10.1016/j.brainresbull.2022.11.005

Hossain, M. S., Mineno, K., & Katafuchi, T. (2016). Neuronal orphan G-protein coupled receptor proteins mediate plasmalogens-induced activation of ERK and Akt signaling. *PLoS ONE*, *11*(3), e0150846. https://doi.org/10.1371/journal.pone.0150846

Huber, T., Rajamoorthi, K., Kurze, V. F., Beyer, K., & Brown, M. F. (2002). Structure of docosahexaenoic acid-containing phospholipid bilayers as studied by (2)H NMR and molecular dynamics simulations. *Journal of the American Chemical Society*, *124*(2), 298–

309. https://doi.org/10.1021/JA011383J

Humphrey, W., Dalke, A., & Schulten, K. (1996). VMD: Visual molecular dynamics. *Journal of Molecular Graphics*, *14*(1), 33–38. https://doi.org/10.1016/0263-7855(96)00018-5

Hung, N. D., Kim, M. R., & Sok, D. E. (2011). Oral administration of 2-docosahexaenoyl lysophosphatidylcholine displayed anti-inflammatory effects on zymosan A-induced peritonitis. *Inflammation*, *34*(3), 147–160. https://doi.org/10.1007/S10753-010-9218-Z/FIGURES/10

Hussain, G., Wang, J., Rasul, A., Anwar, H., Imran, A., Qasim, M., Zafar, S., Kamran, S. K. S., Razzaq, A., Aziz, N., Ahmad, W., Shabbir, A., Iqbal, J., Baig, S. M., & Sun, T. (2019). Role of cholesterol and sphingolipids in brain development and neurological diseases. *Lipids in Health and Disease*, *18*(1), 1–12. https://doi.org/10.1186/S12944-019-0965-Z/FIGURES/5

Ifuku, M., Katafuchi, T., Mawatari, S., Noda, M., Miake, K., Sugiyama, M., & Fujino, T. (2012). Anti-inflammatory/anti-amyloidogenic effects of plasmalogens in lipopolysaccharide-induced neuroinflammation in adult mice. *Journal of Neuroinflammation*, *9*, 197. https://doi.org/10.1186/1742-2094-9-197

Ingólfsson, H. I., Carpenter, T. S., Bhatia, H., Bremer, P. T., Marrink, S. J., & Lightstone, F. C. (2017). Computational lipidomics of the neuronal plasma membrane. *Biophysical Journal*, *113*(10), 2271–2280. https://doi.org/10.1016/j.bpj.2017.10.017

Jacobs, M. L., Faizi, H. A., Peruzzi, J. A., Vlahovska, P. M., & Kamat, N. P. (2021). EPA and DHA differentially modulate membrane elasticity in the presence of cholesterol.

Biophysical Journal, *120*(11), 2317–2329. https://doi.org/10.1016/j.bpj.2021.04.009

Janssen, C. I. F., Zerbi, V., Mutsaers, M. P. C., de Jong, B. S. W., Wiesmann, M., Arnoldussen, I. A. C., Geenen, B., Heerschap, A., Muskiet, F. A. J., Jouni, Z. E., van Tol, E. A. F., Gross, G., Homberg, J. R., Berg, B. M., & Kiliaan, A. J. (2015). Impact of dietary n-3 polyunsaturated fatty acids on cognition, motor skills and hippocampal neurogenesis in developing C57BL/6J mice. *The Journal of Nutritional Biochemistry*, *26*(1), 24–35. https://doi.org/10.1016/J.JNUTBIO.2014.08.002

Javanainen, M., Martinez-Seara, H., & Vattulainen, I. (2017). Nanoscale membrane domain formation driven by cholesterol. *Scientific Reports*, *7*(1), 1–10. https://doi.org/10.1038/s41598-017-01247-9

Jia, X., Pakseresht, M., Wattar, N., Wildgrube, J., Sontag, S., Andrews, M., Subhan, F. B., McCargar, L., & Field, C. J. (2015). Women who take n-3 long-chain polyunsaturated fatty acid supplements during pregnancy and lactation meet the recommended intake. *Applied Physiology, Nutrition and Metabolism*, *40*(5), 474–481. https://doi.org/10.1139/apnm-2014-0313

Joardar, A., Pattnaik, G. P., & Chakraborty, H. (2021). Effect of phosphatidylethanolamine and oleic acid on membrane fusion: Phosphatidylethanolamine circumvents the classical Stalk model. *The Journal of Physical Chemistry. B*, *125*(48), 13192–13202. https://doi.org/10.1021/ACS.JPCB.1C08044

Joffre, C., Grégoire, S., De Smedt, V., Acar, N., Bretillon, L., Nadjar, A., & Layé, S. (2016). Modulation of brain PUFA content in different experimental models of mice.

Prostaglandins Leukotrienes and Essential Fatty Acids, *114*, 1–10. https://doi.org/10.1016/j.plefa.2016.09.003

Jurevics, H., & Morell, P. (1995). Cholesterol for synthesis of myelin is made locally, not imported into brain. *Journal of Neurochemistry*, *64*(2), 895–901. https://doi.org/10.1046/J.1471-4159.1995.64020895.X

Kalmijn, S., Foley, D., White, L., Burchfiel, C. M., Curb, J. D., Petrovitch, H., Ross, G. W., Havlik, R. J., & Launer, L. J. (2000). Metabolic cardiovascular syndrome and risk of dementia in Japanese-American elderly men. *Arteriosclerosis, Thrombosis, and Vascular Biology*, *20*(10), 2255–2260. https://doi.org/10.1161/01.ATV.20.10.2255

Katafuchi, T., Ifuku, M., Mawatari, S., Noda, M., Miake, K., Sugiyama, M., & Fujino, T. (2012). Effects of plasmalogens on systemic lipopolysaccharide-induced glial activation and β-amyloid accumulation in adult mice. *Annals of the New York Academy of Sciences*, *1262*(1), 85–92. https://doi.org/10.1111/J.1749-6632.2012.06641.X

Katakura, M., Hashimoto, M., Shahdat, H. M., Gamoh, S., Okui, T., Matsuzaki, K., & Shido, O. (2009). Docosahexaenoic acid promotes neuronal differentiation by regulating basic helix-loop-helix transcription factors and cell cycle in neural stem cells. *Neuroscience*, *160*(3), 651–660. https://doi.org/10.1016/J.NEUROSCIENCE.2009.02.057

Kawakita, E., Hashimoto, M., & Shido, O. (2006). Docosahexaenoic acid promotes neurogenesis in vitro and in vivo. *Neuroscience*, *139*(3), 991–997. https://doi.org/10.1016/J.NEUROSCIENCE.2006.01.021

Keimpema, E., Alpar, A., Howell, F., Malenczyk, K., Hobbs, C., Hurd, Y. L., Watanabe, M.,

Sakimura, K., Kano, M., Doherty, P., & Harkany, T. (2013). Diacylglycerol lipase α manipulation reveals developmental roles for intercellular endocannabinoid signaling. *Scientific Reports*, *3*(1), 1–9. https://doi.org/10.1038/srep02093

Khammari, A., Arab, S. S., & Ejtehadi, M. R. (2020). The hot sites of α-synuclein in amyloid fibril formation. *Scientific Reports*, *10*(1), 1–14. https://doi.org/10.1038/s41598-020-68887-2

Kim, H., Kim, H., Lee, E., Kim, Y., Ha, E. H., & Chang, N. (2017). Association between maternal intake of n-6 to n-3 fatty acid ratio during pregnancy and infant neurodevelopment at 6 months of age: Results of the MOCEH cohort study. *Nutrition Journal*, *16*(1), 1–10. https://doi.org/10.1186/s12937-017-0242-9

Kim, H. Y., Akbar, M., & Kim, Y. S. (2010). Phosphatidylserine-dependent neuroprotective signaling promoted by docosahexaenoic acid. *Prostaglandins, Leukotrienes, and Essential Fatty Acids*, *82*(4–6), 165. https://doi.org/10.1016/J.PLEFA.2010.02.025

Kim, H. Y., Huang, B. X., & Spector, A. A. (2014). Phosphatidylserine in the brain: Metabolism and function. *Progress in Lipid Research*, *56*, 1–18. https://doi.org/10.1016/J.PLIPRES.2014.06.002

Kim, H. Y., Huang, B. X., & Spector, A. A. (2022). Molecular and signaling mechanisms for docosahexaenoic acid-derived neurodevelopment and neuroprotection. *International Journal of Molecular Sciences*, *23*, 4635. https://doi.org/10.3390/IJMS23094635

Kim, H. Y., Moon, H. S., Cao, D., Lee, J., Kevala, K., Jun, S. B., Lovinger, D. M., Akbar, M., & Huang, B. X. (2011). N-docosahexaenoylethanolamide promotes development of

hippocampal neurons. *Biochemical Journal*, *435*(2), 327–336. https://doi.org/10.1042/BJ20102118

Kim, T. H., Yoo, J. Y., Choi, K. C., Shin, J. H., Leach, R. E., Fazleabas, A. T., Young, S. L., Lessey, B. A., Yoon, H. G., & Jeong, J. W. (2019). Loss of HDAC3 results in nonreceptive endometrium and female infertility. *Science Translational Medicine*, *11*(474). https://doi.org/10.1126/SCITRANSLMED.AAF7533

Kinney, H. C., Brody, B. A., Kloman, A. S., & Gilles, F. H. (1988). Sequence of central nervous system myelination in human infancy: II. Patterns of myelination in autopsied infants. *Journal of Neuropathology & Experimental Neurology*, *47*(3), 217–234. https://doi.org/10.1097/00005072-198805000-00003

Klein, M. E., Mauch, S., Rieckmann, M., Martínez, D. G., Hause, G., Noutsias, M., Hofmann, U., Lucas, H., Meister, A., Ramos, G., Loppnow, H., & Mäder, K. (2020). Phosphatidylserine (PS) and phosphatidylglycerol (PG) nanodispersions as potential anti-inflammatory therapeutics: Comparison of in vitro activity and impact of pegylation. *Nanomedicine: Nanotechnology, Biology and Medicine*, *23*, 102096. https://doi.org/10.1016/J.NANO.2019.102096

Koldsø, H., Shorthouse, D., Hélie, J., & Sansom, M. S. P. (2014). Lipid clustering correlates with membrane curvature as revealed by molecular simulations of complex lipid bilayers. *PLoS Computational Biology*, *10*(10), e1003911. https://doi.org/10.1371/journal.pcbi.1003911

Kuipers, R. S., Luxwolda, M. F., Offringa, P. J., Rudy Boersma, E., Janneke Dijck-Brouwer, D.

A., & Muskiet, F. A. J. (2012). Gestational age dependent changes of the fetal brain, liver and adipose tissue fatty acid compositions in a population with high fish intakes. *Prostaglandins, Leukotrienes and Essential Fatty Acids*, *86*(4–5), 189–199. https://doi.org/10.1016/J.PLEFA.2012.02.007

Kulig, W., Mikkolainen, H., Czerniak, T., Jurkiewicz, P., Cwiklik, L., Rog, T., Hof, M., Jungwirth, P., & Vattulainen, I. (2020). Tail-oxidized cholesterol enhances membrane permeability for small solutes. *Langmuir*, *36*, 10438−10447. https://doi.org/10.1021/acs.langmuir.0c01590

Kutchai, H., Chandler, L. H., & Zavoico, G. B. (1983). Effects of cholesterol on acyl chain dynamics in multilamellar vesicles. *Bwchimica et Biophysica Acta, 736*, 137–149.

Kutzner, C., Kniep, C., Cherian, A., Nordstrom, L., Grubmüller, H., De Groot, B. L., & Gapsys, V. (2022). GROMACS in the cloud: A global supercomputer to speed up alchemical drug design. *Journal of Chemical Information and Modeling*, *62*(7), 1691–1711. https://doi.org/10.1021/ACS.JCIM.2C00044/ASSET/IMAGES/LARGE/CI2C00044_0011.JPEG

Ladjohounlou, R., Louati, S., Lauret, A., Gauthier, A., Ardail, D., Magne, N., Alphonse, G., & Rodriguez-Lafrasse, C. (2020). Ceramide-enriched membrane domains contribute to targeted and nontargeted effects of radiation through modulation of PI3K/AKT signaling in HNSCC cells. *International Journal of Molecular Sciences*, *21*, 7200. https://doi.org/10.3390/IJMS21197200

Lahiri, S., & Futerman, A. H. (2007). The metabolism and function of sphingolipids and

glycosphingolipids. *Cellular and Molecular Life Sciences*, *64*(17), 2270–2284. https://doi.org/10.1007/s00018-007-7076-0

Lands, W. E. M., Morris, A., & Libelt, B. (1990). Quantitative effects of dietary polyunsaturated fats on the composition of fatty acids in rat tissues. *Lipids*, *25*(9), 505–516. https://doi.org/10.1007/BF02537156

Larqué, E., Gil-Sánchez, A., Prieto-Sánchez, M. T., & Koletzko, B. (2012). Omega 3 fatty acids, gestation and pregnancy outcomes. *British Journal of Nutrition*, *107*(S2), S77–S84. https://doi.org/10.1017/S0007114512001481

Larqué, E., Krauss-Etschmann, S., Campoy, C., Hartl, D., Linde, J., Klingler, M., Demmelmair, H., Caño, A., Gil, A., Bondy, B., & Koletzko, B. (2006). Docosahexaenoic acid supply in pregnancy affects placental expression of fatty acid transport proteins. *The American Journal of Clinical Nutrition*, *84*(4), 853–861. https://doi.org/10.1093/AJCN/84.4.853

Lauritzen, L., Brambilla, P., Mazzocchi, A., Harsløf, L. B. S., Ciappolino, V., & Agostoni, C. (2016). DHA Effects in Brain Development and Function. *Nutrients*, *8*(1). https://doi.org/10.3390/NU8010006

Lee, J. W., Huang, B. X., Kwon, H. S., Rashid, M. A., Kharebava, G., Desai, A., Patnaik, S., Marugan, J., & Kim, H. Y. (2016). Orphan GPR110 (ADGRF1) targeted by N-docosahexaenoylethanolamine in development of neurons and cognitive function. *Nature Communications 2016 7:1*, *7*(1), 1–16. https://doi.org/10.1038/ncomms13123

Lee, L. L., Aung, H. H., Wilson, D. W., Anderson, S. E., Rutledge, J. C., & Rutkowsky, J. M. (2017). Triglyceride-rich lipoprotein lipolysis products increase blood-brain barrier transfer

coefficient and induce astrocyte lipid droplets and cell stress. *American Journal of Physiology - Cell Physiology*, *312*(4), C500–C516. https://doi.org/10.1152/AJPCELL.00120.2016/ASSET/IMAGES/LARGE/ZH00031780950008.JPEG

Lee, S. R., Park, Y., & Park, J. W. (2020). Curvature effect of a phosphatidylethanolamine-included membrane on the behavior of cinnamycin on the membrane. *Journal of Physical Chemistry B*, *124*(41), 8984–8988. https://doi.org/10.1021/ACS.JPCB.0C06029/SUPPL_FILE/JP0C06029_SI_001.PDF

Leftin, A., Molugu, T. R., Job, C., Beyer, K., & Brown, M. F. (2014). Area per lipid and cholesterol interactions in membranes from separated local-field 13C NMR spectroscopy. *Biophysical Journal*, *107*(10), 2274–2286. https://doi.org/10.1016/j.bpj.2014.07.044

Li, L. H., Dutkiewicz, E. P., Huang, Y. C., Zhou, H. B., & Hsu, C. C. (2019). Analytical methods for cholesterol quantification. *Journal of Food and Drug Analysis*, *27*(2), 375–386. https://doi.org/10.1016/j.jfda.2018.09.001

Li, M., Gao, Y., Wang, D., Hu, X., Jiang, J., Qing, Y., Yang, X., Cui, G., Wang, P., Zhang, J., Sun, L., & Wan, C. (2022). Impaired membrane lipid homeostasis in schizophrenia. *Schizophrenia Bulletin*, *48*(5), 1125. https://doi.org/10.1093/SCHBUL/SBAC011

Liebisch, G., Binder, M., Schifferer, R., Langmann, T., Schulz, B., & Schmitz, G. (2006). High throughput quantification of cholesterol and cholesteryl ester by electrospray ionization tandem mass spectrometry (ESI-MS/MS). *Biochimica et Biophysica Acta - Molecular and Cell Biology of Lipids*, *1761*(1), 121–128. https://doi.org/10.1016/j.bbalip.2005.12.007

Lindahl, E., Hess, B., & van der Spoel, D. (2001). GROMACS 3.0: A package for molecular simulation and trajectory analysis. *Journal of Molecular Modeling*, *7*(8), 306–317. https://doi.org/10.1007/S008940100045/METRICS

Liu, G., Lee, D. P., Schmidt, E., & Prasad, G. L. (2019). Pathway analysis of global metabolomic profiles identified enrichment of caffeine, energy, and arginine metabolism in smokers but not moist snuff consumers. *Bioinformatics and Biology Insights*, *13*, 1–11. https://doi.org/10.1177/1177932219882961

Logan, A. M., Mammel, A. E., Robinson, D. C., Chin, A. L., Condon, A. F., & Robinson, F. L. (2017). Schwann cell-specific deletion of the endosomal PI 3-kinase Vps34 leads to delayed radial sorting of axons, arrested myelination, and abnormal ErbB2-ErbB3 tyrosine kinase signaling. *Glia*, *65*(9), 1452–1470. https://doi.org/10.1002/glia.23173

Lv, Y. Bin, Mao, C., Gao, X., Yin, Z. X., Kraus, V. B., Yuan, J. Q., Zhang, J., Luo, J. S., Zeng, Y., & Shi, X. M. (2019). Triglycerides paradox among the oldest old: "The lower the better?" *Journal of the American Geriatrics Society*, *67*(4), 741–748. https://doi.org/10.1111/JGS.15733

Madore, C., Nadjar, A., Delpech, J. C., Sere, A., Aubert, A., Portal, C., Joffre, C., & Layé, S. (2014). Nutritional n-3 PUFAs deficiency during perinatal periods alters brain innate immune system and neuronal plasticity-associated genes. *Brain, Behavior, and Immunity*, *41*(1), 22–31. https://doi.org/10.1016/J.BBI.2014.03.021

Maeba, R., Araki, A., & Fujiwara, Y. (2018). Serum ethanolamine plasmalogen and urine myo-inositol as cognitive decline markers. *Advances in Clinical Chemistry*, *87*, 69–111.

https://doi.org/10.1016/BS.ACC.2018.08.001

Magaquian, D., Delgado Ocaña, S., Perez, C., & Banchio, C. (2021). Phosphatidylcholine restores neuronal plasticity of neural stem cells under inflammatory stress. *Scientific Reports*, *11*(1), 1–12. https://doi.org/10.1038/s41598-021-02361-5

Makrides, M., Neumann, M. A., Byard, R. W., Simmer, K., & Gibson, R. A. (1994). Fatty acid composition of brain, retina, and erythrocytes in breast- and formula-fed infants. *American Journal of Clinical Nutrition*, *60*(2), 189–194. https://doi.org/10.1093/ajcn/60.2.189

Mallick, R., Basak, S., & Duttaroy, A. K. (2021). Fatty acids and evolving roles of their proteins in neurological, cardiovascular disorders and cancers. *Progress in Lipid Research*, *83*, 101116. https://doi.org/10.1016/J.PLIPRES.2021.101116

Mani, I., & Kurpad, A. V. (2016). Fats & fatty acids in Indian diets: Time for serious introspection. *The Indian Journal of Medical Research*, *144*(4), 507. https://doi.org/10.4103/0971-5916.200904

Marcucci, H., Paoletti, L., Jackowski, S., & Banchio, C. (2010). Phosphatidylcholine biosynthesis during neuronal differentiation and its role in cell fate determination. *Journal of Biological Chemistry*, *285*(33), 25382–25393. https://doi.org/10.1074/jbc.M110.139477

Mason, R. P., Jacob, R. F., Shrivastava, S., Sherratt, S. C. R., & Chattopadhyay, A. (2016). Eicosapentaenoic acid reduces membrane fluidity, inhibits cholesterol domain formation, and normalizes bilayer width in atherosclerotic-like model membranes. *Biochimica et Biophysica Acta (BBA) - Biomembranes*, *1858*(12), 3131–3140. https://doi.org/10.1016/J.BBAMEM.2016.10.002

Mathai, J. C., Tristram-Nagle, S., Nagle, J. F., & Zeidel, M. L. (2008). Structural determinants of water permeability through the lipid membrane. *Journal of General Physiology*, *131*(1), 69–76. https://doi.org/10.1085/jgp.200709848

Matsumoto, J., Nakanishi, H., Kunii, Y., Sugiura, Y., Yuki, D., Wada, A., Hino, M., Niwa, S. I., Kondo, T., Waki, M., Hayasaka, T., Masaki, N., Akatsu, H., Hashizume, Y., Yamamoto, S., Sato, S., Sasaki, T., Setou, M., & Yabe, H. (2017). Decreased 16:0/20:4-phosphatidylinositol level in the post-mortem prefrontal cortex of elderly patients with schizophrenia. *Scientific Reports*, *7*(October 2016), 6–7. https://doi.org/10.1038/srep45050

Matyash, V., Liebisch, G., Kurzchalia, T. V., Shevchenko, A., & Schwudke, D. (2008). Lipid extraction by methyl-terf-butyl ether for high-throughput lipidomics. *Journal of Lipid Research*, *49*(5), 1137–1146. https://doi.org/10.1194/jlr.D700041-JLR200

McEvoy, J., Baillie, R. A., Zhu, H., Buckley, P., Keshavan, M. S., Nasrallah, H. A., Dougherty, G. G., Yao, J. K., & Kaddurah-Daouk, R. (2013). Lipidomics reveals early metabolic changes in subjects with schizophrenia: Effects of atypical antipsychotics. *PLoS ONE*, *8*(7), 1–12. https://doi.org/10.1371/journal.pone.0068717

McNamara, R. K. (2010). DHA deficiency and prefrontal cortex neuropathology in recurrent affective disorders. *The Journal of Nutrition*, *140*(4), 864–868. https://doi.org/10.3945/JN.109.113233

McNamara, R. K., & Carlson, S. E. (2006). Role of omega-3 fatty acids in brain development and function: Potential implications for the pathogenesis and prevention of psychopathology. *Prostaglandins, Leukotrienes and Essential Fatty Acids*, *75*(4), 329–349.

https://doi.org/10.1016/J.PLEFA.2006.07.010

McNamara, R. K., Jandacek, R., Rider, T., Tso, P., Hahn, C. G., Richtand, N. M., & Stanford, K. E. (2007). Abnormalities in the fatty acid composition of the postmortem orbitofrontal cortex of schizophrenic patients: Gender differences and partial normalization with antipsychotic medications. *Schizophrenia Research*, *91*(1–3), 37–50. https://doi.org/10.1016/J.SCHRES.2006.11.027

Messias, M. C. F., Mecatti, G. C., Priolli, D. G., & De Oliveira Carvalho, P. (2018). Plasmalogen lipids: Functional mechanism and their involvement in gastrointestinal cancer. *Lipids in Health and Disease*, *17*(1), 1–12. https://doi.org/10.1186/S12944-018-0685-9/FIGURES/3

Miranda, M., Morici, J. F., Zanoni, M. B., & Bekinschtein, P. (2019). Brain-derived neurotrophic factor: A key molecule for memory in the healthy and the pathological brain. *Frontiers in Cellular Neuroscience*, *13*(August), 1–25. https://doi.org/10.3389/fncel.2019.00363

Montaner, A., Da Silva Santana, T. T., Schroeder, T., Einiker-Lamas, M., Girardini, J., Costa, M. R., & Banchio, C. (2018). Specific phospholipids regulate the acquisition of neuronal and astroglial identities in post-mitotic cells. *Scientific Reports*, *8*(1), 1–13. https://doi.org/10.1038/s41598-017-18700-4

Montgomery, C., Speake, B. K., Cameron, A., Sattar, N., & Weaver, L. T. (2003). Maternal docosahexaenoic acid supplementation and fetal accretion. *British Journal of Nutrition*, *90*(1), 135–145. https://doi.org/10.1079/bjn2003888

Morita, S., & Ikeda, Y. (2022). Regulation of membrane phospholipid biosynthesis in mammalian cells. *Biochemical Pharmacology*, *206*(October), 115296.

https://doi.org/10.1016/j.bcp.2022.115296

Mota-Martorell, N., Andrés-Benito, P., Martín-Gari, M., Galo-Licona, J. D., Sol, J., Fernández-Bernal, A., Portero-Otín, M., Ferrer, I., Jove, M., & Pamplona, R. (2022). Selective brain regional changes in lipid profile with human aging. *GeroScience*, *44*(2), 763–783. https://doi.org/10.1007/S11357-022-00527-1/TABLES/3

Mukherjee, S., & Chattopadhyay, A. (1996). Membrane organization at low cholesterol concentrations : A study using 7-Nitrobenz-2-oxa-1,3-diazol-4-yl-labeled cholesterol. *Biochemistry*, *35*, 1311–1322.

Murray, N. R., Fields, A. P., Natl, A. P. P., Sci, A., & Chem, J. B. (1998). Phosphatidylglycerol is a physiologic activator of nuclear protein kinase C. *Journal of Biological Chemistry*, *273*(19), 11514–11520. https://doi.org/10.1074/jbc.273.19.11514

Nagahara, A. H., Merrill, D. A., Coppola, G., Tsukada, S., Schroeder, B. E., Shaked, G. M., Wang, L., Blesch, A., Kim, A., Conner, J. M., Rockenstein, E., Chao, M. V., Koo, E. H., Geschwind, D., Masliah, E., Chiba, A. A., & Tuszynski, M. H. (2009). Neuroprotective effects of brain-derived neurotrophic factor in rodent and primate models of Alzheimer's disease. *Nature Medicine*, *15*(3), 331–337. https://doi.org/10.1038/nm.1912

Nägga, K., Gustavsson, A. M., Stomrud, E., Lindqvist, D., Van Westen, D., Blennow, K., Zetterberg, H., Melander, O., & Hansson, O. (2018). Increased midlife triglycerides predict brain β-amyloid and tau pathology 20 years later. *Neurology*, *90*(1), E73–E81. https://doi.org/10.1212/WNL.0000000000004749

Nakajima, R., Hagihara, H., & Miyakawa, T. (2021). Similarities of developmental gene

expression changes in the brain between human and experimental animals: Rhesus monkey, mouse, zebrafish, and drosophila. *Molecular Brain*, *14*(1), 1–5. https://doi.org/10.1186/s13041-021-00840-4

Namiecinska, M., Piatek, P., & Lewkowicz, P. (2024). Nervonic Acid Synthesis Substrates as Essential Components in Profiled Lipid Supplementation for More Effective Central Nervous System Regeneration. *International Journal of Molecular Sciences*, *25*(7). https://doi.org/10.3390/ijms25073792

Newville, J., Ortega, M. C., & Maxwell, J. R. (2018). Babies born early can have brain injury. *Frontiers for Young Minds*, *6*, 20. https://doi.org/10.3389/FRYM.2018.00020

Nguyen, L. N., Ma, D., Shui, G., Wong, P., Cazenave-Gassiot, A., Zhang, X., Wenk, M. R., Goh, E. L. K., & Silver, D. L. (2014). Mfsd2a is a transporter for the essential omega-3 fatty acid docosahexaenoic acid. *Nature*, *509*(7501), 503–506. https://doi.org/10.1038/nature13241

Nordström, V., Willershäuser, M., Herzer, S., Rozman, J., von Bohlen und Halbach, O., Meldner, S., Rothermel, U., Kaden, S., Roth, F. C., Waldeck, C., Gretz, N., de Angelis, M. H., Draguhn, A., Klingenspor, M., Gröne, H. J., & Jennemann, R. (2013). Neuronal expression of glucosylceramide synthase in central nervous system regulates body weight and energy homeostasis. *PLoS Biology*, *11*(3), e1001506. https://doi.org/10.1371/JOURNAL.PBIO.1001506

Noutsi, P., Gratton, E., & Chaieb, S. (2016). Assessment of Membrane Fluidity Fluctuations during Cellular Development Reveals Time and Cell Type Specificity. *PLoS ONE*, *11*(6), e0158313. https://doi.org/10.1371/JOURNAL.PONE.0158313

Numakawa, T., Odaka, H., & Adachi, N. (2018). Actions of brain-derived neurotrophin factor in the neurogenesis and neuronal function, and its involvement in the pathophysiology of brain diseases. *International Journal of Molecular Sciences*, *19*(11), 3650. https://doi.org/10.3390/ijms19113650

Nussbaum, J. L., Neskovic, N., & Mandel, P. (1971). The fatty acid composition of phospholipids and glycolipids in Jimpy mouse brain. *Journal of Neurochemistry*, *18*(8), 1529–1543. https://doi.org/10.1111/J.1471-4159.1971.TB00015.X

O'Brien, J. S., Fillerup, D. L., & Mead, J. F. (1964). Quantification and fatty acid and fatty aldehyde composition of ethanolamine, choline, and serine glycerophosphatides in human cerebral grey and white matter. *Journal of Lipid Research*, *5*(3), 329–338. https://doi.org/10.1016/S0022-2275(20)40201-9

O'Brien, J. S., & Sampson, E. L. (1965). Lipid composition of the normal human brain: Gray matter, white matter, and myelin. *Journal of Lipid Research*, *6*(4), 537–544. https://doi.org/10.1016/S0022-2275(20)39619-X

Oh, Y., Song, E. S., & Sung, B. J. (2021). The effects of the lipid type on the spatial arrangement and dynamics of cholesterol in binary component lipid membranes. *Journal of Chemical Physics*, *154*, 135101. https://doi.org/10.1063/5.0043212

Ollila, S., Hyvönen, M. T., & Vattulainen, I. (2007). Polyunsaturation in lipid membranes: Dynamic properties and lateral pressure profiles. *Journal of Physical Chemistry B*, *111*(12), 3139–3150. https://doi.org/10.1021/jp065424f

Olsen, A. S. B., & Færgeman, N. J. (2017). Sphingolipids: Membrane microdomains in brain

development, function and neurological diseases. *Open Biology*, *7*(5), 170069. https://doi.org/10.1098/RSOB.170069

Onodera, T., Futai, E., Kan, E., Abe, N., Uchida, T., Kamio, Y., & Kaneko, J. (2015). Phosphatidylethanolamine plasmalogen enhances the inhibiting effect of phosphatidylethanolamine on γ-secretase activity. *The Journal of Biochemistry*, *157*(5), 301–309. https://doi.org/10.1093/JB/MVU074

Orr, S. K., Palumbo, S., Bosetti, F., Mount, H. T., Kang, J. X., Greenwood, C. E., Ma, D. W. L., Serhan, C. N., & Bazinet, R. P. (2013). Unesterified docosahexaenoic acid is protective in neuroinflammation. *Journal of Neurochemistry*, *127*(3), 378–393. https://doi.org/10.1111/JNC.12392

Orsi, M., & Essex, J. W. (2012). Physical properties of mixed bilayers containing lamellar and nonlamellar lipids: Insights from coarse-grain molecular dynamics simulations. *Faraday Discussions*, *161*(0), 249–272. https://doi.org/10.1039/C2FD20110K/

Otoki, Y., Kato, S., Nakagawa, K., Harvey, D. J., Jin, L. W., Dugger, B. N., & Taha, A. Y. (2021). Lipidomic analysis of postmortem prefrontal cortex phospholipids reveals changes in choline plasmalogen containing docosahexaenoic acid and stearic acid between cases with and without Alzheimer's disease. *NeuroMolecular Medicine*, *23*(1), 161–175. https://doi.org/10.1007/s12017-020-08636-w

Paigen, B., Ishida, B. Y., Verstuyft, J., Winters, R. B., & Albee, D. (1990). Atherosclerosis susceptibility differences among progenitors of recombinant inbred strains of mice. *Arteriosclerosis*, *10*(2), 316–323. https://doi.org/10.1161/01.atv.10.2.316

Pakkanen, K. I., Duelund, L., Qvortrup, K., Pedersen, J. S., & Ipsen, J. H. (2011). Mechanics and dynamics of triglyceride-phospholipid model membranes: Implications for cellular properties and function. *Biochimica et Biophysica Acta - Biomembranes*, *1808*(8), 1947–1956. https://doi.org/10.1016/j.bbamem.2011.04.006

Palacios-Pelaez, R., Lukiw, W. J., & Bazan, N. G. (2010). Omega-3 essential fatty acids modulate initiation and progression of neurodegenerative disease. *Molecular Neurobiology*, *41*(2–3), 367–374. https://doi.org/10.1007/S12035-010-8139-Z/FIGURES/1

Páll, S., Abraham, M. J., Kutzner, C., Hess, B., & Lindahl, E. (2015). Tackling exascale software challenges in molecular dynamics simulations with GROMACS. *Lecture Notes in Computer Science (Including Subseries Lecture Notes in Artificial Intelligence and Lecture Notes in Bioinformatics)*, *8759*, 3–27. https://doi.org/10.1007/978-3-319-15976-8_1/FIGURES/7

Pandit, S. A., Vasudevan, S., Chiu, S. W., Mashl, R. J., Jakobsson, E., & Scott, H. L. (2004). Sphingomyelin-cholesterol domains in phospholipid membranes: Atomistic simulation. *Biophysical Journal*, *87*(2), 1092–1100. https://doi.org/10.1529/biophysj.104.041939

Papadopoulos, T., Rhee, H. J., Subramanian, D., Paraskevopoulou, F., Mueller, R., Schultz, C., Brose, N., Rhee, J. S., & Betz, H. (2017). Endosomal phosphatidylinositol 3-phosphate promotes gephyrin clustering and GABAergic neurotransmission at inhibitory postsynapses. *Journal of Biological Chemistry*, *292*(4), 1160–1177. https://doi.org/10.1074/jbc.M116.771592

Park, T., Chen, H., Kevala, K., Lee, J. W., & Kim, H. Y. (2016). N-

Docosahexaenoylethanolamine ameliorates LPS-induced neuroinflammation via cAMP/PKA-dependent signaling. *Journal of Neuroinflammation*, *13*(1), 1–15. https://doi.org/10.1186/s12974-016-0751-z

Park, Y. J., Kim, S., Shim, H. P., Park, J. H., Lee, G., Kim, T. Y., Jo, M. C., Kwon, A. Y., Lee, M., Lee, S., Yeo, J., Chung, H. L., Bellen, H. J., Kwon, S. H., & Jeon, S. H. (2021). Phosphatidylserine synthase plays an essential role in glia and affects development, as well as the maintenance of neuronal function. *IScience*, *24*(8), 102899. https://doi.org/10.1016/J.ISCI.2021.102899

Parrinello, M., & Rahman, A. (1980). Crystal structure and pair potentials: A molecular-dynamics study. *Physical Review Letters*, *45*(14), 1196. https://doi.org/10.1103/PhysRevLett.45.1196

Parrinello, M., & Rahman, A. (1981). Polymorphic transitions in single crystals: A new molecular dynamics method. *Journal of Applied Physics*, *52*(12), 7182–7190. https://doi.org/10.1063/1.328693

Parthasarathy, V., Frazier, D. T., Bettcher, B. M., Jastrzab, L., Chao, L., Reed, B., Mungas, D., Weiner, M., DeCarli, C., Chui, H., & Kramer, J. H. (2017). Triglycerides are negatively correlated with cognitive function in non-demented aging adults. *Neuropsychology*, *31*(6), 682–688. https://doi.org/10.1037/NEU0000335

Patel, D., & Witt, S. N. (2017). Ethanolamine and phosphatidylethanolamine: Partners in health and disease. *Oxidative Medicine and Cellular Longevity*, *2017*, 4829180. https://doi.org/10.1155/2017/4829180

Paula, S., Volkov, A. G., Van Hoek, A. N., Haines, T. H., & Deamer, D. W. (1996). Permeation of protons, potassium ions, and small polar molecules through phospholipid bilayers as a function of membrane thickness. *Biophysical Journal*, *70*(1), 339–348. https://doi.org/10.1016/S0006-3495(96)79575-9

Peng, Y., Jiang, B. H., Yang, P. H., Cao, Z., Shi, X., Lin, M. C. M., He, M. L., & Kung, H. F. (2004). Phosphatidylinositol 3-kinase signaling is involved in neurogenesis during Xenopus embryonic development. *Journal of Biological Chemistry*, *279*(27), 28509–28514. https://doi.org/10.1074/jbc.M402294200

Petrov, A. M., Kasimov, M. R., & Zefirov, A. L. (2016). Brain cholesterol metabolism and its defects: Linkage to neurodegenerative diseases and synaptic dysfunction. *Acta Naturae*, *8*(1), 58–73. https://doi.org/10.32607/20758251-2016-8-1-58-73

Petursdottir, A. L., Farr, S. A., Morley, J. E., Banks, W. A., & Skuladottir, G. V. (2008a). Effect of dietary n-3 polyunsaturated fatty acids on brain lipid fatty acid composition, learning ability, and memory of senescence-accelerated mouse. *Journals of Gerontology - Series A Biological Sciences and Medical Sciences*, *63*(11), 1153–1160. https://doi.org/10.1093/gerona/63.11.1153

Petursdottir, A. L., Farr, S. A., Morley, J. E., Banks, W. A., & Skuladottir, G. V. (2008b). Effect of dietary n-3 polyunsaturated fatty acids on brain lipid fatty acid composition, learning ability, and memory of senescence-accelerated mouse. *The Journals of Gerontology: Series A*, *63*(11), 1153–1160. https://doi.org/10.1093/GERONA/63.11.1153

Pham, T. H., Zaeem, M., Fillier, T. A., Nadeem, M., Vidal, N. P., Manful, C., Cheema, S.,

Cheema, M., & Thomas, R. H. (2019). Targeting modified lipids during routine lipidomics analysis using HILIC and C30 reverse phase liquid chromatography coupled to mass spectrometry. *Scientific Reports, 9*(1), 1–15. https://doi.org/10.1038/s41598-019-41556-9

Philips, M. C. (1972). The physical state of phospholipids and cholesterol in monolayers, bilayers, and membranes. *Progress in Surface and Membrane Science*, *5*, 139–221. https://doi.org/10.1016/B978-0-12-571805-9.50009-9

Power, M. C., Rawlings, A., Sharrett, A. R., Bandeen-Roche, K., Coresh, J., Ballantyne, C. M., Pokharel, Y., Michos, E. D., Penman, A., Alonso, A., Knopman, D., Mosley, T. H., & Gottesman, R. F. (2018). Association of midlife lipids with 20-year cognitive change: A cohort study. *Alzheimer's & Dementia: The Journal of the Alzheimer's Association*, *14*(2), 167–177. https://doi.org/10.1016/J.JALZ.2017.07.757

Pronk, S., Páll, S., Schulz, R., Larsson, P., Bjelkmar, P., Apostolov, R., Shirts, M. R., Smith, J. C., Kasson, P. M., Van Der Spoel, D., Hess, B., & Lindahl, E. (2013). GROMACS 4.5: A high-throughput and highly parallel open source molecular simulation toolkit. *Bioinformatics (Oxford, England)*, *29*(7), 845–854. https://doi.org/10.1093/BIOINFORMATICS/BTT055

Quan, G., Xie, C., Dietschy, J. M., & Turley, S. D. (2003). Ontogenesis and regulation of cholesterol metabolism in the central nervous system of the mouse. *Brain Research. Developmental Brain Research*, *146*(1–2), 87–98. https://doi.org/10.1016/J.DEVBRAINRES.2003.09.015

Ramstedt, B., & Slotte, J. P. (2006). Sphingolipids and the formation of sterol-enriched ordered

membrane domains. *Biochimica et Biophysica Acta*, *1758*, 1945–1956. https://doi.org/10.1016/j.bbamem.2006.05.020

Rao, J. S., Ertley, R. N., DeMar, J. C., Rapoport, S. I., Bazinet, R. P., & Lee, H. J. (2007). Dietary n-3 PUFA deprivation alters expression of enzymes of the arachidonic and docosahexaenoic acid cascades in rat frontal cortex. *Molecular Psychiatry*, *12*(2), 151–157. https://doi.org/10.1038/sj.mp.4001887

Reddy, A. S., Warshaviak, D. T., & Chachisvilis, M. (2012). Effect of membrane tension on the physical properties of DOPC lipid bilayer membrane. *Biochimica et Biophysica Acta - Biomembranes*, *1818*(9), 2271–2281. https://doi.org/10.1016/j.bbamem.2012.05.006

Reitz, C., Luchsinger, J., Tang, M. X., Manly, J., & Mayeux, R. (2005). Impact of plasma lipids and time on memory performance in healthy elderly without dementia. *Neurology*, *64*(8), 1378–1383. https://doi.org/10.1212/01.WNL.0000158274.31318.3C

Rey, C., Nadjar, A., Buaud, B., Vaysse, C., Aubert, A., Pallet, V., Layé, S., & Joffre, C. (2016). Resolvin D1 and E1 promote resolution of inflammation in microglial cells in vitro. *Brain, Behavior, and Immunity*, *55*, 249–259. https://doi.org/10.1016/J.BBI.2015.12.013

Riganti, L., Antonucci, F., Gabrielli, M., Prada, I., Giussani, P., Viani, P., Valtorta, F., Menna, E., Matteoli, M., & Verderio, C. (2016). Sphingosine-1-phosphate (S1P) impacts presynaptic functions by regulating synapsin I localization in the presynaptic compartment. *Journal of Neuroscience*, *36*(16), 4624–4634. https://doi.org/10.1523/JNEUROSCI.3588-15.2016

Rommel, A. S., James, S. N., McLoughlin, G., Brandeis, D., Banaschewski, T., Asherson, P., &

Kuntsi, J. (2017). Association of preterm birth with attention-deficit/hyperactivity disorder–like and wider-ranging neurophysiological impairments of attention and inhibition. *Journal of the American Academy of Child and Adolescent Psychiatry*, *56*(1), 40–50. https://doi.org/10.1016/J.JAAC.2016.10.006

Rukmini, R., Rawat, S. S., Biswas, S. C., & Chattopadhyay, A. (2001). Cholesterol organization in membranes at Low concentrations: Effects of curvature stress and membrane thickness. *Biophysical Journal*, *81*(4), 2122–2134. https://doi.org/10.1016/S0006-3495(01)75860-2

Ruxton, C. H. S., Calder, P. C., Reed, S. C., & Simpson, M. J. A. (2005). The impact of long-chain n-3 polyunsaturated fatty acids on human health. *Nutrition Research Reviews*, *18*(1), 113–129. https://doi.org/10.1079/NRR200497

Sacket, S. J., Chung, H. Y., Okajima, F., & Im, D. S. (2009). Increase in sphingolipid catabolic enzyme activity during aging. *Acta Pharmacologica Sinica*, *30*(10), 1454–1461. https://doi.org/10.1038/aps.2009.136

Saher, G., Brügger, B., Lappe-Siefke, C., Möbius, W., Tozawa, R. I., Wehr, M. C., Wieland, F., Ishibashi, S., & Nave, K. A. (2005). High cholesterol level is essential for myelin membrane growth. *Nature Neuroscience*, *8*(4), 468–475. https://doi.org/10.1038/nn1426

Sakamoto, T., Cansev, M., & Wurtman, R. J. (2007). Oral supplementation with docosahexaenoic acid and uridine-5′-monophosphate increases dendritic spine density in adult gerbil hippocampus. *Brain Research*, *1182*(1), 50–59. https://doi.org/10.1016/J.BRAINRES.2007.08.089

Salem, N., Litman, B., Kim, H. Y., & Gawrisch, K. (2001). Mechanisms of action of

docosahexaenoic acid in the nervous system. *Lipids*, *36*(9), 945–959. https://doi.org/10.1007/S11745-001-0805-6

Sarnat, H. B. (2023). Sequences of synaptogenesis in the human fetal and neonatal brain by synaptophysin immunocytochemistry. *Frontiers in Cellular Neuroscience*, *17*, 1105183. https://doi.org/10.3389/FNCEL.2023.1105183/BIBTEX

Sarnat, H. B., & Flores-Sarnat, L. (2015). Synaptogenesis and myelination in the nucleus/tractus solitarius. *Journal of Child Neurology*, *31*(6), 722–732. https://doi.org/10.1177/0883073815615227

Schneider, N., Hauser, J., Oliveira, M., Cazaubon, E., Mottaz, S. C., O'Neill, B. V., Steiner, P., & Deoni, S. C. L. (2019). Sphingomyelin in brain and cognitive development: Preliminary data. *ENeuro*, *6*(4), ENEURO.0421-18.2019. https://doi.org/10.1523/ENEURO.0421-18.2019

Schumann-gillett, A., & Mara, M. L. O. (2019). The effects of oxidised phospholipids and cholesterol on the biophysical properties of POPC bilayers. *BBA - Biomembranes*, *1861*(1), 210–219. https://doi.org/10.1016/j.bbamem.2018.07.012

Schurman, L. D., Carper, M. C., Moncayo, L. V., Ogasawara, D., Richardson, K., Yu, L., Liu, X., Poklis, J. L., Liu, Q. S., Cravatt, B. F., & Lichtman, A. H. (2019). Diacylglycerol lipase-alpha regulates hippocampal-dependent learning and memory processes in mice. *Journal of Neuroscience*, *39*(30), 5949–5965. https://doi.org/10.1523/JNEUROSCI.1353-18.2019

Sheng, R., Chen, Y., Yung Gee, H., Stec, E., Melowic, H. R., Blatner, N. R., Tun, M. P., Kim, Y., Källberg, M., Fujiwara, T. K., Hye Hong, J., Pyo Kim, K., Lu, H., Kusumi, A., Goo

Lee, M., & Cho, W. (2012). Cholesterol modulates cell signaling and protein networking by specifically interacting with PDZ domain-containing scaffold proteins. *Nature Communications*, *3*, 1–9. https://doi.org/10.1038/ncomms2221

Shinoda, W. (2016). Permeability across lipid membranes. *Biochimica et Biophysica Acta - Biomembranes*, *1858*(10), 2254–2265. https://doi.org/10.1016/j.bbamem.2016.03.032

Shoji, H., Takao, K., Hattori, S., & Miyakawa, T. (2016). Age-related changes in behavior in C57BL/6J mice from young adulthood to middle age. *Molecular Brain*, *9*(1), 1–18. https://doi.org/10.1186/s13041-016-0191-9

Simopoulos, A. P. (2016). An increase in the omega-6/omega-3 fatty acid ratio increases the risk for obesity. *Nutrients*, *8*(3), 128. https://doi.org/10.3390/NU8030128

Siskind, L. J., & Colombini, M. (2000). The lipids C2- and C16-ceramide form large stable channels: Implications for apoptosis. *The Journal of Biological Chemistry*, *275*(49), 38640. https://doi.org/10.1074/JBC.C000587200

Skannal, D. G., Brockman, D. E., Eis, A. L. W., Xue, S., Siddiqi, T. A., & Myatt, L. (1997). Changes in activity of cytosolic phospholipase A2 in human amnion at parturition. *American Journal of Obstetrics and Gynecology*, *177*(1), 179–184. https://doi.org/10.1016/S0002-9378(97)70459-9

Smith, P., & Lorenz, C. D. (2021). LiPyphilic: A python toolkit for the analysis of lipid membrane simulations. *Journal of Chemical Theory and Computation*, *17*(9), 5907–5919. https://doi.org/10.1021/acs.jctc.1c00447

Smith, S. L., & Rouse, C. A. (2017). Docosahexaenoic acid and the preterm infant. *Maternal Health, Neonatology and Perinatology*, *3*(1), 1–8. https://doi.org/10.1186/s40748-017-0061-1

Son, H., Madelian, V., & Carpenter, D. O. (1996). The translocation and involvement of protein kinase C in mossy fiber-CA3 long-term potentiation in hippocampus of the rat brain. *Brain Research*, *739*, 282–292.

Stiban, J., Tidhar, R., & Futerman, A. H. (2010). Ceramide synthases: Roles in cell physiology and signaling. *Advances in Experimental Medicine and Biology*, *688*, 60–71. https://doi.org/10.1007/978-1-4419-6741-1_4

Stonehouse, W., Conlon, C. A., Podd, J., Hill, S. R., Minihane, A. M., Haskell, C., & Kennedy, D. (2013). DHA supplementation improved both memory and reaction time in healthy young adults: A randomized controlled trial. *American Journal of Clinical Nutrition*, *97*(5), 1134–1143. https://doi.org/10.3945/ajcn.112.053371

Su, X. Q., Wang, J., & Sinclair, A. J. (2019). Plasmalogens and Alzheimer's disease: A review. *Lipids in Health and Disease*, *18*(1). https://doi.org/10.1186/s12944-019-1044-1

Sugasini, D., Thomas, R., Yalagala, P. C. R., Tai, L. M., & Subbaiah, P. V. (2017). Dietary docosahexaenoic acid (DHA) as lysophosphatidylcholine, but not as free acid, enriches brain DHA and improves memory in adult mice. *Scientific Reports*, *7*(1), 1–11. https://doi.org/10.1038/s41598-017-11766-0

Sui, L., Wang, J., & Li, B. M. (2008). Role of the phosphoinositide 3-kinase-Akt-mammalian target of the rapamycin signaling pathway in long-term potentiation and trace fear

conditioning memory in rat medial prefrontal cortex. *Learning & Memory (Cold Spring Harbor, N.Y.)*, *15*(10), 762–776. https://doi.org/10.1101/LM.1067808

Sun, J., Wang, L., Bao, H., Premi, S., Das, U., Chapman, E. R., & Roy, S. (2019). Functional cooperation of α-synuclein and VAMP2 in synaptic vesicle recycling. *Proceedings of the National Academy of Sciences of the United States of America*, *116*(23), 11113–11115. https://doi.org/10.1073/PNAS.1903049116

Suzuki, H., Park, S. J., Tamura, M., & Ando, S. (1998). Effect of the long-term feeding of dietary lipids on the learning ability, fatty acid composition of brain stem phospholipids and synaptic membrane fluidity in adult mice: A comparison of sardine oil diet with palm oil diet. *Mechanisms of Ageing and Development*, *101*(1–2), 119–128. https://doi.org/10.1016/s0047-6374(97)00169-3

Swanson, D., Block, R., & Mousa, S. A. (2012). Omega-3 Fatty Acids EPA and DHA: Health Benefits Throughout Life. *Advances in Nutrition*, *3*(1), 1–7. https://doi.org/10.3945/AN.111.000893

Sweatt, J. D., Atkins, C. M., Johnson, J., English, J. D., Roberson, E. D., Chen, S., Newton, A., & Klann, E. (1998). Protected-site phosphorylation of protein kinase C in hippocampal long-term potentiation. *Journal of Neurochemistry*, *71*, 1075–1085.

Tahaei, H., Gignac, F., Pinar, A., Fernandez-Barrés, S., Romaguera, D., Vioque, J., Santa-Marina, L., Subiza-Pérez, M., Llop, S., Soler-Blasco, R., Arija, V., Salas-Salvadó, J., Tardón, A., Riaño-Galán, I., Sunyer, J., Guxens, M., & Julvez, J. (2022). Omega-3 fatty acid intake during pregnancy and child neuropsychological development: A multi-centre

population-based birth cohort study in Spain. *Nutrients*, *14*(3), 518. https://doi.org/10.3390/NU14030518

Tam, E. W. Y., Chau, V., Barkovich, A. J., Ferriero, D. M., Miller, S. P., Rogers, E. E., Grunau, R. E., Synnes, A. R., Xu, D., Foong, J., Brant, R., & Innis, S. M. (2016). Early postnatal docosahexaenoic acid levels and improved preterm brain development. *Clinical Investigation*, *79*(5), 723–730. https://doi.org/10.1038/pr.2016.11

Tasseva, G., Daniel Bai, H., Davidescu, M., Haromy, A., Michelakis, E., & Vance, J. E. (2012). Phosphatidylethanolamine deficiency in mammalian mitochondria impairs oxidative phosphorylation and alters mitochondrial morphology. *Journal of Biological Chemistry*, *288*, 4158–4173. https://doi.org/10.1074/jbc.M112.434183

Teigler, A., Komljenovic, D., Draguhn, A., Gorgas, K., & Just, W. W. (2009). Defects in myelination, paranode organization and Purkinje cell innervation in the ether lipid-deficient mouse cerebellum. *Human Molecular Genetics*, *18*(11), 1897–1908. https://doi.org/10.1093/HMG/DDP110

The Dutch-Belgian Fragile X Consorthium, Bakker, C. E., Verheij, C., Willemsen, R., van der Helm, R., Oerlemans, F., Vermey, M., Bygrave, A., Hoogeveen, A. T., Oostra, B. A., Reyniers, E., De Boule, K., D'Hooge, R., Cras, P., van Velzen, D., Nagels, G., Martin, J. J., De Deyn, P. P., Darby, J. K., & Willems, P. J. (1994). Fmr1 knockout mice: A model to study fragile X mental retardation. *Cell*, *78*(1), 23–33. https://doi.org/10.1016/0092-8674(94)90569-X

Thomas, M. H., Paris, C., Magnien, M., Colin, J., Pelleïeux, S., Coste, F., Escanyé, M. C., Pillot,

T., & Olivier, J. L. (2017). Dietary arachidonic acid increases deleterious effects of amyloid-β oligomers on learning abilities and expression of AMPA receptors: Putative role of the ACSL4-cPLA2 balance. *Alzheimer's Research and Therapy*, *9*(1), 1–24. https://doi.org/10.1186/S13195-017-0295-1/TABLES/4

Treen, M., Uauy, R. D., Jameson, D. M., Thomas, V. L., & Hoffman, D. R. (1992). Effect of docosahexaenoic acid on membrane fluidity and function in intact cultured Y-79 retinoblastoma cells. *Archives of Biochemistry and Biophysics*, *294*(2), 564–570. https://doi.org/10.1016/0003-9861(92)90726-D

Tu-Sekine, B., & Raben, D. M. (2011). Regulation and roles of neuronal diacylglycerol kinases: A lipid perspective. *Critical Reviews in Biochemistry and Molecular Biology*, *46*(5), 353–364. https://doi.org/10.3109/10409238.2011.577761

Udagawa, J., & Hino, K. (2022). Plasmalogen in the brain: Effects on cognitive functions and behaviors attributable to its properties. *Brain Research Bulletin*, *188*(March), 197–202. https://doi.org/10.1016/j.brainresbull.2022.08.008

Ueda, Y., Ishitsuka, R., Hullin-Matsuda, F., & Kobayashi, T. (2014). Regulation of the transbilayer movement of diacylglycerol in the plasma membrane. *Biochimie*, *107*(Part A), 43–50. https://doi.org/10.1016/j.biochi.2014.09.014

Ul Amin, F., Shah, S. A., & Kim, M. O. (2017). Vanillic acid attenuates Aβ1-42-induced oxidative stress and cognitive impairment in mice. *Scientific Reports*, *7*(December 2016), 1–15. https://doi.org/10.1038/srep40753

Van Der Spoel, D., Lindahl, E., Hess, B., Groenhof, G., Mark, A. E., & Berendsen, H. J. C.

(2005). GROMACS: Fast, flexible, and free. *Journal of Computational Chemistry*, *26*(16), 1701–1718. https://doi.org/10.1002/JCC.20291

Vance, J. E. (2015). Phospholipid synthesis and transport in mammalian cells. *Traffic*, *16*(1), 1–18. https://doi.org/10.1111/tra.12230

Vanes, L. D., Murray, R. M., & Nosarti, C. (2022). Adult outcome of preterm birth: Implications for neurodevelopmental theories of psychosis. *Schizophrenia Research*, *247*, 41–54. https://doi.org/10.1016/J.SCHRES.2021.04.007

Velasco, A., Tabernero, A., & Medina, J. M. (2003). Role of oleic acid as a neurotrophic factor is supported in vivo by the expression of GAP-43 subsequent to the activation of SREBP-1 and the up-regulation of stearoyl-CoA desaturase during postnatal development of the brain. *Brain Research*, *977*(1), 103–111. https://doi.org/10.1016/S0006-8993(03)02772-0

Vozella, V., Basit, A., Misto, A., & Piomelli, D. (2017). Age-dependent changes in nervonic acid-containing sphingolipids in mouse hippocampus. *Biochimica et Biophysica Acta - Molecular and Cell Biology of Lipids*, *1862*(12), 1502–1511. https://doi.org/10.1016/j.bbalip.2017.08.008

Wainwright, P. E. (2002). Dietary essential fatty acids and brain function: A developmental perspective on mechanisms. *Proceedings of the Nutrition Society*, *61*(1), 61–69. https://doi.org/10.1079/pns2001130

Wainwright, P. E., Huang, Y. S., Bulman-Fleming, B., Mills, D. E., Redden, P., & McCutcheon, D. (1991). The role of n-3 essential fatty acids in brain and behavioral development: A cross-fostering study in the mouse. *Lipids*, *26*(1), 37–45.

https://doi.org/10.1007/BF02544022

Wang, D. D., Wu, F., Zhang, L. Y., Zhao, Y. C., Wang, C. C., Xue, C. H., Yanagita, T., Zhang, T. T., & Wang, Y. M. (2021). Effects of dietary n-3 PUFA levels in early life on susceptibility to high-fat-diet-induced metabolic syndrome in adult mice. *The Journal of Nutritional Biochemistry*, *89*, 108578. https://doi.org/10.1016/J.JNUTBIO.2020.108578

Wang, G., & Bieberich, E. (2018). Sphingolipids in neurodegeneration (with focus on ceramide and S1P). *Advances in Biological Regulation*, *70*(September), 51–64. https://doi.org/10.1016/j.jbior.2018.09.013

Wang, P. Y., Weng, J., & Anderson, R. G. W. (2005). OSBP is a cholesterol-regulated scaffolding protein in control of ERK1/2 activation. *Science*, *307*(5714), 1472–1476. https://doi.org/10.1126/science.1107710

Wang, Z. J., Li, G. M., Tang, W. L., & Yin, M. (2006). Neuroprotective effects of stearic acid against toxicity of oxygen/glucose deprivation or glutamate on rat cortical or hippocampal slices. *Acta Pharmacologica Sinica*, *27*(2), 145–150. https://doi.org/10.1111/j.1745-7254.2006.00259.x

Wassenaar, T. A., Ingólfsson, H. I., Böckmann, R. A., Tieleman, D. P., & Marrink, S. J. (2015). Computational lipidomics with insane: A versatile tool for generating custom membranes for molecular simulations. *Journal of Chemical Theory and Computation*, *11*(5), 2144–2155. https://doi.org/10.1021/ACS.JCTC.5B00209/SUPPL_FILE/CT5B00209_SI_001.PDF

Wechsler, A., Brafman, A., Shafir, M., Heverin, M., Gottlieb, H., Damari, G., Gozlan-Kelner, S., Spivak, I., Moshkin, O., Fridman, E., Becker, Y., Skaliter, R., Einat, P., Faerman, A.,

Björkhem, I., & Feinstein, E. (2003). Generation of viable cholesterol-free mice. *Science*, *302*(5653), 2087. https://doi.org/10.1126/SCIENCE.1090776/SUPPL_FILE/WECHSLER.SOM.PDF

Wei, D., Allsop, S., Tye, K., & Piomelli, D. (2017). Endocannabinoid signaling in the control of social behavior. *Trends in Neurosciences*, *40*(7), 385–396. https://doi.org/10.1016/j.tins.2017.04.005

Wei, D., Lee, D., Li, D., Daglian, J., Jung, K., & Piomelli, D. (2016). A role for the endocannabinoid 2-arachidonoyl- sn -glycerol for social and high-fat food reward in male mice. *Psychopharmacology*, *233*, 1911–1919. https://doi.org/10.1007/s00213-016-4222-0

West, A., Zoni, V., Teague, W. E., Leonard, A. N., Vanni, S., Gawrisch, K., Tristram-Nagle, S., Sachs, J. N., & Klauda, J. B. (2020). How do ethanolamine plasmalogens contribute to order and structure of neurological membranes? *The Journal of Physical Chemistry. B*, *124*(5), 828–839. https://doi.org/10.1021/ACS.JPCB.9B08850

Westmark, C. J., Filon, M. J., Maina, P., Steinberg, L. I., Ikonomidou, C., & Westmark, P. R. (2022). Effects of soy-based infant formula on weight gain and neurodevelopment in an autism mouse model. *Cells*, *11*(8), 1350. https://doi.org/10.3390/CELLS11081350/S1

Whelan, J., & Fritsche, K. (2013). Linoleic acid. *Advances in Nutrition*, *4*(3), 311–312. https://doi.org/10.3945/an.113.003772

Williams, C. M., & Burdge, G. (2006). Long-chain n −3 PUFA: plant v . marine sources . *Proceedings of the Nutrition Society*, *65*(1), 42–50. https://doi.org/10.1079/pns2005473

Wilson, K. A., Fairweather, S. J., Macdermott-Opeskin, H. I., Wang, L., Morris, R. A., & O'mara, M. L. (2021). The role of plasmalogens, Forssman lipids, and sphingolipid hydroxylation in modulating the biophysical properties of the epithelial plasma membrane. *The Journal of Chemical Physics*, *154*(9), 095101. https://doi.org/10.1063/5.0040887

Wilson, K. A., MacDermott-Opeskin, H. I., Riley, E., Lin, Y., & O'Mara, M. L. (2020). Understanding the link between lipid diversity and the biophysical properties of the neuronal plasma membrane. *Biochemistry*, *59*(33), 3010–3018. https://doi.org/10.1021/acs.biochem.0c00524

Wilson, K. A., Wang, L., & O'Mara, M. L. (2021). Site of cholesterol oxidation impacts its localization and domain formation in the neuronal plasma membrane. *ACS Chemical Neuroscience*, *12*(20), 3873–3884. https://doi.org/10.1021/acschemneuro.1c00395

Wong, H. H. W., Chou, C. Y. C., Watt, A. J., & Sjöström, P. J. (2023). Neural circuits: Comparing mouse and human brains. *ELife*, *12*, e90017. https://doi.org/10.7554/ELIFE.90017

Wu, C., Ifa, D. R., Manicke, N. E., & Cooks, R. G. (2009). Rapid, direct analysis of cholesterol by charge labeling in reactive desorption electrospray ionization. *Analytical Chemistry*, *81*(18), 7618–7624. https://doi.org/10.1021/ac901003u

Wu, H., Zhang, W., Huang, M., Lin, X., & Chiou, J. (2023). Prolonged high-fat diet consumption throughout adulthood in mice induced neurobehavioral deterioration via gut-brain axis. *Nutrients*, *15*(2), 392. https://doi.org/10.3390/NU15020392

Wu, Y. Z., Medjane, S., Chabot, S., Kubrusly, F. S., Raw, I., Chignard, M., & Touqui, L. (2003).

Surfactant protein-A and phosphatidylglycerol suppress type IIA phospholipase A2 synthesis via nuclear factor-κB. *American Journal of Respiratory and Critical Care Medicine*, *168*(6 I), 692–699. https://doi.org/10.1164/rccm.200304-467OC

Xiao, Y., Huang, Y., & Chen, Z. (2005). Distribution , depletion and recovery of docosahexaenoic acid are region-specific in rat brain. *British Journal of Nutrition*, *94*, 544–550. https://doi.org/10.1079/BJN20051539

Xing, Y., Tang, Y., Zhao, L., Wang, Q., Qin, W., Ji, X., Zhang, J., & Jia, J. (2016). Associations between plasma ceramides and cognitive and neuropsychiatric manifestations in Parkinson ' s disease dementia. *Journal of the Neurological Sciences*, *370*, 82–87. https://doi.org/10.1016/j.jns.2016.09.028

Xu, D., Omura, T., Masaki, N., Arima, H., Banno, T., Okamoto, A., Hanada, M., Takei, S., Matsushita, S., Sugiyama, E., Setou, M., & Matsuyama, Y. (2016). Increased arachidonic acid-containing phosphatidylcholine is associated with reactive microglia and astrocytes in the spinal cord after peripheral nerve injury. *Scientific Reports*, *6*(April), 1–11. https://doi.org/10.1038/srep26427

Xu, X., & London, E. (2000). The effect of sterol structure on membrane lipid domains reveals how cholesterol can induce lipid domain formation. *Biochemistry*, *39*(5), 843–849.

Yang, G., Kitagawa, K., Matsushita, K., Mabuchi, T., Yagita, Y., Yanagihara, T., & Matsumoto, M. (1997). C57BL/6 strain is most susceptible to cerebral ischemia following bilateral common carotid occlusion among seven mouse strains: Selective neuronal death in the murine transient forebrain ischemia. *Brain Research*, *752*(1–2), 209–218.

https://doi.org/10.1016/S0006-8993(96)01453-9

Yarnykh, V. L., Prihod'ko, I. Y., Savelov, A. A., & Korostyshevskaya, A. M. (2018). Quantitative assessment of normal fetal brain myelination using fast macromolecular proton fraction mapping. *AJNR: American Journal of Neuroradiology*, *39*(7), 1341. https://doi.org/10.3174/AJNR.A5668

Yesylevskyy, S. O., Schäfer, L. V., Sengupta, D., & Marrink, S. J. (2010). Polarizable Water Model for the Coarse-Grained MARTINI Force Field. *PLOS Computational Biology*, *6*(6), e1000810. https://doi.org/10.1371/JOURNAL.PCBI.1000810

Yusuf, H. K. M., Dickerson, J. W. T., Hey, E. N., & Waterlow, J. C. (1981). Cholesterol Esters of the Human Brain During Fetal and Early Postnatal Development: Content and Fatty Acid Composition. *Journal of Neurochemistry*, *36*(2), 707–714. https://doi.org/10.1111/J.1471-4159.1981.TB01646.X

Zhang, J., & Liu, Q. (2015). Cholesterol metabolism and homeostasis in the brain. *Protein & Cell*, *6*(4), 254–264. https://doi.org/10.1007/S13238-014-0131-3

Zhang, Y., Li, X., Becker, K. A., & Gulbins, E. (2009). Ceramide-enriched membrane domains—Structure and function. *Biochimica et Biophysica Acta (BBA) - Biomembranes*, *1788*(1), 178–183. https://doi.org/10.1016/J.BBAMEM.2008.07.030

Zhao, R., Jiang, J., Li, H., Chen, M., Liu, R., Sun, S., Ma, D., Liang, X., & Wang, S. (2018). Phosphatidylserine-microbubble targeting-activated microglia/macrophage in inflammation combined with ultrasound for breaking through the blood-brain barrier. *Journal of Neuroinflammation*, *15*(1), 1–10. https://doi.org/10.1186/s12974-018-1368-1

Appendix 1

Composition of the semi-purified diet used for preparing 20% fat experimental diets

Constituents	Amount in g per kg diet
Casein	200
D/L-methionine	3
Sucrose	305
Corn starch	190
Alphacel non-nutritive bulk	50
Vitamin mix[a]	12
Mineral mix[b]	40

[a]**Vitamin Mix:** Thiamine hydrochloride (0.6 g), riboflavin (0.6 g), pyridoxine hydrochloride (0.7 g), nicotinic acid (3.0 g), D-calcium pantothenate (1.6 g), folic acid (0.2 g), D-biotin (0.02 g), cyanocobalamin (0.001 g), retinyl palmitate - pre-mix (250,000 IU/g) (1.6 g), D/L-α-tocopherol acetate (250 IU/g) (20 g), cholecalciferol (400,000 IU/g) (0.25 g), menaquinone (0.005 g), and finely powdered sucrose (972.9 g).

[b]**Mineral Mix:** Calcium phosphate dibasic (500.0 g/kg), sodium chloride (74.0 g/kg), potassium citrate monohydrate (220.0 g/kg), potassium sulfate (52.0 g/kg), magnesium oxide (24.0 g/kg), manganese carbonate (43-48% Mn, 3.50 g/kg), ferric citrate (16-17% Fe, 6.0 g/kg), zinc carbonate (70% ZnO, 1.6 g/kg), cupric carbonate (53-55% Cu, 0.30 g/kg), potassium iodate (0.01 g/kg), sodium selenite (0.01g/kg), chromium potassium sulfate (0.55 g/kg) and finely powdered sucrose (118.0 g/kg).

Appendix 2

Sources of fat added to the semi-purified fat-free diet

Fat sources	**Amount (g) in high n-3 PUFA diet**	**Amount (g) in low n-3 PUFA diet**
Menhaden fish oil	46	5
Safflower oil	92	113
Olive oil	32	31
Lard	30	51
Total	**200**	**200**

Appendix 3

Fatty acid composition of the experimental diets

Fatty acids (%)	High n-3 PUFA diet (n-6:n-3 PUFA, 5:1)	Low n-3 PUFA diet (n-6:n-3 PUFA, 40:1)
C14:0	2.42	0.66
C16:0	11.94	11.70
C18:0	4.36	5.16
∑ SFA	**18.72**	**17.53**
C16:1n-7	3.70	0.94
C18:1	22.80	25.32
C20:1n9	0.35	0.05
∑ MUFA	**26.85**	**26.30**
C18:2n6	45.23	54.81
C20:4n6	0.42	ND
∑ Omega (n)-6 PUFA	**45.65**	**54.81**
C18:3n3	0.81	0.82
C18:4n3	0.56	0.26
C20:5n3	4.13	0.16
C22:5n3	0.66	0.12
C22:6n3	2.59	ND
∑ Omega (n)-3 PUFA	**8.75**	**1.36**
n-6/n-3 PUFA	**5.2**	**40.1**

Values represented percentages in total fatty acid composition of oil extracted from the diet. Saturated fatty acids (SFA), monounsaturated fatty acids (MUFA), polyunsaturated fatty acids (PUFA).

Appendix 4

Chemical composition of the acyl tails of lipid species used to simulate the fetal neuronal membrane

Lipid species	Lipid class	MARTINI *			Atomistic #			Total unsaturation
		***sn-1* tail**	***sn-2* tail**	***sn-3* tail**	***sn-1* tail**	***sn-2* tail**	***sn-3* tail**	
LPC	LPC	CCCC			14:0			0
PPC		CCCC			16:0, 18:0			0
OPC		CDCC			16:1, 18:1			2
FPC		DDDC			18:3			3
APC		DDDD			20:4			4
DLPC	PC	CCCC	CCCC		14:0	14:0		0
LPPC		CCCC	CCCC		14:0	16:0		0
LOPC		CCCC	CDCC		14:0	16:1		1
DPPC		CCCC	CCCC		16:0;2	16:0, 18:0		0
POPC		CCCC	CDCC		16:0;2	16:1, 18:1		1
DOPC		CDCC	CDCC		16:1;2, 18:1	16:1, 18:1;2		2
OIPC		CDCC	CDDC		16:1	18:2		3
PSPC		CCCC	DDDD		16:0	18:4		4
OPPC		CDCC	CCCC		18:1	18:0		1
PQPC		CCCC	DDDC		16:0, 18:0	20:3;2		3
PAPC		CCCC	DDDD		16:0, 18:0	20:4;2		4
OAPC		CDCC	DDDD		16:1, 18:1	20:4;2		5
OBPC		CDCC	CCCC		18:1	20:0		1
OGPC		CDCC	CDCC		18:1	20:1		2
PUPC		CCCC	DDDDDD		16:0, 18:0	22:6;2		6
OUPC		CDCC	DDDDDD		16:1, 18:1	26:6;2		7
SGPC		DDDD	CDCC		18:4	22:1		5
DPAC		CCCC	CCCC		16:0;2	16:0, 18:0		0

DPMC		CCCC	CCCC	18:0	16:0	0
PPE	LPE	CCCC		16:0, 18:0		0
APE		DDDD		20:4		4
DPPE	PE	CCC	CCCC	18:0	16:0	0
DOPE		CCCC	CDCC	16:1, 18:1	18:1, 18:1	2
POPE		CCCC	CDCC	16:0;2, 18:0	16:1, 18:1;2	1
OIPE		CDCC	CDDC	18:1	18:2	3
PQPE		CCCC	DDDC	18:0	20:3	3
PAPE		CCCC	DDDD	16:0, 18:0, 16:0	20:4;2, 22:4	4
PUPE		CCCC	DDDDD	16:0;2, 18:0;2	22:5, 22:6, 22:5, 22:6	6
DPME	P-PE	CCCC	CCCC	16:0, 18:0	16:0;2	0
POME		CCCC	CDCC	16:0, 18:0	18:1;2	1
PAME		CCCC	DDDD	16:0;2, 18:0	20:4;2, 22:4	4
PUME		CCCC	DDDDD	16:0;2,18:0;2	22:5, 22:6, 22:5, 22:6	6
OAAE	O-PE	CCCC	DDDD	16:1,18:1	20:4;2	5
OUAE		CCCC	DDDDDD	16:1, 18:1	22:6;2	7
DOPG	PG	CDCC	CDCC	18:1,	18:1	2
POPG		CCCC	CDCC	18:0, 16:0;2	18:1;2, 16:1	1
PAPI	PI	CCCC	DDDD	18:0,	20:4	4
OAPI		CDCC	DDDD	18:1,	20:4	4
POPS	PS	CCCC	CDCC	18:0,	18:1	1
PAPS		CCCC	DDDD	18:0;2	20:4, 22:4	4
PUPS		CCCC	DDDDD	18:0,	22:5, 22:6	6

DPCE	Cer	CCCC	CCCC		d18:1	16:0, 18:0		1
OPCE		CCCC	CCCC		d18:2	18:0		2
PBCE		CCCC	CCCC		d18:1	20:0, 22:0		1
PXCE		CCCC	CCCC		d18:1	24:0		1
PNCE		CCCC	CDCC		d18:1	24:1		2
PWCE		CCCC	CDDC		d18:1	24:2		3
PNSM	SM	CCCC	CDCC		d18:1	24:1		2
PPDG	DG	CCCC	CCCC		16:0, 18:0;2	16:0;2, 18:0		0
PODG		CCCC	CDCC		16:0;2	16:1, 18:1		1
LCAP	O-TG	CCCC	CCCC	DDDD	12:0	6:0	20:4	4
TPG	TG	CCCC	CCCC	CCCC	16:0	16:0	16:0	0
PPOG		CCCC	CCCC	CDCC	16:0	16:0	18:1	1
POOG		CCCC	CDCC	CDCC	16:0;2	16:1,18:1	18:1;2	2
POIG		CCCC	CDCC	CDDC	16:0	18:1	18:2	3
PIIG		CCCC	CDDC	CDDC	16:0	18:2	18:2	4
TOG		CDCC	CDCC	CDCC	18:1	18:1	18:1	3
OOIG		CDCC	CDCC	CDDC	18:1	18:1	18:2	4
OIIG		CDCC	CDDC	CDDC	18:1	18:2	18:2	5
DPUG		CCCC	CCCC	DDDDDD	16:0	16:0	22:6	6
POUG		CCCC	CDCC	DDDDDD	16:0	18:1	22:6	7
CHYO	CE	CDCC			18:1			1
CHYI		CDDC			18:2			2
CHYA		DDDD			20:4			4
CHYU		DDDDDD			22:6			6

* = Tail saturation from MARTINI beads; # = acyl tails of lipid species from LC- MS/MS lipidomics data; C = saturated carbons (C1 bead), D = cis-unsaturated carbon (C4 bead). Cer = ceramides, SM = sphingomyelin, CE = cholesteryl ester, PE = phosphatidylethanolamine, P-PE = plasmalogens ethanolamine, O-PE = plasmanyl ethanolamine, LPE = lyso-phosphatidylethanolamine, PC = diacyl phosphatidylcholine, P-PC = choline plasmalogen, O-PC = plasmanyl choline, LPC = lyso-phosphatidylcholine, PS = phosphatidylserine, PI = phosphatidylinositol, DG = diacylglycerol, TG = triacylglycerol

Appendix 5

Chemical composition of lipid species head groups and linkers used to simulate the fetal neuronal membrane

Lipid (sub)class	**Linker[a]**	**MARTINI headgroups**	**Linker**	**Atomistic headgroups**
PC	GL1/GL2[a]	PO4-NC3[d]	glycerol	Phosphocholine
PE	GL1/GL2[a]	PO4-NH3[d]	glycerol	Phosphoethanolamine
PS	GL1/GL2[a]	PO4-CN0[d]	glycerol	Phosphoserine
PG	GL1/GL2[a]	PO4-GL0[d]	Glycerol	Phosphoglycerol
PI	GL1/GL2[a]	PO4-C1-C2-C3[d]	Glycerol	Phosphoinositol
DG	GL1/GL2[a]	–	Glycerol	-
TG	GL1/GL2[a]	–	Glycerol	-
MC	GL1/PL2[a,b]	PO4-NC3[d]	vinyl ether	Phosphocholine
ME	GL1/PL2[a,b]	PO4-NH3[d]	vinyl ether	Phosphoethanolamine
AC	GL1/PL2[a,b]	PO4-NC3[d]	Ether	Phosphocholine
AE	GL1/PL2[a,b]	PO4-NH3[d]	Ether	Phosphoethanolamine
SM	AM1/AM2[c]	PO4-NC3[d]	Sphingoid	GalNAcα1-3GalNAcβ1-3Galα1-4Galβ1-4Glcβ1
Cer	-	-	Sphingoid	GalNAcα1-3GalNAcβ1-3Galα1-4Galβ1-4Glcβ1

Appendix 6

Simulated composition of the fetal neuronal plasma membrane by experimental groups

Lipid species	Upper/lower leaflet ratio	Low GD12.5					Low GD18.5					High GD12.5					High GD18.5				
		Total	Upper		Lower		Total	Upper		lower		Total	Upper		lower		Total	Upper		lower	
		Count	Count	Fraction	Count	Fraction	Count	Count	Fraction	Count	Fraction	Count	Count	Fraction	Count	Fraction	Count	Count	Fraction	Count	Fraction
Lysophosphatidylcholine (LPC)																					
LPC	0.67/0.33	2	2	0.001	-	-	1	1	0.001	-	-	2	2	0.001	-	-	4	4	0.002	-	-
PPC		14	10	0.005	4	0.002	24	17	0.009	7	0.004	25	18	0.009	7	0.004	46	36	0.018	10	0.005
OPC		6	4	0.002	2	0.001	6	5	0.003	1	0.001	9	8	0.004	1	0.001	18	14	0.007	4	0.002
FPC		-	-	-	-	-	1	1	0.001	-	-	2	2	0.001	-	-	4	2	0.001	2	0.001
APC		-	-	-	-	-	1	1	0.001	-	-	-	-	-	-	-	-	-	-	-	-
Phosphatidylcholine (PC)																					
DLPC	0.65/0.35	4	2	0.001	2	0.001	9	8	0.004	1	0.001	5	4	0.002	1	0.001	18	14	0.007	4	0.002
LPPC		60	40	0.020	20	0.010	643	615	0.309	28	0.014	93	67	0.033	26	0.013	68	52	0.026	16	0.008
LOPC		12	8	0.004	4	0.002	21	14	0.007	7	0.004	13	10	0.005	3	0.002	26	20	0.010	6	0.003
DPPC		512	340	0.169	172	0.086	252	171	0.086	81	0.041	455	323	0.160	132	0.066	247	191	0.095	56	0.028
POPC		1006	668	0.332	338	0.168	505	341	0.171	164	0.082	712	505	0.251	207	0.104	497	384	0.191	113	0.056

DOPC		215	142	0.071	73	0.036	105	71	0.036	34	0.017	160	114	0.057	46	0.023	87	67	0.033	20	0.010
OIPC		18	12	0.006	6	0.003	10	7	0.004	3	0.002	17	12	0.006	5	0.003	6	4	0.002	2	0.001
PSPC		16	10	0.005	6	0.003	5	4	0.002	1	0.001	15	12	0.006	3	0.002	6	4	0.002	2	0.001
OPPC		48	32	0.016	16	0.008	82	55	0.028	27	0.014	80	57	0.028	23	0.012	107	83	0.041	24	0.012
PQPC		50	34	0.017	16	0.008	18	13	0.007	5	0.003	41	30	0.015	11	0.006	24	18	0.009	6	0.003
PAPC		143	95	0.047	48	0.024	89	61	0.031	28	0.014	99	71	0.035	28	0.014	52	40	0.020	12	0.006
OAPC		58	38	0.019	20	0.010	138	23	0.012	115	0.058	33	24	0.012	9	0.005	20	16	0.008	4	0.002
OBPC		-	-	-	-	-	-	-	-	-	-	-	-	-	-	-	2	2	0.001	-	-
OGPC		6	4	0.002	2	0.001	1	1	0.001	-	-	5	4	0.002	1	0.001	2	2	0.001	-	-
PUPC		38	26	0.013	12	0.006	26	17	0.009	9	0.005	61	44	0.022	17	0.009	42	32	0.016	10	0.005
OUPC		10	6	0.003	4	0.002	8	5	0.003	3	0.002	13	10	0.005	3	0.002	12	10	0.005	2	0.001
SGPC		22	14	0.007	8	0.004	6	5	0.003	1	0.001	13	10	0.005	3	0.002	2	2	0.001	0	-
Choline plasmalogen (P-PC)																					
DPAC	0.65/0.35	4	2	0.001	2	0.001	3	2	0.001	1	0.001	5	4	0.002	1	0.001	6	4	0.002	2	0.001
Plasmanyl choline (O-PC)																					
DPMC	0.65/0.35	38	26	0.013	12	0.006	18	13	0.007	5	0.003	43	30	0.015	13	0.007	16	12	0.006	4	0.002
Lysophosphatidylethanolamine (LPE)																					

PPE	0.33/0.67	10	4	0.002	6	0.003	14	5	0.003	9	0.005	5	2	0.001	3	0.002	22	10	0.005	12	0.006
APE		10	4	0.002	6	0.003	11	4	0.002	7	0.004	5	2	0.001	3	0.002	16	8	0.004	8	0.004
Phosphatidylethanolamine (PE)																					
DPPE	0.35/0.65	6	2	0.001	4	0.002	4	1	0.001	3	0.002	5	2	0.001	3	0.002	8	4	0.002	4	0.002
DOPE		68	24	0.012	44	0.022	23	8	0.004	15	0.008	74	30	0.015	44	0.022	40	20	0.010	20	0.010
POPE		111	40	0.020	71	0.035	94	35	0.018	59	0.030	145	61	0.030	84	0.042	162	81	0.040	81	0.040
OIPE		12	4	0.002	8	0.004	1	0	-	1	0.001	13	6	0.003	7	0.004	4	2	0.001	2	0.001
PQPE		12	4	0.002	8	0.004	14	5	0.003	9	0.005	19	8	0.004	11	0.006	20	10	0.005	10	0.005
PAPE		186	67	0.033	119	0.059	237	89	0.045	148	0.074	180	75	0.037	105	0.053	306	152	0.076	154	0.077
PUPE		100	36	0.018	64	0.032	206	77	0.039	129	0.065	172	71	0.035	101	0.051	359	179	0.089	180	0.089
Plasmalogen ethanolamine (P-PE)																					
DPME	0.35/0.65	10	4	0.002	6	0.003	9	4	0.002	5	0.003	7	4	0.002	3	0.002	8	4	0.002	4	0.002
POME		44	16	0.008	28	0.014	27	10	0.005	17	0.009	35	14	0.007	21	0.011	26	12	0.006	14	0.007
PAME		206	75	0.037	131	0.065	132	49	0.025	83	0.042	149	61	0.030	88	0.044	88	44	0.022	44	0.022
PUME		166	61	0.030	105	0.052	206	77	0.039	129	0.065	206	85	0.042	121	0.061	206	103	0.051	103	0.051
Plasmanyl ethanolamine (O-PE)																					
OAAE	0.35/0.65	94	34	0.017	60	0.030	82	30	0.015	52	0.026	103	42	0.021	61	0.031	98	48	0.024	50	0.025

OUAE		28	-	-	28	0.014	106	39	0.020	67	0.034	119	48	0.024	71	0.036	237	118	0.059	119	0.059
Phosphatidylserine (PS)																					
POPS	0.0/1.00	48	-	-	48	0.024	11	-	-	11	0.006	44	-	-	44	0.022	34	-	-	34	0.017
PAPS		95	-	-	95	0.047	106	-	-	106	0.053	71	-	-	71	0.036	87	-	-	87	0.043
PUPS		91	-	-	91	0.045	291	-	-	291	0.146	136	-	-	136	0.068	405	-	-	405	0.201
Phosphatidylinositol (PI)																					
PAPI	0.0/1.00	178	-	-	178	0.089	210	-	-	210	0.105	340	-	-	340	0.171	235	-	-	235	0.117
OAPI		38	-	-	38	0.019	36	-	-	36	0.018	40	-	-	40	0.020	46	-	-	46	0.023
Phosphatidylglycerol (PG)																					
DOPG	0.50/0.50	4	2	0.001	2	0.001	7	4	0.002	3	0.002	13	8	0.004	5	0.003	18	12	0.006	6	0.003
POPG		28	14	0.007	14	0.007	60	32	0.016	28	0.014	64	36	0.018	28	0.014	139	91	0.045	48	0.024
Sphingomyelin (SM)																					
PNSM	0.80/0.20	4	4	0.002	-	-	2	2	0.001	-	-	4	4	0.002	-	-	4	4	0.002	-	-
Ceramide (CE)																					
DPCE	0.51/0.49	16	8	0.004	8	0.004	24	13	0.007	11	0.006	13	8	0.004	5	0.003	22	14	0.007	8	0.004
OPCE		-	-	-	-	-	3	2	0.001	1	0.001	-	-	-	-	-	4	2	0.001	2	0.001
PBCE		32	16	0.008	16	0.008	49	26	0.013	23	0.012	29	16	0.008	13	0.007	44	28	0.014	16	0.008

PXCE		4	2	0.001	2	0.001	1	1	0.001	-	-	2	2	0.001	-	-	2	2	0.001	-	-
PNCE		4	2	0.001	2	0.001	3	2	0.001	1	0.001	3	2	0.001	1	0.001	6	4	0.002	2	0.001
PWCE		16	8	0.004	8	0.004	8	1	0.001	7	0.004	2	2	0.001	-	-	2	2	0.001	-	-
Cholesteryl ester (CHY)																					
CHYO	0.51/0.49	6	4	0.002	2	0.001	-	-	-	-	-	9	6	0.003	3	0.002	2	2	0.001	-	-
CHYI		14	8	0.004	6	0.003	1	1	0.001	-	-	21	12	0.006	9	0.005	6	4	0.002	2	0.001
CHYA		8	4	0.002	4	0.002	2	2	0.001	-	-	7	4	0.002	3	0.002	2	2	0.001	-	-
CHYU		-	-	-	-	-	2	2	0.001	-	-	6	3	0.001	3	0.002	6	4	0.002	2	0.001
Diglycerides (DG)																					
DPDG	0.50/0.50	28	14	0.007	14	0.007	10	7	0.004	3	0.002	25	14	0.007	11	0.006	16	10	0.005	6	0.003
PODG		12	6	0.003	6	0.003	8	5	0.003	3	0.002	11	6	0.003	5	0.003	12	8	0.004	4	0.002
1-O-alkyl-diglycerides																					
LCAP	0.50/0.50	4	2	0.001	2	0.001	3	2	0.001	1	0.001	3	2	0.001	1	0.001	6	4	0.002	2	0.001
Triglycerides (TG)																					
TPG	0.50/0.50	4	2	0.001	2	0.001	1	1	0.001	-	-	2	2	0.001	-	-	2	2	0.001	-	-
PPOG		6	4	0.002	2	0.001	2	1	0.001	1	0.001	5	4	0.002	1	0.001	6	2	0.001	4	0.002
POOG		8	4	0.002	4	0.002	2	1	0.001	1	0.001	3	2	0.001	1	0.001	2	2	0.001	-	-

POIG		8	4	0.002	4	0.002	-	-	-	-	-	3	2	0.001	1	0.001	-	-	-	-	-
PIIG		6	4	0.002	2	0.001	-	-	-	-	-	3	2	0.001	1	0.001	-	-	-	-	-
TOG		4	2	0.001	2	0.001	1	1	0.001	-	-	-	-	-	-	-	-	-	-	-	-
OOIG		4	2	0.001	2	0.001	1	1	0.001	-	-	-	-	-	-	-	-	-	-	-	-
OIIG		6	4	0.002	2	0.001	-	-	-	-	-	5	4	0.002	1	0.001	-	-	-	-	-
PPUG		-	-	-	-	-	-	-	-	-	-	-	-	-	-	-	2	2	0.001	-	-
POUG		-	-	-	-	-	-	-	-	-	-	2	2	0.001	-	-	2	2	0.001	-	-
Total		4021	2010	1.000	2011	1.000	3982	1991	1.000	1991	1.000	4004	2015	1.000	1989	1.000	4024	2011	1.000	2013	1.000
Water		82865						82368					82573					81812			
Na^+		957						953					976					1005			
Cl^-		877						875					855					814			

Appendix 7

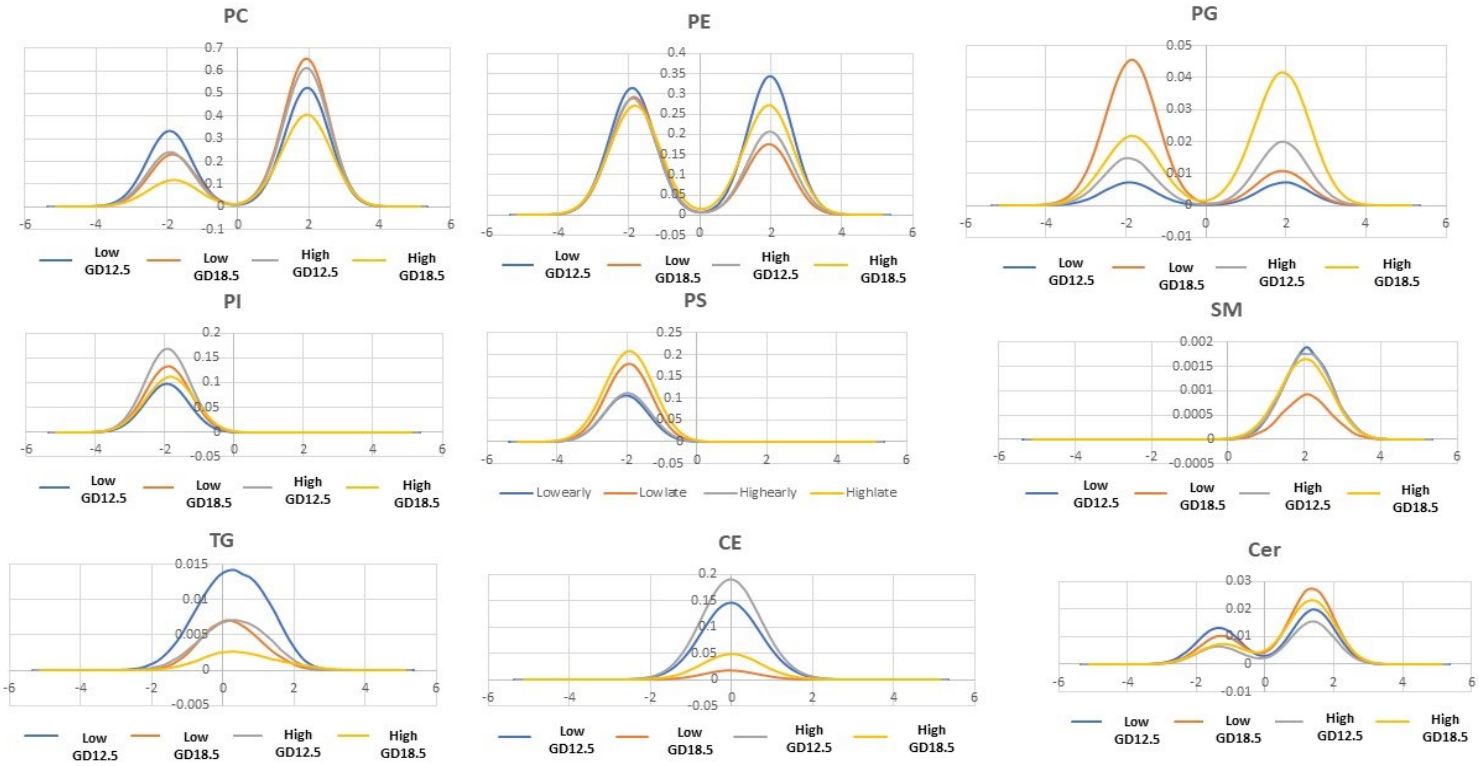

Illustration of the density of each lipid class between leaflets of the neuronal membranes. Phosphatidylcholine (PC), phosphatidylethanolamine (PE), phosphatidylserine (PS), phosphatidylglycerol (PG), phosphatidylinositol (PI), di/triacylglycerols (DG/TG), cholesteryl esters (CE), sphingomyelins (SM), and ceramides (Cer).

Appendix 8

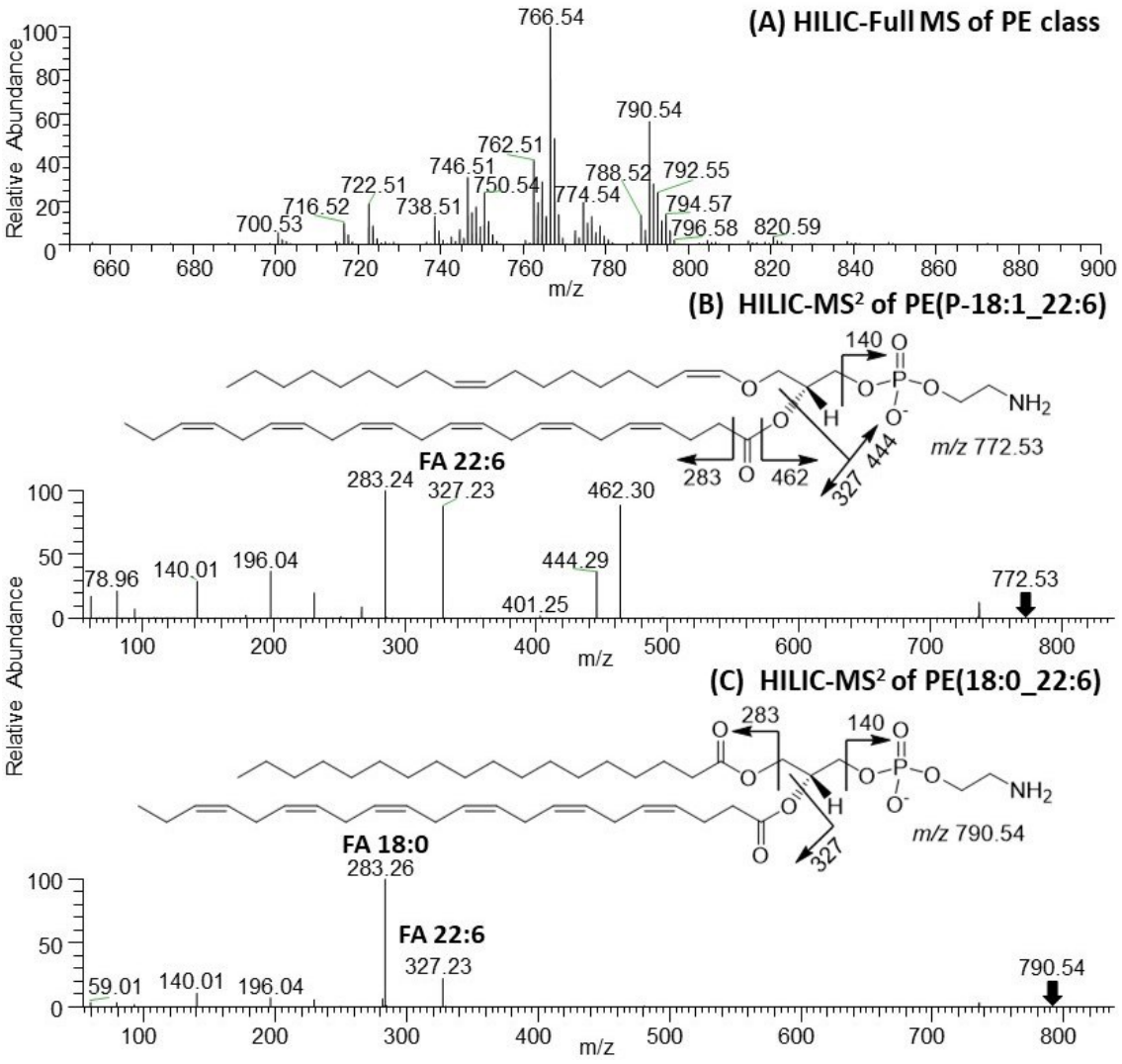

High-resolution mass spectra (HRMS) obtained from HILIC-MS chromatogram of fetal brain lipid extract in negative ion mode. (**A**) Full MS spectrum of PE class by averaging scans from 21-24 mins in the HILIC-MS chromatogram. (**B-E**) HILIC-MS^2 spectra showing the fragmentation of PE and plasmalogen PE precursor ions: (**B**) plasmalogen PE(P-18:1_22:6) $[M-H]^-$ at *m/z* 772.53, (**C**) plasmalogen PE(P-18:0_22:5) $[M-H]^-$ at *m/z* 776.56, (**D**) PE(18:0_22:6) $[M-H]^-$ at *m/z* 790.54 and (**E**) PE(18:0_22:5) $[M-H]^-$ at *m/z* 792.55.

Appendix 9

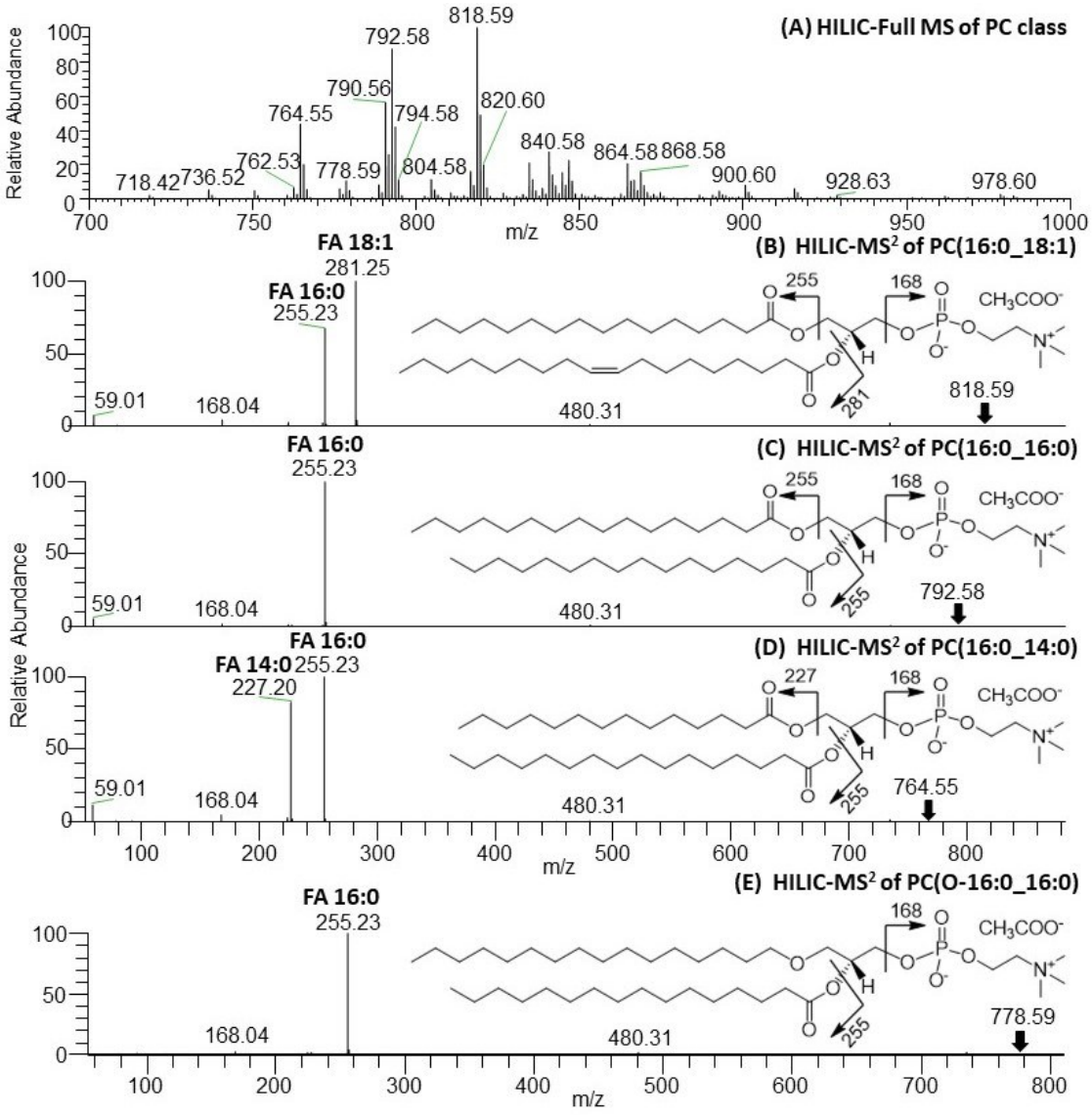

High-resolution mass spectra (HRMS) achieved from HILIC-MS chromatogram of fetal brain lipid extract in negative ion mode. (**A**) Full MS spectrum of PC class by averaging scans from 27.5-29 mins in the HILIC-MS chromatogram. (**B-E**) HILIC-MS^2 spectra showing the fragmentation of PC and ether PC precursor ions: (**B**) PC(16:0/18:1) $[M+CH_3COO]^-$ at *m/z* 818.59, (**C**) PC(16:0_16:0) $[M+CH_3COO]^-$ at *m/z* 792.58, (**D**) PC(16:0_14:0) $[M+CH_3COO]^-$ at *m/z* 764.55 and (**E**) ether PC(O-16:0_16:0) $[M+CH_3COO]^-$ at *m/z* 778.59.

Appendix 10

Lipid species detected in fetal brain at both gestation stages

No	Lipid class	Lipid group	Lipid species	Lipid Ion	*m/z*	RT (min)
1.	Cer	Cer(d34:1)	Cer(d18:1_16:0)	$[M+H]^+$	538.519	16.301
2.	Cer	Cer(d36:1)	Cer(d18:1_18:0)		566.551	16.845
3.	Cer	Cer(d36:2)	Cer(d18:2_18:0)		564.535	16.312
4.	Cer	Cer(d38:1)	Cer(d18:1_20:0)		594.582	17.272
5.	Cer	Cer(d40:1)	Cer(d18:1_22:0)		622.613	17.705
6.	Cer	Cer(d42:1)	Cer(d18:1_24:0)		650.645	18.154
7.	Cer	Cer(d42:2)	Cer(d18:1_24:1)		648.629	17.615
8.	Cer	Cer(d42:3)	Cer(d18:1_24:2)		646.613	17.165
9.	SM	SM(d40:2)	SM(d18:1_22:1)	$[M+H]^+$	785.653	17.112
10.	SM	SM(d42:2)	SM(d18:1_24:1)		813.684	17.486
11.	CE	CE(18:1)	CE(18:1)	$[M+NH_4]^+$	668.634	23.896
12.	CE	CE(18:2)	CE(18:2)		666.618	22.863
13.	CE	CE(20:4)	CE(20:4)		690.618	22.045
14.	CE	CE(22:6)	CE(22:6)		714.618	21.530
15.	DG	DG(32:0)	DG(16:0_16:0)	$[M+NH_4]^+$	586.541	17.157

16.	DG	DG(32:1)	DG(16:0_16:1)		584.525	16.765
17.	DG	DG(34:0)	DG(18:0_16:0)		614.572	17.601
18.	DG	DG(34:1)	DG(16:0_18:1)		612.556	17.122
19.	DG	DG(36:0)	DG(18:0_18:0)		642.603	18.047
20.	LPC	LPC(14:0)	LPC(14:0)	$[M+H]^+$	468.308	2.669
21.	LPC	LPC(16:0)	LPC(16:0)		496.340	4.318
22.	LPC	LPC(16:1)	LPC(16:1)		494.324	2.935
23.	LPC	LPC(18:0)	LPC(18:0)		524.371	7.724
24.	LPC	LPC(18:1)	LPC(18:1)		522.355	4.724
25.	LPC	LPC(18:2)	LPC(18:2)		520.340	3.414
26.	LPC	LPC(18:3)	LPC(18:3)		518.324	4.319
27.	LPC	LPC(18:4)	LPC(18:4)		516.308	1.491
28.	LPC	LPC(20:4)	LPC(20:4)		544.340	3.135
29.	LPC	LPC(22:6)	LPC(22:6)		568.340	2.974
30.	LPE	LPE(16:0)	LPE(16:0)	$[M-H]^-$	452.278	1.491
31.	LPE	LPE(18:0)	LPE(18:0)		480.310	8.008
32.	LPE	LPE(20:4)	LPE(20:4)		500.278	1.478
33.	PC	PC(28:0)	PC(14:0_14:0)	$[M+H]^+$	678.507	15.137
34.	PC	PC(30:0)	PC(14:0_16:0)		706.538	15.253

35.	PC	PC(30:1)	PC(14:0_16:1)	704.522	15.884
36.	PC	PC(32:0)	PC(16:0_16:0)	734.569	16.044
37.	PC	PC(32:1)	PC(16:0_16:1)	732.554	15.396
38.	PC	PC(32:2)	PC(16:1_16:1)	730.538	15.977
39.	PC	PC(34:0)	PC(16:0_18:0)	762.601	17.263
40.	PC	PC(34:1)	PC(16:0_18:1)	760.585	16.418
41.	PC	PC(34:2)	PC(16:1_18:1)	758.569	17.058
42.	PC	PC(34:3)	PC(16:1_18:2)	756.554	17.805
43.	PC	PC(34:4)	PC(16:0_18:4)	754.538	15.081
44.	PC	PC(36:1)	PC(18:1_18:0)	788.616	15.608
45.	PC	PC(36:2)	PC(18:1_18:1)	786.601	16.097
46.	PC	PC(36:3)	PC(16:0_20:3)	784.585	16.516
47.	PC	PC(36:4)	PC(16:0_20:4)	782.569	17.127
48.	PC	PC(36:5)	PC(16:1_20:4)	780.554	15.137
49.	PC	PC(38:1)	PC(18:1_20:0)	816.648	15.938
50.	PC	PC(38:2)	PC(18:1_20:1)	814.632	15.991
51.	PC	PC(38:3)	PC(18:0_20:3)	812.616	16.578
52.	PC	PC(38:4)	PC(18:0_20:4)	810.601	17.165
53.	PC	PC(38:5)	PC(18:1_20:4)	808.585	15.075

54.	PC	PC(38:6)	PC(16:0_22:6)		806.569	15.564
55.	PC	PC(38:7)	PC(16:1_22:6)		804.554	15.831
56.	PC	PC(40:5)	PC(18:4_22:1)		836.616	16.471
57.	PC	PC(40:6)	PC(18:0_22:6)		834.601	16.738
58.	PC	PC(40:7)	PC(18:1_22:6)		832.585	17.005
59.	O-PC	PC(32:0e)	PC(O-16:0_16:0)	$[M+H]^+$	720.554	17.646
60.	O-PC	PC(33:1e)	PC(O-16:0_16:1)		732.590	15.618
61.	O-PC	PC(34:0e)	PC(O-16:0_18:0)		748.621	16.204
62.	P-PC	PC(34:0p)	PC(P-18:0_16:0)	$[M+H]^+$	746.606	16.310
63.	PE	PE(32:1)	PE(16:0_16:1)	$[M-H]^-$	688.492	15.848
64.	PE	PE(34:0)	PE(18:0_16:0)		718.539	16.884
65.	PE	PE(34:1)	PE(16:0_18:1)		716.524	16.381
66.	PE	PE(34:2)	PE(16:1_18:1)		714.508	15.926
67.	PE	PE(36:1)	PE(18:0_18:1)		744.555	16.887
68.	PE	PE(36:2)	PE(18:1_18:1)		742.539	16.402
69.	PE	PE(36:3)	PE(18:1_18:2)		740.524	16.055
70.	PE	PE(36:4)	PE(16:0_20:4)		738.508	15.858
71.	PE	PE(38:3)	PE(18:0_20:3)		768.555	16.438
72.	PE	PE(38:4)	PE(18:0_20:4)		766.539	16.441

73.	PE	PE(38:5)	PE(16:0_22:5)		764.524	15.885
74.	PE	PE(38:6)	PE(16:0_22:6)		762.508	15.717
75.	PE	PE(40:4)	PE(18:0_22:4)		794.571	16.441
76.	PE	PE(40:5)	PE(18:0_22:5)		792.555	16.623
77.	PE	PE(40:6)	PE(18:0_22:6)		790.539	16.304
78.	P-PE	PE(32:0p)	PE(P-16:0_16:0)	$[M+H]^+$	676.528	16.746
79.	P-PE	PE(34:0p)	PE(P-18:0_16:0)		704.559	17.122
80.	P-PE	PE(34:1p)	PE(P-16:0_18:1)		702.543	16.684
81.	P-PE	PE(36:1p)	PE(P-18:0_18:1)		730.575	17.058
82.	P-PE	PE(36:4p)	PE(P-16:0_20:4)		724.528	16.044
83.	P-PE	PE(38:4p)	PE(P-16:0_22:4)		752.559	16.641
84.	P-PE	PE(38:5p)	PE(P-16:0_22:5)		750.543	16.044
85.	P-PE	PE(38:6p)	PE(P-16:0_22:6)		748.528	15.938
86.	P-PE	PE(40:4p)	PE(P-18:0_22:4)		780.590	16.952
87.	P-PE	PE(40:5p)	PE(P-18:0_22:5)		778.575	16.791
88.	P-PE	PE(40:6p)	PE(P-18:0_22:6)		776.559	16.588
89.	P-PE	PE(40:7p)	PE(P-18:1_22:6)		774.543	16.055
90.	O-PE	PE(36:5e)	PE(O-16:1_20:4)	$[M-H]^-$	722.513	16.179
91.	O-PE	PE(38:5e)	PE(O-18:1_20:4)		750.544	16.666

92.	O-PE	PE(38:7e)	PE(O-16:1_22:6)		746.513	16.029
93.	O-PE	PE(40:7e)	PE(O-18:1_22:6)		774.544	16.581
94.	PG	PG(36:1)	PG(18:0_18:1)	$[M-H]^-$	775.549	8.167
95.	PG	PG(36:2)	PG(18:1_18:1)	(HILIC	773.533	8.165
96.	PG	PG(34:1)	PG(16:0_18:1)	column)	747.518	8.411
97.	PG	PG(32:1)	PG(16:0_16:1)		719.486	8.545
98.	PG	PG(32:0)	PG(16:0_16:0)		721.502	8.630
99.	PI	PI(38:4)	PI(18:0_20:4)	$[M-H]^-$	885.550	15.937
100	PI	PI(38:5)	PI(18:1_20:4)		883.534	15.344
101	PS	PS(36:1)	PS(18:0_18:1)	$[M-H]^-$	788.545	16.535
102	PS	PS(38:4)	PS(18:0_20:4)		810.529	16.045
103	PS	PS(40:4)	PS(18:0_22:4)		838.560	16.371
104	PS	PS(40:5)	PS(18:0_22:5)		836.545	16.234
105	PS	PS(40:6)	PS(18:0_22:6)		834.529	15.873
106	TG	TG(24:0)	TG(8:0_8:0_8:0)	$[M+NH_4]^+$	488.395	13.633
107	TG	TG(46:0)	TG(16:0_14:0_16:0)		796.739	20.415
108	TG	TG(48:0)	TG(16:0_16:0_16:0)		824.770	21.252
109	TG	TG(48:1)	TG(16:0_16:0_16:1)		822.755	20.326
110	TG	TG(50:0)	TG(18:0_16:0_16:0)		852.801	22.213

111	TG	TG(50:1)	TG(16:0_16:0_18:1)		850.786	21.109
112	TG	TG(50:2)	TG(16:0_16:1_18:1)		848.770	20.397
113	TG	TG(52:1)	TG(18:0_16:0_18:1)		878.817	22.070
114	TG	TG(52:2)	TG(16:0_18:1_18:1)		876.801	21.037
115	TG	TG(52:3)	TG(16:0_18:1_18:2)		874.786	20.362
116	TG	TG(52:4)	TG(16:0_18:2_18:2)		872.770	19.791
117	TG	TG(52:4)	TG(16:0_16:0_20:4)		872.770	20.103
118	TG	TG(54:3)	TG(18:1_18:1_18:1)		902.817	20.914
119	TG	TG(54:4)	TG(18:1_18:1_18:2)		900.801	20.291
120	TG	TG(54:4)	TG(16:0_16:0_22:4)		900.801	20.904
121	TG	TG(54:5)	TG(18:1_18:2_18:2)		898.786	9.755
122	TG	TG(54:5)	TG(18:1_18:1_18:3)		898.786	20.050
123	TG	TG(54:6)	TG(16:0_16:0_22:6)		896.770	9.943
124	TG	TG(56:5)	TG(18:0_18:1_20:4)		926.817	20.851
125	TG	TG(56:6)	TG(16:0_20:3_20:3)		924.801	20.691
126	TG	TG(56:7)	TG(16:0_18:1_22:6)		922.786	19.827
127	O-TG	TG(38:4e)	TG(O-12:0_6:0_20:4)	$[M+NH_4]^+$	662.572	7.165

Information in the above table represents the lipid species found in the fetal brain. Ceramides (Cer), sphingomyelin (SM), cholesteryl ester (CE), phosphatidylethanolamine (PE), ethanolamine

plasmalogens (P-PE), plasmanyl ethanolamine (O-PE), lyso-phosphatidylethanolamine (LPE), diacyl phosphatidylcholine (PC), plasmalogen choline (P-PC), plasmanyl choline (O-PC), lyso-phosphatidylcholine (LPC), phosphatidylserine (PS), phosphatidylinositol (PI), diacylglycerols (DG), triacylglycerols (TG), and 1-*O*-alkyl-diglyceride (O-TG).

Appendix 11

Effects of maternal n-3 PUFA diet on lateral diffusion rate of lipids in fetal neuronal membrane (10^{-7} cm^2/s)

Lipids	Low GD12.5	Low GD18.5	High GD12.5	High GD18.5	Diet	Gestation	Diet* Gestation
PC	6.21 ± 0.15^b	6.79 ± 0.03^a	6.33 ± 0.20^a	6.85 ± 0.11^b	NS	p = 0.0005	NS
PE	6.23 ± 0.12^b	6.60 ± 0.27^a	6.33 ± 0.19^a	6.79 ± 0.11^b	NS	p = 0.01	NS
PG	6.55 ± 0.95^a	6.45 ± 0.93^a	6.43 ± 0.17^a	7.33 ± 0.04^a	NS	NS	NS
PS	6.18 ± 0.46^b	6.60 ± 0.31^a	5.94 ± 0.20^a	5.94 ± 0.03^b	p = 0.04	NS	NS
PI	5.30 ± 0.29^b	6.10 ± 0.11^a	5.94 ± 0.20^a	5.94 ± 0.03^a	NS	p = 0.01	p = 0.01
DG	7.26 ± 0.43^a	9.58 ± 1.06^a	10.06 ± 0.85^a	9.39 ± 1.04^a	NS	NS	NS
TG	6.76 ± 0.30^b	9.48 ± 0.24^a	7.24 ± 1.48^a	7.32 ± 0.63^a	NS	p = 0.04	NS
CE	12.39 ± 2.01^a	9.74 ± 3.16^a	12.90 ± 2.74^a	11.99 ± 2.96^a	NS	NS	NS
SM	2.75 ± 0.68^a	5.55 ± 1.48^a	6.88 ± 2.23^a	6.75 ± 4.18^a	NS	NS	NS
Cer	7.49 ± 0.52^a	8.64 ± 0.55^a	7.90 ± 0.63^a	7.81 ± 1.16^a	NS	NS	NS
ADR	**6.25 ± 0.20^a**	**6.73 ± 0.17^a**	**6.42 ± 0.25^a**	**6.86 ± 0.15^a**	**NS**	**NS**	**NS**

Data were analysed using two-way ANOVA to determine the main effects and the interactions between maternal diet and gestation stage; pairwise comparison using Bonferroni's correction was used to determine differences when there was an observed interaction. Data represent the mean ± standard error of mean (SEM). Mean values with different superscript letters (a, b, c & d) are significantly different; $p < 0.05$ (n = 3 replicates). PC = species with choline head group (diacyl phosphatidylcholine, lysophosphatidylcholine, plasmanyl choline, and choline plasmalogen), PE = species with ethanolamine head group (diacyl phosphatidylethanolamine, lysophosphatidylethanolamine, plasmanyl ethanolamine and ethanolamine plasmalogen), phosphatidylserine (PS), phosphatidylglycerol (PG), phosphatidylinositol (PI), di/triacylglycerols (DG/TG), cholesteryl esters (CE), sphingomyelins (SM), ceramides (Cer), and average diffusion rate (ADR).

Appendix 12

Effect of n-3 PUFA diets on domain formation in the fetal neuronal membrane during gestation

Domains	Groups			
	Low-GD12.5	Low-GD18.5	High-GD12.5	High-GD18.5
Domains that were enriched in all the membranes				
CE/PI	1.20 ± 0.02	1.22 ± 0.01	1.30 ± 0.02	1.47 ± 0.01
CE/Cer	1.45 ± 0.07	1.73 ± 0.11	1.73 ± 0.15	2.03 ± 0.09
Cer/Cer	1.40 ± 0.15	1.28 ± 0.91	2.26 ± 0.35	1.99 ± 1.00
Cer/PE	1.46 ± 0.06	1.75 ± 0.02	1.64 ± 0.04	1.79 ± 0.01
Cer/SM	1.21 ± 0.13	1.33 ± 0.06	1.50 ± 0.07	1.67 ± 0.27
PC/PC	1.83 ± 0.02	1.90 ± 0.00	1.89 ± 0.00	1.93 ± 0.00
PE/PG	1.62 ± 0.04	1.97 ± 0.08	1.77 ± 0.03	2.00 ± 0.06
PE/Cer	1.45 ± 0.06	1.74 ± 0.17	1.63 ± 0.03	1.75 ± 0.02
PI/PS	1.83 ± 0.41	1.87 ± 0.43	1.91 ± 0.45	1.89 ± 0.44
SM/SM	1.92 ± 0.01	1.96 ± 0.02	1.98 ± 0.00	2.00 ± 0.00
SM/PC	1.89 ± 0.00	1.98 ± 0.00	1.97 ± 0.00	2.00 ± 0.00
Domains that were neither enriched nor depleted in all the membranes				
CE/PS	0.95 ± 0.01	0.83 ± 0.02	0.93 ± 0.00	1.00 ± 0.00
PC/PG	1.02 ± 0.01	1.04 ± 0.03	1.06 ± 0.03	1.14 ± 0.07
PC/Cer	1.02 ± 0.01	1.06 ± 0.02	1.06 ± 0.02	1.15 ± 0.08
PG/Cer	1.05 ± 0.04	1.03 ± 0.01	1.08 ± 0.06	1.19 ± 0.10
PI/PG	0.96 ± 0.02	1.02 ± 0.04	1.06 ± 0.04	1.16 ± 0.01
PI/PI	0.80 ± 0.04	0.90 ± 0.01	0.89 ± 0.01	0.99 ± 0.00
Domains depleted in all the membranes				
Cer/CE	0.37 ± 0.09	0.53 ± 0.07	0.40 ± 0.04	0.43 ± 0.03
Cer/PS	0.75 ± 0.14	0.50 ± 0.07	0.57 ± 0.11	0.45 ± 0.13
Cer/PI	0.73 ± 0.14	0.52 ± 0.07	0.55 ± 0.12	0.48 ± 0.06
PC/PI	0.68 ± 0.16	0.54 ± 0.23	0.58 ± 0.21	0.47 ± 0.23
PC/PE	0.63 ± 0.00	0.26 ± 0.01	0.53 ± 0.02	0.40 ± 0.01
PC/CE	0.19 ± 0.01	0.27 ± 0.03	0.18 ± 0.01	0.15 ± 0.02
PE/SM	0.70 ± 0.02	0.56 ± 0.01	0.60 ± 0.01	0.48 ± 0.01
PE/PC	0.22 ± 0.00	0.17 ± 0.01	0.20 ± 0.02	0.18 ± 0.01
PG/CE	0.56 ± 0.20	0.52 ± 0.13	0.40 ± 0.10	0.40 ± 0.11
PG/PC	0.63 ± 0.00	0.28 ± 0.00	0.52 ± 0.00	0.40 ± 0.00
PG/PS	0.24 ± 0.00	0.28 ± 0.00	0.25 ± 0.00	0.27 ± 0.00

PG/PE	0.45 ± 0.01	0.61 ± 0.02	0.49 ± 0.00	0.55 ± 0.02
PI/CE	0.60 ±0.05	0.32 ± 0.03	0.61 ± 0.04	0.36 ± 0.03
PI/PC	0.68 ± 0.16	0.54 ± 0.23	0.58 ± 0.21	0.47 ± 0.25
PI/SM	0.00 ± 0.00	0.00 ± 0.00	0.00 ± 0.00	0.00 ± 0.00
PS/PC	0.71 ± 0.14	0.55 ± 0.23	0.61 ± 0.20	0.48 ± 0.27
PS/CE	0.47 ± 0.05	0.49 ± 0.03	0.48 ± 0.04	0.36 ± 0.04
SM/PG	0.71 ± 0.00	0.52 ± 0.02	0.67 ± 0.01	0.61 ± 0.01
SM/PS	0.00 ± 0.00	0.00 ± 0.00	0.00 ± 0.00	0.00 ± 0.00

Molecular dynamic simulation of the fetal neuronal membrane was done in triplicate for 10 µs. *The contact fractions - the number of contacts between the headgroups of two lipids within 1.2 nm were calculated using LiPyphilic software (P. Smith & Lorenz, 2021) (to determine the formation of lipid domains in the membrane). The mean ± standard error of the mean (SEM) (n = 3 per group) was determined and presented in Table 3.3. Lipid domains with contact fraction values < 0.8 (in red color cells) represent depleted domains, domains with contact fraction values > 0.8 and less than 1.2 (in yellow color cells) represent domains that were neither depleted nor enriched, and domains with contact fraction values ≥ 1.2 (in blue color cells) represent enriched domains.*

Appendix 13

Summary of effect of diet and gestation on selected fetal brain lipids and fatty acyl species

Lipid group/class/fatty acyl species	Diet	Gestation
∑Ethanolamine-based GP	↑	↑
∑PE	↑	↑
MUFA-containing PE		
PE(16:0_16:1)	NS	↓
PE(16:0_18:1)	↑	↓
PE(18:1_18:1)	NS	↓
PE(16:1_18:1)	NS	↓
PE(P-16:0_18:1)	↓	↓
N-6 PUFA-containing PE		
PE(18:1_18:2)	NS	↓
N-3 PUFA-containing PE		
PE(16:0_22:6)	↑	↑
PE(18:0_22:6)	↑	↑
∑P-PE	↓	NS
N-6 PUFA-containing P-PE		
PE(P-16:1_20:4)	NS	↓
PE(P-16:0_20:4)	↓	↓
PE(P-16:0_22:4)	↓	↓
PE(P-18:0_22:4)	↓	↓
N-3 PUFA-containing P-PE		
PE(P-16:0_22:5)	↓	↓
PE(P-18:0_22:5)	↓	↓
∑O-PE	↑	↑
PE(O-16:1_22:6)	↑	↑
PE(O-18:1_22:6)	↑	↑
∑Choline-based GP	↓	↓
∑PC	↓	↓
SFA-containing PC		
PC(18:1_18:0)	↑	↑
PC(16:0_18:0)	↑	↑
N-6 PUFA-containing PC		
PC(18:1_20:4)	↓	NS
PC(16:0_20:4)	↓	↑
N-3 PUFA-containing PC		

PC(16:0_22:6)	↑	↑
PC(16:1_22:6)	↑	NS
∑P-PC	NS	↓
∑LPC	↑	↑
LPC(22:6)	↑	↑
Minor brain lipids	↑	↑
SFA-containing minor brain lipids		
PG(16:0_16:0)	↑	NS
Cer(d18:1_16:0)	↓	↓
Cer(d18:1_18:0)	↓	↑
Cer(d18:2_18:0)	↑	↓
MUFA-containing minor brain lipids		
PG(18:1_18:1)	↑	↓
PG(18:0_18:1)	↑	↑
PG(16:0_18:1)	↑	↑
N-6 PUFA-containing minor brain lipids		
PS(18:0_22:4)	↓	↓
PI(18:0_20:4)	NS	↓
N-3 PUFA-containing minor brain lipids		
PS(18:0_22:5)	↓	NS
PS(18:0_22:6)	↑	↑
CE(22:6)	↑	↓
∑Glycerolipids	NS	↓
MUFA-containing glycerolipids		
DG(16:0_18:1)	↑	↑
N-6 PUFA-containing glycerolipids		
TG(16:0_20:3_20:3)	↑	↑
N-3 PUFA-containing glycerolipids		
TG(16:0_16:0_22:6)	↑	↑
TG(16:0_18:1_22:6)	↑	↓

Under diet column, ↑ = higher in high n-3 PUFA diet compared with low n-3 PUFA diet, whereas ↓ = lower in high n-3 PUFA diet compared with low n-3 PUFA diet; under gestation column: ↑ increase as gestation progressed from GD12.5 to GD18.5, whereas ↓ = decrease as gestation progressed. NS = no significant effect.

Appendix 14

Summary of effect of diet and gestation on selected fetal neuronal membrane dynamics

Membrane dynamics	Diet	Gestation
Membrane thickness	↓at GD12.5 and ↑ at GD18.5	↓
Area per lipids	↑	↑
CE flip-flop rate	↓	↓
Average LDR	NS	NS

Under diet column, ↑ = higher in high n-3 PUFA diet compared with low n-3 PUFA diet, whereas ↓ = lower in high n-3 PUFA diet compared with low n-3 PUFA diet; under gestation column: ↑ increase as gestation progressed from GD12.5 to GD18.5, whereas ↓ = decrease as gestation progressed. LDR = lipid diffusion rate. NS = no significant effect.